Essays in Evolutionary Theory

Essays in Evolutionary Theory

A DISSERTATION PRESENTED
BY
CARL VELLER
TO
THE DEPARTMENT OF ORGANISMIC AND EVOLUTIONARY BIOLOGY

IN PARTIAL FULFILLMENT OF THE REQUIREMENTS
FOR THE DEGREE OF
DOCTOR OF PHILOSOPHY
IN THE SUBJECT OF
ORGANISMIC AND EVOLUTIONARY BIOLOGY

HARVARD UNIVERSITY
CAMBRIDGE, MASSACHUSETTS
APRIL 2019

Thesis advisor: Professor Martin A. Nowak Carl Veller

Essays in Evolutionary Theory

Abstract

Chapter 1 proposes and empirically tests a model for the evolution of long, synchronous flowering intervals in bamboos. Chapter 2 develops a mathematical method for studying the interaction of multiple populations in stochastic evolutionary games. Chapter 3 applies this methodology to antagonistic and mutualistic species interactions, showing that faster evolution is beneficial in antagonisms, but that slower evolution can be beneficial in some mutualisms. Chapter 4 uses a stochastic model of evolutionary games to show that assortment favors the evolution of cooperation under very general conditions, including when Hamilton's rule fails. Chapter 5 uses a simple model and economic intuition to show that the Trivers-Willard hypothesis of sex allocation—mothers in good condition should (i) have more sons and (ii) care more for sons—holds more generally in case (i) than in case (ii). Chapter 6 identifies and mathematically characterizes a novel selective force, induced by genetic drift, operating in transitions between male and female heterogamety. This 'drift-induced selection' favors epistatically dominant sex determining mutations, possibly explaining their observed preponderance. Chapter 7 proposes a new genetic model to explain the rarity of environmental sex determination (ESD) relative to genetic sex determination (GSD), based on the inevitable coupling of sex-biasing alleles (e.g., of genes underlying temperature thresholds) and 'sexually antagonistic' alleles (which increase fitness in one sex but reduces fitness in the other). Chapter 8 proposes and implements a new metric for genome-wide recombination, $\bar{r}$, that takes into account the positions of crossovers, as well as independent assortment of homologs. Chapter 9 discovers a deeply-conserved form of crossover

patterning: the number of crossovers covaries positively across the chromosomes within individual meiotic nuclei. Crossover covariation causes an increase in the frequencies of gametes with either many or few crossovers, which population genetic modelling shows to be advantageous in a fluctuating environment.

Contents

Author List

The following authors contributed to Chapter 1: Martin A. Nowak and Charles C. Davis.
The following authors contributed to Chapter 2: Laura K. Hayward.
The following authors contributed to Chapter 3: Laura K. Hayward, Christian Hilbe, and Martin A. Nowak.
The following authors contributed to Chapter 4: Daniel B. Cooney and Benjamin Allen.
The following authors contributed to Chapter 5: David A. Haig and Martin A. Nowak.
The following authors contributed to Chapter 6: Pavitra Muralidhar, George W. A. Constable, and Martin A. Nowak.
The following authors contributed to Chapter 7: Pavitra Muralidhar.
The following authors contributed to Chapter 8: Nancy Kleckner and Martin A. Nowak.
The following authors contributed to Chapter 9: Shunxin Wang, Fei Sun, Aurora Ruiz-Herrera, Yongliang Shang, Hongbin Liu, Denise Zickler, Zijang Chen, Nancy Kleckner, and Liangran Zhang.

Listing of figures

Dedicated to Martin and Denise Veller.

Acknowledgments

I am grateful to Martin Nowak, my advisor, for many things. First, for welcoming into his research group a dispirited economics graduate student with an interest in, but little knowledge of, theoretical biology. Second, for providing a free and exciting academic environment in which to think about and discuss research. Third, for always being available for stimulating conversations about work and life.

Each of the members of my committee—David Haig, Dan Hartl, Nancy Kleckner, and Naomi Pierce—could separately count as my PhD advisor, so generous and influential have they been with their thoughts and advice. I have benefited tremendously from discussions and collaborations with them.

Finally, I am grateful to my parents, Martin and Denise Veller, for supporting my education at every step.

Introduction

The essays in this dissertation fall under the broad heading of theoretical evolutionary biology. Evolutionary theory is based on the principle of selection, and its subfield of evolutionary genetics is additionally based on the principles of Mendelian genetics. The solidity of these principles is what first attracted me to evolutionary theory as a graduate student in economics who had become disillusioned with the type of theory being done there.

Chapter 6 in this dissertation is an example of how these principles aid the theoretician in evolutionary genetics. It concerns transitions between male- and female-heterogametic sex determination, which have been common, for example, in reptiles and amphibians [49]. At first, this evolutionary lability seems mysterious—why would the genetic basis of such a fundamental, conserved trait as sex change so often?

Suppose that we begin with a system of XX/XY male heterogamety, and ask how a transition to ZW/ZZ female heterogamety can occur. One obvious starting point is the appearance of a mutation that will define the W chromosome in the desired ZW/ZZ system. Suppose that this dominant feminizing mutation occurs on an X chromosome (it could also occur on an autosome), and call the mutated chromosome

X′. Thus far, all we have done is to posit a mutation with certain effects. In the simplest version of the model, the population dynamics are then entirely governed by random mating (an assumption that can be relaxed) and fair segregation of the sex chromosomes (Mendel's first law). The setting up of the model is done. Studying the deterministic dynamics of this model, Bull and Charnov [53] found that continuous paths of equilibria link male and female heterogamety (here, XX/XY and X′Y/YY). This revealed that evolutionary transitions between the two systems are not mysterious at all, as they can occur simply by drift along the equilibrium paths. Chapter 6 in this dissertation studies the same model in the context of a finite population, and shows that genetic drift in fact induces a selective force along the equilibrium paths—in favor of epistatically dominant sex determining mutations (possibly explaining why these are empirically the most common type).

The points I wish to make here are: (i) The foundational principles of Mendelian genetics, as they do so often in evolutionary genetics, make the construction of the appropriate model extremely simple: posit a mutation, assume Mendelian genetics, and analyze the resulting dynamics. No *ad hoc* assumptions are required, such as choices of functional forms (e.g., logistic growth, logarithmic utility); the only assumptions made—random mating and no exogenous selection on the different genotypes—have natural interpretations and can easily be relaxed. This is unusual in the mathematical modelling of natural phenomena. (ii) The fact that the basic ingredients of the model are well-established empirical laws allows the theoretician great epistemological confidence in interpreting the results of the model. Thus, subtle and surprising findings such as Bull and Charnov's equilibrium paths and the 'drift-induced selection' discovered in Chapter 6 can be trusted as real phenomena, with no suspicion that they are instead spurious consequences of *ad hoc* modelling

decisions. Such confidence would usually be unwarranted in, say, ecological and economic modelling. (A social corollary is that, because ten theorists in a room would often all write down the same model of a given problem in evolutionary genetics, there is consequently less disagreement about theoretical results than there is in other fields.)

I have found it exhilarating to explore some of the consequences of selection and Mendelian genetics in the papers that form this dissertation. The dissertation is organized as follows. Chapter 1 uses a simple model to hypothesize that the long, synchronous flowering intervals of bamboos (e.g., 120 years for *Phyllostachys bambusoides*) evolved by successive discrete multiplication from shorter ancestral intervals. A prediction of the hypothesis is that observed flowering intervals should factorize into small prime numbers. Support for this prediction is found in a historical data set of bamboo flowering observations. Chapter 2 develops a mathematical method for studying the interaction of multiple populations in evolutionary games, when the mutation rates to new strategies are small. Chapter 3 applies this methodology to species interactions, asking when it is better for a species to evolve quickly, and whether it can ever be better to evolve slowly. Faster evolution by any means (higher mutation rate, shorter generation time, and more efficient selection) is shown to be favored in antagonistic interactions—a 'Red Queen' effect. Slower evolution is shown to be favored in an important class of mutualisms. This 'Red King' effect operates predominantly via less efficient selection, rather than lower mutation rates or longer generation times. Chapter 4 uses a stochastic model of evolutionary games to show that assortment favors the evolution of cooperation under very general conditions, including when Hamilton's rule fails to predict the direction of selection on the cooperative trait. Chapter 5 uses a simple model and economic intuition to

show that the Trivers-Willard hypothesis of sex allocation—mothers in good condition should (i) have more sons and (ii) care more for sons—holds more generally in case (i) than in case (ii). Chapter 6 identifies and mathematically characterizes a novel selective force, induced by genetic drift, operating in transitions between the sex-determining systems of male and female heterogamety. This 'drift-induced selection' favors epistatically dominant sex determining mutations, possibly explaining their observed preponderance in heterogametic systems. Chapter 7 proposes a new genetic model to explain the rarity of environmental sex determination (ESD) relative to genetic sex determination (GSD). In a species with ESD, an allele that biases development towards one sex (e.g., by shifting temperature thresholds) can couple with a 'sexually antagonistic' allele that increases fitness in that sex but reduces fitness in the other. The invasion of this haplotype selects for its subsequent expansion and strengthening, together with the elimination of recombination along its length, leading eventually to a new sex chromosome and thus GSD. Chapter 8 proposes a new metric for genome-wide recombination, $\bar{r}$, that takes into account the positions of crossovers (since terminal crossovers cause less recombination than central crossovers) as well as the contribution of independent assortment of homologous chromosomes (Mendel's second law). $\bar{r}$ is increased by crossover interference, suggesting a possible adaptive advantage for this classical but mysterious phenomenon. Measuring $\bar{r}$ in humans reveals that genetic shuffling is nearly maximal, and that this is due largely to independent assortment, which contributes about 30 times more shuffling than crossovers do. Chapter 9 documents a new form of crossover patterning, conserved across eukaryotes: the number of crossovers covaries positively across the chromosomes within individual meiotic nuclei. This effect results from a similar covariation of chromosome axis lengths at meiotic prophase, and causes an

increase in the frequencies of gametes with either many or few crossovers. This can be advantageous in a sporadically fluctuating environment, because high-crossover gametes are useful when the environment changes, while low-crossover gametes are useful in periods of stasis between environmental changes.

1

Extended flowering intervals of bamboos evolved by discrete multiplication

1.1 Abstract

Numerous bamboo species collectively flower and seed at dramatically extended, regular intervals—some as long as 120 years. These collective seed releases, termed 'masts', are thought to be a strategy to overwhelm seed predators or to maximize pollination rates. But why are the intervals so long, and how did they evolve? We

propose a simple mathematical model that supports their evolution as a two-step process: First, an initial phase in which a mostly annually-flowering population synchronizes onto a small multi-year interval. Second, a phase of successive small multiplications of the initial synchronization interval, resulting in the extraordinary intervals seen today. A prediction of the hypothesis is that mast intervals observed today should factorize into small prime numbers. Using a historical data set of bamboo flowering observations, we find strong evidence in favour of this prediction. Our hypothesis provides a first concrete theoretical explanation for the mechanism underlying this remarkable phenomenon.

1.2 Introduction

Understanding the basis of species' phenology—the timing of life history events such as plant flowering and bird migration—is a key area of ecological and evolutionary research [552]. Easily one of the most captivating phenomena in this regard is the extended synchronous flowering and fruiting intervals exhibited by woody bamboos [196, 250]. Although numerous woody bamboo species flower and fruit at more modest time intervals, there are numerous extraordinary examples of bamboos with greatly extended intervals (Fig. 1.2.1). For example, the Asian bamboos *Bambusa bambos*, *Phyllostachys nigra f. henonis*, and *P. bambusoides* flower every 32, 60, and 120 years, respectively [84, 250, 268, 402, 463, 473, 474]. Historical records of this phenomenon for the latter two species date back as far as 813 C.E. and 999 C.E., respectively [268]. In each of these cases, individuals of a species collectively flower and fruit in enormous quantities (referred to as 'masting') only to die back, leaving behind seeds which subsequently germinate. The cycle then repeats itself. In some documented cases, this synchrony is maintained even after plants are transplanted

far from their native ranges [36, 84, 377, 473].

Though other plant species exhibit an ability to mast—most notably Dipterocarpaceae in Southeast Asia [12, 249]—none is known to exhibit either the regularity or the extraordinary interval length of the mast cycles observed in bamboos. Despite its broad interest to biologists, however, the evolution of these prolonged regular flowering intervals has received surprisingly little theoretical investigation.

The leading explanation for masting in bamboos is attributed to Janzen [249, 250], who proposed that the enormous number of propagules (fruits or seeds) released during these episodes satiate local predator populations, ensuring that more seeds survive than with sporadic, and thus less abundant, propagule release [273, 274]. In the case of bamboos, these predators typically include rats, birds, and pigs [250]. The stabilizing selection underlying the predator-satiation hypothesis requires that a plant releasing its propagules out of synchrony with its cohort will likely have them all consumed by predators. Support for this comes from measurements of seed predation rates during and outside of masting episodes, including for bamboos [284] and other masting species [106, 113, 391, 583].

A second explanation for bamboo masting is that, in wind-pollinated plants like bamboos, synchronous pollen production may increase outcross pollination rates, providing a benefit to individuals who seed during a mast episode [391, 393, 488]. Evidence for this hypothesis comes from the higher fertilization rates typically observed during mast episodes in wind-pollinated plants, including beech [391], rimu [393], and oak [289].

A third explanation, the so-called fire cycle hypothesis [270], argues that the large seed release during a mast can act as fuel for wildfires (sparked by lightning, for example). Under this scenario, bamboo seeds are hypothesized to be resilient

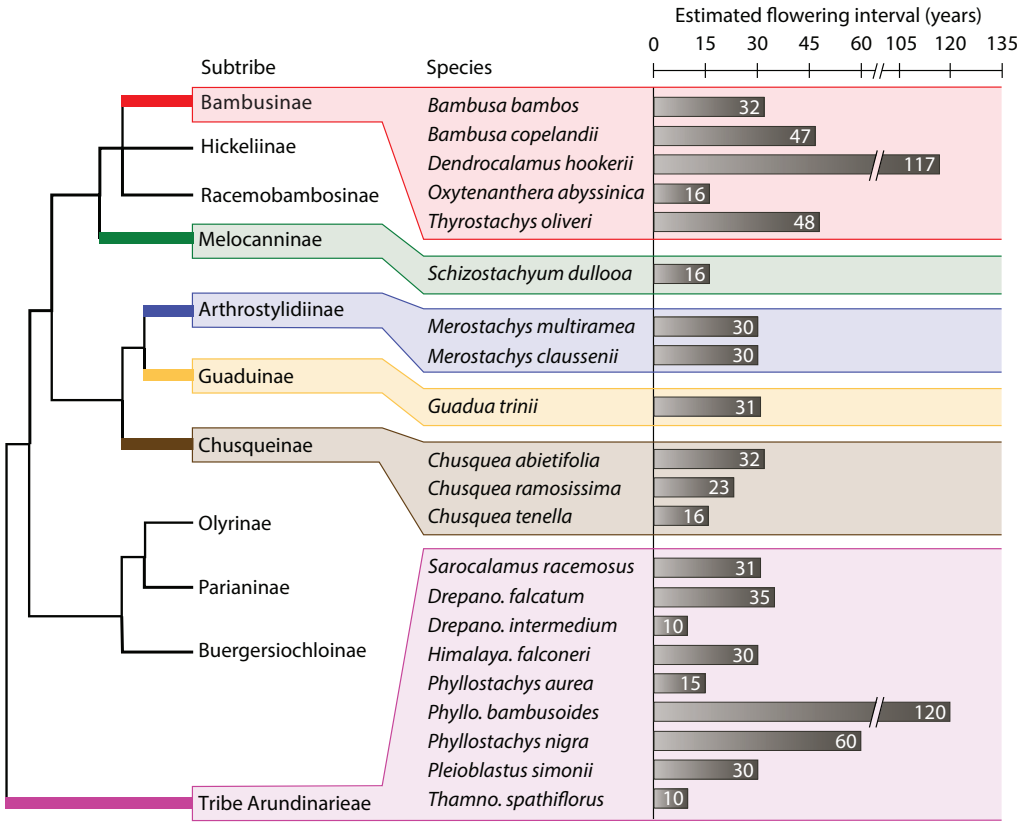

Figure 1.2.1: Long-intervalled flowering in bamboos. A recent phylogeny of the bamboos as inferred by Kelchner et al. [271]. Twenty-one species with long-intervalled flowering are displayed across their associated bamboo tribes and subtribes. These are species whose flowering intervals can be estimated from the data summarized by Janzen [250] (see [544, Appendix S2] for details of interval estimation). Species names have been updated to reflect current taxonomy.

to fire, while competing vegetation is not. However, most masting bamboo species live in humid, tropical forests, where wildfires are unlikely to have been a factor in their long-term evolution [451]. Moreover, it is difficult to see how the stabilizing selection required for continued synchrony could be maintained without wildfires recurring frequently and predictably. The predator-satiation and wind-pollination hypotheses, on the other hand, clearly involve perpetual stabilizing selection.

While these theories of stabilizing selection provide explanations for the existence of synchronous seeding in bamboos, a more intriguing puzzle remains: what explains the remarkable regularity and length of bamboo mast cycles? Here, we propose and test a novel mathematical model of the evolution of bamboo masting to solve this puzzle. The puzzle is twofold. First, how was synchrony achieved on the shorter, regular multi-year intervals that have been hypothesized to be ancestral in bamboos [250]? Second, given the strong stabilizing selection for maintaining a regular interval, how did the shorter ancestral intervals lengthen to the extraordinary intervals seen today?

In the mathematical models we develop to answer these questions, we shall primarily make use of the language of the predator satiation hypothesis, simply because it is the best known and most widely accepted explanation for masting in bamboos. The models do not depend on the veracity of the predator satiation hypothesis, however, only on the existence of stabilizing selection. In general, they can be written in the language of any of the theories of stabilizing selection proposed for bamboo masting, including the commonly-invoked wind-pollination hypothesis.

1.3 Model of initial synchronization

We first hypothesized that initial synchronization on a multi-year interval could occur naturally in a population of annual flowerers when two conditions are met. First, plants that wait longer to flower may accumulate greater energy resources to invest in producing more seeds, and/or seeds that are better protected [151]. (The latter scenario, involving better-protected seeds, seems less applicable to bamboos, whose ancestral fruit type is a caryopsis, i.e., fruits with seeds that are generally less well protected than those of many other flowering plants.) In bamboos, this investment might, for example, take the form of increased shoot production between masts. Second, total potential seed predation varies from year to year, but is typically high, amounting to a significant proportion of maximum possible seed release. Evidence for this assertion comes from observations of enormous predation rates in minor mast years among well studied woody tree species [106, 113, 391, 583].

These conditions can be incorporated into a simple mathematical model (Fig. 1.3.1; full mathematical details in [544, Appendix S1]). Here, we assume a fixed environmental carrying capacity, and begin with a population comprising mostly plants that seed annually, but with some variation in seeding time, so that a small number of plants seed every two years. These two-year plants may be distributed across odd and even years in this two year cycle, forming two reproductively distinct 'cohorts'. Under a broad class of parameterizations, a common outcome of our model is synchronization onto a single cohort of two-year plants, following a year where all annual plants and one cohort of two-year plants are eliminated because their entire seed set is lost to predation (see Fig. 1.3.1 for additional details of the population dynamics involved). Importantly, our model is not restricted to synchronization onto only a two-year cycle: longer intervals of synchronization are possible in a sim-

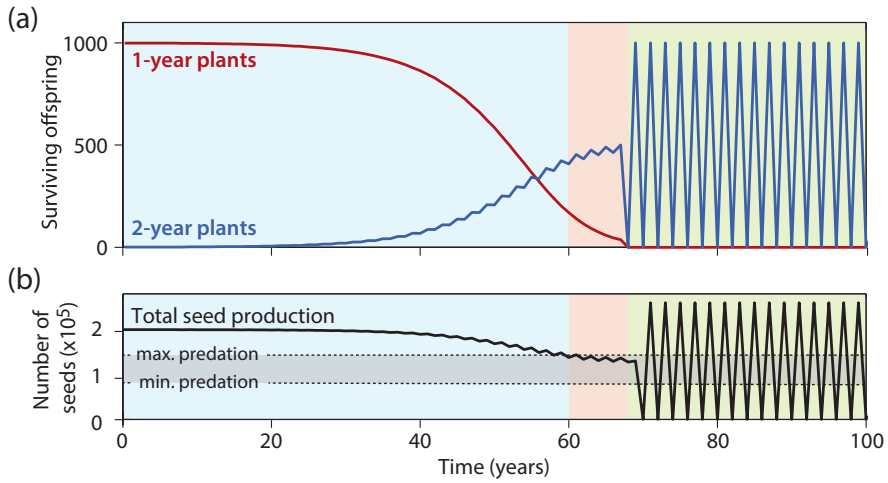

Figure 1.3.1: A model of initial synchronization in bamboos. Blue phase: Initially, the population comprises mostly annual-flowering bamboos, with a small number flowering every two years (symmetric across odd and even years). Owing to their higher individual seed release, the two-year plants increase in numbers over time (a). Total annual seed release declines, as the population's seeding becomes increasingly diluted over the odd and even years of the two-year cohorts (b). Red phase: When total annual seed release declines below maximum potential predation (b), the population is at risk of having an annual seed release completely consumed by predators. When this eventually occurs, all of the annual plants, together with the two-year cohort seeding that year, are eliminated (a). Green phase: If predation is not unusually high the following year, the seed release of the remaining two-year cohort will fill the environmental carrying capacity, establishing synchrony onto that cohort's two year cycle.

ilar model if we extend the variation in the initial population to include plants with longer flowering intervals, including three, four, and five years (Fig. 1.3.2). Also, by altering the parameters of the model, we can hasten or lengthen the transition to a multi-year mast cycle, so that the transition times in Figs. 2 and 3 should not be seen as characteristic of the model (see [544, Appendix S1]).

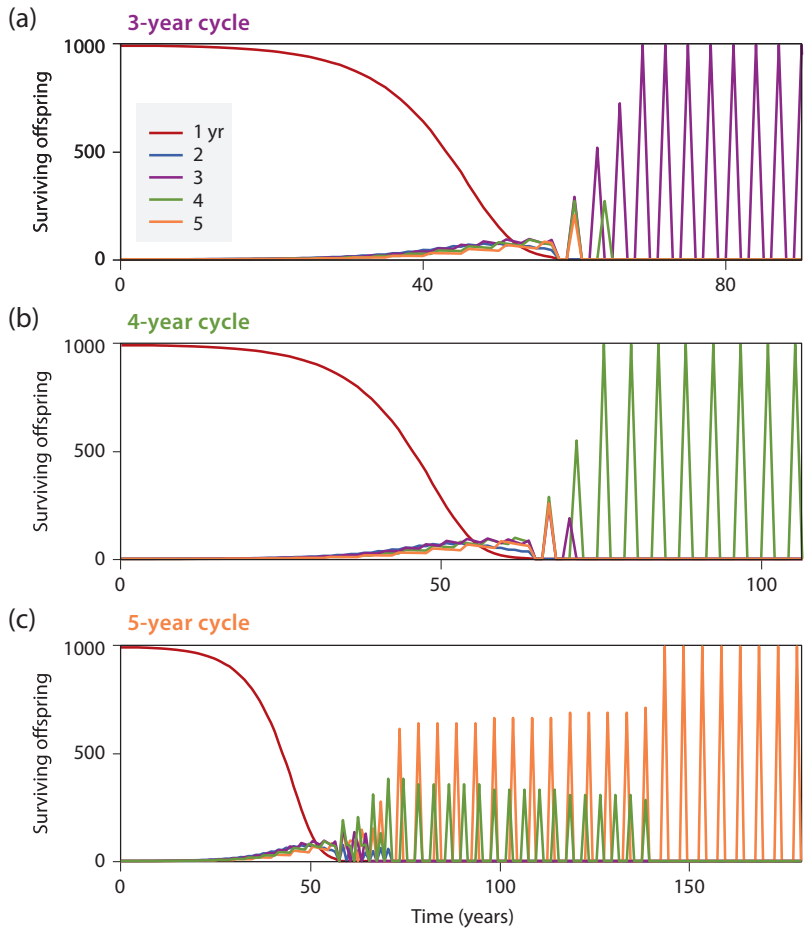

Figure 1.3.2: Initial evolution of mast intervals longer than two years. Our model of initial synchronization can also explain the initial evolution of mast intervals longer than two years, if sufficient variation exists in the original (mostly annual-flowering) population. Because of the stochastic nature of the model, the same original setup can result in the evolution of a three year (a), four year (b), or five year (c) mast cycle.

1.4 Model of interval growth by multiplication

Once synchronization has been established in a population, say, on a three year mast interval, stabilizing selection should maintain synchrony. This is because plants flowering out of sync—e.g., after two or four years—would release its seeds alone, and thus consumed by predators. Given such strong selection for synchrony, how then could flowering intervals have increased to the extraordinary lengths observed today? Janzen [250] noted that a plant flowering at an interval twice that of its population—at six years, in the case of a three year population mast cycle—would always flower during a masting year (i.e., every second mast), and thus be buffered against predation. Indeed, this holds for a mutant flowering at any multiple of the initial population mast interval, not just double. And since plants waiting longer to flower release more propagules, such mutants would likely be favoured during times of low population growth, when delaying seeding would not represent a significant 'missed opportunity'.

For example, suppose a mutant with a flowering interval twice that of its population releases $s\%$ more seeds than the average single-interval plant (or, equivalently, seeds that are better protected, and thus suffer $s\%$ less predation). Suppose too that average population growth is $g\%$ per period. Then a simple population growth model predicts that selection will favour the mutant if $s > g$. Over two population masts, an average population member will yield $(1 + g)^2$ descendants, while the mutant will yield $(1 + g)(1 + s)$ descendants; the latter is larger than the former when $s > g$. This is likely to hold especially when population growth, g, is low (and owing to the nature of exponential growth, g cannot be large for too extended a period of time). Analogous conditions for mutants of higher-multiple intervals can also be derived. In general, if the population growth rate is $g\%$, a mutant that

flowers only every n mast periods and releases $s_n\%$ more seeds than the average population member will face positive selection if $1 + s_n > (1 + g)^{n-1}$. For small integers n, this is likely to hold for reasonable long-term values of g. So when population growth is low, multiple-interval mutants can emerge, be selected for, and fix. Under this scenario, the population's flowering period increases to a multiple of its initial synchronization interval.

The converse, however, is not true: if a population's growth rate increases, mutants with intervals a fraction—say half—of the cohort's would not survive, because they would seed out of synch with the population every second period of their reduced interval. So, earlier initial flowering intervals are not recoverable, and thus the population's flowering interval can only increase in our multiplicative model. The evolution of extended flowering intervals in bamboos may therefore represent an instance of Dollo's law, or irreversibility in evolution [124].

The rival hypothesis for the evolution of very long mast intervals is one of gradual growth. Because mast episodes are not instantaneous, instead lasting from a few weeks to even a few years in the case of species with very long mast intervals, such as *Phyllostachys bambusoides* [250], seed release is in fact distributed across a mast episode. If plants that release their seeds later in the episode are selectively favoured, then selection over time would gradually shift the distribution in the direction of longer intervals. However, both theory and empirical evidence suggest that plants releasing their seeds later in mast episodes would in fact be selected against. Since mast episodes tend to result in a surge in local seed predator populations, either through migration or rapid reproductive growth, predation pressure is expected to increase as a mast episode progresses. Seeds released late in a mast are thus expected to suffer the highest predation rates, and yield fewer successful offspring [250]. This

is borne out in studies that observe predation rates across entire mast episodes, both for bamboos [192, 284] and for Dipterocarpaceae [113, 114].

On the other hand, seeds released early in a mast episode do not enjoy the safety in numbers that seeds released during the mast's peak do. Despite predator levels initially being low, therefore, these early seeds are very vulnerable to predation by the predators that are present. Thus, while the above argument against gradual interval growth suggests that gradual interval reduction is a possibility, we do not expect such reductions to significantly affect mast interval lengths.

It has been claimed that the very long mast intervals observed in, for example, *Phyllostachys bambusoides* (120 years) and *P. nigra f. henonis* (60 years) constitute evidence against the predator satiation hypothesis [270]. The arguments given for this would similarly pit these observations against other theories of stabilizing selection in bamboos, such as the wind-pollination hypothesis. In the case of predator satiation, it has been assumed that integral to the hypothesis is that long mast intervals have evolved to starve seed predators between masts, ensuring that predator numbers are low when a mast eventually occurs [250, 273, 274]. But since the longest known mast intervals greatly exceed the lifespans of typical seed predators, the predator satiation hypothesis cannot alone explain why selection favoured increases of mast intervals to the extremes observed today [270]. In our theory of interval growth by successive multiplication, we have reconciled the predator satiation hypothesis (and, indeed, any theory of stabilizing selection) with the existence of extreme mast interval lengths. Though the key selective factor in longer intervals is greater seed release, rather than predation (or any other stabilizing factor), that these longer intervals must be discrete multiples of their preceding intervals is a direct result of the heavy predation faced by plants releasing their seeds in isolation

(or, again, any perpetual stabilizing force that maintains synchrony).

1.5 Statistical testing

The logic underlying this mechanism of interval growth yields a simple, testable numerical prediction. If the extraordinary flowering intervals observed today are the result of successive multiplications of the initial synchronization interval, then they should be decomposable back into those multiples (and the initial interval). Though the theory is consistent with multiples of any size if population growth is sufficiently low, and though the mechanics of the genetic clock in bamboos are poorly understood [384], small multiples seem more likely than larger ones. The physiological and underlying genetic adjustments necessary for much larger single interval multiplications would likely render such multiplications implausible. Thus, we hypothesize that the extended mast intervals of bamboos should factorize into small positive integers, so that their unique prime factorization should include only small prime numbers.

Do the data support this hypothesis? An initial survey of the most well-studied examples is promising (Fig. 1): *Phyllostachys bambusoides* (120 yrs = 5 yr initial synchronization interval $\times$ 3 $\times$ 2 $\times$ 2 $\times$ 2), *P. nigra f. henonis* (60 yrs = 5 yr initial synchronization interval $\times$ 3 $\times$ 2 $\times$ 2), and *Bambusa bambos* (32 yrs = 2 yr initial synchronization interval $\times$ 2 $\times$ 2 $\times$ 2 $\times$ 2) [84, 250, 268, 402, 463, 473, 474]. These examples support our hypothesis on several fronts. First, all of these intervals are factorizable into small primes (5 or smaller). Second, the smallest primes appear most often in each factorization, consistent with smaller prime multiples being more likely. Third, the 120 year mast interval of *P. bambusoides* is a small multiple of the 60 year interval of the closely related *P. nigra f. henonis*, suggesting a common

ancestral interval from which the two have evolved.

Other bamboo species with extended intervals are less well studied. For these species, a number of factors are likely to increase measurement error in estimates of mast intervals [250]. These include geographic variation in observations of masting, observations gathered at different stages of consecutive masting episodes (many of which can last more than one year), and misidentification of species, as well as natural variation around mean flowering intervals within species [165]. A more detailed discussion of the factors that contribute to mast interval measurement error is included in [544, Appendix S2].

Nonetheless, a broader inspection of the estimated mast intervals of these less well-studied species, together with their phylogenetic placement, corroborates our hypothesis. In the two monophyletic genera in our data that exhibit variation in mast intervals across more than two species, *Phyllostachys* and *Chusquea*, these mast intervals demonstrate evidence of having arisen through a multiplicative process (Fig. 1.5.1). The three *Phyllostachys* species in our data share a common base interval of 15 years (15 yrs, 60, 120), which under our hypothesis would itself have arisen from a shorter (3 or 5 yr) initial synchronization interval. Allowing for measurement error, the three *Chusquea* species appear to share a base interval of 8 years (16 yrs, 23, 32). Similar patterns of multiples in bamboo flowering intervals have previously been noted as anomalous [202]—this anomaly is resolved as a natural consequence of our multiplication model.

To test our hypothesis more formally, we developed a simple, robust nonparametric test to determine if estimated mast intervals (Fig. 1.2.1) are more tightly clustered around numbers factorizable into small primes ('NFSP', here defined as primes 5 or smaller) than would be expected by chance under an appropriate null

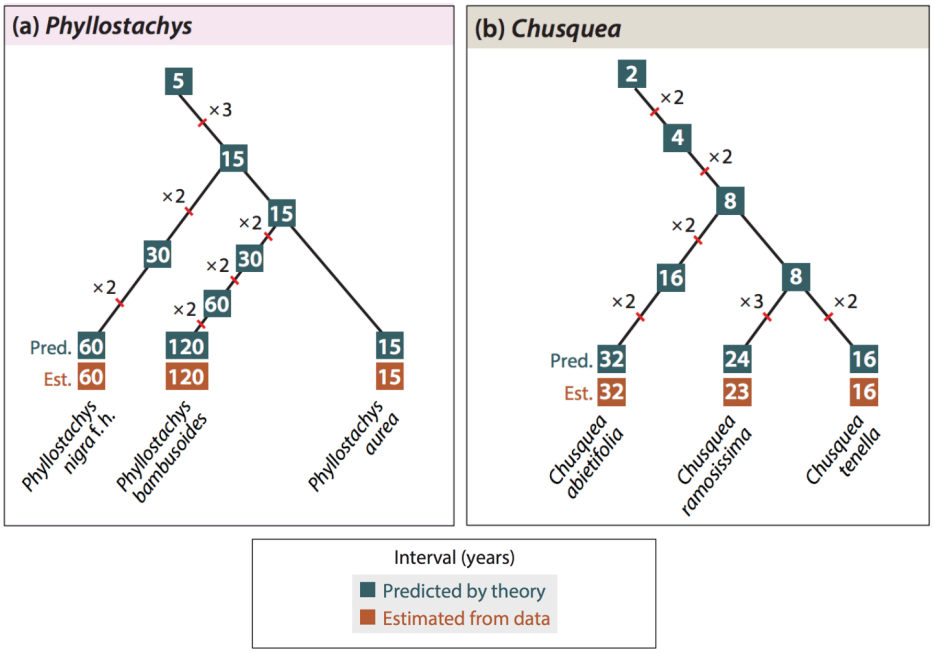

Figure 1.5.1: Mast intervals within bamboo subclades appear to have arisen from a multiplication process. Two hypothesized patterns of small multiplications of intervals along phylogenies [153, 523] of *Phyllostachys* (a) and *Chusquea* (b), the two genera in our data set for which flowering intervals can be estimated for more than two species. The mast intervals of these species are consistent with the multiplication model we propose, allowing for small measurement error in the case of *C. ramosissima* (estimated interval 23 yrs vs. predicted interval 24 yrs). Hypothesized intervals, ancestral and extant, are displayed in boxes; measured intervals from our data set are displayed on the bottom lines.

hypothesis. Here, our null hypothesis is that extended mast intervals evolved gradually (instead of via the discrete multiplications we have hypothesized), resulting in a smooth, continuous distribution of interval lengths (see [544, Appendix S3] for details of the estimation of the null distribution). Compared to samples generated from this null distribution, the measured flowering intervals were significantly closer to NFSP ($p = 0.0041$) and contained significantly more NFSP ($p = 0.0024$). These results strongly support the small primes hypothesis. Moreover, they are robust to changes in the construction of the null distribution, and alternative definitions of NFSP (see [544, Appendix S3]).

1.6 Discussion

To our knowledge, our study is the first to develop a mathematical theory of the mechanism underlying extended mast intervals in bamboos. In our model, an initial phase of synchronization onto a small interval is followed by successive multiplication of the interval by small numbers. Three key assumptions underlie our multiplication model: i.) strong stabilizing selection that maintains interval synchrony, ii.) that later seed release allows for greater seed release (and/or for better protected seeds), and iii.) approximately regular, endogenously-timed mast intervals. These assumptions may explain why other masting plant species, such as members of the Dipterocarpaceae clade, do not exhibit such greatly extended intervals as the bamboos do. In particular, while assumptions i.) and ii.) above are likely to apply to many masting plants, assumption iii.), which is likely under genetic regulation, appears to be unique to bamboos. This assumption, which is crucial to the survival of multiple-interval mutants in our model, may thus be the key distinction that has allowed bamboos to achieve such dramatically extended flowering intervals.

The only other organisms that are well known to exhibit long-intervalled synchrony are the periodical cicadas (genus *Magicicada*), whose synchronized emergence from an underground larval state on 13- and 17-year intervals has similarly been attributed to predator satiation [56, 329, 330]. Evolutionary explanations have been proposed for their large-prime lifecycles [191, 345, 589], which clearly cannot be factorized into small primes, and thus stand in contrast to our hypothesis for the evolution of long-intervalled masting in bamboos. This suggests distinct evolutionary and genetic mechanisms underlying the periodical lifecycle of cicadas in comparison to long-intervalled masting in bamboos. For example, a leading explanation for the large-prime lifecycles of the periodical cicadas is that they minimize the possible frequency of subharmonic resonances with the multi-year lifecycle of a predator or parasite [580]. This evolutionary mechanism appears not to apply to masting bamboos, since the major predators of their seeds are typically either fast-breeding (e.g., rats) or migratory (e.g., fowl and pigs).

In conclusion, our multiplicative model provides the first theoretical explanation of long-intervalled masting in bamboos, and offers a framework upon which comparative analyses can be devised to explore the genetic and developmental basis of this striking biological phenomenon.

2

Finite-population evolution with rare mutations in asymmetric games

2.1 Abstract

We model evolution according to an asymmetric game as occurring in multiple finite populations, one for each role in the game, and study the effect of subjecting individuals to stochastic strategy mutations. We show that, when these mutations occur sufficiently infrequently, the dynamics over all population states simplify to an

ergodic Markov chain over just the pure population states (where each population is monomorphic). This makes calculation of the stationary distribution computationally feasible. The transition probabilities of this embedded Markov chain involve fixation probabilities of mutants in single populations. The asymmetry of the underlying game leads to fixation probabilities that are derived from frequency-independent selection, in contrast to the analogous single-population symmetric-game case [170]. This frequency independence is useful in that it allows us to employ results from the population genetics literature to calculate the stationary distribution of the evolutionary process, giving sharper, and sometimes even analytic, results. We demonstrate the utility of this approach by applying it to a battle-of-the-sexes game, a Crawford-Sobel signalling game, and the beer-quiche game of Cho and Kreps [87].

2.2 Introduction

In evolutionary game theory, games are played within populations, and the prevalence of different strategies changes over time according to natural-selection-like dynamics [238, 349, 396, 454, 457, 566]. This provides a natural method by which to model biological evolution [349] and various learning processes [172], and offers a 'rationality-light' approach to equilibrium selection [454].

In the classical approach, populations are infinitely large and dynamics are deterministic; the focus is typically on the equilibrium refinement of evolutionary stability [238, 349]. More recently, stochastic finite-population dynamics have been introduced into evolutionary game theory [160, 170, 263, 352, 396, 591]. These often take the form of an ergodic Markov chain—for example, when there is a positive mutation rate—the state space of which is all possible strategy compositions of the population [170]. Ranking the various population states' weights in the stationary

distribution is then a natural method of equilibrium selection [160, 263], and solves many problems of the deterministic approach.

A drawback is that the state space is often very large, making calculation of the stationary distribution infeasible. Addressing this, Fudenberg and Imhof [170] study the case of a symmetric game played within a single, finite population, and show that, when the mutation rate is very small, the evolutionary process simplifies significantly. The intuition is straightforward: Starting from a pure (monomorphic) population state, we wait a very long time for a new strategy to appear in the population, because the mutation rate is small. When it does, it either goes extinct or takes over the population ('fixes'). Because this resolution of the mutant's fate occurs on a much shorter timescale than the waiting time for another mutation to occur, it typically re-establishes a pure state. The process therefore approximates a simpler process over just the pure states. This dramatic reduction of the state space makes calculation of the stationary distribution computationally simple.

The transition probabilities of this simpler process depend critically on the various mutants' fixation probabilities—the probability that a given strategy, having arisen in a population otherwise pure for a different strategy, subsequently fixes in that population. Because the game is symmetric, the payoffs that determine these fixation probabilities are frequency dependent—the payoff to a mutant strategy changes as its frequency in the population increases. For most evolutionary processes, frequency-dependent fixation probabilities either do not exist in closed form, or are intractable when they do [396]. This significantly limits the analytical use of Fudenberg and Imhof's result.

Here, we employ the basic machinery of Fudenberg and Imhof [170] to derive a result similar to theirs for asymmetric games. There are several reasons why such a

result is desirable. First, many situations in which we might want to study evolutionary or learning dynamics are best modelled as asymmetric games—for example, signalling games [105, 198, 494], games of entry and entry-deterrence [350, 369, 453], and games of time consistency and commitment [301]. Second, because only strict Nash equilibria of asymmetric games are evolutionarily stable [455], the deterministic approach based on evolutionary stability often fails. This is especially true for multi-stage asymmetric games, which typically have no strict Nash equilibria (because alternative strategies that induce the same path of play, prescribing the same actions on that path but different actions off it, are payoff equivalent).

In our model, evolution occurs in multiple interacting populations, one for each role in the underlying asymmetric game. When the mutation rate is very small, the evolutionary process simplifies to one over just the pure states (each population is monomorphic). Transition probabilities between pure states in this embedded process again depend on the fixation probabilities of single mutants, but these turn out to be much simpler than in the symmetric game case of Fudenberg and Imhof. To see this, suppose we start in a pure state. A mutant eventually arises in one of the populations, and either goes extinct or fixes in that population before another mutant arises in any of the populations. The other populations are therefore monomorphic for the duration of the mutant's extinction or fixation. But because the game is asymmetric, payoffs to different strategies in one population depend only on the states of the other populations, and so the payoffs that determine the fixation probability of the mutant (and therefore the transition probabilities in the embedded evolutionary process) are *frequency independent*. Frequency-independent selection is a standard assumption in the population genetics literature [111, 143], and closed-form fixation probabilities (exact and approximate) exist for many evo-

lutionary processes of interest. Using our result, we can employ these to derive sharper, and sometimes even analytical, characterizations of long run evolutionary behaviour in many asymmetric games of interest. This allows for powerful evolutionary equilibrium selection in these games.

We illustrate the utility of our result with three examples. First, in a 'battle of the sexes' game, we show that a closed-form characterization of the stationary distribution is possible. Second, we consider a discrete Crawford-Sobel signalling game [105]. We show that, when multiple signalling equilibria of differing information content exist for a given misalignment of signaller and receiver interests, the most informative is evolutionarily dominant. This gives a more foundational support to Crawford and Sobel's heuristic argument in favour of the most informative signalling equilibria, which they base on Schelling's [461] concept of 'focal points'. Finally, we apply our methodology to the 'beer-quiche' game of Cho and Kreps [87], and show that, while it supports the Intuitive Criterion in its selection between the two Bayesian Nash equilibria of the game, non-equilibrium states are also evolutionarily significant, especially for small population sizes.

2.3 Evolution with mutations in multiple finite populations

Asymmetric games are characterized by the existence of multiple 'roles' ('Player 1', 'Player 2', etc.). In the evolutionary approach, the simplest way to incorporate multiple roles is to model evolution as occurring in multiple interacting populations [26, 156, 236–238, 349, 406, 591].[1]

Suppose that we have an underlying game Γ with roles $i = 1, \ldots, I$, each role associated with a finite strategy set S_i, and the payoff to a player in role i when

[1] In Section 2.6, we discuss how our results relate to the alternative modelling choice of a single population, in which each generation, each member draws a role from some distribution.

play is $\langle s_1, \ldots, s_I \rangle \in \prod_{i=1}^{I} S_i$ given by $\pi_i(s_1, \ldots, s_I) \in \mathbb{R}$.

We assume the existence of I populations, one for each role, with the size of each population i constant through time at $N_i \in \mathbb{N}$. The overall population state at a given time is defined as the I-tuple of strategy frequencies in the respective populations at that time: $p^t \in \prod_{i=1}^{I} \Delta^{|S_i|}$, where Δ^n is the unit simplex in $\mathbb{R}^n$.[2] We shall be interested in the evolution of this population state over time.

Evolution proceeds as a stochastic process in discrete time. Each generation, each member of each population receives the expected value of interacting, according to Γ, with a group comprising one member from each other population, randomly chosen, and with each group equally likely. (The use of expected payoffs, rather than true payoffs received from single random interactions, is for the sake of tractability.) If $p_j^t(s_j^k)$ denotes the proportion of members of population j that are playing strategy $s_j^k \in S_j$ at time t, then, for example, the expected payoff to a member of population 1 who employs strategy $s_1^1 \in S_1$ in period t is

$$\mathbb{E}\pi_1(s_1^1|p^t) = \mathbb{E}\pi_1(s_1^1|p_{-1}^t) = \sum_{k_2=1}^{|S_2|} \cdots \sum_{k_I=1}^{|S_I|} p_2^t(s_2^{k_2}) \ldots p_I^t(s_I^{k_I}) \pi_1(s_1^1, s_2^{k_2}, \ldots, s_I^{k_I}).$$

Here, p_{-1}^t denotes the population states in all populations other than population 1, and signifies that the expected payoff to a strategy in population 1 depends only on the strategy frequencies in the other populations $2, \ldots, I$, a consequence of the asymmetry of the underlying game.

These expected payoffs in each population i are then translated to non-negative *fitnesses* $f_i(s_i^k|p_{-i})$ according to some positive monotonic transformation (possibly different for each population).[3] In the case of no mutations, the fitnesses within each

[2] Since the populations are finite, p^t is in fact confined to a finite subset of this space.

[3] Popular choices in the evolutionary game theory literature include linear fitness, $f_i(\mathbb{E}\pi_i) =$

population can be used to update that population to its next-period state according to an evolutionary or imitation dynamic, usually following the general Darwinian, or 'monotonicity', principle that strategies with high fitness increase in proportion relative to those with low fitness.

Some notation: let $\mathcal{P}_i$ denote the (finite) set of all possible population states for population i, let $\mathcal{P} = \prod_{i=1}^{I} \mathcal{P}_i$ denote the set of all possible overall population states, and let $\mathcal{P}_{-i}$ denote the set of all possible population states for populations other than i. The set of 'pure' states for population i, $\mathcal{P}_i^{\text{pure}}$, comprises all states in $\mathcal{P}_i$ where every member of population i is playing the same strategy (in which case we say that population i is 'monomorphic'). Abusing notation a little, we label such states by the strategy that all members are playing, i.e., $\mathcal{P}_i^{\text{pure}} = S_i$. Finally, the set of overall pure states, $\mathcal{P}^{\text{pure}} = \prod_{i=1}^{I} \mathcal{P}_i^{\text{pure}}$, is the set of overall population states in which every population is pure.

The evolutionary process with no mutations in each population i is a stochastic process $\{X_i^0(t), t = 0, 1, \ldots\}$, with state space $\mathcal{P}_i$, and transition probabilities $T_i^0(p_i, p_i'|p_{-i})$ for $p = \langle p_i, p_{-i} \rangle \in \mathcal{P}, p_i' \in \mathcal{P}_i$. The transition probabilities depend on the population state p_{-i} because this determines fitnesses within population i.

For each population i, we require two basic assumptions of this no-mutation evolutionary process defined by $T_i^0(p_i, p_i'|p_{-i})$:

Assumption 1. If in some period a strategy in population i is absent, then it is absent in all future periods. Formally, for all $\langle p_i, p_{-i} \rangle \in \mathcal{P}$, $p_i' \in \mathcal{P}_i$, and $s_i \in S_i$, if $p_i(s_i) = 0$ and $T(p_i, p_i'|p_{-i}) > 0$, then $p_i'(s_i) = 0$.

$1 + \eta_i \mathbb{E}\pi_i$, and exponential fitness, $f_i(\mathbb{E}\pi_i) = \exp(\eta_i \mathbb{E}\pi_i)$; in each case, the parameter $\eta_i > 0$ mediates the strength of selection, i.e., the sensitivity of fitness to changes in expected payoff.

Assumption 2. No matter the population state of other populations, any strategy currently played in i, unless it is played by all members of i, has positive probability of having increased representation next period. For any $\langle p_i, p_{-i} \rangle \in \mathcal{P}$, and for each $s_i \in S_i$ such that $0 < p_i(s_i) < 1$, there exists $p_i' \in \mathcal{P}_i$ such that $p_i'(s_i) > p_i(s_i)$ and $T_i^0(p_i, p_i'|p_{-i}) > 0$.

Assumptions 1 and 2 are satisfied by many finite-population stochastic processes studied in evolutionary game theory and population genetics when there are no mutations, selection is finitely strong, and fitnesses are positive. These include stochastic models of imitation learning [172], the Moran process [375], and the Wright-Fisher process [154, 584]. Processes that are excluded include best-response dynamics and fictitious play [172].

Loosely, Assumption 1 ensures that the pure states for population i are absorbing. In a learning context, it distinguishes imitation learning from other learning processes: strategies not employed by anyone in a population cannot be imitated [31, 170, 458]. It is also a natural assumption in a biological context: without mutations, the creation of novel genes, and therefore novel strategies, is not possible.

Assumption 2 ensures that non-pure states in population i are transient. This we take to be the essence of stochastic dynamics. It is important to note that the 'positive probability' of Assumption 2 can be very small. It is not restrictive, for example, that unsuccessful strategies can spread in a population, since the probability that they do so can be appropriately small.

One context in which assumption 2 might appear, at first glance, to be too strong is that of imitation learning in multi-stage games, where some decision nodes are not reached given the strategies currently employed in the populations, so that 'play'

at these nodes cannot be directly observed.[4] This is a problem for assumption 2 only if a particular condition holds, which we consider to constitute a somewhat 'knife-edge' case: learning is by imitation based only on *direct observation* of play.

If imitation can also be based, even if only to a very small degree, on communication between agents in a population, then actions at currently-unobserved nodes could be discussed and imitated, and so assumption 2 would be valid. This we take to be far more realistic. It is implicit in Young's [591] assumption that 'each time an agent plays he starts afresh and must ask around to find out what is going on', and a similar logic underlies many models of social learning (e.g., [138]). Again, we should stress that *any* amount of such communication validates assumption 2; the condition under which it is invalid is therefore a knife-edge case.[5] Communication is especially relevant for situations where membership of the populations is not fixed through time, instead being affected by exits and entries (as modelled by birth-death processes, for example). In this case, if a decision node is currently unreached for a given population, then new entrants in that population must nonetheless have strategies that prescribe actions at the unreached nodes; in a pure imitation dynamics, they can only get these by 'asking around'.

We make the further assumption that the evolutionary processes occur independently within each population, in the sense that, although the probability that population i transitions from p_i to p_i' between periods t and $t+1$ depends on the period-t population states of the other populations, the transitions that these other populations make between periods t and $t+1$ do not influence the transition in

[4] We are grateful to a referee for emphasizing this point, and prompting the present discussion.

[5] It might be objected that changing one's strategy at an unreached decision node would not alter one's payoff, so that imitative strategy changes of this sort would not be expected, but this objection fails to take into account the fundamental stochasticity of the process: even detrimental strategy changes are expected to occur with some positive probability.

population i. This is similar to the assumption that expected, rather than realized, payoffs are relevant for fitnesses, in the sense that it too is an abstraction from the true, random, matching of players in a given period. Like the expected payoffs assumption, it is made for tractability.

Under this assumption, the no-mutation processes $\{T_i^0\}_{i=1}^I$ aggregate to an overall no-mutation Markov process T^0 over the state space $\mathcal{P}$, where for $p = \langle p_1, \ldots, p_I \rangle, p' = \langle p'_1, \ldots, p'_I \rangle \in \mathcal{P}$, $T^0(p, p') = \prod_{i=1}^I T_i^0(p_i, p'_i | p_{-i})$.

We now incorporate mutations into this general evolutionary process. We specify for each population i a mutation rate $\varepsilon\mu_i > 0$, with μ_i a population-specific parameter that governs the between-population relative frequency of mutations, and ε an across-population parameter governing the overall frequency of mutations. We then alter the above no-mutation evolutionary process as follows: From a population state p^t in period t, a *preliminary* (pre-mutation) population state $p_{(0)}^{t+1}$ for period $t+1$ is chosen according to the transition probabilities T^0, i.e., according to the no-mutation evolutionary process.

This preliminary population state is then subjected to random mutations of the following form: in each population i, each member has probability $\varepsilon\mu_i$ of discarding her strategy and randomly selecting another from the strategy space S_i, with each strategy (including the one she just discarded) equally likely.[6] This mutation process is carried out independently across the members of a population, and similarly across populations, resulting in the final population state for period $t+1$, p^{t+1}.

The evolutionary process with mutations can be summarized by the following

[6] We can easily allow for the possibility that not all mutations between strategies within a population are equally likely; this case is discussed in Section 2.6.

scheme:

$$p^t \quad \rightarrow \quad \text{selection (stochastic)} \quad \rightarrow \quad \text{mutation (stochastic)} \quad \rightarrow \quad p^{t+1}.$$

Within each population i, this is a stochastic process governed by the transition probabilities $T_i^{\varepsilon}(p_i, p_i'|p_{-i})$. These individual population processes aggregate to an overall Markov process over the state space $\mathcal{P}$, defined by the transition probabilities $T^{\varepsilon}(p, p') = \prod_{i=1}^{I} T_i^{\varepsilon}(p_i, p_i'|p_{-i})$ (because the independence of the within-population processes is not compromised by the mutations process we have defined).

Since $\mu_i > 0$ for each population i, there is positive probability that, from any given population state, any state can be reached in one generation (it just requires the appropriate mutations). Consequently, the evolutionary process $T^{\varepsilon}(p, p')$ with positive mutation rates μ_i is an ergodic Markov chain. It therefore has a unique stationary distribution, which it approaches in the long run.

In principle, this stationary distribution is analytically calculatable, but in reality, for many games of interest, the state space (all possible population states) will usually be so large that this calculation is infeasible. In general, the size of the state space is $|\mathcal{P}| = \prod_{i=1}^{I} \binom{N_i+|S_i|-1}{|S_i|-1}$. In the case of just two populations, each of size 20 members, and each with 4 strategies available to its members, the size of the state space is approximately 3×10^6: calculating the stationary distribution thus involves solving a system of about 3×10^6 linear equations. This problem intensifies as the population sizes increase.

In the next section, we employ a theorem of Fudenberg and Imhof [170] to show that, when the mutation rate is very small for each population ($\varepsilon \ll 1$), the stationary distribution of the evolutionary process with mutations approximates an embedded Markov process on a much-reduced state space, the set of all pure states $\mathcal{P}^{\text{pure}}$

(the size of which does not increase with increasing population size). Moreover, the asymmetry of the underlying game will render selection frequency-independent in the rare-mutations regime. This will make calculation of the transition probabilities of this embedded Markov chain much simpler than for symmetric games.

2.4 The stationary distribution when mutations are rare

Assumptions 1 and 2, which concern the within-population no-mutation evolutionary processes T_i^0, translate into the following two straightforward propositions, stated without proof, concerning the aggregate no-mutation process T^0:

Proposition 1. Under T^0, all pure population states $p \in \mathcal{P}^{\text{pure}}$ are absorbing.

Proposition 2. Under T^0, all population states $p \in \mathcal{P} \backslash \mathcal{P}^{\text{pure}}$ are transient.

Label pure population states by $s = \langle s_1, \ldots, s_I \rangle \in \mathcal{P}^{\text{pure}}$: here, all members of population i play strategy $s_i \in S_i$. Denote by s/s_i' the population state where every population $j \neq i$ is monomorphic for the strategy s_j, and population i is monomorphic for the strategy s_i except for one individual, who plays $s_i' \neq s_i$. Let the set of all such states be $\mathcal{P}^{\text{pure}/i}$.

Proposition 3. Fix $s \in \mathcal{P}^{\text{pure}}$, and consider the limit $\lim_{\varepsilon \to 0} \frac{T^\varepsilon(s,p)}{\varepsilon}$ for states $p \in \mathcal{P} \backslash \{s\}$. This limit exists for all states $p \in \mathcal{P} \backslash \{s\}$. However, $\lim_{\varepsilon \to 0} \frac{T^\varepsilon(s,p)}{\varepsilon} > 0$ if, and only if, $p \in \mathcal{P}^{\text{pure}/i}$ for some i. Otherwise, $\lim_{\varepsilon \to 0} \frac{T^\varepsilon(s,p)}{\varepsilon} = 0$.

To prove this, note that $T^\varepsilon(s,\, p)$ is a polynomial in ε for all p. For $T^\varepsilon(s,\, s/s_i')$, this polynomial has lowest-order term $\frac{N_i\mu_i}{|S_i|}\varepsilon$, and so $\lim_{\varepsilon\to 0}\frac{T^\varepsilon(s,\, s/s_i')}{\varepsilon} = \frac{N_i\mu_i}{|S_i|} > 0$. On the other hand, if the states s and p differ by the strategy played by more than one individual, then a one-step transition from the former to the latter requires more than one mutation, so $T^\varepsilon(s,\, p)$ has lowest-order term of order ε^k, $k \geq 2$. Thus, for such states p, $\lim_{\varepsilon\to 0}\frac{T^\varepsilon(s,p)}{\varepsilon} = 0$.

Proposition 3 states that mutations from a pure state to a state where only one individual in one of the populations deviates from the pure state are, for small mutation rates, at least an order of magnitude more likely than other transitions from the pure state (and, owing to the pure states being absorbing under the no-mutation process, mutations are the only way to transition out of pure states).

Now suppose that, from a pure state s, the system transitions to the state s/s_i'. Since interior states in population i are transient, absent further mutations in population i, the process will absorb either back into the pure state s (the mutant strategy s_i' has 'gone extinct') or into the pure state $\langle s_i', s_{-i}\rangle = \langle s_1, \ldots, s_{i-1}, s_i', s_{i+1}, \ldots, s_I\rangle$ (the mutant strategy s_i' has 'fixed').

But when the mutation rates are very small, we should expect this extinction or fixation of strategy s_i' to occur before another mutant appears in population i, and indeed before a mutant subsequently appears in any other population. This latter fact, that no mutant is expected to appear in any of the other populations during the extinction/fixation event in population i, is key in determining the probability that fixation of s_i' will occur in population i. Because the underlying payoffs to, and thus fitnesses of, strategies s_i (the 'incumbent' strategy) and s_i' (the 'mutant' strategy) depend only on the population states in the other populations, and since these are fixed at s_{-i} for the duration of the extinction or fixation of s_i', the fitness

difference between s_i and s_i' is constant for the duration of this event. Thus, selection is *frequency-independent* in this regime, a fact that will make the calculation of the various fixation probabilities significantly simpler.

To formalize this intuition, for states $s \in \mathcal{P}^{\text{pure}}$ and $s/s_i' \in \mathcal{P}^{\text{pure}/i}$ define $\hat{\mu}_i(s_i, s_i') := \lim_{\varepsilon \to 0} \frac{T^\varepsilon(s, s/s_i')}{\varepsilon} = \frac{N_i \mu_i}{|S_i|} = \hat{\mu}_i$, and let $\rho_i(s_i, s_i'|s_{-i})$ be the 'fixation probability' that, given that populations $-i$ remain monomorphic for strategies s_{-i}, a s_i' mutant who appears in population i that is otherwise monomorphic for strategy s_i subsequently fixes. Assumption 2 ensures that this probability is always positive.

Now let $K = |\mathcal{P}^{\text{pure}}| = \prod_{i=1}^{I} |S_i|$, and let $1, \ldots, K$ be some enumeration of the pure population states.[7] Construct a $K \times K$ transition probability matrix Λ as follows:

- If the pure states labelled m and n are $s = \langle s_i, s_{-i} \rangle$ and $\langle s_i', s_{-i} \rangle$ respectively (i.e., pure states that differ by only one population's strategy), then $\Lambda_{mn} = \hat{\mu}_i \rho_i(s_i, s_i'|s_{-i})$.
- If the pure states m and n differ by more than one population's strategy, $\Lambda_{mn} = 0$.
- Having thus defined Λ_{mn} for all distinct m and n, define $\Lambda_{mm} = 1 - \sum_{n \neq m} \Lambda_{mn}$.

Λ is the transition probability matrix for a homogeneous Markov chain over the (finite) state space $\mathcal{P}^{\text{pure}}$.[8] Moreover, this Markov chain is irreducible, since any pure state can be reached from any other with positive probability in a number of

[7] A particular enumeration that we have found useful: writing $K_i = \prod_{j=i+1}^{I} |S_i|$, enumerate the pure state $\langle s_1^{m_1}, \ldots, s_I^{m_I} \rangle$ by $\sum_{i=1}^{I-1} K_i(m_i - 1) + m_I$. The population states in the pure state enumerated n can then be recovered as follows: $m_I - 1 = n \mod |S_I|$, and $m_i - 1 = \left\lfloor \frac{n}{K_i} \right\rfloor \mod |S_i|$ for each $i < I$.

[8] If there are some m such that $\Lambda_{mm} < 0$ in the above construction of Λ, one can rescale all mutation rates μ_i by an appropriately small factor to render all $\Lambda_{mm} > 0$. Any such rescaling will result in the same stationary distribution induced by Λ.

steps equal to the number of populations on whose strategies the two pure states differ.

This establishes the final proposition that we require, that Λ induces a unique stationary distribution on the state space of pure population states [265]:

Proposition 4. There is a unique vector $\lambda = (\lambda_1, \ldots, \lambda_K)$ such that $\lambda_j \geq 0$ for all j, $\lambda_1 + \ldots + \lambda_K = 1$, and $\lambda\Lambda = \lambda$.

We are now in a position to state our main result. Propositions 1-4 ensure that T^0, T^ε, and Λ satisfy Assumptions 6-9 of Fudenberg and Imhof [170]. Employing their Theorem 2,[9] we arrive at the following theorem.

Theorem 1. *For each ε, denote by λ^ε the unique stationary distribution of the Markov process T^ε. If n corresponds, in the enumeration of pure states, to the pure state s, then*

$$\lim_{\varepsilon \to 0} \lambda^\varepsilon(s) = \lambda_n.$$

That is, the stationary distributions of T^ε approach λ as mutation rates become small.

2.5 The usefulness of the result

Our result is useful on two fronts. First, it extends to asymmetric games our ability to compute the limiting stationary distributions of finite-population evolutionary or imitation processes. We have argued that it is these games, and asymmetric multi-

[9] A simple proof of a generalization of Fudenberg and Imhof's [170] result, holding for more general evolutionary processes, has recently been given by McAvoy [351].

stage games in particular, for which stochastic finite-population dynamics are most relevant.

Second, the fixation probabilities used to calculate Λ derive from frequency-independent selection. Since frequency-independent selection has long been a standard assumption of the population genetics literature, we can make use of the many results about fixation probabilities in that literature. This bridge between evolutionary game theory and classical population genetics could allow for analytical calculation of the rare-mutations stationary distribution, where this would be impossible or infeasible in a single-population symmetric game setup [170] (where the fixation probabilities that compose Λ derive from frequency-dependent selection, and therefore typically do not exist in closed form, or are intractable when they do [396][10])

To illustrate this, we consider three examples: a 'battle of the sexes' game, a discrete Crawford-Sobel signalling game [105], and the 'beer-quiche' game of Cho and Kreps [87].

Example 1: Battle of the sexes

The well-known 'battle of the sexes' game involves a man and a woman hoping to coordinate their weekend activities, which are either going to a ballet performance (the woman's preference) or going to a rugby match (the man's preference). Both

[10] In the particular case where the evolutionary process is a birth-death process [265, 396], a closed form for fixation probabilities exists—see, e.g., [265, Sec. 4.7] and [396, Eq. 6.13]. In general, it is a complicated expression involving the relative fitnesses of the incumbent and mutant strategies at each possible intermediate frequency of the mutant strategy. One case for which this expression simplifies to a tractable form is the Moran process, if fitnesses are calculated as exponential functions of game payoffs [102, 520]. For some other frequency-dependent evolutionary processes, fixation probabilities can be shown to approach tractable representations as the population size becomes very large—see, e.g., [171]. However, as we shall discuss in Section 2.6, the cases to which the 'rare mutations' approximation studied here best applies are specifically those where population sizes are not too large.

the man and the woman prefer coordination on either activity to not coordinating. The simple example we shall study is summarized by the payoff matrix:

		Woman	
		B	R
Man	B	$1, 2$	$0, 0$
	R	$0, 0$	$2, 1$

To cast this into an evolutionary model, assume two separate populations of men and women, of size N_m and N_w respectively. Each period, each member of each population goes either to the ballet or to the rugby, and receives his/her expected payoff from interacting with a random member of the other population. (This corresponds to members of each group preferring to be at an event attended by many members of the other group, though males would prefer this to be at the rugby, and females would prefer it to be at the ballet.)

Expected payoffs $\mathbb{E}\pi$ within both populations translate to fitnesses via the linear transformation $f_\theta(\mathbb{E}\pi) = 1 + \eta_\theta \mathbb{E}\pi$, where θ is either m ('man') or w ('woman'), and η_m and η_w are the strengths of selection in the men's and women's populations respectively. The evolutionary or imitation dynamics within each population are assumed to be a Moran process [375, 396], occurring with mutations in the manner set out in Section 2.3. The per-person mutation, or experimentation/error, rates in the men's and women's populations are $\varepsilon\mu_m$ and $\varepsilon\mu_w$ respectively.

In populating the rare-mutations Markov matrix Λ, we need only consider transitions between pure states where either the male population's strategy is different or the female population's strategy is different, but not both. For example, consider the transition from the pure state where the men all go to the rugby and

the women all to the ballet, $(\mathbf{R}, \mathbf{B})$, to the pure state where everyone goes to the rugby, $(\mathbf{R}, \mathbf{R})$. (The bold font indicates that these are population strategies.) In the former 'incumbent' female population, members all had fitness $1+\eta_w(0) = 1$. A mutant woman going instead to the rugby has fitness $1 + \eta_w(1) = 1 + \eta_w$, and thus has (frequency-independent) selective advantage η_w over the ballet-going members of the female population.

This frequency independence allows us to make use of the well-known formula for fixation probability under a Moran process [396]: If a single mutant has selective advantage s over the other members of the (size N) population, then its fixation probability is

$$\rho(s) = \frac{1 - 1/(1+s)}{1 - 1/(1+s)^N}$$

for $s \neq 0$, and $\rho(0) = 1/N$. The corresponding formula for the case of frequency-dependent selection is significantly more complicated [265, 396].

The entry of Λ corresponding to the transition $(\mathbf{R}, \mathbf{B}) \to (\mathbf{R}, \mathbf{R})$ is therefore

$$\Lambda_{(\mathbf{R},\mathbf{B})\to(\mathbf{R},\mathbf{R})} = \hat{\mu}_w \rho_w(\eta_w) = \frac{N_w \mu_w}{2} \frac{1 - 1/(1+\eta_w)}{1 - 1/(1+\eta_w)^{N_w}}.$$

For the reverse transition $(\mathbf{R}, \mathbf{R}) \to (\mathbf{R}, \mathbf{B})$, mutant women have fitness 1, while incumbents have fitness $1 + \eta_w$. Mutants are thus at relative selective disadvantage $\frac{(1)-(1+\eta_w)}{1+\eta_w} = -\eta_w/(1+\eta_w)$, and the relevant entry of Λ is

$$\Lambda_{(\mathbf{R},\mathbf{R})\to(\mathbf{R},\mathbf{B})} = \hat{\mu}_w \rho_w \left(\frac{-\eta_w}{1+\eta_w} \right) = \frac{N_w \mu_w}{2} \frac{1 - (1+\eta_w)}{1 - (1+\eta_w)^{N_w}}.$$

The other entries of Λ are calculated similarly. Enumerating the pure states

$(\mathbf{B},\mathbf{B})$, $(\mathbf{B},\mathbf{R})$, $(\mathbf{R},\mathbf{B})$, and $(\mathbf{R},\mathbf{R})$ as 1, 2, 3, and 4 respectively,

$$\Lambda = \begin{pmatrix} 1-\ldots & \hat{\mu}_w\rho_w(\frac{-2\eta_w}{1+2\eta_w}) & \hat{\mu}_m\rho_m(\frac{-\eta_m}{1+\eta_m}) & 0 \\ \hat{\mu}_w\rho_w(2\eta_w) & 1-\ldots & 0 & \hat{\mu}_m\rho_m(2\eta_m) \\ \hat{\mu}_m\rho_m(\eta_m) & 0 & 1-\ldots & \hat{\mu}_w\rho_w(\eta_w) \\ 0 & \hat{\mu}_m\rho_m(\frac{-2\eta_m}{1+2\eta_m}) & \hat{\mu}_w\rho_w(\frac{-\eta_w}{1+\eta_w}) & 1-\ldots \end{pmatrix},$$

where the ellipses abbreviate that the rows must each sum to one.

We have a number of free parameters in this model; to wit: the sizes of, selection strengths in, and mutation rates in the two populations. As an example, suppose we set the sizes of, and selection strengths in, the two populations equal at N and η respectively. Making use of the fact that, for the Moran process, $\rho(s)/\rho(-s/[1+s]) = (1+s)^{N-1}$, we calculate the stationary distribution of the Markov chain defined by Λ:

$$\lambda = \left[1, \frac{1}{(1+2\eta)^{N-1}}, \frac{1}{(1+\eta)^{N-1}}, 1\right]/\bar{\lambda},$$

where $\bar{\lambda}$ is a normalization constant. Notice that, in the rare mutations limit, the mutation rates, though possibly different in the two populations, do not affect the long-term distribution of states.

The proportions of time the populations spend both at the rugby and both at the ballet are equal, and are higher for larger values of the common selection strength η and population size N. The intuition for this effect of η is straightforward: A higher η increases the fixation probabilities of positively selected mutants, and decreases the fixation probabilities of negatively selected mutants. In this coordination game, the former are always mutants leading towards the coordination equilibria $(\mathbf{B},\mathbf{B})$ and $(\mathbf{R},\mathbf{R})$, while the latter are always mutants leading away from these coordination equilibria.

The effect of population size can most easily be seen from the ratio of transition probabilities from a non-coordination to a coordination state (positive selection s) and vice-versa (negative selection $-s/[1+s]$): $\rho(s)/\rho(-s/[1+s]) = (1+s)^{N-1}$. This ratio increases with N, and so, for each path into and out of a coordination equilibrium, a higher N increases the transition probability into, relative to the symmetric probability out.

Example 2: Crawford-Sobel signalling

The next game to which we apply our result is a discrete variant of a signalling game from Crawford and Sobel [105, Sec. 4]. Suppose that there are three possible states of the world, $\theta \in \{0, 1, 2\}$, with each equally likely. A signaller observes the state of the world, and sends a costless signal $s \in \{a, b, c\}$ to a receiver, who observes only the signal, and not the state of the world. Having observed the signal, the receiver makes a decision r. Payoffs to signaller and receiver are as follows:

$$\begin{aligned} \pi_S(\theta, r) &= -(r - \theta - \gamma)^2, \\ \pi_R(\theta, r) &= -(r - \theta)^2, \end{aligned}$$

where $\gamma \geq 0$ is a parameter that characterizes the signaller and receiver's misalignment of interests (for every θ, the receiver's optimal decision is γ lower than the signaller would most want it to be). For simplicity, we restrict the receiver's possible decisions r to the set $\{0, 0.5, 1, 1.5, 2\}$, which covers all possible optimal decisions the receiver could make given some posterior over the state space, having observed a signal.

For all $\gamma \geq 0$, Nash equilibria exist where the signaller sends the same signal no matter the state of the world, and the receiver, observing that signal, makes decision

$r = 1$. We call these equilibria 'uninformative', and label them 'xxx', since the same signal $x \in \{a, b, c\}$ is sent for each state of the world $\{0, 1, 2\}$. Also, for all γ, Nash equilibria exist where the signaller sends the same signal for states $\theta = 0$ and $\theta = 2$, and a different signal for state $\theta = 1$: to all sent signals, the receiver responds with decision 1. Since no practical (decision-changing) information is transmitted by the signaller, we also call these equilibria, labelled 'xyx', 'uninformative'.

For sufficiently low γ, there also exist 'partially informative' equilibria where, for two adjacent states of the world (i.e., {0,1} or {1,2}), the signaller sends the same signal, but for the other state of the world, sends a different signal. For such 'xxy' and 'xyy' equilibria, these threshold values for γ are 0.25 and 0.75 respectively.

Finally, for $\gamma \leq 0.5$, there exist 'informative' equilibria, where the signaller sends a different signal for each state ('xyz'), and the receiver makes a decision equal to the state that the signal is sent from.

A full characterization of the Nash equilibria of this game, including the receiver's responses to unsent signals required to sustain each equilibrium, is included in [543, Appendix].

Crawford and Sobel [105] argue, somewhat informally, that for a given value of γ, the most reasonable equilibria are the most informative ones possible for that γ. This, they claim, is because these equilibria are Pareto-superior to less informative equilibria, and are salient—or 'focal' in Schelling's [461] language—in that they are the *most* informative equilibria (the other salient equilibria are the *least* informative ones, but these are ruled out on the former grounds of being Pareto-inferior to the most informative equilibria).

The methodology developed in the present paper allows us to test this equilibrium selection prediction more formally, in the context of learning by agents. Notice

that none of the equilibria that are not perfectly informative is strict, so that a deterministic infinite-population approach would be of little use here, particularly for higher values of the misalignment parameter γ (for which the informative equilibria do not exist). Instead, our finite-population approach is better-suited to this game.

We assume two populations, one of signallers and one of receivers. The size of each population is N. Each signaller is equipped with a response to each possible state of the world, and each receiver with a response to each possible signal. States of the world are drawn independently for each individual interaction (i.e., there is no aggregate state of the world), and fitnesses are calculated according to expected payoffs.

Evolution within each population is assumed to be a Wright-Fisher process [154, 584], which has been used as a model for both biological evolution [219] as well as imitation learning [509, 518]. Expected payoffs translate to fitnesses exponentially, $f(\mathbb{E}\pi) = \exp(\eta\mathbb{E}\pi)$, with selection strength η and per-person mutation rate $\varepsilon\mu$ in both populations.

In constructing Λ, frequency-independent selection allows us to make use of the well-known 'diffusion approximation' formula for the fixation probability, under the Wright-Fisher process, of a single mutant at selective advantage s in a population of size N [279]:

$$\rho(s) \approx \frac{1 - \exp(-s)}{1 - \exp(-Ns)}$$

for $s \neq 0$, and $\rho(0) = 1/N$.[11] Again, the case of frequency-dependent selection is

[11] The diffusion approximation formula cited above is known to be very accurate [141, 142], and we would expect our results to alter very little were we to use near-exact numerical approximations of the true fixation probabilities. Such numerical estimation of fixation probabilities is computationally very expensive, which further highlights the value of our result: when selection is frequency dependent, as in the single-population symmetric-game case, fixation probabilities will usually *have to be* estimated numerically, whereas in our asymmetric-game case, where selection is frequency independent, we may make use of well-known exact or approximate closed-form fixation probabili-

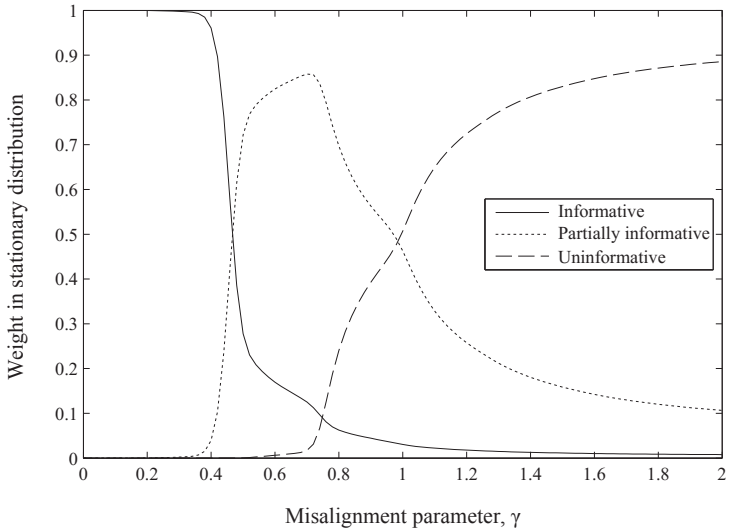

Figure 2.5.1: Frequencies of the signalling profiles of different levels of information transmission in the long-run dynamics of the Crawford-Sobel game, plotted for various values of the misalignment parameter γ. Both signaller and receiver populations are of size $N = 100$; fitness is exponential in expected payoffs, with equal selection strength $\eta = 1$; mutation rates are equal in the two populations. The results are broadly consistent with Crawford and Sobel's prediction that the most informative equilibria supportable by a given value of γ are the most reasonable for that γ.

significantly more complicated [7, 247, 317].

We use these fixation probabilities to populate Λ according to the method set out in Section 2.4, and calculate its stationary distribution. Fig. 2.5.1 plots, for the case $N = 100$ and $\eta = 1$, and for various values of the misalignment parameter γ, the relative frequencies of equilibria of different information levels in this stationary distribution.[12]

It can be seen from Fig. 2.5.1 that the results of the learning/evolutionary dy-

ties.

[12]The frequencies that we plot for a given equilibrium type are in fact those of all population states whose signalling profile is consistent with that equilibrium type: because the populations are large and selection is strong, the plotted frequencies correspond closely with those of the equilibria (which would take into account receiver behaviour too).

namics in this game broadly support Crawford and Sobel's prediction that the most informative equilibria supportable by a given γ are the most reasonable for that γ. For low levels of misalignment $\gamma < 0.4$, the informative equilibria dominate, and information transmission is almost always perfect in the long run. For intermediate levels of misalignment ($0.4 < \gamma < 1$), partially informative equilibria, especially those of the form xyy, are dominant. For high levels of misalignment ($\gamma > 1$), only uninformative equilibria can be supported, and indeed such equilibria dominate the long-run dynamics.

Note that the equilibria involving signalling of the forms xxy and xyx do not have analogs in the equilibria of the game with continuous state, signal, and decision spaces [105]; they are artefacts of the discrete structure of the game we have set up. It is reassuring, then, that they play little role in the long-run dynamics for all values of γ.

Example 3: The beer-quiche game

Our final example is the beer-quiche game of Cho and Kreps [87], employed by them to illustrate the equilibrium refinement method they advance, the 'Intuitive Criterion'. The extensive form of the game is given in Fig. 2.5.2. Player 1 is either a wimp (type t_w) or surly (type t_s), with probabilities 0.1 and 0.9 respectively. Player 1 knows his type; player 2 does not. Player 1 either has beer or quiche for breakfast, observed by player 2, who then chooses whether to fight player 1 or not. The payoffs are such that player 2 should choose to fight player 1 if the posterior probability he holds that player 1 is a wimp is greater than 0.5. For any action by player 2, player 1 prefers beer for breakfast if he is surly, but quiche if he is a wimp. Regardless of player 1's type, he would prefer to avoid fighting.

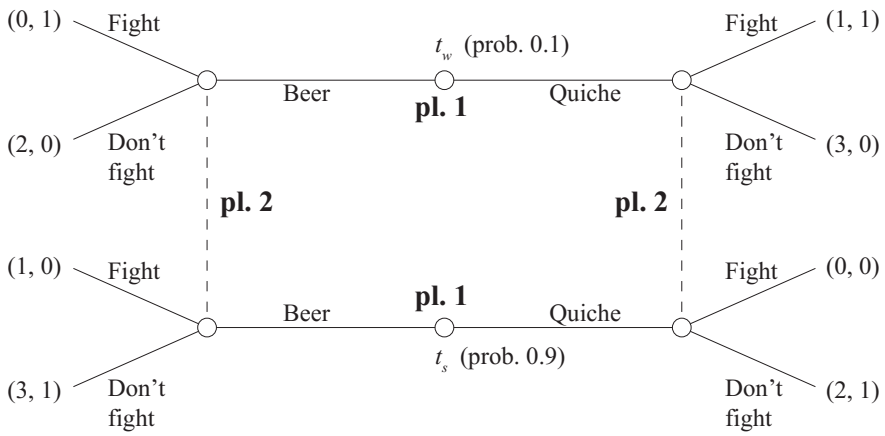

Figure 2.5.2: Extensive-form setup of the beer-quiche game of Cho and Kreps [87].

The game has two Bayesian Nash equilibria, both of the 'pooling' kind: one in which player 1 eats quiche no matter his type, and one in which player 1 drinks beer no matter his type. In both cases, player 2 chooses not to fight in response to the observed behaviour of player 1, but would fight in response to the unobserved behaviour. Both pooling equilibria are sustained by player 2's 'out-of-equilibrium' belief that, if he were to observe player 1 having the opposite breakfast to that consumed in equilibrium, there would be a greater-than-half chance that player 1's type was wimp. Cho and Kreps's Intuitive Criterion, however, rules out the always-quiche equilibrium, by the argument that the out-of-equilibrium beliefs that player 2 is required to hold do not survive forward-inductive reasoning [87] [173, Ch. 11.2].

The Intuitive Criterion has been criticized as being, in some cases, too rationality-heavy [173]. Our methodology allows us to test whether its prediction in the beer-quiche game holds up under a rationality-light learning process, where players need not even know the other players' payoffs.

We assume two populations, one for each role. Evolution proceeds in each population as a Wright-Fisher process with mutations. The population of player i's, 'popu-

lation i', is of size N_i, with selection strength η_i, exponential fitness $f_i = \exp(\eta_i \mathbb{E}\pi)$, and per-individual mutation rate μ_i. Each member of population 1 has a strategy prescribing his breakfast choice (beer or quiche) if he turns out to be wimpish (with probability 0.1) and if he turns out to be surly (with probability 0.9). Each member of population 2 has a strategy prescribing his response (fight or don't fight) to seeing a member of population 1 drink beer for breakfast, and to seeing a member of population 1 eat quiche. Each round, each member of each population receives his expected ex-ante (i.e., before types are chosen in population 1) payoff from interacting with a random member of the other population.

We label pure population states by the tuple $b(t_w), b(t_s); r(B), r(Q)$: respectively, breakfast had when wimpish, breakfast had when surly; response to beer-drinking, response to quiche-eating. For the former two, **B** and **Q** represent 'beer' and 'quiche', while, for the latter two, **F** and **N** represent 'fight' and 'no fight'. Again, the bold font is used to indicate that these are population strategies.

The weights of the most popular states in the stationary distribution are displayed in Fig. 2.5.3, for the parameter settings $\eta_1 = \eta_2 = 0.2$, $\mu_1 = \mu_2$, and for various population sizes $N = N_1 = N_2$. For large population sizes ($N > 20$), the pooling equilibrium predicted by the Intuitive Criterion, **BB**; **NF**, is the modal state in the stationary distribution. For all population sizes, the other pooling equilibrium, 'all-quiche', has low weight in the stationary distribution; this supports its rejection by the Intuitive Criterion.

Apart from the fact that, of the two Bayesian Nash equilibria, the one predicted by the Intuitive Criterion is dominant, it is also of interest that non-equilibrium population states occur so frequently in the long run. These states are, in order of their weights in the stationary distribution, **QB**; **NF**, **QB**; **NN**, and **BB**; **NN**.

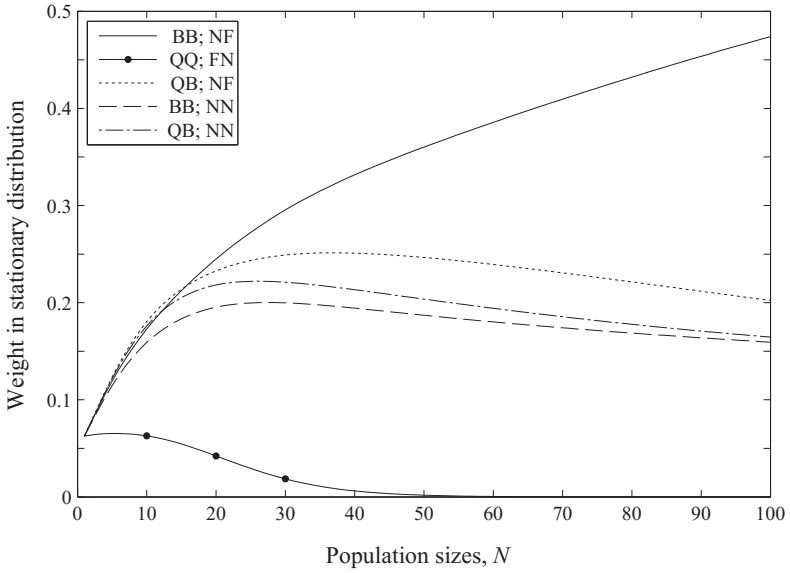

Figure 2.5.3: The frequencies of various population states in the long run dynamics of the beer-quiche game, plotted for various common population sizes $N = N_1 = N_2$. For reference, population state '$\mathbf{QB}; \mathbf{NF}$' is that where members of population 1 eat quiche ($\mathbf{Q}$) if wimpish and drink beer ($\mathbf{B}$) if surly, while members of population 2 do not fight ($\mathbf{N}$) if they see beer-drinking and do fight ($\mathbf{F}$) if they see quiche-eating. The equilibrium predicted by the Intuitive Criterion, $\mathbf{BB}; \mathbf{NF}$, is modal for large (> 20), but not for low (< 20), population sizes. The equilibrium ruled out by the Intuitive Criterion, $\mathbf{QQ}; \mathbf{FN}$, is infrequent in the long-run dynamics for all population sizes.

Indeed, for small population sizes ($N < 20$), the state **QB**; **NF** has highest weight in the stationary distribution.

The success of these non-equilibrium states is a result of neutral and nearly-neutral drift. Starting from the equilibrium state **BB**; **NF**, members of population 2 who instead play NN achieve the same expected payoff (0.9) as those playing NF, and so can neutrally invade the population. If they fix, the pure population state **BB**; **NN** is established. From this state, members of population 1 who play QB are slightly favoured over the incumbents playing BB (expected payoff 3 versus 2.9), and so can invade and fix, establishing the pure state **QB**; **NN**. From this state, members of population 2 who play NF are slightly favoured (expected payoff 1 versus incumbent expected payoff 0.9). If they invade and fix, pure state **QB**; **NF** is established. But from this pure state, members of population 1 who play BB are slightly favoured (expected payoff 2.9 versus incumbent 2.8). If they invade and fix, the equilibrium pure state **BB**; **NF** is re-established. Notice that, because the reverse directions involve only neutral and slightly disfavourable mutations, they also occur with non-negligible probability, and are therefore likely to influence the stationary distribution.

The intuition for the fact that increased population size here results in the system spending more time in the Nash equilibrium state is similar to that for the same observation in the battle of the sexes. When the population size is small, mutants that are weakly selected against still have non-negligible probability of fixing, and so transitions out of **BB**; **NF** to, say, **QB**; **NF** (mutant's expected payoff only 0.1 less than incumbents') play a role in the long-run dynamics. When the population size is very large, mutants that are weakly selected against have very little chance of fixing, and so these paths out of equilibrium are shut down, leaving only neutral

paths such as $\mathbf{BB}; \mathbf{NF} \to \mathbf{BB}; \mathbf{NN}$. Increasing selection strength η would have the same effect.

2.6 Discussion

Our model involves a number of assumptions and simplifications, four major ones of which we discuss below: (i) the assumption of multiple populations, (ii) that, in the no-mutations process, only pure states are absorbing, (iii) that mutations can, in reality, be sufficiently rare for the evolutionary dynamics to behave like the limiting case, and (iv) that mutation rates within populations are uniform. Thereafter, we briefly discuss the relevance of the approach developed in this paper for mixed-strategy equilibria.

On (i), an alternative approach would be to model evolution as occurring in a single population, wherein each agent has a strategy for every role [353]. Expected payoffs to players could then be computed on the basis of random assignment of roles each period.

In most learning contexts, the multiple-population setup seems more natural: we think of roles as being assigned at the outset, with each agent subsequently learning how best to play her assigned role. An example is the battle of the sexes game studied in Section 2.5, where the gender of each agent is fixed for the duration of his/her learning period. The multiple-population setup is also better suited to modelling the genetical evolution of multiple interacting, though reproductively distinct, species. In the context of genetical evolution within a single species, however, the more natural model is a single population in whose genomes strategies for different roles are encoded at different loci. Strategies are then collections of alleles, one for each locus, and are inherited intact (ignoring genetic recombination). In the course of

the propagation of a strategy, which locus is relevant will change from generation to generation, as different roles are taken on (carrier is male or female, carrier is the incumbent occupant of a territory or the trespasser, etc.).

When should we expect the evolutionary dynamics under this single-population model to resemble those under our multiple-population model (where each locus, or role, is treated as a separate 'population')? Here, the answer is simpler for deterministic infinite-population dynamics. If there is variation within the population for alleles (/strategies) at multiple loci (multiple loci exhibit 'polymorphism'), then the multiple-population approach and the single-population approach yield equivalent dynamics under the deterministic replicator dynamics if a simple condition concerning allele frequencies holds [107]. This condition, known in the population genetics literature as *linkage equilibrium*, amounts to statistical independence of allele frequencies across loci, and is preserved through time under the replicator dynamics [107].

In a finite population, polymorphism at multiple loci will be common if the mutation rate or the population size are sufficiently large. The stochastic nature of the evolutionary process in a finite population ensures that linkage equilibrium will not always hold, and so a 'dynamical equivalence' result such as that described above is not possible. Nonetheless, if mutations at different loci occur independently, then in the regime of rare mutations studied in this paper, it will almost always be the case that at most one locus is polymorphic in the population. Thus linkage equilibrium will almost always hold, since linkage disequilibrium between two loci requires that both loci be polymorphic. In the rare mutations limit, therefore, the dynamics are the same whether we model evolution as occurring in multiple populations of loci, or in a single multi-locus population.

On (ii), we noted that, in multi-stage games, play at unreached decision nodes could not be imitated if imitation were a learning process based only on direct observation of play. Under this condition, interpreting assumption 2 as applying to imitation processes seems unjustified—mixed population states in which one population is polymorphic for an action at an unreached decision node could be maintained in perpetuity. As argued in Section 2.3, this condition represents an unrealistic 'knife-edge' case. In reality, we expect agents to communicate about their strategies. The case of imitation only by direct observation is nonetheless a useful benchmark from which to discuss the influence of the general factors that validate assumption 2 for imitation learning processes. Despite the obvious importance of such a discussion, it has not, to our knowledge, explicitly appeared in the literature on stochastic learning in extensive form games.

On (iii), how rare do mutations have to be for the population dynamics to resemble those in our limiting case? A simple heuristic may be derived as follows: Assume all I populations to be of size N, with a common individual mutation rate of μ. Consider the case where, starting from a monomorphic state, a mutant appears in one of the populations. Under most commonly studied population dynamics (e.g., Wright-Fisher, Moran), the time that it takes this mutant either to go extinct or fix in its population is of order N or less [143, 281]. Say that this time is aN. Then the probability that another mutant appears during the extinction/fixation of this mutant is about $\mu NI \times aN$; for this probability to be below some small threshold ν, we require $\mu < \nu/(aIN^2)$. If this holds, the dynamics should resemble those for the limiting case $\mu \to 0$.

The bound could probably be loosened for most games, as it can be in the single-population symmetric game case (Wu et al. [586]): the analogous loosening of the

bound in Wu et al. [586] is from order $1/N^2$ (our heuristic) to order $1/(N \ln N)$. In their case, this holds for all games except coexistence games, in which mixed equilibria are stable. The reason for this latter fact is that, if selection is very strong in a coexistence game, the population can stabilize around the mixed equilibrium for a very long period of time, long enough for another mutation to occur with non-negligible probability. In the case of coexistence games, the bound must be tightened to order $N^{-1/2}e^{-N}$ [586]. In asymmetric games, an analogous 'negative feedback' issue could arise in a situation where two populations stabilize each other at respective mixed equilibria. A good example is the 'matching pennies' game, where the row player and column player have the same strategy space (heads and tails); if the strategies played match, the row player gets payoff $+1$ and the column player gets -1, and if they don't match, the row player gets -1 and the column player $+1$. In our multi-population context, if the column population predominantly plays heads, the row population moves to predominantly playing heads, which in turn leads to a decrease in the play of heads in the column population, and a subsequent decrease in the play of heads in the row population, etc. If selection is strong enough, this situation could persist for long enough that the chance of another mutation occurring would be non-negligible. (Recent derivations [475] of fixation probabilities in a Moran process when multiple populations are polymorphic should be useful in analyzing such cases.) In this case, a strengthening of the 'rare mutation' bound would be required: following the analysis of Wu et al. [586], we would expect a bound of order $I^{-1}N^{-1/2}e^{-N}$ to suffice.

In any case, it is clear that our rare-mutations result is most relevant either if mutations (or experimentation and errors) occur at a low per-period rate, or if the populations under study are small, or both. In learning dynamics, interpretation of

this 'rare mutations' condition is difficult, since the rate of mutations is calibrated to the timescale over which strategy revisions are made. Thus, a 'generation' might in fact constitute a very short period of time, and we might expect experimentation or errors to be very infrequent on such a timescale. Interpretation of this condition is easier for genetical evolution, where the timescale is in generations, and the probabilities of mutations can be reasonably well measured. For example, the point mutation rate at a single nucleotide site in humans (though known to vary across the genome [489, 576, 582], and between the sexes [246]) is of order about 10^{-8} per generation [328, 446]. If we set a threshold of $\nu = 0.05$ and $a = 1$, and consider evolution at two independent loci ('roles'), then the bound $\mu < \nu/(aIN^2)$ holds for populations of up to about 1500 individuals.

On (iv), it may be objected that, in our model, mutation rates within populations are uniform: a mutation from any strategy to any other strategy is equally likely. While this assumption may be valid in certain genetic contexts, in a learning context we might expect certain errors, or examples of experimentation, to be less likely than others [172]. Also, in a genetical context, if we include in our concept of mutation the possibility of structural changes (e.g., rearrangements, translocations), or if we are interested in the evolutionary dynamics of a certain functional genotype relative to all other genotypes (grouped as one class), then asymmetric mutation rates would be natural [355, 395].

Our result can be generalized in a straightforward way to incorporate heterogeneity in mutation rates within populations. If we denote by $\varepsilon\mu_i(s_i, s_i')$ the probability that a member of preliminary period-t population i currently employing strategy s_i will mutate to playing s_i' in the finalized period-t population, then the evolutionary process with mutations is a Markov chain T^ε. It is still the case that, for

$s = \langle s_1, \ldots, s_I \rangle \in \mathcal{P}^{\text{pure}}$, $\lim_{\varepsilon \to 0} \frac{T^\varepsilon(s,p)}{\varepsilon} = 0$ if $p \notin \mathcal{P}^{\text{pure}} \cup \mathcal{P}^{\text{pure}/i}$ for some i. But now, for $s/s_i' \in \mathcal{P}^{\text{pure}/i}$, $\lim_{\varepsilon \to 0} \frac{T^\varepsilon(s,s/s_i')}{\varepsilon} = N_i \mu_i(s_i, s_i')$. The transition probability matrix Λ is then constructed as before.

If it is always the case that $\mu_i(s_i, s_i') > 0$, then the Markov chain defined by Λ is irreducible, and an analogous form of Theorem 1 goes through as before. If, however, we allow there to be some i, s_i, and s_i' such that $\mu_i(s_i, s_i') = 0$, then the T^ε are no longer guaranteed to induce irreducible Markov chains. It is then required that T^ε have a unique stationary distribution for each $\varepsilon > 0$, and that there exists a unique stochastic vector λ such that $\lambda\Lambda = \lambda$, for the analogous Theorem 2 to go through [170, 351].

A final point concerns games with mixed-strategy equilibria. In evolutionary game theory, two kinds of 'mixed strategy' states must be distinguished [25, 197]. The 'population kind' is where individuals within a population each play pure strategies, but different individuals play different strategies. In our setup, when mutations are rare, the system spends almost all of the long-run time in pure states (where individuals within each population all play the same strategy); mixed strategies of the 'population kind' are therefore essentially never observed. The underlying reason is that these polymorphic states are transient under the no-mutations process. For a different reason, these 'population kind' mixed states are also excluded by the evolutionary stability concept of infinite-population deterministic dynamics in asymmetric games: the component strategies of an equilibrium mixed state must have equal fitness, but then any of them could be involved in a 'neutral invasion' of the state [476].

The second kind of mixed strategy state is the 'individual kind', and involves the individuals of a population all playing the same mixed strategy. Unlike the

'population kind', such states can be evolutionarily stable in infinite-population dynamics. They do, however, raise a problem for our finite-population approach. Allowing individuals to play any mixed strategy requires an infinite strategy space (the unit simplex in $\mathbb{R}^{|S_i|}$, for population i with pure-strategy space S_i), and therefore an infinitely large state space. A workaround would be to approximate the infinite strategy space $\mathbb{R}^{|S_i|}$ by a discrete lattice.

3

The Red Queen and King in finite populations

3.1 Abstract

In antagonistic symbioses, such as host-parasite interactions, one population's success is the other's loss. In mutualistic symbioses, such as division of labor, both parties can gain, but they might have different preferences over the possible mutualistic arrangements. The rates of evolution of the two populations in a symbiosis are important determinants of which population will be more successful: faster evolution is thought to be favored in antagonistic symbioses (the 'Red Queen effect'),

but disfavored in certain mutualistic symbioses (the 'Red King effect'). However, it remains unclear which biological parameters drive these effects. Here, we analyze the effects of the various determinants of evolutionary rate: generation time, mutation rate, population size, and the intensity of natural selection. Our main results hold for the case where mutation is infrequent. Slower evolution causes a long-term advantage in an important class of mutualistic interactions. Surprisingly, less intense selection is the strongest driver of this Red King effect, while relative mutation rates and generation times have little effect. In antagonistic interactions, faster evolution by any means is beneficial. Our results provide insight into the demographic evolution of symbionts

3.2 Introduction

Antagonistic symbioses can be conceptualized well in the following simple, constant-sum game [115, 388]:

		Player 2	
		C	D
Player 1	A	$1,0$	$0,1$
	B	$0,1$	$1,0$

(3.1)

Here, player 1's available strategies are A and B, player 2's are C and D, the first payoff in each cell is player 1's, and the second is player 2's. Interacting populations of 'player 1s' and 'player 2s' constitute an antagonistic symbiosis, which we expect to evolve according to arms-race dynamics [121]. To see why, suppose we start with population 1 all playing strategy A and population 2 all playing strategy C, so

that population 1 is doing well at the expense of population 2. Now, a mutant in population 2 who plays strategy D does better (payoff 1) than other members of population 2 (payoff 0), and can take over, at population 1's expense (their payoff decreases from 1 to 0). Population 1 is then expected to switch to strategy B, after which population 2 switches to strategy C, and so on. As the Red Queen said to Alice, "it takes all the running *you* can do, to keep in the same place" [68].

Arms-race dynamics characterize many interactions both in the natural world and in human behavior. In a host-parasite interaction, for example, the host is selected to develop immunity to the parasite, which in turn selects for new 'resistance' mutations in the parasite, which selects for the host to develop immunity to the new mutant parasite, and so on. In Batesian mimicry, a palatable species (of butterfly, for example) evolves to mimic the warning display of an unpalatable species, so that it is mistaken by predators for the unpalatable species. This selects for the unpalatable species to evolve a new display, so as not to be mistaken for the palatable species, which is then under selection to mimic the new display, and so on [527].

Antagonistic interactions play out at an intragenomic level as well. Examples, among many others [59, 362], are the X-linked male-meiotic driving gene *Dox* and its autosomal suppressor *Nmy* in *Drosophila simulans* [507, 508], centromeric repeat sequences seeking to drive in female meiosis and the centromere-histone genes that keep them in check [226, 337], and the mammalian recombination-specifying gene *Prdm9* and the binding sequences of its protein (which are under positive selection to escape PRDM9 binding [19, 35, 421, 528]). Consistent with arms-race dynamics, the conflicting elements in these examples all show genetic evidence of rapid evolution [16, 120, 226, 255, 283, 316, 337, 383, 428, 469].

Mutualistic symbioses with a degree of conflict [123, 227] can also be conceptual-

ized in a simple game [26]:

		Player 2	
		C	D
Player 1	A	$2, 1$	$0, 0$
	B	k, k	$1, 2$

(3.2)

with $0 \leq k < 2$. From either of the two mutualistic coordination states (A, C) and (B, D), neither population is under selection to deviate to one of the non-coordination states (A, D) and (B, C). But population 1 prefers coordination state (A, C), while population 2 prefers coordination state (B, D). Of most interest is the case $k < 1$, where game (3.2) is a true mutualism (both populations prefer the two coordination states to the two non-coordination states).

This game also describes many interactions in both nature and humans. Mutualisms often involve a division of labor [309], such as the production of different nutrients in a microalgal-microbial partnership [240], the separate production of a 'poison' and its 'antidote' by two linked genetic elements in a gamete-killing meiotic drive complex [59, 207], or the economic production of different goods by trading partners when production exhibits increasing returns to scale [299]. In these cases, it is beneficial to both interactants that all tasks be carried out, but there can be conflict over who should do which tasks [555]. For example, it is better to be the antidote producer than the poison producer in the meiotic drive complex, because the gains of their partnership are shared equally, but its disruption (by recombination) is costlier to the poison producer.

Another example, Müllerian mimicry, involves two poisonous species (of butterfly, say) evolving to share a common pattern, one pattern being easier for their

predators to learn than two [483]. But if the species' original patterns evolved to suit differences in their respective habitats, behaviors, or genomic backgrounds, then there might be conflict over which pattern to converge on, with each species enjoying an evolutionary advantage if convergence is on its original pattern.

In both antagonistic and mutualistic symbioses, the relative rates of evolution of the participating populations are thought to be important determinants of their relative evolutionary success. A faster rate of evolution could be achieved through various means [26, 121, 123, 227]. First, it could derive from a shorter generation time, allowing more generations over which to adapt [115]. Second, it could derive from a higher rate of mutation, more rapidly generating new variants that allow a population to escape an unfavorable state of interaction [123, 492, 504]. Finally, it could derive from more effective action of natural selection. This could be because the stakes are higher for one population than the other—'the rabbit is running for his life, while the fox is only running for his dinner' [121]—or because selection acts more effectively in large populations, owing (roughly speaking) to a reduced effect of random drift [302] (a precise formulation of this statement is given in [546, Appendix Section S5.2]).

Common wisdom holds that a faster rate of evolution is advantageous in antagonistic interactions [537], the better to 'keep ahead in the race' [121]. But it has not, to our knowledge, been clearly demonstrated which individual biological parameters drive this 'Red Queen effect' in theory.

In an important paper, Bergstrom and Lachmann [26] (hereafter B&L) demonstrated that a *slower* rate of evolution might be advantageous in some mutualistic interactions, an effect they called the 'Red King effect'. They studied two populations interacting according to the mutualism game (3.2), with deterministic evolu-

tionary dynamics operating in each of the two populations, both of infinite size, and without the possibility of mutations.

In their model, x is the proportion of population 1 playing strategy A (so that the proportion $1-x$ play B), and y the proportion of population 2 playing D ($1-y$ play C). Then the expected payoff to a member of population 1 who plays A when interacting with a random member of population 2 is, from the payoff matrix (3.2), $\pi_1^A = 2(1-y)$. On the other hand, the payoff to a member playing B is $\pi_1^B = k(1-y)+y$, and the average payoff in population 1 is $\bar{\pi}_1 = x\pi_1^A + (1-x)\pi_1^B$. The analogous quantities in population 2, π_2^C, π_2^D, and $\bar{\pi}_2$, are calculated similarly. The strategy frequencies in the two populations evolve according to replicator dynamics:

$$\dot{x} = mx\left[\pi_1^A(y) - \bar{\pi}_1(x,y)\right], \quad \dot{y} = ny\left[\pi_2^D(x) - \bar{\pi}_2(x,y)\right]. \tag{3.3}$$

Here $m, n > 0$ are parameters that calibrate the relative rates of evolution of the two populations by determining how responsive their respective evolutionary dynamics are to fitness differences among strategies.

These dynamics are *deterministic*—evolutionary trajectories are fully determined once their starting points are known—and evolution necessarily leads to one of the two coordination equilibria, (A,C) [$x=1, y=0$; population 1's preference] or (B,D) [$x=0, y=1$; population 2's preference], where evolution then halts.

B&L showed that, when $k>1$ in game (3.2) and population 1 evolves slower than population 2 ($m<n$), then the set of starting points from which evolution proceeds to population 1's favored equilibrium (A,C) (the equilibrium's 'basin of attraction') is larger than the basin of attraction of the equilibrium (B,D). In this sense, slower evolution is beneficial. When $k<1$, the opposite result holds: if population 1 evolves slower, the basin of attraction of (A,C) is smaller than that of (B,D).

Here, we construct a finite-population model of symbiosis evolution, incorporating all of the biological determinants of evolutionary rate. This model allows us to extend B&L's results for mutualisms in several ways, and to apply a similar analysis to antagonistic symbioses, leading to a richer picture of the evolutionary dynamics of symbioses.

First, our model allows for an explicit characterization of which evolutionary rate parameters influence the relative success of the interacting populations. This is unknown for mutualisms (B&L's general rate parameters m and n have no clear biological interpretation), has not been fully disentangled for antagonistic symbioses, and in both cases is crucial for standard empirical measures of evolutionary rate (such as the substitution rate at neutral genetic loci, which depends on mutation rate and generation time, but is insensitive to changes in population size [280]).

Second, our model allows us to uncover a key influence of evolutionary timescale on symbiosis evolution. In the mutualism game (3.2), we shall show that the short-run behavior of our stochastic evolutionary dynamics is very similar to that of the replicator dynamics studied by B&L: from a given starting state, the dynamics rapidly converge to, or near to, one of the two equilibria of the game. Which equilibrium is most likely to be approached depends critically on the starting point, just as in the dynamics of B&L. On a longer timescale, however, we shall show the evolutionary dynamics of this game to be of a very different nature. The long-run dynamics involve transitions between equilibria, driven by sporadic mutation, and eventually become independent of where the dynamics first started. As we shall show, in mutualisms, many of the conclusions concerning the short-run dynamics are either annulled or reversed in the long run.

Our main results are summarized in Table 1.

Table 3.2.1: The biological parameters that drive the Red Queen and King effects in antagonistic and mutualistic symbioses. For each of the parameters that determine evolutionary rate, we ask whether the population with the larger parameter value, and which therefore evolves faster, is more successful (♕Q, a Red Queen effect) or less successful (♔K, a Red King effect) in the interaction, holding the other rate parameters constant and equal between the two populations. The short-run results are numerically computed for particular parameter values (see Figs. 3.4.1, 3.5.1, and 3.5.2). The long-run results are for the weak-mutation limit, and are exact (see text for details). For selection strength and population size in the mutualisms: (i) we set one population's selection strength to w (or both populations', when studying the effect of population size), and assume that the larger parameter value is larger by a small amount. (ii) 'k small' means $k < 1/(1+w)$; 'k large' means $k > 1/(1+w)$, and (iii) we assume the populations to be sufficiently large.

	Antagonistic symbiosis		Mutualism k small		Mutualism k large	
	Short run	Long run	Short	Long	Short	Long
1/Generation time	♕Q	♕Q	♕Q	NE	♔K	NE
Mutation rate	NE	♕Q	NE	NE	NE	NE
Selection strength	♕Q	♕Q	♕Q	♔K	♔K	♕Q
Population size	♕Q	♕Q	♕Q	♔K	♔K	♕Q

♕Q: Red Queen effect. ♔K: Red King effect. NE: no effect

3.3 A finite-population model of symbiosis evolution

Populations 1 and 2 are of sizes N_1 and N_2, and interact according to a two-player, two-strategy game such as games (3.1) and (3.2). The 'populations' here can be broadly construed: they could be all the individuals of two species in a symbiosis, for example, or all the alleles at two distinct loci among the genomes of a single species.

The evolutionary process occurs in discrete time-steps. Each time-step, individuals in each population receive their average payoffs from interacting with a random member of the opposite population. An individual's payoff π in population l is translated to a non-negative fitness value $1 + w_l\pi$, so that the 'selection strengths' $w_1, w_2 > 0$ calibrate the effectiveness of natural selection in the two populations.

In each time-step, a 'birth-death event' occurs in one of the populations. Individuals in the two populations have relative generation times g_1 and g_2: in a given

time-step, the birth-death event occurs in population l with probability proportional to N_l/g_l, independently across time-steps.

A birth-death event in a population involves choosing an individual to reproduce, with probability proportional to fitness, and an individual to die, with each equally likely. These can be the same individual. A single offspring of the reproducing individual replaces the individual that was chosen to die. This within-population process, the Moran process [375, 511], has been used as a model both of biological evolution [219, 396] and of imitation learning [170, 174, 224]. In the Moran process, one 'generation' of a population typically corresponds to a number of birth-death events that is about the same as the population's size [219]. In our two-population framework, we shall label the number of time-steps equal to the sum of the populations' sizes as a common 'generation': each individual experiences on average one birth-death event per generation.

Finally, to account for the possibility of mutation, we assume that, in a birth-death event in population l, the offspring inherits its parent's strategy with probability $1-\varepsilon\mu_l$, or mutates to the alternative strategy with probability $\varepsilon\mu_l$. Thus, μ_1 and μ_2 represent the relative mutation rates of the two populations (they are unitless), while the parameter ε calibrates the overall frequency of mutations in the two populations (in units 'per replication').

In sum, given a payoff matrix such as (3.1) and (3.2), and rate parameters N_1, N_2, g_1, g_2, w_1, w_2, μ_1, μ_2, and ε, and provided $\mu_1, \mu_2, \varepsilon > 0$, the above defines an ergodic Markov chain over a state space comprising all possible strategy compositions of the two populations. If $0 \leq i \leq N_1$ is the number of A-strategists in population 1 at some point in time (so that $N_1 - i$ individuals play B), and $0 \leq j \leq N_2$ is the number of C-strategists in population 2 ($N_2 - j$ play D), then the population state

is (i, j). The behavior of the evolutionary process is characterized by the probability of moving from state (i, j) to (i', j') in one time-step, for all such pairs of states—these probabilities are provided in [546, Appendix Section S1].

Two regimes are of interest in these dynamics, corresponding roughly to their short-run and long-run behavior.

Given some initial population state (i^0, j^0), the short-run dynamics (a) are not affected much by mutations, instead being governed mostly by selection strengths, population sizes, and generation times, (b) depend critically on the starting point (i^0, j^0), (c) have trajectories that are similar to those of the replicator dynamics, especially when the populations are large, and (d) in coordination games, like game (3.2), converge rapidly to or near one of the pure population states (in which each population is monomorphic) associated with the equilibria of the game. For illustration, the upper panels in Figs. 3.5.1, 3.5.2, and especially S1 display the similarity of the short-run behavior of our dynamics to the replicator dynamics, in the context of the mutualism game (3.2) (cf. Fig. 2 of B&L [26]).

The long-run dynamics, on the other hand, are of a very different nature. Because the evolutionary process, as we have defined it, is ergodic, the probability that the system is in some state in the future eventually becomes independent of where the system started [265]. This effect is illustrated for the antagonistic symbiosis game in the lower panels of Fig. 3.4.1, and for the mutualism game in the lower panels of Figs. 3.5.1 and 3.5.2. The state of the system comes to depend not on the early dynamics that emanate from the starting point, but instead on infrequent transitions between equilibria, driven by mutations.

The object of interest in these long-run dynamics is their *stationary distribution*, that is, the proportion of time spent in each population state in the long run. Equiv-

alently, the stationary distribution tells us, were we to observe many independent instances of equivalent symbioses evolving, what proportion of these symbioses we should expect to find in each possible state at some fixed point in time in the long run [265].

While we shall numerically study the stationary distribution of our evolutionary process for large mutation rates and selection strengths, we shall also invoke recent methodological advances in evolutionary game theory [406, 543] to study it analytically in certain limits. Chief among these will be the 'weak-mutation limit', $\varepsilon \to 0$, which approximates the case where mutations are very infrequent: $N_1\varepsilon\mu_1, N_2\varepsilon\mu_2 \ll 1$ [174, 543]. This is a common assumption in the population genetics and evolutionary game theory literatures [174, 355, 564], and is realistic when populations are small, or when the individual mutation rate is very small. For example, in genetical evolution, the mutations we are considering might be single nucleotide substitutions, which occur at rates of order 10^{-8} or smaller per generation for most organisms [334]; if multiple nucleotide substitutions are required to change strategies, then the relevant mutation rates are even lower. Therefore, while the case of infrequent mutations is certainly not general, it is a relevant and interesting case to consider.

In the weak-mutation limit, the dynamics converge to an embedded dynamical process over just the four pure states [170, 543]; concomitantly, the stationary distribution collapses to a probability distribution over these pure states, $\boldsymbol{\lambda} = \left[\lambda_{(A,C)}, \lambda_{(A,D)}, \lambda_{(B,C)}, \lambda_{(B,D)}\right]$. In these embedded dynamics, transitions between the pure states occur with probabilities determined by the relative frequency of appearance of mutants in the two populations, and the probabilities of fixation of these various mutants [543] (full details in [546, Appendix Section S4]).

In this paper, we examine the influence of individual rate parameters—mutation rate, generation time, selection strength, and population size—on the outcomes of antagonistic and mutualistic symbioses. For the majority of our analysis, we take the following 'all else equal' approach: For each rate parameter, we hold equal and constant for the two populations all but that parameter, and then ask whether the population with the larger value of that parameter is, by some relevant criterion, evolutionarily more successful.

This 'all else equal' approach is motivated by two considerations: First, it will be seen to allow for simple mathematical characterization of the long-run dynamics in the weak-mutation limit. Second, it allows us to ask in a clear way, 'What is the contribution of a given parameter to the success of the populations?' For illustration, suppose we see that a large population of parasites does well against a small host population. We might wonder whether it is the parasite's large population size or its rapid generation time that is the main reason for its success. The cleanest way to get at an answer is to ask what the effect of the parasite's large population size would be if we eliminated any benefit from a faster generation time—i.e., by setting the parasite's generation time equal to its host's. We would then do the same for generation time, by setting the parasite and the host population sizes equal.

This approach ignores possible interactions between rate parameters—for example, if the parasite's larger population size is beneficial only if the parasite also has a faster generation time than its host's. For antagonistic symbioses, in the weak-mutation limit, we will be able to relax the 'all else equal' simplification to prove more general results about the long-run effect of the various rate parameters. For mutualisms, our long-run weak-mutation analytical results do require the 'all else equal' assumption. We also give some numerical suggestion that they hold qualita-

tively when we relax this assumption.

3.4 Antagonistic symbioses

In this section, we study the evolutionary dynamics of populations interacting according to the antagonistic symbiosis game (3.1). An appropriate measure of the relative success of population 1 in a given population state is the proportion of (A, C) and (B, D) matchings (favorable to population 1) minus the proportion of (A, D) and (B, C) matchings (unfavorable to population 1). If this quantity is positive, then population 1 has a larger average payoff than population 2 in that state.

3.4.1 Strong mutation, strong selection

We begin by numerically studying the short and long-run dynamics, when mutations are not very rare and selection is not very weak.

We first set the two populations' sizes, selection strengths, and mutation rates equal ($N_1 = N_2$, $w_1 = w_2$, $\mu_1 = \mu_2$), and vary their relative generation times g_1 and g_2. For the parameter values that we consider, we find a weak Red Queen effect in the short-run dynamics (Fig. 3.4.1A): when population 1 has a longer generation time, the set of initial population states from which, after 50 generations, population 1 is on average more successful is greater than the set of initial population states for which the reverse is true. We find a more pronounced Red Queen effect in the long-run dynamics, when the dynamics have become independent of where they started (Fig. 3.4.1A).

We then set the populations' generation times equal ($g_1 = g_2$), as well as their sizes ($N_1 = N_2$) and mutation rates ($\mu_1 = \mu_2$), and allow their selection strengths w_1 and w_2 to vary. We now find very strong Red Queen effects in both the short

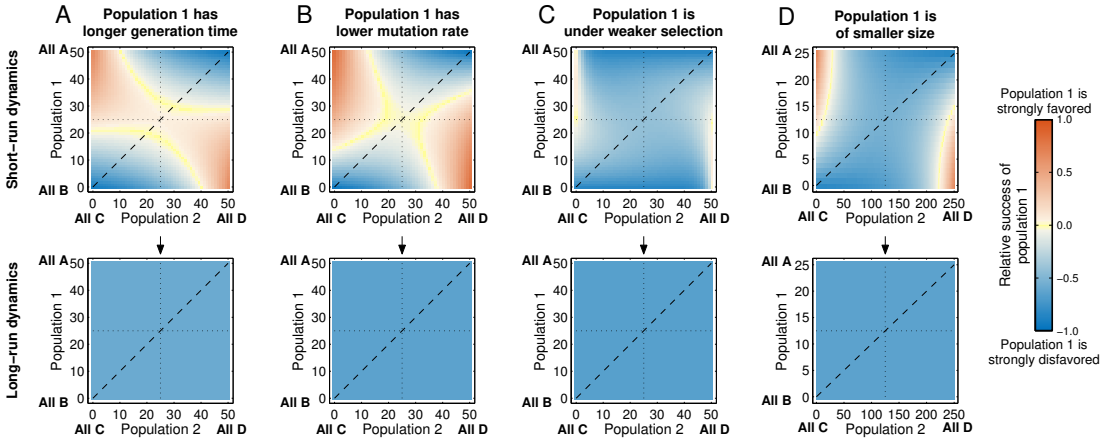

Figure 3.4.1: Evolutionary dynamics of antagonistic symbioses, when population 1 evolves slower than population 2 owing to (A) a longer generation time, (B) a lower mutation rate, (C) weaker selection, and (D) a smaller population size. Each panel shows the numerically computed dynamics, assuming that both populations coincide in their evolutionary rate parameters except for the parameter explicitly varied. The upper panels show, for each initial population configuration in the state space, population 1's relative success after 50 generations. Except when the populations differ only in their mutation rates, a short-run Red Queen effect operates in all cases: as the blue area covers more than 50% of the square, population 1's slower evolution leads to its typically being disfavored after 50 generations for a larger fraction of initial population states. The short-run Red Queen effect is strongest for selection strength and population size. The lower panels show population 1's relative success after $50,000$ generations, by which time the starting configuration no longer influences the dynamics: the panels have a uniform color. A strong long-run Red Queen effect is observed in all cases: population 1's slower evolution causes a larger fraction of long-run time to be spent in states unfavorable to it. Baseline parameters: $N_1 = N_2 = 50$, $w_1 = w_2 = 0.05$, $g_1 = g_2 = 1$, $\mu_1 = \mu_2 = 1$, and $\varepsilon = 0.001$. (A) $g_1 = 10$; (B) $\mu_1 = 0.1$; (C) $w_2 = 0.5$; (D) $N_1 = 25$, $N_2 = 250$. A 'generation' is $N_1 + N_2$ elementary time-steps of the Moran process.

run and the long run (Fig. 3.4.1C). We find similar Red Queen effects, especially in the long run, when populations differ in their mutation rates (Fig. 3.4.1B) or in their sizes (Fig. 3.4.1D).

We have spoken loosely of the 'short run' and 'long run'. While 50 generations are certainly short run, the long run should be more precisely defined as the time by which the distribution over population states is close to the stationary distribution. In the language of Markov chains, this is known as the 'mixing time' of the dynamical process [320].

For small population sizes, the time evolution of the probability distribution over states can feasibly be computed given any starting point. It is shown in [546, Fig. S6] that, in the antagonistic dynamics, for the parameter values used in Fig. 3.4.1 (with small populations, of size 50), we may speak of the 'long run' as being after 100-1,000 generations. For larger population sizes, it is not computationally feasible to compute the time evolution of the probability distribution over states, and we must resort to approximate analytical arguments.

We give such arguments in [546, Appendix Section S3], Section S3. Here, we summarize their conclusions. We assume that mutations are infrequent. When selection acts weakly in at least one of the populations l—that is, when $N_l w_l < 1$—the mixing time of the antagonistic co-evolutionary process is approximately proportional to $1/(\varepsilon\mu_l)$ [if selection acts weakly in both populations, then the mixing time will be proportional to $1/\min_l(\varepsilon\mu_l)$]. When selection acts strongly in both populations ($N_l w_l > 1$), then the mixing time is proportional to $1/\min_l(N_l w_l \varepsilon\mu_l)$. In this latter case, the mixing time *decreases* with increasing population size, owing to a higher substitution rate of beneficial mutations (which drive the evolutionary dynamics of the antagonism game (3.1)) in larger populations (see [546, Appendix

Section S5.2]. That the mixing time in either case does not increase rapidly with increasing population size, and in fact decreases in the case of strong selection, indicates that the stationary distribution will be relevant on realistic timescales.

3.4.2 Weak mutation

To gain a greater understanding of the above results, we study the analytically tractable case of rare mutations, $\varepsilon \to 0$, using the methodology developed in ref. [543].

In this 'weak-mutation limit', the long-run stationary distribution collapses to a distribution over just the four pure states, $\boldsymbol{\lambda} = \left[\lambda_{(A,C)}, \lambda_{(A,D)}, \lambda_{(B,C)}, \lambda_{(B,D)}\right]$. The relative success of population 1, as defined above, then simplifies to $\left(\lambda_{(A,C)} + \lambda_{(B,D)}\right) - \left(\lambda_{(A,D)} + \lambda_{(B,C)}\right)$, which, by symmetry of the underlying states ($\lambda_{(A,C)} = \lambda_{(B,D)}$, $\lambda_{(A,D)} = \lambda_{(B,C)}$), is proportional to $\lambda_{(A,C)} - \lambda_{(A,D)}$.

First, we examine the influence of generation time and mutation rate on the success of population 1. We fix $N_1 = N_2 = N$ and $w_1 = w_2 = w$, and write $\gamma = (1+w)^{N-1} > 1$. Define $r_1 = (\mu_1/g_1)/(\mu_2/g_2)$, the relative arrival rate of mutations in population 1. The stationary distribution of the evolutionary process, $\boldsymbol{\lambda} = \left[\lambda_{(A,C)}, \lambda_{(A,D)}, \lambda_{(B,C)}, \lambda_{(B,D)}\right]$, is then

$$\boldsymbol{\lambda} = \left[\frac{1+\gamma r_1}{r_1+\gamma}, 1, 1, \frac{1+\gamma r_1}{r_1+\gamma}\right] / \bar{\lambda}, \tag{3.4}$$

where $\bar{\lambda}$ ensures that $\boldsymbol{\lambda}$ sums to one (calculations in [546, Appendix Section S5.4]). The relative success of population 1 is then

$$\lambda_{(A,C)} - \lambda_{(A,D)} = \frac{(\gamma-1)(r_1-1)}{(r_1+\gamma)\bar{\lambda}}, \tag{3.5}$$

which is increasing in r_1. Since both a higher mutation rate and a shorter generation time for population 1 increase r_1, they are both associated with greater evolutionary success in Red Queen interactions. In fact, this result can be shown to hold far more generally: it does not require that the population sizes and selection strengths be set equal for the two populations, and holds for all standard evolutionary dynamics, including those exhibiting frequency dependence [396, 401, 406, 475, 511] (proof in [546, Appendix Section S5.3]).

A larger population size and a stronger selection strength of population 1 can also be shown to increase its relative evolutionary success, $\lambda_{(A,C)} - \lambda_{(A,D)}$, although the results cannot be written as neatly as in (3.4) [546, Appendix Sections S5.1, S5.2]. Again, these results hold more generally: for many evolutionary processes, including the Moran and Wright-Fisher processes, they hold even if the generation times, mutation rates, and selection strengths are not set equal for the two populations.

3.5 Mutualistic symbioses

In this section, we study the evolutionary dynamics of populations interacting according to the mutualism game (3.2). We take the measure of relative success of population 1 in a given population state to be the proportion of (A, C) matchings in that state minus the proportion of (B, D) matchings. If this quantity is positive, then population 1 has a larger average payoff than population 2 in that state.

3.5.1 Strong mutation, strong selection

As we did for the antagonistic game in the previous section, we begin here by numerically studying the short- and long-run dynamics, when mutations are not rare and selection is not weak. We consider large and small values of k, specifically

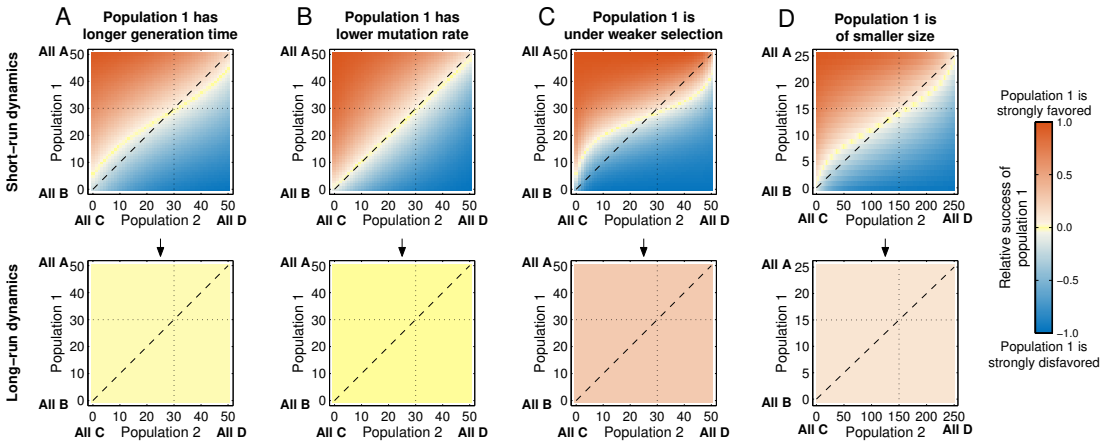

Figure 3.5.1: Evolutionary dynamics of mutualisms when k is small, and population 1 evolves slower than population 2 owing to (A) a longer generation time, (B) a lower mutation rate, (C) weaker selection, and (D) a smaller population size. Population parameters are the same as in Fig. 3.4.1, and $k = 1/2$. A short-run Red Queen effect is observed for generation time, selection strength (especially), and population size. Relative differences in mutation rate again have no discernible short-run effect. In the long run, differences in mutation rate and generation time again have no effect, while a Red King effect is found for selection strength and population size.

$k = 1/2$ and $k = 3/2$.

When $k = 1/2$, and we set the populations' sizes, selection strengths, and mutation rates equal ($N_1 = N_2$, $w_1 = w_2$, $\mu_1 = \mu_2$), and vary their relative generation times g_1 and g_2, we find a weak Red Queen effect in the short-run dynamics for the parameter values we consider: when population 1 has a longer generation time, the set of initial states from which, after 50 generations, the proportion of (A, C) matchings is expected to be less than that of (B, D) matchings is larger than the set of initial states for which the reverse is true (Fig. 3.5.1A). This is similar to Bergstrom and Lachmann's general replicator-dynamics result for $k < 1$ [26].

In the long run, however, the average proportion of (A, C) matchings relative to (B, D) matchings becomes independent of where the dynamics started; this effect

is clear after 50,000 generations (Fig. 3.5.1, lower panels). In this case, we find that differences in generation time between the two populations have almost no effect on their relative success (Fig. 3.5.1A).

We also find that differences in the populations' relative mutation rates μ_1 and μ_2, when their other rate parameters are equal, confer almost no advantage to either population, in both the short run and the long run (Fig. 3.5.1B).

If, instead, we allow the populations' selection strengths w_1 and w_2 to differ, setting their other rate parameters equal, we observe stronger effects. Now, there is a pronounced Red Queen effect in the short-run dynamics, which reverses to a strong Red King effect in the long run (Fig. 3.5.1C). A similar result is found when the populations have equal rate parameters except for their population sizes: when population 1 is smaller (so that it evolves slower—again, see [546, Appendix Section S5.2] for a precise statement of this), it suffers a small disadvantage in the short-run dynamics (a Red Queen effect), but an advantage in the long-run dynamics (a Red King effect) (Fig. 3.5.1D).

When $k = 3/2$, these results reverse (Fig. 3.5.2). We now find a Red King effect in the short-run dynamics, which is largest when evolutionary rate differences between the populations derive from differences in selection strength (Fig. 3.5.2C). This is similar to Bergstrom and Lachmann's general replicator-dynamics result for $k > 1$, and indeed, the upper panels in Figs. 3.5.2A,B,D and Fig. S1 in [546] look very similar to B&L's Fig. 2 [26]. Again, generation time and mutation rate differences have little effect on the long-run dynamics (Fig. 3.5.2A,B). In contrast, a strong Red Queen effect is found in the long-run dynamics when the populations differ in their selection strengths (Fig. 3.5.2C), with population size having a weak Red Queen effect in the long run (Fig. 3.5.2D).

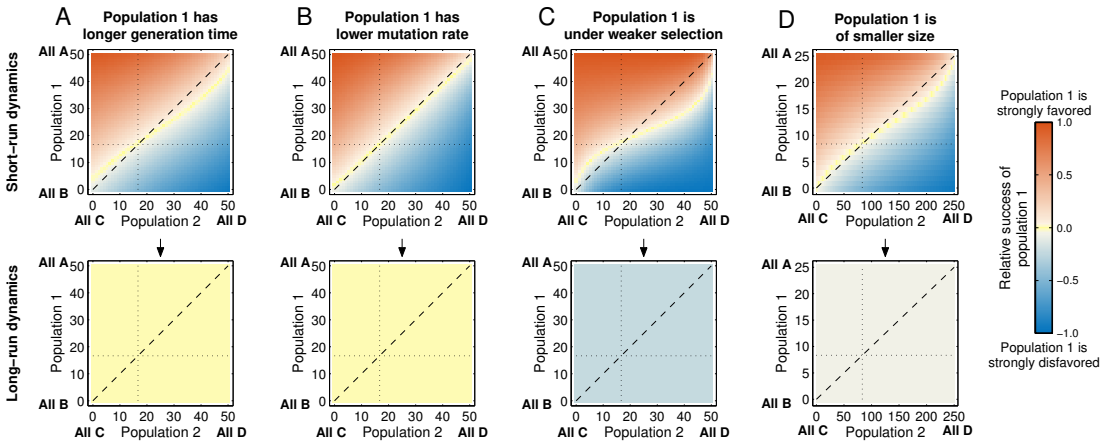

Figure 3.5.2: Evolutionary dynamics of mutualisms when k is large, and population 1 evolves slower than population 2 owing to (A) a longer generation time, (B) a lower mutation rate, (C) weaker selection, and (D) a smaller population size. Population parameters are the same as in Fig. 3.5.1, but now $k = 3/2$. A short-run Red King effect is observed for generation time, selection strength, and population size, with that for selection strength most pronounced. These short-run Red King effects are analogous to that found by Bergstrom and Lachmann [26]. Relative differences in mutation rate have no discernible short-run effect. In the long run, differences in mutation rate and generation time have no effect on the relative success of the populations, while a Red Queen effect is found for selection strength and population size.

To summarize, when mutation rates are not very small, we find, for $k = 1/2$, a Red Queen effect in the short run, and a Red King effect in the long run; for $k = 3/2$, we find a Red King effect in the short run, and a Red Queen effect in the long run. The long-run effects are driven by selection strengths and population sizes; generation times and mutation rates have little effect on the long-run dynamics.

Again, the appropriate definition of the 'long run' is how long it takes for the dynamics to get close to their stationary distribution. This can be computed exactly for small population sizes. In the mutualism game (3.2), for the parameter values we have considered in Figs. 3.5.1 and 3.5.2, Fig. S6 in [546] suggests that the long run could be considered any time after about 1,000-10,000 generations.

For larger population sizes, such computations are not feasible, and we must again resort to approximate analytical arguments. These are detailed in [546, Appendix Section S3]. We summarize their conclusions here. Mutations are assumed to be infrequent. When selection acts weakly in both populations ($N_l w_l < 1$ for $l = 1, 2$), then the mixing time is approximately proportional to $1/\min_l(\varepsilon\mu_l)$. When selection acts strongly in at least one population l, then the mixing time is approximately proportional to $e^{N_l w_l}/(N_l w_l \varepsilon\mu)$ (or, if selection acts strongly in both populations, the largest such value among them).

The exponential term in this last expression is a result of requiring substitutions against selection for the process to mix. It means that the mixing time will be prohibitively long when populations are large and selection acts strongly in them (mixing times increasing exponentially with population size have also been observed in single-population coordination games [32, 263], where transitions between equilibria require evolution against selection too). In these cases, our stationary distributions will not be empirically relevant; evolution over realistic timescales will involve

movement to an equilibrium and then stasis there, as in Bergstrom and Lachmann's analysis [26]. When populations are not large and selection is not very strong, then the stationary distribution will still be reached on a realistic timescale. This will also be true when the *effective* sizes of the populations are not large [73], or when the populations are subdivided into small subpopulations [137, 573], properties that hold for many mutualistic symbionts [61, 101, 374].

3.5.2 Weak mutation

Again, analytical results can be obtained for the long-run dynamics in the weak-mutation limit ($\varepsilon \to 0$), using the methodology developed in ref. [543]. In this limit, the stationary distribution collapses to a distribution over just the pure states, $\boldsymbol{\lambda} = \left[\lambda_{(A,C)}, \lambda_{(A,D)}, \lambda_{(B,C)}, \lambda_{(B,D)}\right]$, and population 1's relative success, as defined above, simplifies to the quantity $\lambda_{(A,C)} - \lambda_{(B,D)}$.

We first examine the influence of generation time and mutation rate. Setting $N_1 = N_2 = N$ and $w_1 = w_2 = w$, but not specifying k, g_1, g_2, μ_1, or μ_2, the stationary distribution of the evolutionary process is

$$\boldsymbol{\lambda} = \left[1, \left(\frac{1}{1+w}\right)^{N-1}, \left(\frac{1+kw}{1+2w}\right)^{N-1}, 1\right] / \bar{\lambda}, \tag{3.6}$$

where $\bar{\lambda}$ ensures that λ sums to one (calculations in [546, Appendix Section S6.1]. As expected, most time in the long run is spent in the two coordination states (A, C) and (B, D), because $w > 0$ and $0 \leq k < 2$. Less intuitively, for small values of k ($< 1/[1+w]$), more time is spent in the worse non-coordination state (A, D) than in the better non-coordination state (B, C).

Similar to the numerical results we obtained for the case where mutations are not very rare, neither the generation times nor the relative mutation rates of the

two populations have any influence on the stationary distribution $\boldsymbol{\lambda}$ in the weak-mutation limit: if populations 1 and 2 are of the same size, and if natural selection acts equally efficiently in them, then they will be equally successful in the long run, no matter their relative generation times or mutation rates. This weak-mutation result in fact holds for all standard evolutionary processes, including those exhibiting within-population frequency dependence, such as the dynamics that govern Müllerian mimicry [546, Appendix Section S6.1].

It turns out (mathematical details in [546, Appendix Section S6.1]) that transitions *against selection* play an important role in this weak-mutation result. For example, while a higher relative mutation rate (or shorter generation time) in population 1 renders the transition from (A, D) to (B, D) more likely than that from (A, D) to (A, C), they also make the reverse transition, from (B, D) to (A, D), more likely than that from (A, C) to (A, D). Because of the symmetry of the fitness changes in these two sets of transitions, these mutations effects (and, similarly, generation effects) cancel out exactly. In words, with a higher mutation rate, population 1 is typically the one that evolves to a coordination equilibrium (in the direction of selection), but it is also typically the one that evolves back out of it (against the direction of selection).

Furthermore, numerical calculations suggest that this weak-mutation result is broadly robust to inequalities in population sizes and selection strengths [546, Fig. S10C,D]: relative mutation rates and generation times have very little effect on the long-run success of the two populations in the weak-mutation limit. (Of course, we have not explored the entire parameter space, and so cannot completely rule out that there exist parameter values where mutation rates and generation times do have an appreciable effect on the relative success of the populations.)

The directional effects of selection strength and population size limit are more subtle. For selection strength, we equate population 1 and 2's sizes at N, and fix population 2's selection strength at $w_2 = w$. Then, if N is sufficiently large, and population 1 has a slightly higher selection strength than population 2, population 1 is less successful when $k < 1/(1+w)$, and more successful when $k > 1/(1+w)$ (proofs in [546, Appendix Section S6.3]). Numerical calculations suggest that the 'sufficiently large' population size is not very large: results for $N = 100$ agree with those above [546, Fig. S10A].

The results are similar if we equate the selection strengths in the two populations at w, and set population 1's size slightly higher than that of population 2: population 1 is less successful when $k < 1/(1+w)$, and more successful when $k > 1/(1+w)$ (proofs in [546, Appendix Section S6.4]). Again, numerical calculations suggest that these results are robust to inequality in mutation rates and generation times, and larger differences in the two populations' sizes when both are sufficiently large [546, Fig. S10B,E,F].

Intuition for these results can be gained by noting that any switch from one coordination state to the other involves two transitions: one transition out of the original equilibrium (against the direction of selection), and a subsequent transition into the new equilibrium state (in the direction of selection). Whether weaker selection (or a smaller population size) favors population 1 depends on which non-equilibrium state is more often passed during these two transitions. This is driven predominantly by the relative probabilities of the transitions against selection, because these probabilities are very sensitive (more so than those of transitions in the direction of selection) to population size, selection strength, and the payoffs involved.

Of the transitions against selection, transitions to (B, C) always involve the fix-

ation of mutants of payoff k in populations of payoff 2, while transitions to (A, D) always involve the fixation of mutants of payoff 0 in populations of payoff 1.

Therefore, when k is large, the passed non-equilibrium state is usually (B, C) [indeed, notice that (B, C) has a higher weight than (A, D) in the stationary distribution (3.6) precisely when $k > 1/(1 + w)$]. Focusing therefore on transitions through (B, C), if population 1 experiences weaker selection (or is of smaller size), the transition from (A, C) to (B, C) occurs more easily than that from (B, D) to (B, C). So we expect more time to be spent in population 1's disfavored equilibrium state (B, D) in the long run—a Red Queen effect.

Contrariwise, if k is small, the passed non-equilibrium state is usually (A, D). So, if selection is less effective in population 1, more time is spent in its favored equilibrium state (A, C)—a Red King effect—because transitions from this state to (A, D), involving fixation of a selected-against mutant in population 2, are relatively very rare.

In contrast to the minor influence of relative mutation rates and generation times on the long-run success of the two populations in the weak-mutation limit, the effect of population size and selection strength is very large. Indeed, when $N_1 = N_2 = 100$ and $w_2 = 0.15$, a small increase in w_1 from 0.15 to 0.16 increases $\lambda_{(A,C)}/\lambda_{(B,D)}$ (another measure of population 1's relative success, useful for illustrating extreme values) about 35% when $k = 1.5$, and decreases it about 30% when $k = 0.8$ [546, Fig. S10A]. Changes of similar magnitude are seen when holding $w_1 = w_2 = 0.15$ and increasing N_1 from 100 to 105 [546, Fig. S10B]. These effects, caused by small changes in population size and selection strength, are larger than those caused by varying relative mutation rates and generation times across ten orders of magnitude [546, Fig. S10C,D]. Larger changes in population size and selection strength

have enormous effects on the long-run relative success of the two populations [546, Fig. S10E,F].

3.5.3 Weak selection

Returning to the effect of mutation rate and generation time, we have shown analytically that these have no effect on the long-run stationary distribution in the weak-mutation limit. To analytically study the long-run effect of mutation rates when they need not be negligibly small, we make use of another recent advance in evolutionary game theory [406]. We impose that the population sizes N, selection strengths w, and generation times g of the two populations be equal. Their mutation rates, $\varepsilon\mu_1$ and $\varepsilon\mu_2$, need not be equal, and we do not impose that $\varepsilon \to 0$. Instead, we assume $w \ll 0$; that is, we assume that selection operates very weakly in the two populations. Long-run Red King and Queen effects consistent with that we have found above for selection strength and population size would have that slower evolution (via a smaller mutation rate) is favored when $k < 1$, and disfavored when $k > 1$ [the threshold for k that was previously relevant, $1/(1 + w)$, tends to 1 as $w \to 0$].

Unlike in the weak-mutation case, the stationary distribution of this process places non-negligible weight on every possible population state, including those where one or both populations are polymorphic. Again, the relative success of population 1 depends on the long-run proportion of (A, C) and (B, D) matchings, which, following the notation in ref. [406], we denote by $\langle p_A q_C \rangle$ and $\langle p_B q_D \rangle$ respectively. Using Eq. (29) in ref. [406], we calculate the long-run advantage to population 1 in the weak-selection limit:

$$\langle p_A q_C \rangle - \langle p_B q_D \rangle = A(1 - k)\varepsilon(\mu_2 - \mu_1), \tag{3.7}$$

where $A = wN(N-1)/[8(1+[N-1]\varepsilon\mu_1)(1+[N-1]\varepsilon\mu_2)] > 0$ (calculations in [546, Appendix Section S7]). Therefore, when $k < 1$, population 1 does better when it evolves slower ($\mu_1 < \mu_2$), while when $k > 1$, population 1 does better when it evolves faster ($\mu_1 > \mu_2$). We have thus analytically recovered long-run Red King and Queen effects of mutation consistent with those for selection strength and population size. When mutation rates are small ($\varepsilon \ll 1$), the two populations do approximately equally well, consistent with our weak-mutation results above.

3.6 Discussion

We have placed the evolution of symbioses, both antagonistic and mutualistic, into a simple finite-population model, and studied the effect of parameters that influence the rate of evolution of the participating populations on those populations' relative success.

Among these 'rate parameters', mutation rate and generation time are perhaps the most obvious and responsive [51, 210, 400, 491, 492, 498, 549, 577]. Selection strengths, though also a clear determinant of evolutionary rate, seem more of a fixed property of an interaction, but could change over time if one population reduces its dependence on the interaction [121], or actively increases the dependence of its interactant [588]. Population size is perhaps the most complicated of the rate parameters, because changes in the relative success of interacting populations (possible driven by differences in their population sizes) are expected to manifest themselves in subsequent changes in the populations' sizes [462].

It is important to realize that, though we have studied differences in the relative success of interacting populations caused by different evolutionary rate parameters, our results do not say anything directly about how the rate parameters themselves

should evolve. For example, it is conceivable that a slower generation time leads to greater success for a population (i.e., that a Red King effect holds), but that a faster generation time is selected for within that population. In this example, slow evolution could be interpreted as a public good.

This has important implications for how results such as ours and those of Bergstrom and Lachmann [26] should be interpreted in studies of molecular evolution (e.g., [449]). Though generation times and mutation rates determine the rate of nucleotide substitution at neutral sites [280], were we to find that a slower generation time or a lower mutation rate lead to greater success for a population in a mutualism, this would not necessarily imply that species involved in mutualisms should exhibit lower neutral substitution rates than closely related species not involved in mutualisms.

Examining the evolution of the rate parameters themselves would require a more complicated model than that we have studied. In a population genetic setting, one could posit in each population two distinct genetic loci: a 'strategy locus', the alleles at which determine which game strategies their bearers play, and a 'rate locus', the alleles at which determine the value of a rate parameter such as mutation rate. The evolutionary dynamics would then inform how both the success of the populations and their evolutionary rates evolve. One setting where we might expect evolutionary rate within a population to evolve to increase that population's relative success is if the interacting populations are subdivided into many isolated symbioses (on 'islands'), between which migration occurs (this model is similar to the 'haystack model' considered by Bergstrom and Lachmann [26]). A rate parameter value that improves a subpopulation's success on an island causes that subpopulation to send out more migrants—who bear the rate parameter value—to colonize other islands. Thus, in symbioses with a high degree of population structure, we might expect the

results we have found in this paper to be informative of how evolutionary rate will evolve within populations.

In antagonistic symbioses, we have shown that faster evolution through any of the rate parameters leads to greater evolutionary success in our model, in both the short run and the long run—a clear Red Queen effect (faster evolution is beneficial). Mutation rate and generation time play similar roles in determining the long-run outcome of antagonistic interactions when mutations are infrequent. As far as our results have implications for evolution within populations, this suggests that one population might compensate for an intrinsically longer generation time by evolving an elevated mutation rate. Consistent with this, bacterial strains subjected to antagonistic interactions with bacteriophages often exhibit much higher mutation rates than do control strains [416]. A similar explanation has been suggested for the finding that, in mammals, generation time is positively correlated with the rate of intra-chromosomal recombination [58], which, like mutation, is a generator of variation [388]. With particular respect to selection strength, the 'life-dinner principle' [121] holds in our model: in an antagonistic interaction, the population for whom the interaction matters more (the rabbit, not the fox) is evolutionarily more successful.

In mutualistic symbioses, we have uncovered an important influence of evolutionary timescale on the relative success of interacting populations, with results in the short-run and long-run often being in opposition.

In the short run, the stochastic evolutionary dynamics that we have studied are similar to the deterministic dynamics studied by Bergstrom and Lachmann [26], and our short-run results replicate theirs. In particular, we find a short-run Red Queen effect when k is small in game (3.2), and a short-run Red King effect (slow evolution

is beneficial) when k is large. Our analysis extends that of B&L by allowing us to determine which of the biological rate parameters drive these effects; to wit: generation times, population sizes, and (especially) selection strengths.

In the long run, we find a Red King effect when k is small, and a Red Queen effect when k is large, contrary to the short-run results. Among the rate parameters that could drive these long-run results, mutation rate and generation time in fact have little to no effect on the long-run relative success of mutualistic populations, unless mutation is frequent. This is a surprising result, given that mutation rate and generation time are perhaps the most prominent determinants of evolutionary rate. This result depends on the possibility of evolution against selection, always present in stochastic evolutionary dynamics. It could not be discovered using deterministic evolutionary dynamics, because in such dynamics, evolution always proceeds in the direction of selection. Deterministic dynamics admit little notion of the strength of selection: selection is either 'positive' or 'negative'. In reality, selection is a continuum—as the Red Queen said to Alice, "*I* could show you hills, in comparison with which you'd call that a valley" [68]—and deleterious mutations do sometimes fix because of random drift, especially in populations that are not very large [280, 333, 356, 404, 405].

The long-run Red King and Queen effects in mutualisms, for small k and large k respectively, instead operate predominantly in our model through the *efficiency of selection* (which increases with selection strength and population size), not the generation of variation (mutation and generation rates).

With short-run and long-run results differing so starkly, timescale clearly matters for evolution in mutualisms in our model. The short-run dynamics depend critically on their starting point. Comparisons of the populations' short-run rela-

tive success, both in our analysis and B&L's [26], involve counting the proportion of non-equilibrium starting states from which evolution leads to each equilibrium. This implicitly assumes every starting state to be equally likely, a problematic assumption. In addition, interpretation of 'starting points' in a continuous process like evolution is itself problematic. Analysis of the long-run dynamics, which become independent of where they started, obviates these problems.

Which results, short-run or long-run, are relevant to a specific case depends on which evolutionary timescale is appropriate. Again, this question is treated quantitatively in [546, Appendix Section S3]. In mutualisms, the long-run dynamics are characterized by transitions between the equilibria—involving evolution first against, and then with, selection—so the applicability of our long-run results depends on the timescale of these transitions. When both populations are very large and under strong selection, the time it takes for a transition between equilibria to occur can be so long as to be empirically irrelevant; here, the short-run dynamics are of more interest. When the populations have small effective population sizes (owing to small census size, or population structure, for example) or selection acts weakly in them, equilibrium transitions can be frequent, and the long-run dynamics apply.

In our analysis, we have made several modeling decisions and simplifying assumptions:

We have assumed that interactions are pairwise, for simplicity. The consideration of multiplayer games [115, 185–188, 354, 587] is a desirable extension, and has been shown to influence the outcome of mutualism games in infinite populations [187] and antagonism and Snowdrift games in finite populations [115].

In deriving our main analytical results, we assumed that mutations are very in-

frequent. This is a realistic assumption in many cases, but not always. Fig. S5 in [546] shows that mutation rates in the two populations do not have to be exceedingly small for our weak-mutation analytical results to be an excellent quantitative match [434, 543, 586], and Figs. S2-5 in [546] suggest that, even for very large mutation rates, the long-run relative success of the populations qualitatively matches our weak-mutation results in most cases. The only notable exceptions, all for the mutualism game (3.2), are (i) for large k, when the populations have different selection strengths, a strong long-run Red Queen effect for small mutation rates reverses to a weak Red King effect when mutation rates are very large [546, Figs. S2C,S5C]; (ii) when the populations have different mutation rates and both their mutation rates are very large, then, contrary to our weak-mutation result where differences in mutation rates have no effect, we find a long-run Red King effect for small k [546, Figs. S3B,S5B] and a Red Queen effect for large k [546, Figs. S2B,S5C] [exception (ii) is consistent with our weak-selection result, (3.7)]; (iii) for small k, generation time has a Red Queen effect for intermediate and large mutation rates [546, Figs. S3A,S5B]. We note that a very recent methodological advance in the study of stochastic evolutionary dynamics [542] suggests that tractable analytical study of the stationary distribution outside the weak-mutation regime may soon be possible.

In finite-population evolutionary game theory, game payoffs π must be translated to positive fitnesses f [396], with this translation calibrated by a strength of selection w. We have employed the commonly-used linear translation $f = 1 + w\pi$, but others are also possible. The exponential translation $f = \exp(w\pi)$ has the advantage that it guarantees fitnesses always to be positive, no matter the range of game payoffs, and also sometimes allows for neater characterization of long-run dynamics [33, 103, 519, 520]. Results are expected to be similar for the two translations, and

they are identical in the weak-selection limit $w \to 0$. Fig. S5 in [546] suggests that our results are essentially unchanged when we employ either translation.

The dynamics in our model, based on the widely-used Moran process, are highly stylized, especially in their assumption of constant population sizes over time. It would be interesting to study the evolutionary dynamics of games (3.1) and (3.2) using more complicated inter-generational population dynamics [189, 417, 493].

Finally, the games themselves are particular simplifications of more complex interactions. One key simplification in games (3.1) and (3.2) is that strategies are discrete: A, B, C, and D. This will be relevant for many antagonistic symbioses; for example, it is probably a realistic summary that a pathogen is either resistant or not to a host's defenses. For mutualisms, we have motivated the discrete game (3.2) with examples that exhibit such discreteness, such as division of labor, and Müllerian mimicry. However, many mutualisms are likely to involve continuous strategies: for example, how much energy to expend on a cooperative or altruistic task, as in the degree to which an ant colony protects from herbivores the plant that houses and feeds it [167], and in turn the energy the plant dedicates to housing and feeding the ants. For such cases, an alternative, continuous-strategy model specification is appropriate.

An attractive option is a simple modification of a Nash bargaining game [386]. Players 1 and 2 choose activity levels x and y. If $x + y > 1$, then both receive zero payoff. If $x + y \leq 1$, then player 1 receives payoff $\alpha x + (1-\alpha)y$, and player 2 receives $\alpha y + (1-\alpha)x$. $\alpha \in (0, 1)$ calibrates the degree to which players' payoffs depend on their own actions. As long as $x + y < 1$, both players' payoffs increase if either player increases its activity, so that the game is mutualistic. But when α is small, each player would prefer to have a lower activity than the other, while when α is

large, each would prefer to have the larger activity. Unlike in the discrete-strategy mutualism game, where there were two discrete equilibria, here there is a continuous path of equilibria (the line $x + y = 1$). In [546, Appendix Section S8], we study the co-evolutionary dynamics of populations of player 1s and 2s. The short-run dynamics in this game involve evolution to the equilibrium line, while the long-run dynamics are characterized by drift-like movement along and around it.

In both the short and long runs, the faster-evolving population is at an advantage when α is large (a Red Queen effect; [546, Fig. S11]), but a disadvantage when α is small (a Red King effect; [546, Fig. S12]). The short-run effects are driven by all rate parameters. However, similar to what we found for the discrete mutualism game, the long-run effects here are driven predominantly selection strength and population size—differences in mutation rate and generation time have little long-run effect. This is because selection strength and population size contribute differentially here to a case of *drift-induced selection*: stochastic jumps off the equilibrium path return with an average directional bias, so that a drift-induced directional flow operates along the path. Drift-induced selection is a newly-recognized phenomenon that has recently gained attention in the stochastic dynamics literature [99, 100, 547]. It can be studied analytically using diffusion approximations and separations of timescales [419]. Such a study in the context of continuous-strategy mutualisms would be an important extension of our preliminary analysis.

In this vein, studying the finite-population dynamics of other games in which slow evolution has been hypothesized to be beneficial [229] would also be desirable.

4

Assortment and the evolution of cooperation in a Moran process with exponential fitness

4.1 Abstract

We study the evolution of cooperation in a finite population interacting according to a simple model of like-with-like assortment. Evolution proceeds as a Moran process, and payoffs from the underlying cooperator-defector game are translated to positive fitnesses by an exponential transformation. These evolutionary dynamics can arise,

for example, in a nest-structured population with rare migration. The use of the exponential transformation, rather than the usual linear one, is appropriate when interactions have multiplicative fitness effects, and allows for a tractable characterization of the effect of assortment on the evolution of cooperation. We define two senses in which a greater degree of assortment can favour the evolution of cooperation, the first stronger than the second: (i) greater assortment increases, at all population states, the probability that the number of cooperators increases, relative to the probability that the number of defectors increases; and (ii) greater assortment increases the fixation probability of cooperation, relative to that of defection. We show that, by the stronger definition, greater assortment favours the evolution of cooperation for a subset of cooperative dilemmas: prisoners' dilemmas, snowdrift games, stag-hunt games, and some prisoners' delight games. For other cooperative dilemmas, greater assortment favours cooperation by the weak definition, but not by the strong definition. We also show that increasing assortment expands the set of games in which cooperation dominates the evolutionary dynamics. Our results hold for any strength of selection.

4.2 Introduction

Whether like-with-like assortment favours the evolution of cooperation is a critical question in social evolution and population biology more generally [139, 159, 197, 327, 399, 424]. Assortment can result if interactions are often between related individuals (e.g., if the population is 'viscous'; [209, 512]), or if individuals prefer to interact with those to whom they are similar (homophily; [169, 363]). Any theoretical analysis of the relationship between assortment and cooperation requires the synthesis of two models: one for cooperative interactions, and one for population

assortment.

The simplest models of cooperation are games between two players, where each player has available to it the same two strategies: cooperate (C) and defect (D). The paradigmatic example is the prisoners' dilemma [13, 397, 435], but many other two-strategy games can be interpreted as cooperative dilemmas as well [275, 398, 487].

A simple model of assortment in two-strategy games was developed by Grafen [197]. In his model, individuals can be of two types, corresponding to the two strategies in the underlying game. In a given time-step, an individual interacts with a same-type individual with probability r, and a random member of the population (possibly same-type, possibly not) with probability $1 - r$. Higher values of r correspond to greater degrees of assortment in the population. This model has been extended in many ways [1, 3, 27, 139, 248, 532, 539, 540]

Does increased assortment tend to favour cooperation? Of course, this question is not new, and has been approached from numerous angles. Most analyses have been in a deterministic, infinite-population setting. In such a setting, Hamilton [212, App. A] determines, for several particular games of interest, whether selection is in favour of cooperators or defectors in a population with an interaction structure identical to that in [197]. Extending this, Eshel and Cavalli-Sforza [139] analyze the effect of Grafen's assortment parameter on the conditions for evolutionary stability of cooperation and defection. They show that, for cooperative dilemmas broadly defined (two cooperators do better than two defectors, and a defector does better than a cooperator when faced with a cooperator), there are threshold assortment levels $0 < r^{**} < r^{*} < 1$ such that, if $r > r^{*}$, cooperation is the only ESS, but if $r < r^{**}$, defection is an ESS (and the only one in the case of a prisoners' dilemma). That is, sufficiently high relatedness renders cooperation evolutionarily stable, while

sufficiently low relatedness renders defection evolutionarily stable.

More recently, the effect of assortment on the evolution of cooperation has been studied in the context of finite populations subject to stochastic evolution. In this setting, a natural measure of the success of a strategy is the weight of its pure state (where the population is monomorphic for that strategy) in the stationary distribution of the evolutionary process [4, 170, 533, 543]. In a two-strategy game (such as the usual cooperative dilemmas) with symmetric, small mutation rates, the superiority of one strategy over the other corresponds to its having a higher fixation probability [4, 170]. In a very general model of social evolution that allows for arbitrary dependence of payoffs on strategy frequencies and population structure of any sort, van Cleve [531] derives, in the limit of weak selection, the conditions under which the fixation probability of cooperation exceeds that of defection.

An alternative way to study whether assortment aids cooperation is to determine the effect on key parameters of the evolutionary process, positive or negative, of marginal changes in the assortment parameter. In the economics literature, this general approach is called 'comparative statics': rather than trying to determine the *exact* effect a change in one variable has on another, we instead try to determine just the *direction* of the effect (its 'comparative static'). Many empirical studies of social evolution test the broad 'comparative statics' statement that increased relatedness should be associated with more cooperation, and much of social evolutionary theory is interpreted in this way [164]. It is therefore important that the comparative statics of social evolution be studied extensively from a theoretical perspective.

A step in this direction was recently provided by Allen and Nowak [3], who studied the effect of assortment on the evolution of cooperation in a finite population subject to Wright-Fisher evolution. Interaction each period accords with Grafen's

assortment process, with expected payoffs derived from an underlying two-strategy game. Expected payoffs are translated to fitnesses according to a linear mapping mediated by a selection strength parameter w, and the next period's population composition is chosen stochastically on the basis of these fitnesses. Allen and Nowak [3] derive analytical results for the 'weak selection limit', $w \to 0$. In this limit, for most cooperative dilemmas, increasing relatedness favours cooperation in the sense that it increases the fixation probability of a single cooperator relative to that of a single defector.

Here, we make use of a relatively recent advance in the study of finite-population evolutionary game theory to give a more general characterization of the comparative statics of assortment in Grafen's model. We model evolution as a Moran process [375], occurring in a finite population that interacts according to Grafen's assortment model. Expected payoffs translate to fitnesses according to an *exponential* mapping mediated by a selection strength parameter w [520].

In this setup, we find that increasing r increases the fixation probability of a cooperator relative to that of a defector for the same set of cooperative dilemmas to which the result in Allen and Nowak [3] applies. However, our result holds for *any* strength of selection, while that of Allen and Nowak [3] holds only for weak selection. We also define a stronger sense in which increased r favours cooperation, and show that this too holds for a natural class of cooperative dilemmas: prisoners' dilemmas, snowdrift games, stag-hunt games, and some prisoners' delight games. To distinguish this stronger definition, we provide an example of a cooperative dilemma where assortment favours cooperation by the weaker definition of Allen and Nowak [3], but not by our stronger definition. Finally, we define what it might mean for assortment to favour cooperation outside the context of any particular game, using

the 'containment order' notion of Peña et al. [424]. We show that assortment favours cooperation in our model according to this definition.

For most of this work, we follow in the footsteps of many others [1, 27, 139, 197, 248, 409, 532] by treating r as an abstract assortment parameter without specifying how this assortment arises mechanistically. In Section 4.7, however, we illustrate how our model could apply to a nest-structured population. In this setting, the parameter r quantifies the frequency of interaction among nest-mates.

4.3 Model

Social interactions are between two individuals, with the payoffs from any one interaction defined by the payoff matrix

	C	D
C	R	S
D	T	P

(4.1)

The population is of constant size N. Each member's type is either cooperator (plays C) or defector (plays D). Each period, each member of the population receives its expected payoff from the following interaction: with probability r, it interacts with an individual of the same type, and with probability $1-r$, it interacts with a random member of the population, with each member equally likely. We allow for the possibility of self-interaction, to simplify the analysis. In [103, Appendix A], we show that our main results, Propositions 1 and 3, also hold when self-interaction is not allowed, while a modified version of Proposition 2 holds.

The population state at a given time is defined by the number of cooperators, i.

If $1 \leq i \leq N-1$, then the expected payoff to a cooperator and a defector are:

$$\begin{aligned} \pi_i^C &= rR + (1-r)\frac{iR + (N-i)S}{N}, \\ \pi_i^D &= rP + (1-r)\frac{iT + (N-i)P}{N}. \end{aligned} \tag{4.2}$$

These expected payoffs in turn translate to positive fitnesses f_i^C and f_i^D according to some positively monotonic transformation f, which we assume for simplicity also to be differentiable ($f > 0, f' > 0$). We discuss the choice of transformation in Section 4.4.

Evolution is modelled as a Moran process [375, 396]. Each period, the fitnesses of the cooperators and defectors in the population are calculated as above. One member is chosen for reproduction; the probability of being chosen is proportional to fitness. One member of the population is chosen to die; each member is equally likely to be chosen. A new individual is then born, taking the place of the one chosen to die. The new individual is of the same type as its parent, the member chosen for reproduction (which can be the same as the individual that was chosen to die).

Thus, if there are i cooperators this period in the population, with $1 \leq i \leq N-1$, then denoting by $p_{i,j}$ the probability that there will be j cooperators next period, we have:

$$\begin{aligned} p_{i,i+1} &= \frac{N-i}{N} \cdot \frac{if_i^C}{if_i^C + (N-i)f_i^D}, \\ p_{i,i-1} &= \frac{i}{N} \cdot \frac{(N-i)f_i^D}{if_i^C + (N-i)f_i^D}, \\ p_{i,i} &= 1 - p_{i,i+1} - p_{i,i-1}, \\ p_{i,j} &= 0 \qquad \text{if } j \notin \{i-1, i, i+1\}. \end{aligned} \tag{4.3}$$

Now consider the probability that a single cooperator, presently in a population that is otherwise all defectors, takes over the population; i.e., its 'fixation probability', ρ^C. For our frequency-dependent Moran process, this is given by [396]:

$$\rho^C = \frac{1}{1 + \sum_{j=1}^{N-1} \prod_{i=1}^{j} \frac{f_i^D}{f_i^C}}.$$

The fixation probability of a single D in a population otherwise all-C is

$$\rho^D = \frac{\prod_{i=1}^{N-1} \frac{f_i^D}{f_i^C}}{1 + \sum_{j=1}^{N-1} \prod_{i=1}^{j} \frac{f_i^D}{f_i^C}}.$$

From these expressions, the 'relative fixation probability of cooperation', ρ^C/ρ^D, simplifies to:

$$\frac{\rho^C}{\rho^D} = \prod_{i=1}^{N-1} \frac{f_i^C}{f_i^D}.$$

4.4 Payoff-to-fitness transformations

To move from game interaction to reproduction, one must specify some transformation of payoff (π_i^C and π_i^D in our model) to fitness (f_i^C and f_i^D, respectively). Here, 'fitness' is shorthand for all those things that determine the rate at which an organism reproduces, i.e., its viability, fecundity, and fertility, although fecundity is the most natural interpretation in the Moran process that we study. We require that the payoff-to-transformation f be monotonic, so that fitness increases with payoff, and that it be positive. A common choice is a linear transformation such as $f = 1 + w\pi$, where $w > 0$ represents selection strength.

Some of our results will apply to any transformation that is monotonic, positive, and differentiable. For most of our results, however, we follow Blume [33] and

Traulsen et al. [520] by using an exponential transformation $f(x) = \exp(wx)$, so that

$$f_i^C = \exp\left(w\pi_i^C\right),\ f_i^D = \exp\left(w\pi_i^D\right), \tag{4.4}$$

where w is the strength of selection. This choice of transformation is for the most part arbitrary [520]. But in the common linear transformation, $f = 1 + w\pi$, when some payoffs are negative, the selection strength needs to be sufficiently small to ensure that all fitnesses are positive. In contrast, the exponential transformation that we use guarantees that all fitnesses are positive, even if some payoffs in the underlying game are negative.

Moreover, the exponential transformation is conducive to a 'multiplicative fitness effects' interpretation. If an individual has a total of K interactions, with each interaction k having a small fitness consequence $\exp\left(w\pi^k/K\right) \approx 1 + w\pi^k/K$, and if these fitness consequences combine multiplicatively, then the total fitness consequence is

$$f = \prod_{k=1}^{K} \exp\left(w\pi^k/K\right) = \exp\left(w\frac{1}{K}\sum_{k=1}^{K}\pi^k\right).$$

If the π^k are interpreted as payoffs from an underlying game, then the expression above can be read as $\exp(w\pi)$, where π is the average payoff to the individual. Treating averages as expectations, this is the same as the expression in (4.4).

Finally, we note that in the weak selection limit $w \to 0$, the exponential fitness transformation (4.4) coincides with the usual linear fitness transformation $f = 1 + w\pi$, since Taylor expanding (4.4) around $w = 0$ gives $\exp(w\pi) = 1 + w\pi + \mathcal{O}(w^2)$. Thus, models that use the linear fitness transformation and the weak selection limit (e.g. [3, 401]) can be thought of as special cases of the exponential fitness formulation

[585].

4.5 Defining when assortment favours cooperation

We are interested in whether, and under what conditions, assortment favours cooperation. To proceed, we must address two semantic questions. First, how is cooperation defined? Second, given a suitable definition of cooperation, what does it mean for it to be favoured by assortment?

For strategy C in game 4.1 to be represent cooperation, there are three comparisons one might consider:

C1. $R \geq P$ (Mutual cooperation is better than mutual defection)

C2. $R \geq S$ (Cooperation helps opposing cooperators)

C3. $T \geq P$ (Cooperation helps opposing defectors)

One may also consider strict versions of these inequalities; these will be denoted with primes (for example, C1$'$ denotes $R > P$). For the game to be a dilemma, there must be some temptation to defect, which could be any of the following:

D1. $T \geq R$ (Better to defect vs. cooperators)

D2. $P \geq S$ (Beter to defect vs. defectors)

D3. $T \geq S$ (Defector is favoured in C-D interaction)

The six conditions C1–C3 and D1–D3 include all possible pairwise comparisons of payoffs. If all are satisfied in their strict form, the game is a Prisoner's Dilemma ($T > R > P > S$). Following Nowak [398], we define a *cooperative dilemma* to be any game satisfying C1$'$, and at least one of D1$'$–D3$'$. This definition can be considered

minimal, in that other definitions in the literature [3, 223, 275, 424] require more stringent conditions.

Having defined a cooperative dilemma, we now consider what it might mean for assortment to favour cooperation. Our first definition centers on the quantities $p_{i,i+1}/p_{i,i-1}$, which we term the 'relative rate of increase of cooperation' at population state i. We can say assortment favours cooperation if it increases the relative rate of increase of cooperation for all interior i:

Definition 1. *For a given cooperative dilemma, assortment favours cooperation in the* strong sense *if* $\frac{\partial}{\partial r}\frac{p_{i,i+1}}{p_{i,i-1}} > 0$ *for all* $i = 1, \ldots, N-1$.

In our second definition, we say that assortment favours cooperation if it increases the relative fixation probability of cooperation, ρ_C/ρ_D:

Definition 2. *For a given cooperative dilemma, assortment favours cooperation in the* weak sense *if* $\frac{\partial}{\partial r}\frac{\rho^C}{\rho^D} > 0$.

The use of the terminology 'weak' and 'strong' for these definitions is justified by the fact that the strong definition implies the weak definition: if $\frac{\partial}{\partial r}\frac{f_i^C}{f_i^D} > 0$ for all $i = 1, \ldots, N-1$, then clearly $\frac{\partial}{\partial r}\prod_{i=1}^{N-1}\frac{f_i^C}{f_i^D} > 0$.

Definitions 1 and 2 characterize what it means for assortment to favour cooperation in a given cooperative dilemma. One can also ask what it means for assortment to favour cooperation generally, outside the context of any particular game. To address this question, we propose a third definition, based on the 'containment order' notion of Peña et al. [424]. Informally, this definition asserts that assortment favours cooperation if it expands the set of games for which cooperation is favored. For the formal definition, let $\mathcal{C}$ denote the set of games satisfying C1′, C2, and C3. (These games can be seen as 'strongly cooperative'). For any $r > 0$, let $\mathcal{S}(r) \subset \mathcal{C}$ be the subset of games for which $\rho_C > \rho_D$.

Definition 3. *Assortment favours cooperation in the* containment order sense *if* $\mathcal{S}(r_1) \subset \mathcal{S}(r_2)$ *whenever* $r_1 < r_2$.

Equivalently, assortment favours cooperation in the containment order sense if, for any game in the set $\mathcal{C}$ and any $r_1 > 0$, $\rho_C > \rho_D$ for $r = r_1$ implies that $\rho_C > \rho_D$ for $r > r_1$. Peña et al. [424] also define a 'volume order' notion under which assortment can favour cooperation: if it increases the volume of the set of games for which cooperation is favoured. This is weaker than the containment order notion, and so if in our model assortment favours cooperation in the containment order sense, it does so in the volume order sense as well.

4.6 Results

We first consider the question of when assortment favours cooperation in the strong sense of Definition 1. Notice that, given the Moran process transition probabilities in (4.3), $p_{i,i+1}/p_{i,i-1} = f_i^C/f_i^D$. So the condition for assortment to favour cooperation in the strong sense simplifies to $\frac{\partial}{\partial r}\frac{f_i^C}{f_i^D} > 0$ for all $i = 1, \ldots, N-1$. This allows us to analyze for which games assortment favours cooperation in the strong sense, having made no assumptions about the nature of payoff-to-fitness transformation f beyond the requirement that it be positively monotonic, positive, and differentiable:

Proposition 1. *Assortment favours cooperation in the strong sense for any game satisfying C2 and C3 (that is,* $R \geq S$ *and* $T \geq P$*), with at least one inequality strict.*

Proof. Suppose $R \geq S$ and $T \geq P$, with at least one inequality strict. We have from

(4.2) that, for $1 \leq i \leq N-1$,

$$\begin{aligned}\frac{\partial}{\partial r}\pi_i^C &= R - \frac{iR + (N-i)S}{N} = \frac{N-i}{N}(R-S) \geq 0,\\ \frac{\partial}{\partial r}\pi_i^D &= P - \frac{iT + (N-i)P}{N} = \frac{i}{N}(P-T) \leq 0,\end{aligned}$$

with at least one of these inequalities strict. But, because the fitnesses f_i^C and f_i^D are increasing with respect to π_i^C and π_i^D respectively,

$$\begin{aligned}\frac{\partial}{\partial r}f_i^C &= f'(\pi_i^C)\frac{\partial}{\partial r}\pi_i^C \geq 0,\\ \frac{\partial}{\partial r}f_i^D &= f'(\pi_i^D)\frac{\partial}{\partial r}\pi_i^D \leq 0,\end{aligned}$$

with at least one inequality strict. It follows that $\frac{\partial}{\partial r}\frac{f_i^C}{f_i^D} > 0$. □

The assumption that f be differentiable is for neatness, but can be safely dropped with an obvious restatement of Definition 1 that f_i^C/f_i^D just be increasing in r.

An alternative definition of the 'relative rate of increase of cooperation' at population state i is the expected increase in the share of cooperators, $p_{i,i+1} - p_{i,i-1}$, which can also be shown to be increasing in r when $R \geq S$ and $T \geq P$, with at least one inequality strict. This follows from Proposition 1 and the fact that $p_{i,i+1}$ is increasing, and $p_{i,i-1}$ decreasing, in f_i^C/f_i^D.

For the remainder of our results, we use the exponential transformation (4.4). With this transformation, the relative rate of increase of cooperation is calculated by successively applying (4.3) and (4.4):

$$p_{i,i+1}/p_{i,i-1} = f_i^C/f_i^D = \exp\left(w\left[\pi_i^C - \pi_i^D\right]\right), \tag{4.5}$$

with π_i^C and π_i^D as specified in (4.2). Using this, we can prove a partial converse to

Proposition 1 in the case of exponential fitness, which shows that Proposition 1 can be strengthened to an 'if, and only if' statement provided the population size N is sufficiently large.

Proposition 2. *If assortment favours cooperation in the strong sense, then one of the following three sets of conditions is satisfied:*

(2a) $R \geq S$ *and* $T \geq P$*, with at least one inequality strict.*

(2b) $R > S$*,* $T < P$*, and* $N < \frac{R-S+P-T}{P-T}$*.*

(2c) $R < S$*,* $T > P$*, and* $N < \frac{S-R+T-P}{S-R}$*.*

Proof. We have from (4.5) that

$$\frac{\partial}{\partial r}\frac{p_{i,i+1}}{p_{i,i-1}} = \exp\left(w\left[\pi_i^C - \pi_i^D\right]\right) w \frac{\partial}{\partial r}\left[\pi_i^C - \pi_i^D\right],$$

and since the exponential is positive, the sign of $\frac{\partial}{\partial r}\frac{p_{i,i+1}}{p_{i,i-1}}$ is the same as the sign of $\frac{\partial}{\partial r}\left[\pi_i^C - \pi_i^D\right]$. Writing $x := i/N$, so that $x \in (0,1)$, we have from (4.2) that this quantity is given by

$$\begin{aligned} \frac{\partial}{\partial r}\pi_i^C - \frac{\partial}{\partial r}\pi_i^D &= [R - xR - (1-x)S] - [P - xT - (1-x)P] \\ &= (1-x)(R-S) + x(T-P). \end{aligned} \tag{4.6}$$

We prove Proposition 2 by considering all possible cases for the signs of $R - S$ and $T - P$.

- From Proposition 1, we know that if $T \geq P$ and $R \geq S$ (with at least one inequality strict), $\frac{\partial}{\partial r}\frac{p_{i,i+1}}{p_{i,i-1}} > 0$.
- If $R \leq S$ and $T \leq P$, both terms in (4.6) are non-positive, and so $\frac{\partial}{\partial r}\frac{p_{i,i+1}}{p_{i,i-1}} \leq 0$.

- If $R < S$ and $T > P$, the term $R - S$ in (4.6) is negative, and the term $T - P$ is positive. The expression (4.6) is therefore increasing in $x := i/N$, and therefore smallest when $i = 1$. So, in this case, $\frac{\partial}{\partial r}\frac{p_{i,i+1}}{p_{i,i-1}} > 0$ for each $i = 1, \ldots, N-1$ if, and only if, (4.6) is positive when $i = 1$. When $i = 1$, (4.6) equals $[(N-1)(R-S) + (T-P)]/N$, which is positive if, and only if, $N < (S - R + T - P)/(S - R)$.

- If $R > S$ and $T < P$, the term $R - S$ in (4.6) is positive, and the term $T - P$ is negative. The expression (4.6) is therefore decreasing in $x := i/N$, and therefore smallest when $i = (N-1)/N$. So, in this case, $\frac{\partial}{\partial r}\frac{p_{i,i+1}}{p_{i,i-1}} > 0$ for each $i = 1, \ldots, N-1$ if, and only if, (4.6) is positive when $i = (N-1)/N$. When $i = (N-1)/N$, (4.6) equals $[(R-S) + (N-1)(T-P)]/N$, which is positive if, and only if, $N < (R - S + P - T)/(P - T)$.

□

We now determine how much broader the conditions are under which assortment favours cooperation in the weaker sense of Definition 2.

As noted by Traulsen et al. [520], the ratio of fixation probabilities ρ^C/ρ^D in the frequency-dependent Moran process simplifies significantly with the exponential fitness transformation (4.4):

$$\begin{aligned} \frac{\rho^C}{\rho^D} &= \prod_{i=1}^{N-1} \frac{f_i^C}{f_i^D} = \prod_{i=1}^{N-1} \exp\left(w\left[\pi_i^C - \pi_i^D\right]\right), \\ &= \exp\left(w \sum_{i=1}^{N-1} \left[\pi_i^C - \pi_i^D\right]\right). \end{aligned} \tag{4.7}$$

But in our case, we have from (4.2) that for each i, $\pi_i^C + \pi_{N-i}^C = 2rR + (1-r)(R+S)$

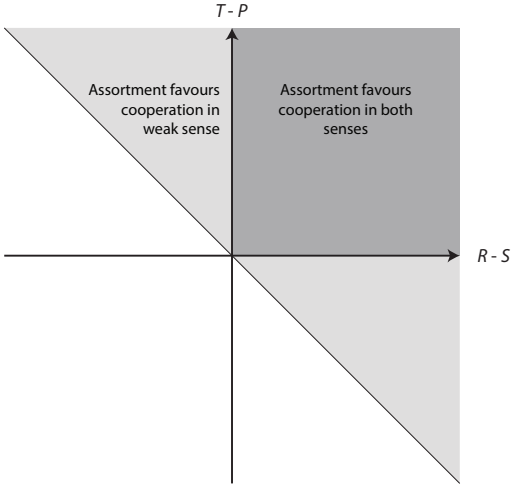

Figure 4.6.1: A summary of our results for two-player games. Assortment favours cooperation in the *strong sense* (increases the relative rate of increase of cooperators for all intermediate population states) if $R \geq S$ and $T \geq P$, with at least one inequality strict (blue and red cross-hatch). For large enough population sizes, this is a necessary condition as well. Assortment favours cooperation in the *weak sense* (increases the fixation probability of a single cooperator, relative to a single defector) if, and only if, $R - S > P - T$ (blue).

and $\pi_i^D + \pi_{N-i}^D = 2rP + (1-r)(T+P)$ [if N is even, $\pi_{N/2}^C = rR + (1-r)(R+S)/2$ and $\pi_{N/2}^D = rP + (1-r)(T+P)/2$]. Grouping payoff terms for i and $N-i$ in (4.7), we see that, for both odd and even N,

$$\begin{aligned} \frac{\rho^C}{\rho^D} &= \exp\left(w\frac{N-1}{2}[2rR + (1-r)(R+S) - 2rP - (1-r)(T+P)]\right) \\ &= \exp\left(w\frac{N-1}{2}[(R-P+S-T) + r(R-P-S+T)]\right). \end{aligned} \tag{4.8}$$

This allows us to analyze for which games assortment favours cooperation in the weak sense of Definition 2 (Fig. 4.6.1).

Proposition 3. *Assortment favours cooperation in the weak sense if, and only if,* $R - S > P - T$.

Proof. From (4.8), we have that

$$\frac{\partial}{\partial r}\frac{\rho^C}{\rho^D} = \exp\left(w\frac{N-1}{2}[(R-P+S-T)+r(R-P-S+T)]\right)w\frac{N-1}{2}(R-P-S+T).$$

Since the exponential is positive, $\frac{\partial}{\partial r}\frac{\rho^C}{\rho^D} > 0 \;\Leftrightarrow\; R-P-S+T>0$. □

This condition corresponds to that found by Allen and Nowak [3] for assortment favouring cooperation in the same weak sense, but their result applies only in the weak selection limit ($w \to 0$), whereas our result holds for all selection strengths.

A corollary of Proposition 3 follows from a result due to Fudenberg and Imhof [170]. Consider an evolving finite population of cooperators and defectors, where cooperators mutate to defectors and defectors to cooperators at the same rate. If this rate of mutation is very small (the 'weak mutation limit'), the long-run distribution of the (ergodic) evolutionary process over all population states $i = 1, 2, \ldots, N$ is close to a distribution over just the two pure states all-D ($i = 0$) and all-C ($i = N$). This distribution is given by $\left(\frac{\rho^D}{\rho^D+\rho^C}, \frac{\rho^C}{\rho^D+\rho^C}\right)$, whose dependence on ρ^C/ρ^D can explicitly be seen in the form $\left(\frac{1}{1+\rho^C/\rho^D}, 1-\frac{1}{1+\rho^C/\rho^D}\right)$. If greater assortment increases the ratio ρ^C/ρ^D (i.e., if assortment favours cooperation in our weak sense), it also increases the weight on the cooperative state in this weak mutation limit.

Corollary 1. *In the Moran process with symmetric mutation rates, in the weak-mutation limit, greater assortment increases the stationary distribution's weight on the cooperative state all-C if, and only if,* $R-P-S+T>0$.

If the condition $R-P-S+T>0$ holds and mutations are very infrequent, then this corollary can be interpreted as follows: at a time point far in the future, a population with a high degree of assortment is more likely to be all cooperating than is a population with a low degree of assortment. Alternatively, among many evolving

populations, cooperation will be more common among those with high assortment than those with low assortment.

We have demonstrated that, for a large class of cooperative dilemmas, assortment favours cooperation in our strong sense, and that for an even broader class, assortment favours cooperation in the weak sense. To demonstrate the utility of the distinction between our weak and strong definitions, we provide an example of a game in which assortment favours cooperation in the weak sense but not the strong sense.

Suppose we have a population of size $N > 10$ interacting according to Grafen's assortment model, with payoffs specified by the game

	C	D
C	$R = 10$	$S = 1$
D	$T = 8$	$P = 9$

.

This is a 'cooperative dilemma' in the sense of Nowak [398] in that it satisfies C1′, C2′, D2′, and D3′. Here, assortment favours cooperation in the weak sense, because $R - P - S + T = 8 > 0$. But assortment does not favour cooperation in the strong sense, because none of the conditions (2a), (2b), and (2c) holds: (2a) and (2c) fail because $T < P$; (2b) fails because $\frac{R-S+P-T}{P-T} = 10 < N$.

Eq. (4.8) tells us that, for a given game (4.1) and value of r, cooperation is favoured in the sense $\rho_C > \rho_D$ if and only if

$$(R - P + S - T) + r(R - P - S + T) > 0. \tag{4.9}$$

This condition allows us to show that assortment favours cooperation in general for

our model, according to Definition 3:

Proposition 4. *Assortment favours cooperation in the containment order sense.*

Proof. For any game in the set $\mathcal{C}$, the coefficient of r in (4.9) is nonnegative, since both $R - S$ and $T - P$ are. The left-hand side of (4.9) is therefore nondecreasing in r. It follows that, for a particular game in $\mathcal{C}$ and a particular assortment value $r_1 > 0$, if $\rho_C > \rho_D$ for $r = r_1$ then $\rho_C > \rho_D$ for $r > r_1$. □

4.7 Realization of the model in a nest-structured population

So far we have described the model in abstract terms. Here we show how the model can be realized in a nest-structured population, with r describing the relative frequency of interaction among nest-mates.

Consider a population with N nests, each containing a single adult. Each time-step corresponds to a single (non-overlapping) generation. Each generation, each adult produces a large number of juveniles. Each juvenile interacts with a large number of others, a proportion r of these being with juveniles from the same nest, and the remaining proportion $1 - r$ being with juveniles chosen uniformly from the population at large. These interactions determine a juvenile's fitness multiplicatively, so that fitness is an exponential function of the sum of individual payoffs.

After interaction, a new head for each nest is chosen, forming the next generation of adults. With high probability ($1 - \mu$, where $\mu \ll 1$ represents the migration rate) the new head of a nest is chosen from among the juveniles who were born at this nest. Otherwise (with probability μ) the new head is chosen from the juvenile population at large. In each case, the choice is made proportionally to fitness.

In the limit $\mu \to 0$, the dynamics of the above model coincide with those of the simple model we have studied in this paper (up to a rescaling of time). The reason

is that, as the migration rate becomes very small, the probability of there being two migrants in a given generation becomes negligible compared to that of there being only one migrant. Thus at most one nest changes its strategy per generation, consistent with the Moran process.

4.8 Games with more than two players

In reality, many cooperative dilemmas are not pairwise interactions, but involve more than two players [159, 188, 407, 423, 539]. Here, we shall demonstrate that our methodology can extend to a particularly simple n-player cooperative dilemma, a linear public goods game. We shall show that increased assortment favours the evolution of cooperation in this case.

Interactions occur in groups of size n, where each interactant is either a cooperator (C) or a defector (D). Assortment is defined as $r = \mathbb{P}(C|C) - \mathbb{P}(C|D)$, where $\mathbb{P}(C|D)$ is the probability that a randomly chosen interactant of a defector is a cooperator, and $\mathbb{P}(C|C)$ is the probability that a randomly chosen interactant of a cooperator is a cooperator [27, 538]. (It is easily seen that $\mathbb{P}(C|C) - \mathbb{P}(C|D) = \mathbb{P}(D|D) - \mathbb{P}(D|C)$, so that this definition does not depend on the labelling of strategies. The definition is also consistent with that used in our two-player setup above and with regression-based definitions of relatedness; see e.g. [30].)

Assortment derives from a 'population structure', which determines, from the number of cooperators in the population, their distribution among the interacting groups. Formally, in a population of size N, a population structure m (for 'matching function') is a vector-valued function that specifies, for each possible number i of cooperators in the population, a probability distribution $(m_{[0]}(i), m_{[1]}(i), \ldots, m_{[n]}(i))$ over the $n+1$ possible group compositions, so that $m_{[j]}(i)$ is the probability that,

when there are i cooperators in the whole population, a randomly chosen group contains exactly j cooperators. (The subscript in $m_{[j]}(i)$ is bracketed to distinguish that this is the number of cooperators in the group, while we have throughout used an unbracketed subscript to indicate the number of cooperators in the whole population.)

One complication arises. In an infinite-population setting [256, 443, 539], where the proportion $x \in [0, 1]$ of cooperators is specified, it is required that the population structure f, applied to the proportion of cooperators x, recapitulate that proportion: $x = \sum_{j=0}^{n} j m_{[j]}(x)$. In our finite-population case, the law of large numbers does not apply: N/n groups drawn independently from the distribution $m(i)$ need not contain a total of i cooperators. To sidestep this complication, we shall make an assumption analogous to that of self-interaction in the two-player game setup: interactants in a group are drawn *with replacement* from the population, according to the distribution $m(i)$. That is, we shall assume that an individual can take on multiple positions in the group, so that a group of n need not contain n distinct individuals.

We shall be interested in the population structures that maintain, for all intermediate $i = 1, 2, \ldots, N-1$, a constant assortment parameter r. One such population structure, and a natural extension of the population structure we analyzed for two-player games, is this: A cooperator's $n-1$ group-mates are, with probability r, all cooperators, and with probability $1-r$ are drawn randomly and independently from the population (i.e., they constitute a binomial sample of size $n-1$). When there are no cooperators in the population (respectively, no defectors), then all groups comprise only defectors (respectively, only cooperators). The exact population structure that leads to a constant r will not matter in what follows, because the game we shall consider is linear. For general (nonlinear) n-player games, the population structure

will matter.

The game played by the n constituents of a group is a linear, or additive, public goods game. A cooperator produces, at individual payoff cost c to itself, a public good that provides benefit b to each member of the group. A defector enjoys the benefits of the public good produced by cooperators in the group, but does not produce any itself. The payoff to a cooperator in a group with j cooperators is $\pi^C_{[j]} = jb - c$, while the payoff to a defector in a group with j cooperators is $\pi^D_{[j]} = jb$.

When there are i cooperators in the population, the expected payoff to a cooperator and a defector are, respectively:

$$\begin{aligned} \pi^C_i &= -c + b + (n-1)\mathbb{P}(C|C)b; \\ \pi^D_i &= (n-1)\mathbb{P}(C|D)b. \end{aligned} \tag{4.10}$$

With a constant-r assortment process, we have [539]:

$$\pi^C_i - \pi^D_i = (n-1)[\mathbb{P}(C|C) - \mathbb{P}(C|D)]b - c + b = (n-1)rb - c + b.$$

As before, we calculate fitness exponentially from expected payoffs, and update the population according to a Moran process. Checking our strong condition by which assortment favours cooperation, Definition 1:

$$p_{i,i+1}/p_{i,i-1} = f^C_i/f^D_i = \exp\left(w[\pi^C_i - \pi^D_i]\right) = \exp\left(w[(n-1)rb - c + b]\right),$$

so that

$$\frac{\partial}{\partial r}\frac{p_{i,i+1}}{p_{i,i-1}} = w(n-1)b\exp\left(w[(n-1)rb - c + b]\right) > 0.$$

Therefore, assortment favours the evolution of cooperation in the strong sense here.

The above results apply to a linear public goods game. For nonlinear public goods games, a single assortment parameter does not suffice to characterize the effects of population structure on natural selection; rather, a full probability distribution over all possible group compositions is required [407, 538]. Therefore, while nonlinear public goods games are important from both a theoretical [11, 188, 423] and empirical [193] perspective, an analysis of how assortment affects cooperation in such games is beyond the scope of the current work.

4.9 Discussion

We have studied the effect of assortment on the evolution of cooperation, making use of a simple model of like-with-like assortment in two-strategy games. We have demonstrated that, for many cooperative games of interest (including prisoners' dilemmas, snowdrift games, and stag-hunt games), increased assortment favours the evolution of cooperation in two senses: it increases the rate at which the cooperative strategy increases in the population, and it increases the fixation probability of cooperators relative to that of defectors.

Most studies of stochastic game theory—for example, Allen and Nowak [3] in a setting similar to ours—assume selection to be weak. This assumption is made because standard stochastic models are otherwise intractable, with analytical results impossible. Here, making use of an exponential transformation of payoffs to fitnesses [520] instead of the usual linear one, we have demonstrated that informative analytical results may be obtained in the more general case allowing any strength of selection. This exponential transformation is not simply a mathematical expediency. We have argued that it is the appropriate transformation of average payoff to fitness when fitness derives from many interactions with multiplicative fitness effects.

Multiplicative fitness effects are a common assumption in population genetics [143], but not in evolutionary game theory, where additive fitness effects are standard. Our results highlight the usefulness of this exponential payoff-fitness transformation in the Moran process, and suggest that this transformation could lead to tractable results for other questions in social evolution and evolutionary game theory more broadly.

Our results give exact conditions for the success of cooperation under arbitrary selection strength. Specifically, Eq. (4.8) implies that cooperation is favored in the sense $\rho_C > \rho_D$ if and only if

$$\sigma R + S > T + \sigma P, \tag{4.11}$$

where

$$\sigma = (1 + r)/(1 - r) \tag{4.12}$$

is the *structure coefficient* [5, 510] of this model. That the condition for success takes the form (4.11) is significant: Tarnita et al. [510] proved that the condition for success takes this form for a large class of models, but only under weak selection. The fact that condition (4.11) applies under any selection strength can be traced to our use of the exponential payoff-to-fitness transformation; one would not expect the same outcome for other models or other transformations.

We observe that σ is increasing in r according to Eq. (4.12). This implies that all of our comparative statics results with respect to r (i.e., pertaining to Definitions 1 and 2) also hold as comparative statics with respect to σ. It also gives another way to understand our containment order result (Proposition 4). Peña et al. [424] show that, for two-strategy games in structured populations, comparing population

structures according to the containment order amounts to comparing their structure coefficients, higher structure coefficients being better for cooperation. Since the structure coefficient for our model is increasing in r, it follows that higher r favours cooperation in the containment order sense.

The structure coefficient in Eq. (4.12) matches that found by Allen and Nowak [3] for a similar discrete-generation model, although the latter result holds only under weak selection. Interestingly, in both cases, σ is independent of the population size. These results can also be understood in terms of the *scaled relatedness coefficient* κ [308, 533], which is related to the structure coefficient by $\sigma = (1+\kappa)/(1-\kappa)$ [531]. Comparing with Eq. (4.12), we see that, for our model and for that of Allen and Nowak [3], the scaled relatedness coefficient κ is equal to the assortment parameter r. This is a consequence of the fact that both models use a *global update rule* [387], meaning that, after game interaction, individuals compete globally for the opportunity to reproduce. Thus, in these models, assortment affects game payoff, but does not further affect the probability of reproduction. For other models such as games on graphs [2, 408, 514], which do not have global updating, local competition effects can cause κ to be different from the degree of assortment.

5

The Trivers-Willard hypothesis: sex ratio or investment?

5.1 Abstract

The Trivers-Willard hypothesis has commonly been considered to predict two things. First, that a mother in good condition should bias the sex ratio of her offspring towards males (if males exhibit greater variation in reproductive value). Second, that a mother in good condition should invest more per son than per daughter.

These two predictions differ empirically, mechanistically, and, as we demonstrate here, theoretically too. We construct a simple model of sex allocation that allows simultaneous analysis of both versions of the Trivers-Willard hypothesis. We show that the sex ratio version holds under very general conditions, being valid for a large class of male and female fitness functions. The investment version of the hypothesis, on the other hand, is shown to hold only for a small subset of male and female fitness functions. Our results help to make sense of the observation that the sex ratio version is empirically more successful than the investment version.

5.2 Introduction

The Trivers-Willard hypothesis (TWH) [525] predicts that, when one sex exhibits more variation in reproductive value, then mothers in good condition should 'prefer' offspring of that sex, and vice-versa for mothers in poor condition. (In polygynous species, the sex with more variable reproductive value is usually males; for convenience we shall adopt this convention throughout.) What should be meant by 'prefer', however, is not entirely clear. Two definitions can be found in the empirical literature.

One definition is that mothers in good condition should bias their individual *sex ratios* towards sons, and mothers in poor condition towards daughters. This interpretation is suggested by the title of Trivers and Willard's original paper, 'Natural selection of parental ability to vary the sex ratio of offspring'. This 'sex ratio version' of the TWH has been the subject of a large empirical literature—well known examples exist for red deer [92, 93], feral horses [66], parasitoid wasps [83], and humans [63, 365].

The second definition is that mothers in good condition should bias their *parental*

care towards sons, and mothers in poor condition towards daughters. This definition also seems to be implied by Trivers and Willard [525]: 'In species with a long period of PI [parental investment] after birth of young, one might expect biases in parental behavior toward offspring of different sex, according to parental condition; parents in better condition would be expected to show a bias toward male offspring.' Many empirical tests of this 'investment version' of the TWH have also been conducted. For example, Fujita et al. [175] conclude that the TWH is supported by their finding that mothers of low socioeconomic status in agropastoral villages in northern Kenya produce more nutritious milk when breastfeeding daughters than sons, and vice-versa for mothers of high socioeconomic status. The assumption that biased parental investment is part of the TWH extends far into the empirical literature—see, e.g., [24, 43, 64, 108, 179, 228, 234, 235, 430, 556], and the references in these papers—and is explicitly defended in [65].

The two versions of the TWH clearly make very different empirical predictions. A broad observation is that the sex ratio version is empirically more successful than the investment version [272]. On the sex ratio version, for example, of the 37 studies of ungulate mammals surveyed by Sheldon and West [480], 29 found a sex ratio effect in the direction predicted by the TWH. 15 of the 37 studies returned significant results ($p < 0.05$); of these 15, 13 were in the direction predicted by the TWH.[1] In a statistical meta-analysis of these studies, Sheldon and West [480] found a significant positive correlation between maternal condition and the proportion of male offspring. In humans, adequately powered empirical tests tend to find a small sex ratio bias in the direction predicted by the TWH [6, 134].

[1] Insignificant results can be explained either by inadequate sample size or constraints imposed by genetic sex determination. Significant results in the opposite direction can be explained by demographic factors [310, 464].

Empirical tests of the investment version, on the other hand, tend to show more mixed results. Only 4 of the 8 studies of nonhuman mammals surveyed by Keller et al. [272] found an investment effect in the direction predicted by the TWH, and studies in humans have proven similarly inconclusive [272]. There could be methodological reasons for this. For example, while it is obvious what outcome to measure when testing for biased sex ratios, it is not as obvious when testing for biases in parental care, since parental care can take many forms [272]. There also does not yet exist an extensive review of empirical tests of the investment version, and so any statements about its empirical success must be preliminary. With these caveats in mind, it is still safe to conclude that the sex ratio version has thus far been empirically more successful.

The two versions of the TWH also differ mechanistically, an observation which has significant implications for research into the physiological and behavioural bases of the parental biases predicted by the hypothesis. The aim of the present paper is to characterize how the two versions differ in theory. This issue has been raised by Carranza [67], who gave a simple graphical example for which the sex ratio version holds while the investment version does not—though see [65] for a critical review of this example.

Though much theoretical work has been carried out on the TWH and sex allocation in general, it has typically not focussed on the distinction between the two versions of the hypothesis that are tested in the empirical literature. Most models of sex allocation—e.g., [162, Sec. 1-3]—combine sex ratio and investment costs into a single variable for each sex, 'parental expenditure' (or 'allocation'). This variable is useful for a number of general arguments, most notably Fisher's principle [129, 154] that, under certain assumptions, total population parental expenditure on offspring

of the two sexes should be equal. Other models of sex allocation have held brood composition fixed, and derived conditions under which parental investment should be biased towards male or female offspring—e.g., [348], [162, Sec. 5], and [318]. Others have focussed simultaneously on sex ratio and clutch size in cases where sibling interaction is relevant, but have not studied the level of parental investment/care in individual offspring [184, 199, 385, 569].

A unified model allowing for simultaneous analysis of the sex ratio and investment versions of the TWH is therefore lacking. Here, we construct a simple model to expose the logic underpinning both the sex ratio and investment versions of the TWH. We show that, while the sex ratio version holds under very general specifications of how adult condition translates to fitness for males and females, the investment version is very sensitive to the nature of these condition-to-fitness translations. This theoretical result helps to make sense of the disparity in empirical success between the two versions of the hypothesis, as noted by Keller et al. [272].

5.3 The general model

The TWH is based on three assumptions. First, that parental condition (usually taken to be mother's) correlates with offspring condition. Second, that offspring condition persists into adulthood, so that it is relevant for reproductive value. Third, that 'Adult males will be differentially helped in [reproductive success] (compared to adult females) by slight advantages in condition' [525].

'Condition' is not explicitly defined in the original paper of Trivers and Willard [525]. Its definition has remained vague in much of the biological literature [90], but in the context of the TWH, can involve many physical factors, including the ability of a parent to provision its offspring, as well as heritable factors such as traits under

direct genetic control (sexual ornaments, for example) and social status. It is important to note that condition cannot be intepreted simply as reproductive value—either of parent or offspring—because the TWH requires that condition translate to reproductive value differently for males and females. In the Discussion section, we provide a more detailed consideration of problems with the definition of 'condition' in the TWH.

We capture the three assumptions of the TWH in the following simple model.

Each mother is of a certain physical condition, c_m (continuously distributed), and has a single brood of precisely two offspring. A mother's total investment capability, which she apportions fully between her two offspring, is limited by her physical condition to $I(c_m)$, assumed to be non-decreasing in c_m (mothers in better condition are able to invest more) and smooth. The post-investment condition of an offspring whose mother was of condition c_m and who received investment i is, regardless of its sex, $c(c_m, i)$, increasing in both arguments ($\frac{\partial}{\partial c_m} c(c_m, i) > 0$ and $\frac{\partial}{\partial i} c(c_m, i) > 0$) and concave in investment ($\frac{\partial^2}{\partial i^2} c(c_m, i) < 0$). This post-investment condition is assumed to persist into adulthood, and to be the quantity that is relevant for offspring fitness. To avoid confusion, we should note at this stage that condition—a physical measure—is treated as distinct from fitness.

That c should depend on i is clear. In our model, 'investment' is taken to mean the level of direct parental care for a single offspring. It is plain that, by this definition, offspring condition should increase with investment.

Why does c depend directly on c_m too? Mother's condition can affect offspring's condition directly (as opposed to indirectly, through greater investment capacity) in several ways, examples of which are: (i) if condition is defined by social rank, and rank is hereditary—as, for example, in baboons [225], spotted hyenas [130], and

red grouse [378]; (ii) if condition is in part determined genetically (this could apply either to maternal or paternal condition: in our model, c_m could equally well refer to either). This genetic mechanism of condition transmission is especially clear for sexually selected traits [136, 147, 300, 422].[2]

The model thus far captures the first two assumptions of Trivers and Willard [525]. Their third assumption, in the context of our model, means at the very least that adult condition $c(c_m, i)$ translates differently into reproductive success for males than it does for females. (In fact, the focal quantity should be reproductive value, not reproductive success [310]. We shall abbreviate this to 'fitness'.) A son in condition c will be assumed to have fitness $f_{\male}(c)$, while a daughter in the same condition will have fitness $f_{\female}(c)$.

The optimization problem for a mother in condition c_m is one of backwards induction: first, to choose the optimal investment decision for each possible brood (male-male, male-female, and female-female), and then, using the maximum fitness sums that arise from these investment decisions, to choose the sex ratio that maximizes the expected sum of her offspring's fitnesses. Denoting by p the probability of having a son (the same probability is assumed to apply independently for each of the two offspring), the optimization problem can be formally written:

$$\begin{aligned}\max_{p\in[0,1]} \max_{\substack{i_1,i_2,i_3\\ \in[0,I(c_m)]}} \quad & p^2[f_{\male}(i_1) + f_{\male}(I(c_m) - i_1)] \\ + \quad & 2p(1-p)[f_{\male}(i_2) + f_{\female}(I(c_m) - i_2)] \\ + \quad & (1-p)^2[f_{\female}(i_3) + f_{\female}(I(c_m) - i_3)],\end{aligned}$$

[2] Note that all results in this paper hold in the simplified cases where (a) the improved condition of offspring of high-condition mothers derives only from those mothers' ability to invest more in their offspring ($\frac{\partial}{\partial c_m} c(c_m, i) = 0$ and $\frac{\partial}{\partial i} c(c_m, i) > 0$), and (b) there is no difference in investment ability between high and low quality mothers, and the translation of their condition to offspring condition is purely hereditary ($\frac{\partial}{\partial c_m} c(c_m, i) > 0$ and $\frac{\partial}{\partial i} c(c_m, i) = 0$).

where $f_{♂}(i_1)$, for example, is shorthand for $f_{♂}(c(c_m, i_1))$.

In the context of our model, the sex ratio version of the TWH may be stated as follows: There exists a threshold maternal condition such that a mother in better condition has an optimal sex ratio that is male-biased, while a mother in worse condition has an optimal sex ratio that is female-biased. The question of whether a mother should have a male- or female-biased sex ratio is shown in [545, Appendix 1] to be equivalent to the simpler question of whether she would prefer to have two male or two female offspring (which is not to say that her optimal sex ratio is then necessarily one or zero—this is just a 'litmus test' for the optimal sex ratio being biased by any amount).

The investment version of the TWH, on the other hand, is this: There exists a threshold maternal condition such that a mother in better condition, upon having a mixed brood (one male and one female offspring), will invest more in her son than in her daughter, while a mother in worse condition will invest more in her daughter than in her son.

It should be noted, in light of the facts that checking the sex ratio version amounts to comparing the fitness sum of an all-male brood with that of an all-female brood, and checking the investment version amounts to comparing investment patterns in a mixed brood, that our results are based on simultaneous optimization, by backwards induction, of the sex ratio and investment decisions. In particular, the optimal sex ratio will itself depend on the optimal investment patterns for the various possible brood compositions, as is made clear in [545, Appendix 1].

The model presented above is not meant to represent reality in full detail, but rather to make accessible the logic underpinning the two versions of the TWH. More complex models that extend our framework to more realistic settings would

also be desirable. For example, we have ignored possible demographic differences between the sexes, though these have recently been shown to influence predictions of the TWH [464]. Our assumption that each mother has exactly two offspring is not realistic but simplifies the analysis considerably, and is the smallest brood number that still allows for simultaneous analysis of sex ratio and investment bias. It is argued in the Discussion section and [545, Appendix 3] that the case of a monotocous species, where single offspring are raised in sequence, will not differ much from our simple single-period, two-offspring model.

It will also be noted that our model applies best to contexts where (i) the sex ratio and parental care decisions are separable (in time, for example), and (ii) parental care is of a continuous, quantitative form (for example, the length of the period of parental care—duration of gestation, or time until weaning, say—or the fat content of breast milk). In such cases, the conceptual difference between the sex ratio and investment versions of the TWH is clear. (i) excludes cases where the sex ratio and investment decisions coincide, such as in parasitoid wasps. It applies, on the other hand, to vertebrate species where parental care is given post-conception and post-birth. (ii) excludes those discrete parental care decisions that are harder, conceptually, to distinguish from sex ratio decisions, such as sex-biased brood reduction [205, 348].

5.4 An example where the investment version fails

A simple case that satisfies Trivers and Willard's assumption 3, and which results in a mother always investing more in the male of a mixed brood, no matter her condition (and thus contra the investment version of the TWH), is where the fitness-condition profiles are linear for both males and females: $f_{\male}(c) = \lambda c$ and $f_{\female}(c) =$

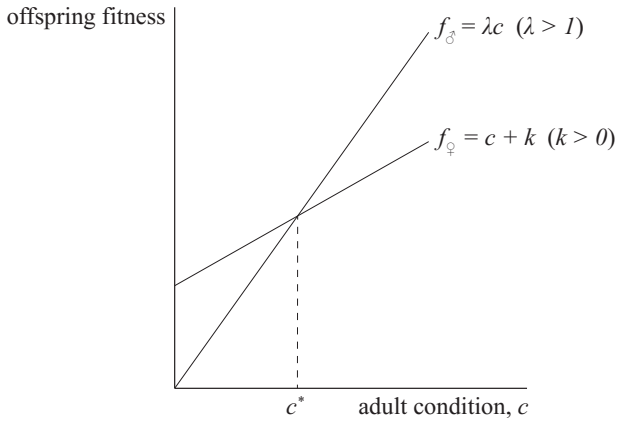

Figure 5.4.1: The 'classic' Trivers-Willard fitness functions, for which the sex ratio version of the Trivers-Willard hypothesis holds, while the investment version does not. Because male fitness always increases faster with condition than does female fitness, fitness returns to investment in a male offspring are always greater than in a female offspring of the same initial condition, and so a mother with a mixed brood will always invest more in the male of the brood, no matter her own condition.

$c + k$, with $\lambda > 1$ so that the fitness profile is steeper for males than for females (clearly satisfying Trivers and Willard's assumption 3) (Fig. 5.4.1). $k > 0$ can be adjusted arbitrarily; for example, it can be adjusted so that the average reproductive value of sons and daughters coincides. Alternatively, if offspring of one sex cost more to raise than offspring of the other sex, this could be represented by the fitness function of the more expensive sex shifting downwards for each condition; such a shift would lead to a population sex ratio biased against that sex. These facts concerning the adjustability of the fitness functions—i.e., the average fitness effects of having male and female offspring and therefore the population sex ratio as well—are true of all later specifications as well.

The investment decision of a female in condition c_m who has a mixed brood, denoting by i_s how much she invests in her son, amounts to the following maximization

problem:

$$\begin{aligned} i_s^* &:= \arg\max_{i_s} \; f_{\male}\big(c(c_m, i_s)\big) + f_{\female}\big(c(c_m, I(c_m) - i_s)\big) \\ &= \arg\max_{i_s} \; \big[\lambda c(c_m, i_s)\big] + \big[c(c_m, I(c_m) - i_s) + k\big]. \end{aligned}$$

Her investment will be male-biased if $i_s^* > I(c_m)/2$, i.e., if $i_s^* > I(c_m) - i_s^*$. Assuming an interior solution $i_s^* \in (0, I(c_m))$, the first-order condition for i_s^* amounts to equating the male and female offspring's marginal fitness returns to investment:

$$\begin{aligned} & \frac{\partial}{\partial i_s}\Big([\lambda c(c_m, i_s)] + [c(c_m, I(c_m) - i_s) + k]\Big)\Big|_{i_s = i_s^*} = 0 \\ \Rightarrow \quad & \lambda \partial_2 c(c_m, i_s^*) - \partial_2 c(c_m, I(c_m) - i_s^*) = 0 \\ \Rightarrow \quad & \partial_2 c(c_m, i_s^*) < \partial_2 c(c_m, I(c_m) - i_s^*) \\ \Rightarrow \quad & i_s^* > I(c_m) - i_s^*, \end{aligned}$$

where $\partial_2 c(\cdot, \cdot)$ refers to the partial derivative of c with respect to its second argument, and where the second-to-last step follows from $\lambda > 1$ and the last step from the concavity assumption $\partial_{22} c < 0$ ($\partial_{22} c(\cdot, \cdot)$ is the second partial derivative). Thus, no matter a mother's condition, she always biases investment in favour of the male offspring of a mixed brood. The reason for this is that the marginal returns to investment in a male offspring, $\lambda \partial_2 c(c_m, i)$, are always greater than the returns to investment in a female of the same condition, $\partial_2 c(c_m, i)$.[3]

[3] This result, and the reason behind it, extend to any functions $f_{\male}$ and $f_{\female}$ that satisfy $f'_{\female}(x) < f'_{\male}(y)$ for any x and y, since then the general first-order condition for i_s^* yields

$$\begin{aligned} & f'_{\male}\big(c(c_m, i_s^*)\big)\partial_2 c(c_m, i_s^*) - f'_{\female}\big(c(c_m, I(c_m) - i_s^*)\big)\partial_2 c(c_m, I(c_m) - i_s^*) = 0 \\ \Rightarrow \quad & \frac{\partial_2 c(c_m, i_s^*)}{\partial_2 c(c_m, I(c_m) - i_s^*)} = \frac{f'_{\female}\big(c(c_m, I(c_m) - i_s^*)\big)}{f'_{\male}\big(c(c_m, i_s^*)\big)} < 1 \quad \Rightarrow \quad i_s^* > I(c_m) - i_s^*, \end{aligned}$$

where the last step follows from the concavity of c with respect to its second argument.

We shall show later (Section 5.5) that the sex ratio version of the TWH holds under quite general conditions on $f_{\male}$ and $f_{\female}$. These conditions are satisfied by the linear fitness functions studied in this section. Still, owing to the simplicity of the present fitness functions, it will nonetheless be instructive to demonstrate here that the sex ratio version of the TWH holds for them.

It is proven in [545, Appendix 1] that a mother of condition c_m will have an optimal sex ratio that is male-biased if and only if she would prefer, in fitness terms, to have two male offspring than two female offspring (again, it is important to note that this comparison of the fitness sums of an all-male brood and an all-female brood is a diagnostic test for whether the mother's optimal sex ratio is *at all* male or female biased, and does not imply that her optimal sex ratio is necessarily one or zero). Notice that she always apportions investment equitably among a same-sex brood, owing to the concavity of fitness with respect to investment for both male and female offspring (a result of condition being concave in investment and this concavity being maintained under the linear transformation to fitness). So the condition for a male-biased sex ratio amounts to the following inequality:

$$\begin{aligned} & 2f_{\male}(c_m, I(c_m)/2) > 2f_{\female}(c_m, I(c_m)/2) \\ \Leftrightarrow \quad & 2\lambda c(c_m, I(c_m)/2) > 2[c(c_m, I(c_m)/2) + k] \\ \Leftrightarrow \quad & c(c_m, I(c_m)/2) > \frac{k}{\lambda - 1}. \end{aligned}$$

But since $\frac{\partial}{\partial c_m} c(c_m, I(c_m)/2) = \partial_1 c(c_m, I(c_m)/2) + \partial_2 c(c_m, I(c_m)/2) \frac{I'(c_m)}{2} > 0$, and assuming the existence of some $c_m^* \in (0,1)$ such that $c(c_m^*, I(c_m^*)/2) = \frac{k}{\lambda - 1} =: c^*$, this implies that mothers with condition above c_m^* have a male-biased optimal sex ratio, and mothers with condition below c_m^* have a female-biased optimal sex ratio.

The sex ratio version of the TWH therefore holds in this case, while the investment version does not.

Finally, it is interesting to note that mothers of condition c_m^*, though indifferent between having an all-male brood and an all-female brood, are not indifferent between those choices and having a mixed brood. To see this, note that each male in an all-male brood of such a mother has the same fitness as each female in an all-female brood, and each receives the same investment $I(c_m^*)/2$. Thus, a mother with a mixed brood could achieve the same fitness sum as with a same-sex brood if she invests $I(c_m^*)/2$ in each offspring, male and female. But as the argument above demonstrates, this is not the optimal investment decision for the mother: she should always invest more in the male offspring than in the female offspring of a mixed brood. So her fitness sum from having a mixed brood and apportioning investment optimally is strictly higher than her fitness sum from having a same-sex brood and apportioning investment optimally. And as a result, by continuity, mothers whose condition is sufficiently close to c_m^*, though the bias in their sex ratio is determined by whether their condition is higher or lower than this value, would nonetheless have optimal sex ratios that are mixed (i.e., not zero or one). The intuition for this result is that, with a mixed brood, the mother can divert investment away from the female offspring, for whom it is relatively unproductive (in fitness terms) and towards the male offspring, for whom it is relatively productive. This choice is not available to the mother of a same-sex brood.

This explanation complements other reasons for why selection favours individual sex ratios that are not zero or one. In situations with local within-sex competition for mates, selection can favour extreme sex ratios [211], but it will also not favour those that are zero or one. More generally, in small populations whose overall sex ratio

fluctuates stochastically, intermediate individual sex ratios can be favoured because extreme individual sex ratios confer a greater fitness penalty when the population sex ratio is biased in the same direction as they are, compared to the fitness gain they confer when the population sex ratio is biased symmetrically in the opposite direction [550]. (For most species, however, around the equilibrium population sex ratio, the selective forces in favour of individuals whose sex ratios match it over those with extreme sex ratios are likely to be weak—this follows from the general arguments in [513] and [579]).

5.5 Broad sufficient conditions for the sex ratio version to hold

Assume that the optimal investment decision for the mother of a same-sex brood, no matter her condition, is always to apportion investment equitably between her two offspring. This holds if the functions $f_{\male}(c(c_m, i))$ and $f_{\female}(c(c_m, i))$ are both concave in investment i—loosely speaking, given that $c(c_m, i)$ is already concave in i, this means that either $f_{\male}$ and $f_{\female}$ are themselves (weakly) concave, or that any convexities in them are not sufficient to overturn the concavity of $c(c_m, i)$ in i. This is satisfied, for example, by the linear fitness functions assumed in Section 5.4, by those displayed in Fig. 5.6.3, and by those displayed in Fig. 5.6.2 provided the convex fitness function $f_{\male}(c)$ is not too convex.[4]

With this assumption, a simple and natural set of 'single-crossing' conditions under which the sex ratio version of the TWH always holds is:

[4] More precisely, in this case of convex $f_{\male}(c)$, we require $\frac{\partial^2}{\partial i^2} f_{\male}(c(c_m, i)) < 0$, which translates to the condition $\left|\frac{\partial_{22} c(c_m,i)}{\partial_2 c(c_m,i)}\right| > \left|\frac{f''_{\male}(c(c_m,i))}{f'_{\male}(c(c_m,i))}\right|$, i.e., that c is relatively more concave in i than $f_{\male}$ is convex in c.

(SC1) The condition-fitness profiles for males and females cross only once (at c^*), with the male profile starting below the female profile (in poor adult condition, males are less fit than females: $c < c^* \Rightarrow f_{\male}(c) < f_{\female}(c)$) and ending above it (in good adult condition, males are fitter than females: $c > c^* \Rightarrow f_{\male}(c) > f_{\female}(c)$);

(SC2) There exists some maternal condition c_m^* such that $c^* = c(c_m^*, I(c_m^*)/2))$.

If $f_{\male}(c(c_m, i))$ and $f_{\female}(c(c_m, i))$ are concave in i, and if (SC1) and (SC2) hold, then mothers in condition $c_m > c_m^*$ have optimal sex ratios that are male-biased, while those in condition $c_m < c_m^*$ have optimal sex ratios that are female-biased.

To prove this, first consider the case of a female in condition $c_m > c_m^*$. A sufficient condition for her optimal sex ratio to be male-biased is that she would achieve higher fitness with an all-male brood than with an all-female brood (as shown in [545, Appendix 1]). Since her optimal investment decision in either case is equitable apportionment among the brood, this condition becomes:

$$2f_{\male}(c(c_m, I(c_m)/2)) > 2f_{\female}(c(c_m, I(c_m)/2)).$$

But since $\frac{\partial}{\partial c_m} c(c_m, I(c_m)/2) = \partial_1 c(c_m, I(c_m)/2) + \partial_2 c(c_m, I(c_m)/2) \frac{I'(c_m)}{2} > 0$, we have that $c_m > c_m^* \Rightarrow c(c_m, I(c_m)/2) > c(c_m^*, I(c_m^*)/2) = c^*$, and so, from the single-crossing condition (SC1), $f_{\male}(c(c_m, I(c_m)/2)) > f_{\female}(c(c_m, I(c_m)/2))$.

A female in condition $c_m < c_m^*$ would, by a similar argument, achieve higher fitness with an all-female brood than with an all-male brood, and so her optimal sex ratio would be female-biased.

The case where at least one of $f_{\male}(c(c_m, i))$ or $f_{\female}(c(c_m, i))$ is not everywhere concave in i is more complicated, and in general, the single-crossing conditions do

not guarantee that the sex ratio version holds (a graphical counterexample is given in [545, Appendix 2]).

5.6 Narrow sufficient conditions for the investment version to hold

We have seen in Section 5.4 that, for a simple set of fitness functions that satisfy the Trivers-Willard assumptions, the investment version of the hypothesis does not hold. In this section, we derive conditions under which the investment version of the TWH does hold. They are significantly narrower than the basic set of assumptions stated by Trivers and Willard [525].

To simplify the analysis, we assume that to determine the investment bias (male or female) in a mixed brood of a mother in condition c_m, it suffices to check in which direction natural selection 'points' from an initial state of equitable investment in the male and female offspring (i.e., does it point towards increased, and thus biased, investment in the male or in the female?). If the ancestral state is equitable apportionment of investment within mixed broods, and if maternal behavioural changes are gradual, then this is the investment bias that natural selection would lead to.

Mathematically, this amounts to checking the slope of the mixed brood's fitness sum $f_{\male}(c(c_m, i_s)) + f_{\female}(c(c_m, I(c_m) - i_s))$ with respect to investment i_s in the male offspring, evaluated at the point $i_s = I(c_m)/2$. If the brood's fitness sum is of the 'single-humped' shape displayed in Fig. 5.6.1, i.e., with one local maximum that is also the global maximum, and with no local minima, then this slope indeed points towards the global maximum.

The investment version of the TWH then simplifies to the following: the partial

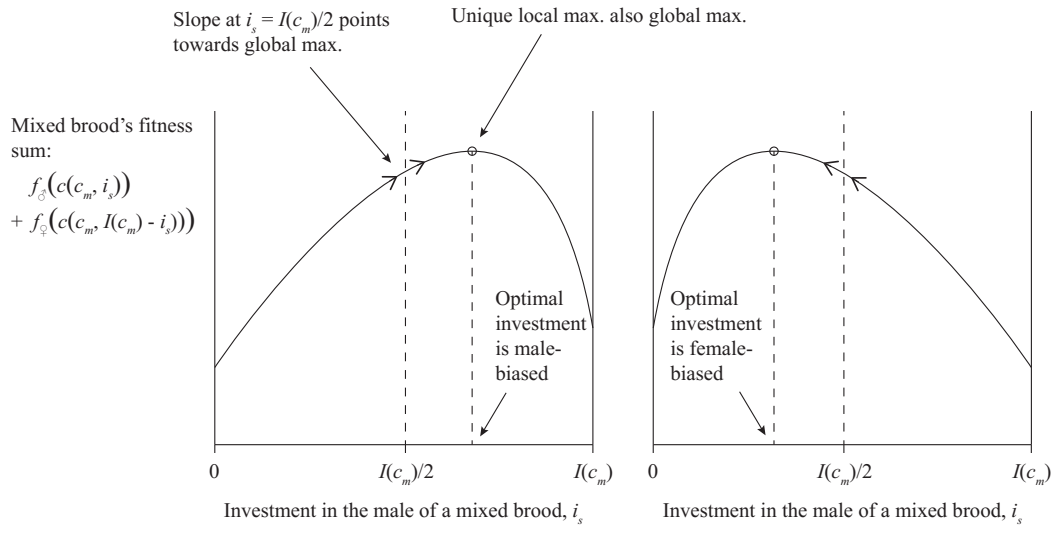

Figure 5.6.1: If the fitness sum of a mixed brood is 'single-humped' with respect to investment in the male of the brood, then the slope of the function at the point of equitable investment points in the direction of the optimal bias in investment, significantly simplifying detection of the latter in our model.

derivative of the fitness sum of a mixed brood, taken with respect to investment in the male offspring, and evaluated at the point of equitable investment $I(c_m)/2$, is negative for maternal conditions below a certain threshold, and positive for maternal conditions above that threshold. This partial derivative, in general form, is given by:

$$\begin{aligned}
&\frac{\partial}{\partial i_s}\left[f_{♂}\big(c(c_m, i_s)\big) + f_{♀}\big(c(c_m, I(c_m) - i_s)\big)\right]\Big|_{i_s = I(c_m)/2} \\
=&f'_{♂}\big(c(c_m, I(c_m)/2)\big)\partial_2 c(c_m, I(c_m)/2) - f'_{♀}\big(c(c_m, I(c_m)/2)\big)\partial_2 c(c_m, I(c_m)/2) \\
=&\Big[f'_{♂}\big(c(c_m, I(c_m)/2)\big) - f'_{♀}\big(c(c_m, I(c_m)/2)\big)\Big]\,\partial_2 c(c_m, I(c_m)/2). \qquad (5.1)
\end{aligned}$$

Since $\partial_2 c(c_m, I(c_m)/2) > 0$, the sign of this expression is the same as the sign of the term in square brackets in the last line. The investment version of the TWH thus

further simplifies to the following: $f'_{\male}\big(c(c_m, I(c_m)/2)\big) < f'_{\female}\big(c(c_m, I(c_m)/2)\big)$ for all c_m below some threshold, and $f'_{\male}\big(c(c_m, I(c_m)/2)\big) > f'_{\female}\big(c(c_m, I(c_m)/2)\big)$ for all c_m above that threshold. In other words, male fitness responds less to increases in adult condition than does female fitness below some threshold adult condition, and male fitness responds more to changes in adult condition than does female fitness above that threshold condition. This condition is rather specific, and will hold for only a subset of the fitness functions that are consistent with Trivers and Willard's original assumptions. Indeed, under a strict reading of Trivers and Willard's 'Assumption 3' (quoted in Section 5.3), it appears that the condition (5.1) we have derived for the investment version to hold is in fact disallowed! Nevertheless, there are some natural instances where we might expect them to be fulfilled, as the following example illustrates.

We keep the female fitness function from before, $f_{\female}(c) = c + k, k > 0$, and specify a convex male fitness function $f_{\male}(c)$ such that the slope of $f_{\male}(c)$ is less than one (the slope of $f_{\female}(c)$) for all adult conditions below a certain (realized) threshold $\hat{c}$ (we keep the notation c^* for the point at which $f_{\male}$ and $f_{\female}$ cross), and greater than one for all adult conditions above that threshold (see Fig. 5.6.2). That is, we require the male fitness function to be *sufficiently convex*. Under this scenario, it is clear that the condition (5.1) is satisfied, and we expect the investment version of the TWH to hold in this case.

If we instead specify that the male fitness function be sufficiently concave, while keeping the female fitness function linear (Fig. 5.6.3), then a situation results that is directly opposed to that predicted by the investment version of the TWH. Now, mothers in poor condition are expected to bias investment towards the male of a mixed brood, while mothers in good condition are expected to bias investment

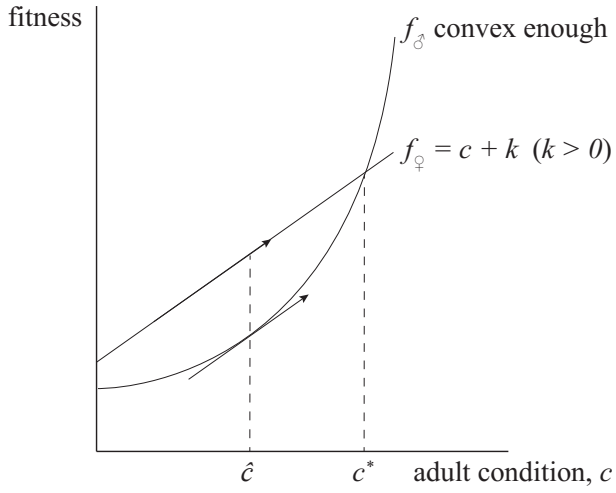

Figure 5.6.2: Fitness functions for which the investment version of the Trivers-Willard hypothesis does hold. If the male fitness function is sufficiently convex, then the very small slope at low conditions makes investment in males in low condition unattractive relative to investment in females, and so mothers in low condition should bias investment towards females. Conversely, investment in males in good condition is very attractive (their fitness function is very steep), and so mothers in good condition should bias their investment towards male offspring.

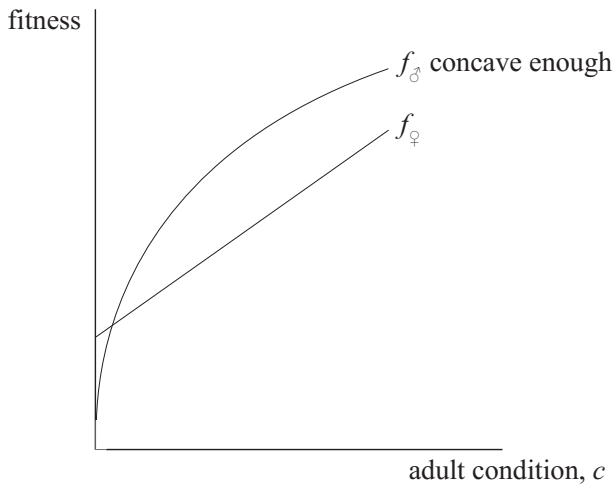

Figure 5.6.3: Fitness functions for which a situation opposite that predicted by the investment version of the Trivers-Willard hypothesis is expected to result. Because the slope of the male fitness function starts out very steep, investment in males in poor condition yields high fitness returns, and so mothers in poor condition would be expected to bias investment towards the male of a mixed brood. Conversely, mothers in good condition are expected to bias investment towards the female of a mixed brood, because the eventual flatness of the male fitness function makes investment in males in good condition relatively unproductive.

towards the female of a mixed brood. Nonetheless, the sex ratio version of the TWH is expected still to hold in this case.

5.7 Discussion

We have demonstrated, in the context of a simple unified model, that the conditions under which the sex ratio version of the TWH holds are significantly broader than those under which the investment version is expected to hold. This helps to make sense of the observation that empirical tests of the former tend to return positive results, while empirical tests of the latter return more mixed results [272].

The difference between the two versions of the hypothesis can be understood in terms of the economic difference between absolute and marginal value. Whether

a mother in a certain condition should bias her sex ratio towards male offspring amounts to asking whether the male fitness function *lies above* the female fitness function for the relevant condition, i.e., whether there exists an absolute difference in fitness between offspring of the two sexes. On the other hand, for a mother with a mixed brood, whether she should bias parental investment towards the male offspring amounts to asking whether the male fitness function is *steeper* than the female fitness function for the relevant condition, i.e., whether improvement of the male's condition yields a greater marginal fitness return. This insight is clearly captured by Keller et al. [272], who find no evidence for an investment-version Trivers-Willard effect in the United States:

> [Resource allocation biasing] should be biased toward the offspring that most improves the parents' fitness per unit invested. However, this bias has no necessary link to the fitness value of the offspring. Rather, it is predicted by cues related to the marginal gains of allocating each particular resource to the sex in question. The assumptions of the TWH (a higher correlation between condition and [reproductive success] among males than females, and a correlation between the parent's and offspring's conditions) are unrelated to these marginal benefits, but they *are* related to the fitness value of offspring.

Loosely, then, the sex ratio version of the TWH is expected to hold when the male and female fitness functions are such that males in poor condition have relatively low fitness (the male fitness function starts out below the female fitness function), males in good condition have relatively high fitness (the male fitness function ends up above the female fitness function), and the fitness functions cross once (e.g., Figs. 5.4.1, 5.6.2, and 5.6.3). This describes the classic picture of male and female

fitness functions in polygynous species, and so we should expect the sex ratio version of the TWH to hold very generally.

The investment version, on the other hand, is expected to hold only if the male fitness function is much flatter than the female fitness function for poor conditions, but much steeper for good conditions (e.g., Fig. 5.6.2). This condition is much more restrictive than that under which the sex ratio version holds, and so we should expect the investment version of the TWH to hold less generally than the sex ratio version.

Our model is simply intended to capture the logic of why the sex ratio and investment versions of the TWH differ. We discuss some of the model's assumptions, and the possibility of their relaxation, below.

First, our analysis optimizes over phenotypes, and therefore ignores both their genetic basis and the evolutionary dynamics that might lead to their optimization. In this sense, it is a heuristic analysis. Studying phenotypes in a static, non-genetic setting was vital both for the simplicity of the exposition and the results (for a defense of this style of modelling, see Parker and Maynard Smith [418]). Nonetheless, it remains possible that the optimal behaviours derived here are not evolvable in a simple population genetic framework. It might be objected that the genetic basis of some of the behaviours we discuss is both unknown and likely to be complicated, but it is a simple retort that, if a behaviour is not evolvable when assumed to have a simple genetic basis, we are unlikely to be able to demonstrate that it is evolvable assuming it to have a more complicated one.

Second, the assumption of a single fixed brood of constant size two is, of course, not realistic in general, having been made for the sake of tractability. One direction in which the model could be made more realistic would be to allow brood size to

vary, and to undergo selection in conjunction with sex ratio and the pattern of parental investment. While it is not clear whether this could be done in a way that still permitted tractable analysis, it could alter the interpretation of our results if there were significant interactions between optimal brood size and the optima of our variables of interest, sex ratio and the pattern of parental investment [579] [163, Sec. 9].

In this vein, another way in which the model could be generalized would be to consider sex ratio and investment patterns across sequential broods. Consider the simplest case, that of two offspring raised one after the other. The optimization problem faced by the mother is then slightly different to that she faces in our single-brood model. For example, she might be able to alter her sex ratio for the second offspring conditional on the sex of her first offspring; this option is not available to the mother of a single brood. In this case, the results of the sequential model are very similar to those of the single-period model we have analyzed—see [545, Appendix 3]. If, on the other hand, her sex ratio cannot change between periods in the sequential model, then a mother whose sex ratio is not zero or one invests in her first offspring without knowing the sex of her second offspring. This case is significantly more complicated, but a tentative analysis [545, Appendix 3] suggests that its results would usually not differ significantly from those of our single-period model.

Third, our model is, in the language of economic theory, a 'partial equilibrium' analysis: the decision problem faced by one mother is independent of the decisions made by other mothers. In our model, for example, the exogenous parameter k, mediating the height of the female fitness function, can be adjusted so that, given the population distribution of maternal condition, the average reproductive success

of sons and daughters is equal. In reality, the mating success of a male in good condition depends on the number of other males in good condition, and this in turn depends on the sex allocation decisions of other mothers in the population. A full general equilibrium model would specify a distribution of maternal conditions, and sex ratio and investment strategies for mothers in each condition, such that (a) each mother's strategies are optimal, given the strategies of other mothers, (b) the average reproductive success of all sons would match that of all daughters, and possibly (c) the distribution of adult condition of the daughters matches that of the mothers. We do not believe that the technical tools of sex allocation theory are yet advanced enough to approach this general equilibrium problem, but it represents an important avenue of future research.[5]

Fourth, our model treats maternal and offspring condition as continuous variables, where in reality the important factor for reproductive success may be discrete, like rank within a social hierarchy. The strategic concerns raised in the previous paragraph apply with even more force here: whether a mother's investment in her son causes him to jump up one place in the male condition ranking clearly depends on the decision of the mother of the son presently 'occupying' that place. A more subtle complication is that the discretization of the fitness functions' domain (here, within-sex rank) makes analysis of the effects of continuous variables (like investment) on fitness significantly less tractable.

A related, but more fundamental problem with the approach adopted here is that

[5] On the strategic considerations, however, we expect that, in equilibrium, a certain monotonicity condition should hold: in particular, within-sex offspring condition rank should covary perfectly with maternal condition rank. If this were not satisfied, we would have the odd scenario that, in equilibrium, a mother in better condition than another neglects her son (say) sufficiently much relative to the other mother that her son's post-investment condition is lower than that of the other mother's son. So, if this monotonicity condition were to hold, we should not expect strategic concerns to alter the structure of the problem, at least in terms of the rank of offspring condition.

'condition' is treated as an abstract, and therefore unobserved, quantitative variable. But many of the contingencies that we have shown to be of theoretical importance involve the shape of reproductive value functions with respect to condition; since condition is not empirically observed, neither can the shape of these functions be. The criteria that we have derived for when the sex ratio and investment versions of the TWH hold are therefore not directly measureable.

Getting around this problem would require substitution of 'condition' for an imperfect but observable proxy variable, such as weight. That is, it would require measurement of the fitness functions with respect to weight, and how weight responds to parental condition and investment. This would detract significantly from the generality of the theory, and would be accurate only in so far as weight correlates closely with true condition. It is possible that a composite proxy involving many variables (such as weight, nutritional status, sexual ornaments, etc.) might improve this correlation.

This problem applies not only to our model, but to all theoretical models of the TWH that treat 'condition' as an intermediate variable [90]. It appears to us to be the chief obstacle to generating testable predictions from such models, and its solution is therefore a crucial line of future research.

6

Drift-induced selection between male and female heterogamety

6.1 Abstract

Evolutionary transitions between male and female heterogamety are common in both vertebrates and invertebrates. Theoretical studies of these transitions have found that, when all genotypes are equally fit, continuous paths of intermediate equilibria link the two sex chromosome systems. This observation has led to a belief that

neutral evolution along these paths can drive transitions, and that arbitrarily small fitness differences among sex chromosome genotypes can determine the system to which evolution leads. Here, we study stochastic evolutionary dynamics along these equilibrium paths. We find non-neutrality, both in transitions retaining the ancestral pair of sex chromosomes and in those creating a new pair. In fact, substitution rates are biased in favor of dominant sex determining chromosomes, which fix with higher probabilities than mutations of no effect. Using diffusion approximations, we show that this non-neutrality is a result of 'drift-induced selection' operating at every point along the equilibrium paths: stochastic jumps off the paths return, on average, with a directional bias in favor of the dominant segregating sex chromosome. Our results offer a novel explanation for the observed preponderance of dominant sex determining genes, and hint that drift-induced selection may be a common force in standard population genetic systems.

6.2 Introduction

In most animals, sex is determined genetically [49]. Among those animals with genetic sex determination, the majority exhibit heterogametic sex determination: the presence or absence of a sex-specific chromosome triggers sexual differentiation [28, 49]. Depending on whether the sex-specific chromosome is in males or in females, the system is, respectively, male heterogamety (XX females, XY males) or female heterogamety (ZW females, ZZ males).

The system of heterogamety is a fundamental genetic property of a species. It is therefore surprising that it is evolutionarily very labile, with transitions between male and female heterogamety having occurred frequently in amphibians [232], reptiles [145, 427], and fishes [144, 339, 340], as well as in invertebrates [20, 260, 551]. A

striking example of a recent transition is found in the frog *Rana rugosa*: populations in northern Japan exhibit female heterogamety while populations in southern Japan exhibit male heterogamety [371, 392].

In a classic theoretical study, Bull and Charnov [53] showed that continuous paths of population genetic equilibria exist between male and female heterogamety. States along these paths are equilibria in the sense that the evolutionary dynamics of an infinite, randomly mating population are stationary at them when all genotypes are equally fit. Intermediate states along the paths involve the presence of multiple genotypes for each sex, a situation observed in several species, e.g., the platyfish *Xiphophorus maculatus* [261, 262], the blue tilapia *Oreochromis aureus* [306], a Lake Malawi cichlid *Metriaclima pyrsonotus* [477], the western clawed frog *Xenopus tropicalis* [447], and the housefly *Musca domestica* [148, 161, 366].

Two of these equilibrium paths are of particular interest. The first, which we shall refer to as 'model 1', governs those transitions between male and female heterogamety that involve the same pair of sex chromosomes [53] (see Figures 6.3.1 and 6.3.3A). The second, which we shall refer to as 'model 2', governs those transitions between male and female heterogamety that involve different pairs of sex chromosomes, i.e., where the sex chromosome pair in one system is autosomal in the other, and vice versa [53, 470, 471] (see Figures 6.3.2 and 6.3.3B).

The existence of these deterministic equilibrium paths has led to a belief that neutral drift along them in finite populations could be responsible for transitions between male and female heterogamety [49, 50, 534], an important baseline model for such transitions [534]. Moreover, arbitrarily small fitness differences between the sexual genotypes can eliminate the equilibrium paths under deterministic evolutionary dynamics, and render one of the heterogametic systems stable and the

other unstable [53]. This has led to a belief that small fitness differences alone can determine which transitions are possible [49, 50, 534].

Here, we examine these claims in the context of finite-population evolutionary dynamics. Using both stochastic simulations and analytical approximations based on the removal of fast variables, we estimate the fixation probabilities of the various sex determining mutations along the two equilibrium paths, starting from a state of simple heterogamety. We find that evolution along these 'neutral' equilibrium paths is in fact not neutral, instead showing a clear bias in favor of dominant sex determining mutations. Selection for otherwise deterministically neutral genotypes has previously been recognized in other settings [88, 100, 183, 290, 326, 420, 513, 550]. Perhaps the most prominent example is Gillespie's criterion [183], which states that if the reproductive rates of two genotypes have equal arithmetic mean but different variance, then the genotype with lower variance will be selected for, owing to higher geometric mean fitness. A key difference is that, in the neutral models we study, we assume no *a priori* differences in the reproductive rates of the various genotypes; these instead emerge naturally in our analysis of the dynamics along and around the equilibrium paths.

When all genotypes are equally fit, we find in both models that the substitution rates of the dominant sex determining mutations (in directions a and c in Figure 6.3.3) are higher than the substitution rates of recessive mutations (in directions b and d in Figure 6.3.3). Thus, in finite populations, stochastic evolutionary dynamics have a clear directionality along the equilibrium paths, owing to a drift-induced selective force. However, this selective force is a weak one—its effect on fixation probabilities in the neutral case is of order $1/N$—and therefore can be dominated by direct selective forces such as viability, fecundity, or fertility differences between

genotypes.

We also study the case where the sex-specific chromosome (the Y or the W) has accumulated deleterious recessive mutations, as it is expected to do over time in its non-recombining region [71, 74]. When the sex-specific chromosome is so degraded that homozygosity for it is lethal (as in mammals and birds), most heterogametic transitions are impossible [49]. However, in many other taxa, the sex-specific chromosome has accumulated only few recessive deleterious mutations—this state is common, for example, in amphibians, reptiles, and fish [15]. In such cases, homozygosity for the sex-specific chromosome is not expected to be lethal, and in fact can be associated with only a small fitness cost, if any at all. When taking into account these natural selective forces, we find in model 1 that the drift-induced selective bias in favor of dominant sex determining mutations is amplified, though the overall substitution rates in both directions are reduced. In model 2, the drift-induced bias in favor of dominant sex determining mutations is reduced when these selective forces are taken into account. Thus, in model 2, when selection is weak and the population is small, dominant sex determining mutations substitute at a higher rate; when selection is strong and the population is large, recessive sex determining mutations substitute at a higher rate.

The potential for drift-induced selection in transitions between sex determining systems has previously been noted by Vuilleumier et al. [554], who use simulations to investigate the stochastic dynamics of model 1, focusing predominantly on the effects of population structure. Our work overlaps with theirs in one particular case, that of a single deme, with no viability differences between the various genotypes. In that case, they too find non-neutral fixation probabilities for new dominant and recessive sex determining mutations, but find fixation probabilities substantially

above the neutral expectation for both classes of mutation. In contrast, we find in this case that dominant sex determining mutations fix with probability above the neutral expectation, but recessive mutations fix with probability lower than the neutral expectation. The fixation probabilities that they report are also orders of magnitude different from those we report, especially for large populations [compare, for example, their Figure 1(a) with our Figure 4A]. They also find mean conditional fixation times that are invariant, and in some cases even decrease, as population size increases; we find mean conditional fixation times that increase linearly with population size, consistent with drift-like dynamics. We have independently simulated their population model for the case that overlaps with ours, and obtain results consistent with ours, but different from those they report. The validity of our results is supported by mathematical analysis, which also allows us to explain them in analytical detail. In addition, we also consider transitions between sex determining systems in model 2, where the sex chromosome locus is changed in the course of a transition; empirically, this scenario is possibly even more common than model 1 [144]. Our results thus suggest that biases favoring dominant sex determining mutations may be general to transitions between male and female heterogamety.

6.3 Characterization of the equilibrium paths

6.3.1 Model 1

Consider an initial male-heterogametic system, XX/XY. Suppose now that a mutation occurs on an X chromosome that renders the feminizing tendency of the resulting chromosome—call the new chromosome X′—dominant to the masculinizing tendency of the Y (so that X′Y individuals are female). Allowing all possible

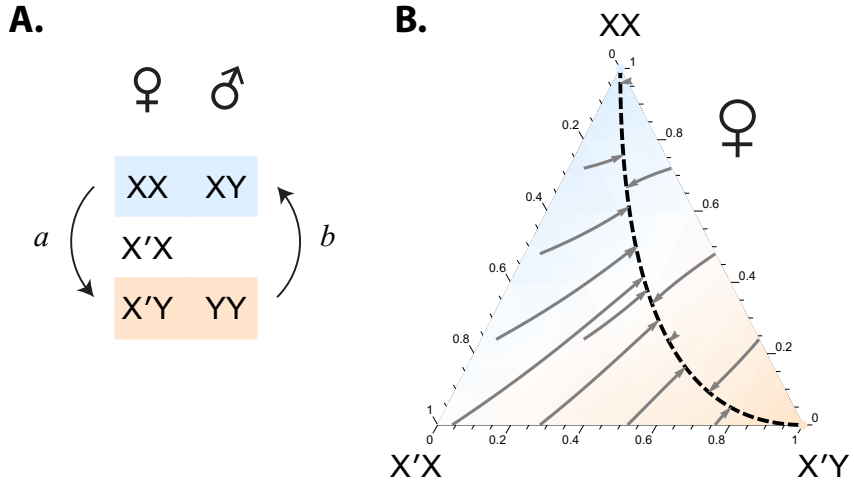

Figure 6.3.1: Transitions between male and female heterogamety without a change in the sex determining locus (model 1). (A) In model 1, heterogametic transitions involve intermediate systems of five sexual genotypes. In the system depicted here, there are three female and two male genotypes. Transition *a* is from male to female heterogamety, and involves fixation of the dominant feminizing X′ chromosome (mutated from an X). The reverse transition, *b*, is from female to male heterogamety, and involves fixation of the recessive feminizing X chromosome (mutated from an X′). A symmetric path, with two female and three male genotypes, also exists (see Figure 6.3.3A). (B) The equilibrium path (dashed line) governing transitions *a* and *b*. For ease of visualization, attention is restricted to the frequencies of the three female genotypes when the sex ratio is $1/2$ (as it is at every point on the equilibrium path). These frequencies are displayed in a de Finetti diagram, where, for example, the relative frequency of XX females at a point is given by the height of that point along a perpendicular line dropped from the XX corner to its opposing side. Some deterministic trajectories to the equilibrium path are displayed with arrowed grey lines. Color shading indicates frequency of XX females (blue) relative to X′Y females (orange). The equation for the equilibrium path is given in Eq. (6.1).

male-female matings between the genotypes results in a closed system of five sexual genotypes: females can be XX, X′X, or X′Y, while males can be XY or YY (Figure 6.3.1A, system arises in direction a). Clearly, this system could also arise in the reverse direction: starting from a female-heterogametic system, X′Y/YY, an X′ chromosome can mutate to an X chromosome with recessive feminizing tendency (Figure 6.3.1A, direction b). (It should of course be noted that the usual sex chromosome labels—X, Y, Z, and W—are arbitrary, so that we could just as validly label those in a female-heterogametic system X′ and Y. We also note that 'sex chromosomes' are defined simply by the presence of a locus at which genes of major sex determining effect segregate—it is possible, for example, that X and Y chromosomes are identical along their entire length, and recombine along their entire length, except at the major sex determining locus.)

Assuming the genotypes all to have equal fitness (i.e., that the system is neutral), enumerating them in the above order (XX, X′X, X′Y, XY, YY), and letting p_i be the population frequency of genotype i, Bull and Charnov [53] showed that, for any value $0 \leq q \leq 1$, the population state

$$p_1 = \frac{(1-q)^2}{2(1+q)^2}, \quad p_2 = \frac{q(1-q)}{(1+q)^2}, \quad p_3 = \frac{q}{1+q},$$
$$p_4 = (1-q)/2, \quad p_5 = q/2, \tag{6.1}$$

is an equilibrium in an infinite, randomly-mating population (Figure 6.3.1B). When $q = 0$, all males are XY and all females XX, so that a system of male heterogamety operates; when $q = 1$, males are YY and females X′Y, and the system is female heterogamety. For intermediate values $0 < q < 1$, all five genotypes are present at positive frequency.

A symmetric, though distinct, path exists where, from an initial female-heterogametic system ZW/ZZ, a dominant masculinizing Z′ arises from a mutated Z, and, if it reaches high enough frequency, establishes a male-heterogametic WW/WZ′ system. The reverse transition along the same path involves fixation of the recessive Z chromosome from an initial WW/WZ′ system. Intermediate states along this path involve two female and three male genotypes.

These symmetric paths, one with three female and two male genotypes (as illustrated in Figure 6.3.1), and the other with two female and three male genotypes (described in the previous paragraph), are illustrated in a general format in Figure 6.3.3A. There, among the transitions involving fixation of dominant sex determining mutations, those from male to female heterogamety are labeled a (as in Figure 6.3.1A), while those from female to male heterogamety are labeled c. Among the transitions involving fixation of recessive sex determining mutations, those from female to male heterogamety are labeled b (as in Figure 6.3.1A), while those from male to female heterogamety are labeled d. We shall use this labeling throughout for model 1 transitions.

Notice that, if there are no demographic differences between males and females, then the dynamics in directions c and d are identical to those in directions a and b, respectively, up to a relabeling of males and females.

For the non-neutral case, the equilibrium path connecting systems of male and female heterogamety no longer exists [53]. The resultant dynamics in this scenario depend on the selective forces acting on each of the genotypes. Transitions in either direction involve the production of individuals homozygous for a previously sex-specific chromosome (the Y for transitions in direction a and the X′ and X for those in direction b). Sex-specific chromosomes are expected to accumulate reces-

sive deleterious mutations in a heterogametic system [71, 74], causing individuals homozygous for them to be selected against weakly in young heterogametic systems (as in many reptiles, amphibians, and fishes) and to be inviable in old systems (as in mammals and birds). In the latter case, model 1 transitions are impossible. In the former case, we expect YY genotypes to be selected against in transitions in direction a, and X′X and XX genotypes to be selected against in transitions in direction b (in direction b, the X chromosome is created simply by mutation at a major sex determining locus on the X′ chromosome; the X is therefore expected to carry the same deleterious mutations that the X′ does).

6.3.2 Model 2

Begin with a male-heterogametic system XX,AA/XY,AA, where A is initially autosomal. Now suppose that a mutation occurs on an A chromosome that confers on the resultant chromosome, A′, a feminizing tendency dominant to the masculinizing tendency of the Y (so that XY,AA′ and YY,AA′ individuals are female). All possible matings then yield a closed system of six sexual genotypes, females being XX,AA, XX,AA′, XY,AA′, or YY,AA′, and males being XY,AA or YY,AA (Figure 6.3.2, direction a). Again, this system could arise in the reverse direction as well, starting from the female-heterogametic system YY,AA′/YY,AA and introducing, as a mutated Y chromosome, a recessive feminizing X (Figure 6.3.2, direction b).

Scudo [470, 471] and Bull and Charnov [53] showed that, when all genotypes are equally fit (i.e. when the system is neutral), enumerating them in the above order (XX,AA, XX,AA′, XY,AA′, YY,AA′, XY,AA, YY,AA), and writing p_i for

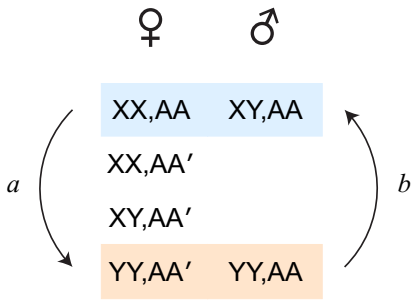

Figure 6.3.2: Transitions between male and female heterogamety with a change in the sex determining locus to a previous autosome (model 2). Model 2 transitional systems involve six sexual genotypes. In the system illustrated here, there are four female and two male genotypes. Transition *a* involves fixation of the dominant feminizing A′ chromosome (mutated from an A), and causes the previous sex chromosome Y to become an autosome. Transition *b* involves fixation of the recessive feminizing X (mutated from a Y), and causes the previous sex chromosome A to become an autosome. The equilibrium path of this system is given in Eq. (6.2). A symmetric path, with two female and four male genotypes, also exists (see Figure 6.3.3B).

the frequency of genotype i, a continuous path of equilibria,

$$p_1 = \frac{(1-q)^2}{2(1+q)^2}, \quad p_2 = \frac{q(1-q)^2}{2(1+q)^2}, \quad p_3 = \frac{q(1-q)}{1+q}, \quad p_4 = q/2,$$
$$p_5 = (1-q)/2, \quad p_6 = q/2, \tag{6.2}$$

connects male heterogamety at one end (XX,AA/XY,AA; $q = 0$) with female heterogamety at the other (YY,AA′/YY,AA; $q = 1$), with intermediate equilibria ($0 < q < 1$) involving all six genotypes.

Notice that, if the former system transitions to the latter (Figure 6.3.2, direction *a*), the Y chromosome becomes autosomal, and the previous autosome A becomes a sex chromosome. Notice too that this transition involves the production of YY individuals. On the other hand, the reverse transition (Figure 6.3.2, direction *b*) does not involve the production of individuals homozygous for the previously sex-specific chromosome (here, the A′ chromosome), an important difference.

Again, a symmetric, though distinct, equilibrium path exists that connects a female-heterogametic system AA,ZW/AA,ZZ with a male-heterogametic system AA′,WW/AA,WW via an intermediate system with two female and four male genotypes. Transitions from female to male heterogamety along this path involve production of WW individuals, the W having been female-specific in the original system of female heterogamety. But transitions from male to female heterogamety along this path do not involve the production of A′A′ individuals, the A′ having been male-specific under male heterogamety. That heterogametic transitions along standard equilibrium paths are possible without the production of WW or YY individuals (using the standard labeling) is an important fact often forgotten in the literature on evolutionary transitions between sex determining mechanisms.

These symmetric equilibrium paths, one with four female and two male genotypes (as in Figure 6.3.2), and the other with two female and four male genotypes (as described in the previous paragraph), are illustrated in a general way in Figure 6.3.3B. There, among model 2 transitions involving fixation of dominant sex determining mutations, those from male to female heterogamety are labeled a, while those from female to male heterogamety are labeled c. Among the reverse transitions involving fixation of recessive sex determining mutations, those from female to male heterogamety are labeled b, while those from male to female heterogamety are labeled d. We shall use this labeling throughout for model 2 transitions. Transitions b and d do not involve the production of individuals homozygous for a previously sex-specific chromosome, while transitions a and c do.

Again, notice that, if there are no demographic differences between males and females, then the dynamics in directions c and d are respectively identical to those in directions a and b up to a relabeling of males and females.

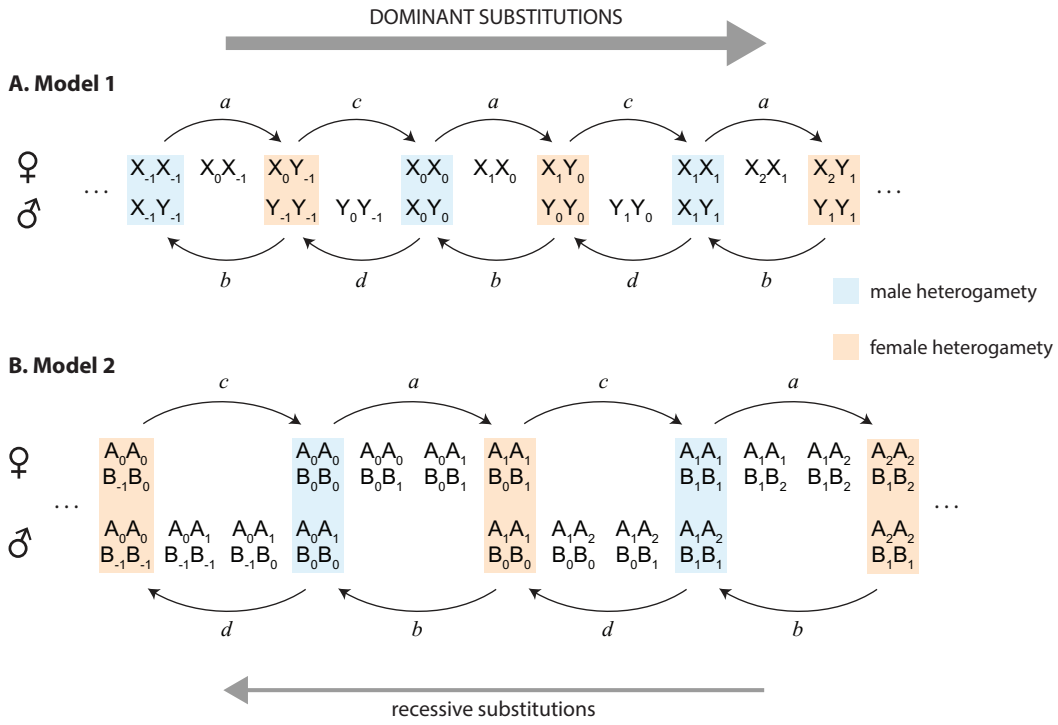

Figure 6.3.3: A general representation of the substitutions involved in changing the heterogametic system, both for model 1 transitions (A) and for model 2 transitions (B). Transitions between heterogametic systems that involve the arrival and fixation ('substitution') of new dominant sex determining mutations are labeled *a* and *c*. Transitions that involve the substitution of new recessive sex determining mutations are labeled *b* and *d*. For model 2 (B), we have used the arbitrary letters A and B to denote the two separate chromosomes/unlinked loci: one switches to a sex chromosome, and the other switches to an autosome, each time the heterogametic system changes.

6.4 Methods

The equilibrium paths described in the previous section arise under deterministic evolutionary dynamics. Our aim is to study stochastic evolution along and around these paths. To do so, we employ Monte Carlo simulations to estimate the substitution rates of the various mutations along the paths, and approximation techniques to analytically investigate the results of these simulations.

For computational efficiency, our simulations are of a non-overlapping generations Wright-Fisher process [154, 219, 584]. For mathematical tractability, on the other hand, our analytical treatment considers models of the overlapping generations Moran type [375]; mapping between these processes in the diffusion limit simply requires rescaling the rate of genetic drift [143]. The agreement of the results under the two processes will demonstrate their robustness to the consideration of overlapping or non-overlapping generations.

6.4.1 Monte Carlo simulations

For both model 1 and model 2, we simulate a population of constant size N, which comprises males and females, and evolves according to a sexual Wright-Fisher process [154, 219, 584]. Each generation, males and females form mating pairs, N in total. An individual can be in more than one pair, and the probability that an individual is in a given pair is proportional to that individual's fitness relative to other members of its sex (and is independent across pairs). Each mating pair produces a single offspring, whose sexual genotype (and therefore sex) is determined by randomly choosing a gamete from each of its parents. The sex chromosomes of heterogametic individuals are assumed to segregate in a Mendelian fashion. After offspring production, all individuals in the parental generation die. (This model is

equivalent to one in which each male contributes a large number of sperm, proportional to his fitness, to a common sperm pool, each female contributes a large number of eggs, proportional to her fitness, to a common egg pool, and each of N offspring is then formed by drawing a random sperm and a random egg from the respective pools.)

As a baseline for both models, we consider the case where each genotype is equally fit (the 'neutral' case), i.e., where each individual within a sex is equally likely to be chosen to be in a given mating pair. Thereafter, we focus on cases where individuals that are homozygous for a previously sex-specific chromosome suffer a selective disadvantage: each such individual is a fraction $1 - s$ as likely as other members of its sex to be chosen to be in a given mating pair.

In all cases, we assume no population structure (mating is random), and no demographic differences between males and females in our simulations. Relaxing these assumptions is an important direction of future work, and would be aided by parallel theoretical developments in the general study of drift-induced selection. In [547, Section S1.3], we give some numerical picture of how demographic differences between males and female (viz. greater variance in male reproductive success) affect our results (also see Discussion section).

6.4.2 Diffusion approximations

In the Moran formulation, we likewise consider a discrete population of N individuals. Males and females of each genotype encounter each other with a probability per unit time proportional to their frequency in the population. On encountering each other, a pair produces a single offspring, which inherits its sexual genotype from its parents in a Mendelian fashion. In order to keep the population size constant

at N, another individual is chosen to die. In the neutral case, each individual in the population is equally likely to be chosen to die. In the case with selection, the probability that an individual is chosen to die is weighted by a normalized death probability, the inverse of that genotype's fitness. This implementation of selection will give similar dynamics to the Wright-Fisher model to leading order in the selection strength (see In [547, Section S2.1].

In order to simplify the probabilistic model, we make use of a diffusion approximation [111]. Denoting the frequency of each genotype by p_i and assuming N to be large but finite, the evolution of the pdf for the system $\phi(\boldsymbol{p}, t)$ is approximately governed by

$$\begin{aligned}\frac{\partial \phi(\boldsymbol{p}, \tau)}{\partial \tau} = &- \sum_i \frac{\partial}{\partial p_i} \left[A_i(\boldsymbol{p}) \phi(\boldsymbol{p}, \tau)\right] \\ &+ \frac{1}{2N} \sum_{i,j} \frac{\partial^2}{\partial p_i \partial p_j} \left[B_{ij}(\boldsymbol{p}) \phi(\boldsymbol{p}, \tau)\right] \end{aligned} \tag{6.3}$$

[178, 361], where the forms of the vector $\boldsymbol{A}(\boldsymbol{p})$ and the matrix $B(\boldsymbol{p})$ can be directly calculated for both models 1 and 2 from their respective probability transition rates (see [547, Section S2.1]. The term $\boldsymbol{A}(\boldsymbol{p})$ primarily controls the time-evolution of the mean of $\phi(\boldsymbol{p}, t)$, and can thus be interpreted as a deterministic selective term. Indeed, in the deterministic limit ($N \to \infty$), the dynamics of the system are described by the ordinary differential equations $\dot{\boldsymbol{p}} = \boldsymbol{A}(\boldsymbol{p})$. Meanwhile, the term $B(\boldsymbol{p})$ controls the diffusion of $\phi(\boldsymbol{p}, t)$, thus capturing the effect of genetic drift.

In comparing this diffusion equation with one for the analogous Wright-Fisher process, we must take account of two scalings. First, genetic drift is larger by a factor of two in the Moran formulation than in the Wright-Fisher formulation [143, 149]. This leads to an additional pre-factor of $1/2$ appearing before the $B(\boldsymbol{P})$ in the

Wright-Fisher formulation of Eq. (6.3). Second, reproduction occurs $4N$ times faster in the Wright-Fisher model. This is because individual reproduction events in the sexual Moran model occur at an average rate proportional to the product of the frequency of males and females in the population (which is 1/4 at equilibrium sex ratios), whereas, in the Wright-Fisher model, N reproduction events occur every time-step. Since we have already taken into account a factor N in timescale in obtaining Eq. (6.3) ($\tau = t/N$), the Wright-Fisher formulation of Eq. (6.3) contains an additional factor of 4 preceding all terms on the right-hand side of Eq. (6.3).

We wish to determine the probabilities of transitions from male to female heterogamety, and vice-versa. The calculation of these quantities is not straightforward; the diffusion equation (6.3) governing the dynamics is non-linear in either four or five variables (for models 1 and 2, respectively). However, analytical progress can be made by exploiting a separation of timescales that is present in both models. Such methods have long been successfully employed in population genetics to solve a wide range of problems [140, 390, 499]. The key to progress is in noting that, in the deterministic neutral systems, a trajectory starting from any initial point will quickly collapse to a point on the equilibrium path of the system, Eq. (6.1) for model 1 (Figure 6.3.1B) and Eq. (6.2) for model 2, where it will then stay. In the current notation, this line is the set of solutions $\boldsymbol{p}$ to the equation $\boldsymbol{A}(\boldsymbol{p}) = 0$. When genetic drift and selection are taken into account, the system will no longer reach and subsequently remain at a position on this line. However, if selection is weak and N is large (such that the rate of genetic drift, $1/N$, is small), then the system will quickly collapse to a subspace in the vicinity of this line; it will then slowly move along this 'slow subspace' until the system fixes in a state of either male or female heterogamety. We exploit this separation of timescales by removing

the fast transient dynamics to obtain an approximation for the system dynamics in the slow subspace. Since this approximate description in the slow subspace is in terms of a single variable, q [see Eqs. (6.1) and (6.2)], fixation probabilities are then straightforward to calculate.

There is no unique way to mathematically implement the approach outlined conceptually above. While methods similar to the projection operator formalism described in [178] have historically found most favor in the population genetics literature (e.g., [140, 499]), in this paper we implement the approach described in [419], which is more intuitive in the present case. The full calculation is provided in the [547, Section S2.2]. Here we simply state the key results. On removing the fast-variables, the dynamics of Eq. (6.3) can be approximated by

$$\begin{aligned}\frac{\partial \psi(q,\tau)}{\partial \tau} = &- \frac{\partial}{\partial q}\left\{\left[\mathcal{D}(q)+\mathcal{S}(q)\right]\psi(q,\tau)\right\} \\ &+ \frac{1}{2N}\frac{\partial^2}{\partial^2 q}\left\{\mathcal{B}(q)\psi(q,\tau)\right\} . \end{aligned} \tag{6.4}$$

Here, $\psi(q,t)$ is the probability density function for q along the slow subspace. In a similar fashion to Eq. (6.3), the terms $\mathcal{D}(q)$ and $\mathcal{S}(q)$ control the time-evolution of the mean of $\psi(q,t)$ and can thus be interpreted as selective terms for q along the slow subspace. Likewise, the term $\mathcal{B}(q)$ controls the diffusion of $\phi(\boldsymbol{p},t)$, and can thus be interpreted as capturing the effect of genetic drift along the slow subspace.

The equation for the slow subspace itself can be approximated by the equation for the equilibrium line, since they lie close to each other in the weak selection limit, and coincide when selection is absent. The equations for $\mathcal{D}(q)$, $\mathcal{S}(q)$, and $\mathcal{B}(q)$ can be determined from $\boldsymbol{A}(\boldsymbol{p})$ and $B(\boldsymbol{p})$ along with the equation for the slow subspace. The terms $\mathcal{D}(q)$ and $\mathcal{B}(q)$ are simply the components of $\boldsymbol{A}(\boldsymbol{p})$ and $B(\boldsymbol{p})$ along the slow

subspace (i.e., respectively, the components of deterministic selection and genetic drift in the subspace). More interesting is the term $\mathcal{S}(q)$, which is a selective term induced by genetic drift. Its origin can be interpreted in various ways. First, it can be graphically understood as resulting from a bias in how fluctuations taking the system off the slow subspace return to the slow subspace (i.e., fluctuations do not return, on average, to the point from which they originated on the slow subspace) [100, 419]. Second, it can be mathematically understood as the result of making a non-linear change of stochastic variables [444] into the system's slow variable. Finally, it can be understood as the result of a selective pressure favoring genotypes with a lower variance in their reproductive output—Gillespie's Criterion [182, 216, 420]. In Eq. (6.4), differences in the variance of the reproductive output of the genotypes emerge naturally from the confinement of the system to the slow subspace.

6.5 Results

6.5.1 Model 1: Transitions using the same chromosomes

In this section, we study transitions between male and female heterogamety where the sex chromosome locus is the same under both systems (Figures 6.3.1 and 6.3.3A).

Monte Carlo simulations

We begin with a male-heterogametic system, XX/XY, in a population of constant size N, initially with $N/2$ females (all XX) and $N/2$ males (all XY). We consider a mutation to one of the X chromosomes, rendering it an X′ chromosome, X′Y and X′X bearers of which are female. YY individuals are male. If the X′ chromosome 'fixes' in the population, a female-heterogametic system, X′Y/YY, is established (direction a in Figures 6.3.1A and 6.3.3A).

Influenced by whether the original X′ mutation occurs in oogenesis or spermatogenesis, the X′ could initially find itself in an X′X or an X′Y female. We consider both cases in our simulations, and in both begin with a population that is $N/2$ females (one of which carries an X′ chromosome) and $N/2$ males.

Initially assuming all five sexual genotypes to be equally fit, what is a reasonable null expectation for the fixation probability of this X′ chromosome? The fixation probability of a mutation on the X chromosome of no effect is simply the inverse of the initial census count of the X chromosome, i.e., $1/(3N/2)$. This we take to be the neutral expectation for $\rho_{\mathrm{X}'}^{\mathrm{null}}$, the fixation probability of the X′ chromosome, so that $N\rho_{\mathrm{X}'}^{\mathrm{null}} = 2/3$.

Instead, we find in our simulations that the fixation probability of the X′ chromosome is higher than this neutral expectation, with $N\rho_{\mathrm{X}'} \approx 1.12$ (Figure 6.5.1A). This is irrespective of the background on which the initial X′ chromosome finds itself [547, Figure S1A]. The average conditional fixation time of the X′ chromosome is close to $2.4N$ for each N considered in our simulations, and again, this is irrespective of the mutation's initial background [547, Figure S1B]. A fixation time that scales linearly with N is strongly suggestive of drift-like evolutionary dynamics.

We now consider evolution in the other direction along the path (direction b in Figures 6.3.1A and 6.3.3A). We begin with an established X′Y/YY female-heterogametic system, and consider a mutation to one of the X′ chromosome that renders it an X. If this X chromosome subsequently fixes in the population of X and X′ chromosomes, an XX/XY male-heterogametic system would be established. Here, the X mutation must occur in oogenesis, since it derives from an X′ chromosome which must have been borne by a female. Therefore, the first individual to carry the new X chromosome must be an XY male. For consistency, we be-

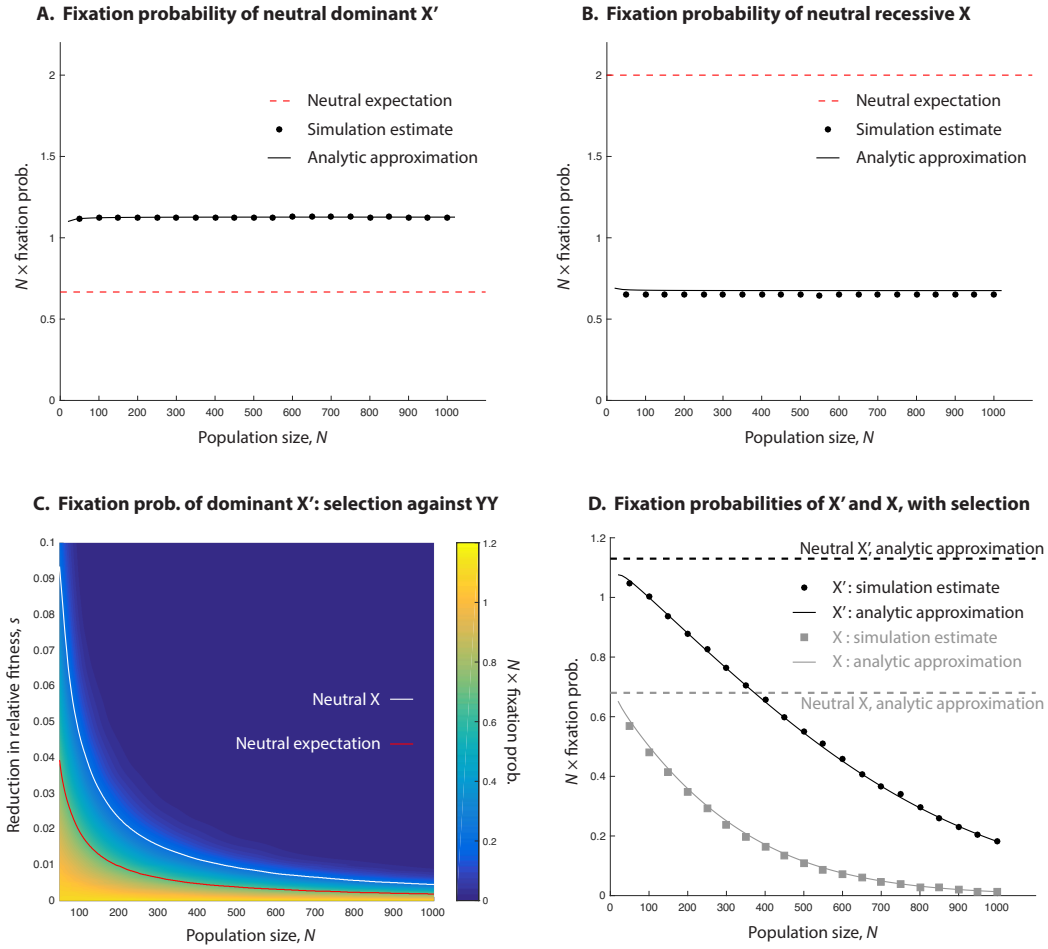

Figure 6.5.1: Fixation probabilities in Model 1 heterogametic transitions. (A, B) The fixation probability of a neutral dominant feminizing X′ arising in an XX/XY system is significantly higher than the neutral expectation (A), while the reverse fixation probability of a neutral recessive feminizing X chromosome arising in an X′Y/YY system is lower than the neutral expectation (B). (C) If YY individuals are selected against in the transition from XX/XY to X′Y/YY, the substitution rate of the X′ chromosome causing this transition is reduced. Still, selection needs to be sufficiently strong to reduce the substitution rate below the neutral expectation (above red line), and even stronger to reduce the substitution rate below that of the neutral X chromosome in the reverse transition (above white line). This is especially true in smaller populations. (D) Fixation probabilities of the X′ and X chromosomes, in directions *a* and *b* of Figure 6.3.1A respectively, when individuals homozygous for a previously sex-specific chromosome have relative fitness reduced by $s = 0.5\%$. Though the fixation probabilities of the two chromosomes decrease when this selection operates, the relative advantage in substitution rates enjoyed by the dominant X′ over the recessive X is exacerbated.

gin our simulations with $N/2$ females and $N/2$ males (one of which carries the X chromosome).

Similar to before, our neutral expectation for the fixation probability of the X is just the inverse of the number of X′ chromosomes initially in the population, i.e., $\rho_{\mathrm{X}}^{\mathrm{null}} = 1/(N/2)$, so that $N\rho_{\mathrm{X}}^{\mathrm{null}} = 2$. Instead, in our simulations we find the fixation probability of the X chromosome to be much lower than this neutral expectation, with $\rho_{\mathrm{X}} \approx 0.65$ (Figure 6.5.1B). The average conditional fixation time of the X chromosome is, like that of the X′, close to $2.4N$ for each N considered [547, Figure S2B].

Thus, the fixation probability of the X′, starting from an initial XX/XY system, is almost twice as great as the fixation probability of the X, starting from an initial X′Y/YY system. However, to properly determine whether evolution along the equilibrium path is biased in favor of the X′ chromosome, we must consider the *substitution rates* of the two chromosomes. In doing so, we assume symmetric mutation rates in the two directions, i.e., that the probability of an X chromosome mutating to an X′ is the same as the probability of an X′ chromosome mutating to an X. We also assume this mutation rate to be sufficiently small that at most one mutation segregates in the population at any given time (a common assumption [355]).

Suppose this mutation rate to be u per chromosome per generation. An XX/XY population with even sex ratio produces X′ mutations at a rate of $\mu_{\mathrm{X}'} = (3N/2)u$ per generation, while an X′Y/YY population produces X mutations at a third of this rate, $\mu_{\mathrm{X}} = (N/2)u$ per generation. Under our naive neutral expectations, the substitution rates of the X and X′ chromosomes should both be u ($= \mu_{\mathrm{X}'}\rho_{\mathrm{X}'}^{\mathrm{null}} = \mu_{\mathrm{X}}\rho_{\mathrm{X}}^{\mathrm{null}}$). Instead, the substitution rate $\mu_{\mathrm{X}'}\rho_{\mathrm{X}'}$ from an XX/XY to an X′Y/YY system (in direction a of Figures 6.3.1A, 6.3.3A) is about $(3N/2)u \times 1.12/N = 1.68u$,

while the substitution rate $\mu_X \rho_X$ from an X′Y/YY to an XX/XY system (direction b of Figures 6.3.1A, 6.3.3A) is about $(N/2)u \times 0.65/N = 0.325u$. That is, the substitution rate of the X′ is more than *five times higher* than that of the X.

Since, in the population model we have simulated, there are no demographic differences between males and females, the transitions symmetric to those above (i.e., in directions c and d in Figure 6.3.3) occur with fixation probabilities and substitution rates equivalent to those we have estimated above (i.e., with reference to Figure 6.3.3, the fixation probabilities in directions a and b match those in directions c and d respectively).

Therefore, the most likely trajectory that the neutral dynamical system will follow in the long term is the recurrent invasion and fixation of successive *dominant* sex determining mutations, flipping the system repeatedly between male and female heterogamety. This corresponds to a bias in favor of rightward transitions in Figure 6.3.3.

We now consider the possibility that some genotypes are fitter than others. In particular, we study the case where individuals homozygous for a previously sex-specific chromosome (including mutated versions of it) are of lower fitness.

The transition from a male-heterogametic XX/XY system to a female-heterogametic X′Y/YY system, via fixation of the dominant X′ chromosome and displacement of the X, involves the production of YY males. Assume that YY males have relative fitness $1 - s$, while all other sexual genotypes are of equal fitness 1. Figure 6.5.1C gives the fixation probability of the X′ chromosome for various values of s and N. As expected, the fixation probability decreases as selection against the YY genotype increases. Nonetheless, it is clear that the YY genotype can suffer appreciable fitness reductions with the X′ chromosome still fixing with probability higher than

the neutral expectation. This is especially true in small populations, in which selection acts less efficiently [302]; we would expect this to carry over to structured populations of larger size, e.g., those that are subdivided into many small demes in which drift is an important force [303, 573].

The reverse transition, from the X′Y/YY to the XX/XY system, involves the production of X′X and XX females. The substitution rate of the X, in direction b of Figure 6.3.1A, was very low even when no genotypes were of reduced fitness; selection against the XX and X′X genotypes (recall that the X′ chromosome is just an X mutated at the sex-determining locus) severely exacerbates this disadvantage (Figures 6.5.1D and S4). Again, given the symmetry between transitions in directions a and c in Figure 6.3.3, and between transitions in directions b and d, the above results imply a bias towards c transitions over d transitions, with this bias exacerbated by selection. That is, selection generally exacerbates the bias in favor of rightward (dominant) transitions in Figure 6.3.3.

Analytical results

To better understand these simulation results, we now study the system analytically in the diffusion limit. We first consider the neutral case. Applying the fast-variable elimination described in *Methods* and detailed in full in [547, Section S2], we find for the model 1 system described in Eq. (6.1) that the system dynamics can be approximated by Eq. (6.4) with $\mathcal{D}(q) = 0$ and

$$\begin{aligned}\mathcal{S}(q) &= \frac{1}{4N}\frac{q(1-q)(1+q)^3(1+q^2)\{1+(2-q)q[4+q(6+q)]\}}{[1+q(2+3q)]^3}\\ \mathcal{B}(q) &= \frac{1}{4}\frac{q(1+q)^3\{1+q\,[1+q(6-q(6+(3-q)q))]\}}{[1+q(2+3q)]^2}\end{aligned} \tag{6.5}$$

(calculations in [547, Section S2.2.1]). As we expect in this neutral scenario, there are no deterministic contributions to selection along the equilibrium path [$\mathcal{D}(q) = 0$]. However, there is a drift-induced selection term [$\mathcal{S}(q) \neq 0$]. The strength of the drift-induced selection is of order $1/N$, generated as it is by demographic fluctuations. Recalling that $q = 0$ corresponds to male heterogamety [XX/XY; $p_1 = 1/2$, $p_4 = 1/2$ in Eq. (6.1)], while $q = 1$ corresponds to female heterogamety [X′Y/YY; $p_3 = 1/2$, $p_5 = 1/2$ in Eq. (6.1)], we find that the drift-induced selection selects for the fixation of the dominant sex determining mutation *at every point* on the equilibrium path [$\mathcal{S}(q) > 0$ for all $q \in (0, 1)$].

How does this drift-induced selection emerge? Essentially, in this 'neutral' stochastic system, demographic fluctuations continually perturb the system away from the equilibrium path (to which the deterministic system is constrained). There is then a selective pressure for the system to return to the equilibrium path. However, the nonlinear trajectories along which these fluctuations return, combined with the curvature of the equilibrium path, give rise to a bias in the average position to which fluctuations return. In other words, fluctuations arising at a point q return on average to a point $q + \delta(q)$ on the equilibrium path.

Mathematically quantifying this bias requires taking account of the probability distribution of fluctuations in each genotype, the form of trajectories back to the equilibrium path, and the curvature of the equilibrium path itself, each of which varies as q is varied. However, further intuition can be gained by decomposing $\mathcal{S}(q)$ into two components: $\mathcal{S}(q) = \mathcal{S}^{\mathrm{NL}}(q) + \mathcal{S}^{\mathrm{C}}(q)$. The first term, $\mathcal{S}^{\mathrm{NL}}(q)$, quantifies contributions to $\mathcal{S}(q)$ arising from the non-linearity of trajectories that take the system back to the equilibrium path. The second term, $\mathcal{S}^{\mathrm{C}}(q)$, quantifies contributions to $\mathcal{S}(q)$ arising from the curvature of the equilibrium path itself. Plotting these

terms together in Figure 6.5.2A, we see that it is the curvature of the equilibrium path that contributes most to the observed drift-induced selection.

Standard methods can be used to numerically calculate the fixation probability of either male or female heterogamety for any initial condition q_0 on the slow subspace (see [178, 444]; and [547, Section S2.3]). Our final task is to calculate how the initial conditions described in the previous section, those of single mutants invading a resident population, map onto initial conditions on the equilibrium path. That is, for a given $\boldsymbol{p}_0$, we wish to determine q_0. This calculation is given in [547, Section S2.3.1]; with it, the neutral fixation probabilities can be calculated.

The results for the fixation probabilities of the mutants are given in Figure 6.5.1A, in which we see excellent agreement between theory and simulations. In particular we find that the fixation probability of the X′ chromosome under the diffusion approximation is $N\rho_{\mathrm{X}'} \approx 1.13$ (Figure 6.5.1A). This is irrespective of the background on which the initial X′ chromosome finds itself, as both of these initial conditions lead to the same initial condition q_0 on the equilibrium path [547, Section S2.3.1]. We may also compute the mean conditional fixation time of the X, which agrees well with our simulation estimates when the differences in variance between the Wright-Fisher and Moran processes are taken into account [547, Figure S1B]. Meanwhile the fixation probability of an X chromosome is $N\rho_{\mathrm{X}} \approx 0.68$, again in close agreement with our simulation results (Figure 6.5.1B), as is the computed mean conditional fixation time [547, Figure S2B].

We now consider the possibility that some genotypes are fitter than others. For transition direction a, assume that YY males (with frequency p_5) have relative death rate $\Delta_5 = 1+s$, while all other sexual genotypes have death rate 1. When s is small, we can still utilize fast-variable elimination to arrive at the approximate description

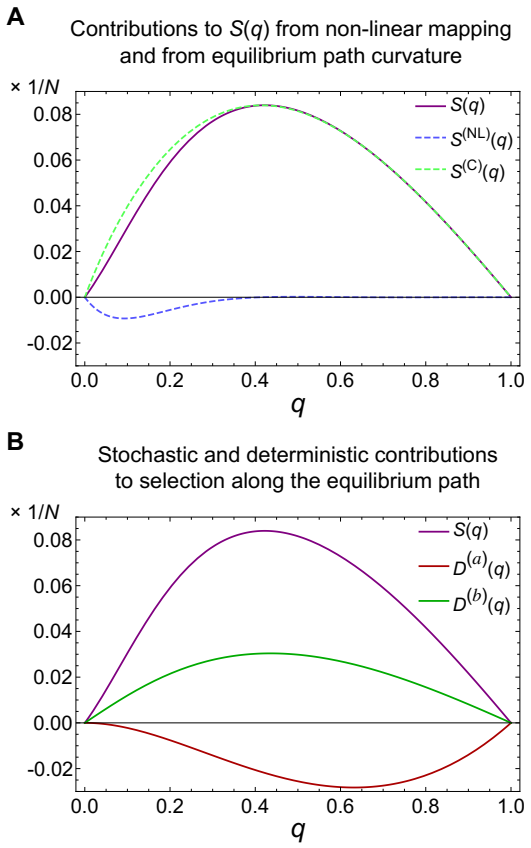

Figure 6.5.2: (A) In model 1, random demographic fluctuations induce a selective gradient $\mathcal{S}(q)$ along the equilibrium path in favor of the dominant sex determining chromosome, i.e., causing q to increase on average [see Eqs. (6.4) and (6.5)]. $\mathcal{S}(q)$ can be divided into two components. The first, $\mathcal{S}^{(\mathsf{NL})}$, is from non-linear components of the mapping of fluctuations back to the equilibrium path; the second, $\mathcal{S}^{(\mathsf{C})}$, is from the curvature of the equilibrium path. In this case, it can be seen that the primary contribution to the drift-induced bias $\mathcal{S}(q)$ is from curvature of the equilibrium path. (B) Contributions to average dynamics along the equilibrium path arising from drift-induced selection, $\mathcal{S}(q)$, and deterministic selection against individuals homozygous for a previously sex-specific chromosome, $\mathcal{D}(q)$ [see Eq. (6.4)]. Note that the form of $\mathcal{D}(q)$ is expected to change depending on whether the initial population exhibits XX/XY male heterogamety [$\mathcal{D}^{(a)}(q)$] or X′Y/YY female heterogamety [$\mathcal{D}^{(b)}(q)$] [Eqs. (6.6) and (6.7)], i.e., whether the transition is in direction *a* or direction *b* of Figure 6.3.1A. In both plots the parameters have been scaled such that $N\delta = 1$ in order to facilitate the comparison of contributions to selection along the slow subspace.

of the system dynamics given by Eq. (6.4). The functions $\mathcal{S}(q)$ and $\mathcal{B}(q)$ retain the forms given in Eq. (6.5), but now $\mathcal{D}(q) = \mathcal{D}^{(a)}(q)$, where

$$\mathcal{D}^{(a)}(q) = -\frac{s}{4}\frac{q^2(1-q)(1+q)^2}{1+2q+3q^2} \tag{6.6}$$

and the superscript '(a)' denotes that this is $\mathcal{D}(q)$ evaluated for transitions in direction a (Figure 6.5.2B; calculations in [547, Section S2.2.1]). This term is of order s as this is the deterministic contribution to the dynamics along the slow subspace.

For the reverse transition b, assume that XX and X′X females (with frequencies p_1 and p_2) have relative death rates $\Delta_1 = 1+s$ and $\Delta_2 = 1+s$ respectively, while all other sexual genotypes have death rate 1. Again utilizing fast variable elimination, we find $\mathcal{D}(q) = \mathcal{D}^{(b)}(q)$, where

$$\mathcal{D}^{(b)}(q) = -\frac{s}{8}\frac{q(1+2q-q^2)(1-q^2)}{1+2q+3q^2} \tag{6.7}$$

and the superscript '(b)' denotes that this is $\mathcal{D}(q)$ evaluated for transitions in direction b (Figure 6.5.2B; calculations in [547, Section S2.2.1]).

We are now in a position to calculate the respective fixation probabilities of mutations arising in directions a and b. We find that, while the fixation probability of X′ in direction a is of course lower than in the neutral case (since YY is selected against), the relative reduction of the fixation probability of X in direction b is even higher (Figure 6.5.1D).

6.5.2 Model 2: Transitions that change the sex chromosome pair

In this section, we study transitions between male and female heterogamety where, in the course of the transitions, a pair of chromosomes that are initially autosomal

are co-opted as new sex chromosomes, while one of the old sex chromosomes becomes autosomal (Figures 6.3.2 and 6.3.3B).

Monte Carlo simulations

Beginning with an XX,AA/XY,AA male-heterogametic system (where X and Y are sex chromosomes and A is an autosome), assume that a mutation appears on an A chromosome, rendering it an A′ such that XX,AA, XX,AA′, XY,AA′, and YY,AA′ individuals are female, while XY,AA and YY,AA individuals are male (Figure 6.3.2). If the A′ chromosome reaches sufficiently high frequency in the population, the X chromosome is eliminated, and a YY,AA′/YY,AA female-heterogametic system establishes (direction a in Figures 6.3.2 and 6.3.3B).

We initially assume all six sexual genotypes to be equally fit. Unlike for the case of transitions involving the same chromosome pair, we do not propose a null *expectation* for the fixation probability of the A′ mutation. This is because, if it fixes, it displaces the unlinked X chromosome from the population: this is not the 'population' in which the A′ arises, being a mutated A chromosome. (In contrast, in model 1, the X′ chromosome for example is a mutated X chromosome, and if it fixes, it displaces the X chromosome.) Therefore, we shall focus predominantly on comparing the substitution rates of the A′ and X chromosomes (i.e., the substitution rates, respectively, in directions a and b of Figure 6.3.2). We may, however, take as a *reference* neutral fixation probability for both mutations, ρ^{ref}, that of a mutation of no effect occurring on an autosome: $N\rho^{\text{ref}} = 1/2$.

In our simulations, we find the fixation probability of the A′ chromosome to be $N\rho_{\text{A}'} \approx 1.07$ (Figure 6.5.3A), substantially higher than our reference value of 1/2. This value is insensitive to the genetic background of the initial mutation [547,

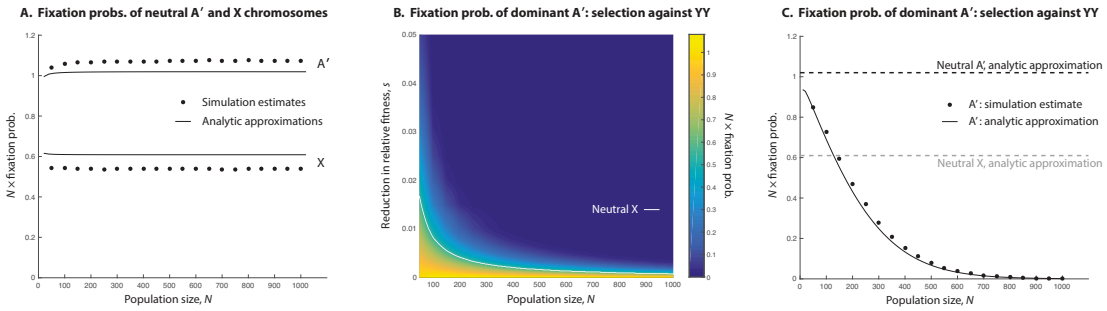

Figure 6.5.3: Fixation probabilities in Model 2 heterogametic transitions. (A) The fixation probability of a neutral dominant feminizing A′ arising in an XX,AA/XY,AA system is substantially higher than the reverse fixation probability, that of a neutral recessive feminizing X chromosome arising in an YY,AA′/YY,AA system. (B) If YY individuals are selected against in the transition from XX,AA/XY,AA male heterogamety to YY,AA′/YY,AA female heterogamety (direction *a* in Figure 6.3.2), the substitution rate of the A′ chromosome causing this transition is reduced. But selection needs to be sufficiently strong to reduce the substitution rate below that of the neutral X chromosome in the reverse transition (above white line), especially in smaller populations. (C) Fixation probability of the A′ chromosome when YY individuals have relative fitness reduction $s = 0.5\%$. Since the reverse transition (direction *b* in Figure 6.3.2) does not involve the production of individuals homozygous for the previously sex specific chromosome (the A′), the substitution rates in the two directions are equal where the declining fixation probability of the A′ intersects the flat neutral fixation probability of the X, here at a population size of only about 150 individuals. For larger populations, the recessive X substitutes at a higher rate than the dominant A′.

Figure S5A]. The average conditional fixation time of the A′ in our simulations is approximately $2.65N$ for each N considered, again regardless of the initial background of the mutation [547, Figure S5B], and again suggestive of drift-like dynamics.

Turning our attention to transitions in the other direction along the equilibrium path (direction *b* in Figures 6.3.2 and 6.3.3B), we begin with a female-heterogametic YY,AA′/YY,AA system, and assume that a mutation on a Y chromosome occurs, rendering the chromosome a recessive feminizing X. If this mutation reaches sufficient frequency, the male-heterogametic system XX,AA/XY,AA establishes.

We estimate in our simulations that the fixation probability of the X is $N\rho_X \approx 0.54$ (Figure 6.5.3A), which is fractionally higher than the reference value of 1/2.

The background on which the mutation arises has no effect on its fixation probability [547, Figure S6A]. The average conditional fixation time of the X chromosome is also close to $2.65N$ for all values of N considered [547, Figure S6B].

To see if there is a directional bias in one direction or the other along the equilibrium path, we assume that these mutations occur at the same rate, u per chromosome per generation, and calculate the substitution rates of the two transitions.

The male-heterogametic system XX,AA/XY,AA generates A′ mutations at rate $\mu_{A'} = 2Nu$, so that the substitution rate from an XX,AA/XY,AA system to a YY,AA′/YY,AA system (in direction a of Figures 6.3.2, 6.3.3B) is about $\mu_{A'}\rho_{A'} = 2Nu \times 1.07/N = 2.14u$. Similarly, the female-heterogametic system YY,AA′/YY,AA generates X mutations at rate $\mu_X = 2Nu$, and so the substitution rate from a YY,AA′/YY,AA system to an XX,AA/XY,AA system (direction b of Figures 6.3.2, 6.3.3B) is about $\mu_X\rho_X = 2Nu \times 0.54/N = 1.08u$, or about half that of the reverse transition.

Again, with no demographic differences between males and females, the transitions symmetric to those above (i.e., in directions c and d in Figure 6.3.3B) occur with fixation probabilities and substitution rates equivalent to those we have estimated above (i.e., the fixation probabilities in directions a and b match those in directions c and d respectively).

We now consider the role of selective differences between the genotypes. This is an especially important question here because, unlike in model 1 heterogametic transitions, model 2 transitions are possible without the production of individuals homozygous for a previously sex-specific chromosome. In particular, the transitions in directions b and d of Figure 6.3.3B change the heterogametic system, but do not involve the production of individuals homozygous for the previously sex-specific

chromosome. In contrast, the reverse transitions (in directions a and c) do involve the production of individuals homozygous for previously sex-specific chromosomes. Since we have found these latter transitions to have higher substitution rates than the reverse transitions in the neutral case, we should expect selection to reduce, and when strong enough to overturn, this bias.

We focus on the transition from the male-heterogametic XX,AA/XY,AA system to the female-heterogametic YY,AA′/YY,AA system (direction a in Figures 6.3.2 and 6.3.3B), involving the substitution of a dominant female-determining A′ chromosome as a mutated A. The Y chromosome is sex-specific in the original XX,AA/XY,AA system, and we assume that it has accumulated deleterious recessive mutations such that the two YY genotypes are of fitness $1 - s$, relative to all other genotypes' fitness of 1. Figure 6.5.3B gives the fixation probability of the A′ chromosome for various values of s and N. Naturally, the fixation probability decreases as selection against the YY genotypes increases, and this effect is stronger in larger populations (in which selection acts more efficiently [302]). Indeed, in large populations, even very small degrees of selection against the YY genotypes are enough to overturn the substitution rate bias in favor of dominant sex determining mutations.

Analytical results

We begin by considering the dynamics of the neutral model. Once again, fast-variable elimination can be used to calculate the effective dynamics of the system along the equilibrium path [see Eq. (6.4)]. For model 2 (as with model 1), $\mathcal{D}(q) = 0$ (that is, there is no deterministic contribution to the dynamics along the equilibrium

path), but there is a drift-induced selection term, which now takes the form

$$\mathcal{S}(q) = \frac{q(1-q)(1+q)^3\left[1+(2-q)q\right]\left\{1+q\left[6-q\left(2-q(10+q)\right)\right]\right\}}{4N\left[1+q(2+5q)\right]^3}, \tag{6.8}$$

which, along with the expression for diffusion along the equilibrium path,

$$\mathcal{B}(q) = \frac{1}{4}\frac{q(1+q)^3\left\{1+q\left[1+q\left(10-q(2+q)(5-q)\right)\right]\right\}}{\left[1+q(2+5q)\right]^2}, \tag{6.9}$$

approximates the stochastic dynamics (calculations in [547, Section S2.2.2]). Recalling that $q = 0$ corresponds to male heterogamety [XX,AA/XY,AA; $p_1 = 1/2$, $p_5 = 1/2$ in Eq. (6.2)], while $q = 1$ corresponds to female heterogamety [YY,AA′/YY,AA; $p_4 = 1/2$, $p_6 = 1/2$ in Eq. (6.2)], we find that the drift-induced selection selects for the fixation of the dominant sex determining mutation *at every point* on the equilibrium path [$\mathcal{S}(q) > 0$ for all $q \in (0,1)$].

As in model 1, we find that demographic fluctuations away from the equilibrium path return to the equilibrium path on average with a bias, described by the drift-induced selection term $\mathcal{S}(q)$. Once again, $\mathcal{S}(q)$ can be split into two components, $\mathcal{S}^{\mathrm{NL}}(q)$ and $\mathcal{S}^{\mathrm{C}}(q)$, that respectively capture the contribution to $\mathcal{S}(q)$ arising from the non-linearity of trajectories taking the system back to the equilibrium path and the curvature of the equilibrium path itself. These terms are plotted in Figure 6.5.4A, in which we see that, as with model 1, it is the curvature of the equilibrium path that contributes most to drift-induced selection in model 2.

Using this single-variable description of the dynamics, the fixation probability for any initial condition q_0 on the equilibrium path can be calculated. In order to determine the fixation probability of mutants in the system starting from a single copy, we need to calculate the mapping, for each initial mutation scenario, from $\boldsymbol{p}_0$

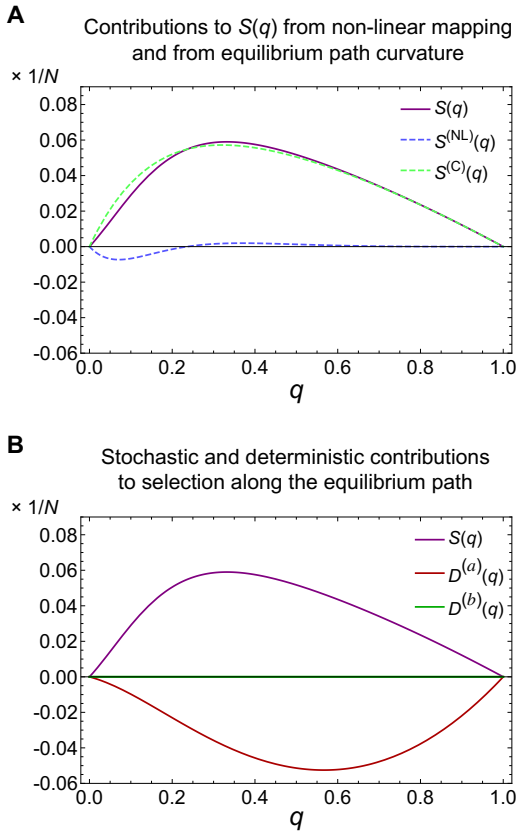

Figure 6.5.4: (A) In model 2, as in model 1, random demographic fluctuations induce a selective gradient $\mathcal{S}(q)$ along the equilibrium path in favor of the dominant sex determining chromosome, i.e., causing q to increase on average [see Eqs. (6.4) and (6.8)]. Again, $\mathcal{S}(q)$ can be divided into two components: $\mathcal{S}^{(\mathrm{NL})}$, from non-linear components of the mapping of fluctuations back to the equilibrium path, and $\mathcal{S}^{(\mathrm{C})}$, from the curvature of the equilibrium path. As in model 1, curvature of the equilibrium path is the primary contributor to drift-induced selection in favor of increasing q. (B) Contributions to average dynamics along the equilibrium path arising from drift-induced selection, $\mathcal{S}(q)$, and deterministic selection against individuals homozygous for a previously sex-specific chromosome, $\mathcal{D}(q)$ [see Eq. (6.4)]. Such individuals are only produced in transitions in direction *a* of Figure 6.3.2, where the initial population is XX,AA/XY,AA male heterogametic, so that $\mathcal{D}^{(a)}(q) < 0$ for all $q \in (0,1)$ [see Eq. (6.10)]. In transitions in direction *b* of Figure 6.3.2, where the initial population is YY,AA′/YY,AA female-heterogametic, no A′A′ individuals are produced, and so $\mathcal{D}^{(b)}(q) = 0$ for all q. In both plots the parameters have been scaled such that $N\delta = 1$ in order to facilitate the comparison of contributions to selection along the slow subspace.

to q_0. This calculation is given in [547, Section S2.3.2]. We can now evaluate our numerical expression for the neutral fixation probability at these initial conditions. Recall that simulations of the Wright-Fisher process showed the fixation probability of the A′ chromosome to be $N\rho_{\mathrm{A}'} \approx 1.07$, higher than our reference value of $1/2$. Our analytical prediction slightly underestimates this fixation probability ($N\rho_{\mathrm{X}} \approx 1.02$; Figure 6.5.3A). The background on which the mutation arises has no effect on its fixation probability, because the two scenarios initially have an identical component q_0 along the slow manifold [547, Section S2.3.2]. The computed mean conditional fixation time of the A′ agrees well with our simulation estimates [547, Figure S5B].

We next consider the fixation probability of an X mutation occurring on an initially autosomal Y. Our Wright-Fisher simulations returned an estimated fixation probability of $N\rho_{\mathrm{A}'} \approx 0.54$. Once again, there is a small discrepancy with our analytical results, which overestimate this value ($N\rho_{\mathrm{X}} \approx 0.61$; Figure 6.5.3A). The fixation probability is again the same irrespective of the background on which the X mutation occurs, because the initial conditions on the equilibrium path are the same [547, Section S2.3.2]. Again, we may compute the mean conditional fixation time of the X, and find good agreement with our simulation estimates when the variance difference between the Wright-Fisher and Moran processes is taken into account [547, Figure S6B].

We now consider the role of selective differences between the genotypes. As we have noted, comparing transitions in directions a and b, only those in direction a involve the production of individuals homozygous for a previously sex-specific chromosome, and so we focus here on transitions in direction a. We assume that the two YY genotypes (with frequencies p_4 and p_6) have elevated death rates $\Delta_4 = 1+s$ and $\Delta_6 = 1+s$ relative to all other genotypes' death rates of 1. The term $\mathcal{D}(q)$ in

Eq. (6.4) now becomes $\mathcal{D}(q) = \mathcal{D}^{(a)}(q)$, where

$$\mathcal{D}^{(a)}(q) = -\frac{s}{16}\frac{q(1-q)(1+q)^2\left[1+(8-q)q\right]}{1+q(2+5q)}. \tag{6.10}$$

$\mathcal{D}^{(a)}(q) < 0$ for all $q \in (0,1)$, and so this term acts in the opposite direction to $\mathcal{S}(q) > 0$ (Figure 6.5.4B; calculations in [547, Section S2.2.2]). There is thus an antagonism between the deterministic contribution to selection $\mathcal{D}^{(a)}(q)$ (favoring transitions in direction b) and the drift-induced selection (favoring transitions in direction a). Which of these dominates depends on the strength of selection and the population size: $\mathcal{D}^{(a)}(q)$ increases with s, while $\mathcal{S}(q)$ decreases with N.

In contrast, since transitions in direction b do not produce individuals homozygous for a previously sex-specific chromosome, none of the genotypes is selected against. Therefore, $\mathcal{D}(q)$ in direction b is $\mathcal{D}^{(b)}(q) = 0$.

Whereas in model 1 selection exacerbated the directionality of switching between sex determining systems (while decreasing the overall switching rate), in model 2 we see that deterministic selection and drift-induced selection work in opposite directions. Thus, for small populations with weak selection, transitions in directions a and c in Figure 6.3.3B occur more often than transitions in directions b and d, while for large populations with strong selection, transitions in b and d occur more often than transitions in directions a and c.

6.6 Discussion

We have studied stochastic evolution along two 'neutral' equilibrium paths connecting male and female heterogamety. We have shown that, even when all genotypes are equally fit, evolution along these paths is not neutral. Instead, it shows significant

substitution rate biases in particular directions, specifically in favor of dominant sex determining mutations. We have demonstrated these biases to be the result of drift-induced selection: random perturbations off the equilibrium path—inevitable in finite populations—return to the equilibrium path with an average directional bias in favor of the dominant segregating sex chromosome. The substitution rates of dominant sex determining mutations that switch the system of heterogamety are, in both of the cases we have studied, higher than those of truly neutral mutations occurring on the same chromosomes.

Evolutionary transitions between male and female heterogamety have been common in the evolutionary history of animals [15, 144, 145, 232, 260, 339, 340, 427], despite the fact that, in any given heterogametic system, the sex-specific chromosome should degrade over time by the operation of Muller's ratchet [71, 74]. To counter this 'evolutionary trap' [54, 442], mechanisms based on direct selective forces have been invoked to explain the frequency of heterogametic transitions (e.g., the operation of sex-specific selection [536]). Our demonstration of drift-induced selection in transitions between male and female heterogamety suggests that mechanisms based on direct selective differences between the sex chromosome genotypes may be unnecessary to explain empirical transitions. We have shown that small fitness reductions to individuals homozygous for previously sex-specific chromosomes are not enough to overturn the biases caused by drift-induced selection (Figures 6.5.1C and 6.5.3B). Large fitness reductions to such individuals (and in the limit, their inviability) render most transitions impossible—the exception being the recessive transitions b and d in model 2.

The influence of drift-induced selection in heterogametic transitions is therefore best understood in terms of evolutionary timescale. From an initial heterogametic

system with homomorphic sex chromosomes, the sex-specific chromosome gradually accumulates recessive deleterious mutations that would reduce the fitness of individuals homozygous for this chromosome. At some threshold period of time of accumulation of these mutations, the fitness reduction of the homozygote reduces the fixation probability of a dominant sex reversal mutation exactly enough to cancel this mutation's drift-induced selective advantage (Figures 6.5.1C and 6.5.3B). Prior to this time threshold, a transition via a dominant sex reversal mutation is likely—it becomes less likely as the threshold is neared. However, progress towards the threshold is reset every time a transition occurs, because each transition creates a new sex-specific chromosome from a chromosome that was previously not sex-specific.

A notable prediction of our findings is that heterogametic transitions should typically involve dominant sex determining mutations. That is, we should expect transitions usually to occur in directions a and c in Figures 6.3.3A and 6.3.3B, and not in directions b and d. This general prediction is not unique to our theory. For example, under the theory that heterogametic transitions are driven by linkage between novel sex determining genes and genes with sex-specific fitness effects [536], dominance of the sex determining mutation is either required for a transition, or substantially increases the parameter range over which a transition may occur. However, our analysis does reveal that this prediction can be recapitulated with a minimal number of biological assumptions.

Evidence in favor of this prediction comes from intermediate 'multi-factorial' systems [14]. In the platyfish *Xiphophorus maculatus*, females are XX, WX, or WY, while males are XY or YY [261, 262]. In principle, such a system could have arisen either in directions a or b of Figure 6.3.3A, depending on the ancestral heteroga-

metic system. Mapping known systems of heterogamety in the genus *Xiphophorus* [522] onto a phylogeny of the clade [112] suggests this ancestral system to be male heterogamety, in which case the intermediate system of *X. maculatus* has arisen in direction *a* of Figure 6.3.3A, via a dominant sex reversal mutation, consistent with our prediction. The western clawed frog, *Xenopus tropicalis*, also has an intermediate system: females are ZW or WW, and males are ZZ, ZY, or WY [447]. This system could have arisen in direction *c* or *d* in Figure 6.3.3A, depending on the ancestral system. The mechanism of sex determination has yet to be determined for most members of the genus *Xenopus* [447, 522], but the well-studied *X. laevis* is female-heterogametic [69], as is *X. borealis* [177]. If female heterogamety is ancestral to the intermediate system of *X. tropicalis*, then this intermediate system would have arisen in direction *c* of Figure 6.3.3A, again consistent with our prediction. Though it is possible that balancing selection operates to stabilize these observed instances of multi-factorial systems (e.g., [411])—with the important suggestion that, because observed instances are rare, most intermediate multi-factorial systems are transitional—the drift-induced selection that we have discovered operating at all points on the slow subspace near the line of equilibria will, even in this case, act so as to make invasion of dominant sex determining mutations more likely.

The prediction that heterogametic transitions should usually involve dominant sex determining mutations can also be tested by reciprocal crosses of species or populations on either side of a recent heterogametic transition, provided the ancestral system is known. In the frog *Rana rugosa*, populations in northern Japan are female-heterogametic, while those in southern Japan are male-heterogametic [371, 392]. The sex chromosomes in these populations are all homologous [529], and so a model 1 transition appears to have occurred. Because the ancestral system

is male heterogamety [403], the candidate directions in Figure 6.3.3A are *a* and *d*. These two directions can be distinguished by crossing a homogametic male (from the north) with a homogametic female (from the south). If the transition occurred in direction *a*, all the offspring from this cross should be male, but if it occurred instead in direction *d*, all the offspring should be female. This test has been carried out using homogametic males from Hirosaki (in the north) and homogametic females from Kumano (in the south), the reciprocal cross of which yielded almost all male offspring [392]. Again, this is consistent with our prediction. [Crossing heterogametic males and females yielded a sex ratio of 1/2 [392], consistent with the model 1 transitions we have studied, though not informative of which direction the transition was in.]

The bias we have found in favor of substitution of dominant sex determining mutations also carries predictions for how the genetic pathways underlying sex determination should look. We have referred throughout to 'sex chromosomes', but in reality we are talking about genes of major sex determining effect, the presence or absence of which acts as a switch to direct development down separate molecular pathways, or sex determining 'cascades', which then produce males and females. The downstream components of these cascades tend to be widely conserved [28], but there is significant lability in the upstream components—through the addition of new sex determining genes to the top of the cascade [575] and the shuffling of genes already in a cascade [460]—suggesting that these cascades evolve 'from the bottom up'. This is consistent with our findings: our model predicts successive transitions involving dominant sex determining mutations, with comparatively few reversals involving fixation of recessive sex determining mutations, and so we expect either the expansion of sex determining cascades, or their shuffling, but seldom their

contraction.

The drift-induced selective force that we have identified is a weak one: when all genotypes are equally fit, it shifts fixation probabilities away from the values expected under neutrality by amounts of order $1/N$. This raises two questions. First, are neutral transitions, even in the direction of the drift-induced bias, empirically relevant, given that they involve fixation probabilities of order $1/N$? Second, would direct selective forces, such as viability differences among genotypes, not overwhelm the drift-induced bias?

On the first question, as with the study of neutral substitutions elsewhere in the genome, this depends on how often the relevant mutations are produced. The extended sex-determining cascades discussed above present a large mutational target: mutations of major sex determining effect can occur at many points along them. These mutations can also occur in many ways, in addition to standard sequence-mutation events: (i) translocation of a gene in a sex determining pathway and a resulting shift in expression or function [78, 521], (ii) duplication and subsequent neo-functionalization of such a gene [29, 460], and (iii) mutation of a major sex determining gene's regulatory elements, such as transcription factors [28, 505]. The frequency of these mutations is evidenced by the heterogeneity of major sex determining genes observed between and within clades [28].

On the second question, it is true that the drift-induced bias we have found becomes very weak as population size increases, while direct selective forces do not. When such selective forces operate—for example, when there is selection against individuals homozygous for a previously sex-specific chromosome—we have argued that drift-induced biases are most likely to be relevant in populations with small effective sizes. One way in which effective population size can be reduced is through

demographic differences between the sexes, for example if males exhibit higher variance in reproductive success. Notice that demographic differences between the sexes also eliminate the symmetry between dominant transitions from male to female heterogamety and from female to male heterogamety, and the same for recessive transitions, so that they also allow the possibility that male or female heterogamety may be favored. In [547, Section S1.3], we have introduced greater variance in male reproductive success for the case of model 1 transitions by altering our baseline population model so that, each generation, a reduced subset of males is randomly chosen to be candidate mates, with the other males denied the possibility of mating. In the neutral case, we find that dominant transitions from male to female heterogamety exhibit a substantially higher substitution rate than in the case with no demographic differences between the sexes [547, Figure S8A], while dominant transitions from female to male heterogamety have a slightly reduced substitution rate [547, Figure S8B]. The substitution rate of recessive transitions from female to male heterogamety is increased marginally relative to the case of no sex differences [547, Figure S8D], while recessive transitions from male to female heterogamety have a significantly reduced substitution rate [547, Figure S8D]. Therefore, the general effect of greater variance in male reproductive success in the neutral case is to exacerbate the bias in favor of dominant sex determining mutations, and to bias evolution towards female heterogamety. When selection against individuals homozygous for a previously sex specific chromosome is taken into account, we expect the results to differ from those under no sex differences for two reasons: because drift-induced selection operates differently in this regime, as for the neutral results just described, and because reducing the number of males eligible to mate reduces the effective population size, rendering the deterministic selection against individuals homozygous

for a previously sex specific chromosome less effective. To illustrate these effects, Figure S10 in [547] displays the fixation probabilities of a dominant X′ chromosome in an initially XX/XY system, with varying strengths of selection against YY males. Compared with the case of no sex differences (Figure 6.5.1C, [547, Figure S10C]), the fixation probabilities of the X′ are greatly increased when males have greater variance in reproductive success [547, Figure S10A,B], so that, even for substantial degrees of selection against YY individuals, the X′ fixes with non-negligible probability. Another effect of the reduced effective population size is that conditional fixation times are substantially smaller than in the case of no sex differences [547, Figure S9].

In comparing the substitution rates of dominant and recessive sex determining mutations, we have assumed that their respective mutation rates, i.e., the rates at which they are generated, are equal. It is possible that this is not the case, and that one class of sex determining mutations is generated more rapidly than the other [14, 232]. If this were the case, it would simply be a distinct mechanism by which we expect one class of sex determining gene to be more prevalent than the other. We should note that this is not as simple as comparing the rates of generation of gain-of-function and loss-of-function mutations. Suppose, for example, that a system is initially XX/XY male heterogametic, and consider a transition in direction a of Figure 6.3.1A, involving fixation of a dominant feminizing X′ mutation. Depending on the molecular functioning of the initial XX/XY system, this dominant X′ could be gain-of-function or loss-of-function. If the Y is initially dominant male-determining (as, e.g., in mammals [28, 296]), then a mutation on the X chromosome that blocks the Y's activity (a gain-of-function mutation) would be dominant feminizing, as we require. If, however, the initial system depends on the ratio of some gene (or

genes) on the X chromosome with respect to autosomes (as in *Drosophila* [28, 39]), then a loss-of-function mutation to a relevant gene on the X chromosome could be dominant feminizing.

We have studied direct transitions between male and female heterogamety. These appear to have been common, at least in vertebrates [144]. However, transitions are also possible between heterogametic and environmental sex determination [48, 49, 239, 432], so that transitions between heterogametic systems could also occur via an intermediate system of environmental sex determination.

We have identified the force driving our results to be drift-induced selection operating along the equilibrium path (in the neutral case) or in its near vicinity (in the case with selection). While drift-induced selection as a force in natural selection has analogs that have been known for some time (e.g., Gillespie's criterion [182, 183], and selection in favor of reduced variance in offspring sex ratios [513, 550]), the demonstration that it acts endogenously in systems of biological interest is relatively recent [88, 100, 290, 326, 420]. We suspect that drift-induced selection will come to be recognized as an important force in many dynamical systems in population biology.

7

Sexual antagonism and the instability of environmental sex determination

7.1 Abstract

The sex of an organism can be determined by its genetics or by its early environment. Across the animal kingdom, genetic sex determination (GSD) is far more common than environmental sex determination (ESD). Here, we propose an explanation for this pattern: the coupling of genes that bias offspring sex ratios toward one sex with

genes that are beneficial in that sex but costly in the other. Gradual strengthening of the sex-specific tendency of this association eventuates in a neo-sex chromosome, i.e., GSD. Our model predicts to which system of heterogamety ESD will evolve when nesting behavior is an important determinant of brood sex ratios. It explains the puzzling observation in some GSD species of sex reversal induced by extreme environments. The model also suggests an approach to discovering sex determining genes in ESD species.

7.2 Introduction

The dominance of GSD over ESD across the animal kingdom is well illustrated in vertebrates (Fig. 7.2.1), where the most prevalent form of GSD, heterogamety, is far more common than the most prevalent form of ESD, temperature-dependent sex determination (TSD) [15, 28, 49]. A similar preponderance of GSD, and heterogamety in particular, is found in invertebrates [15, 28, 49].

This pattern is unexpected, because ESD allows a species to take advantage of environmental variation that differentially affects the fitness of sons and daughters—the Charnov-Bull effect [44, 80, 485, 562, 563]—while GSD does not. For example, it could be that developing at warmer temperatures is beneficial for offspring of both sexes, owing to more rapid development, but that the benefit to female offspring is greater than that to male offspring (Fig. 7.2.2). In this case, a system of TSD where offspring incubated above some threshold temperature develop as female, while those incubated below the threshold temperature develop as male, is evolutionarily stable, including against invasion of GSD [44, 81] (Fig. 7.2.2 and [382, Section S1, S2]). This system—'females high, males low'—is common in reptiles with TSD, especially turtles [47, 252]. If, instead, males benefit more from developing at higher temper-

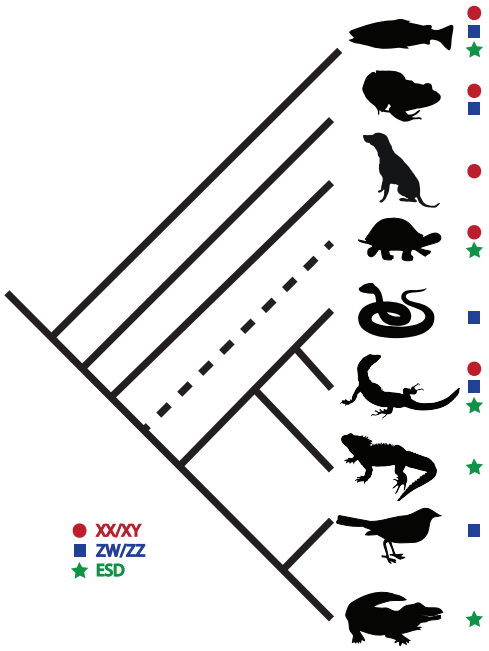

Figure 7.2.1: Genetic sex determination dominates environmental sex determination in vertebrates. Cladogram of vertebrates illustrating the sex determination mechanisms found in all major groups. Genetic sex determination (GSD) has been split into male heterogamety (XX female, XY males) and female heterogamety (ZW females, ZZ males). For fish, only gonochoric species (species with separate males and females) have been included. While information for many species is not available, it is clear that GSD is far more common than environmental sex determination (ESD) across all clades. The ancestral sex determining mechanism for all vertebrates is probably GSD [253], but phylogenetic reconstructions of clades within vertebrates, such as squamates (for whom ESD is probably ancestral [427]), indicate multiple independent transitions from ESD to GSD within each group, with many fewer transitions in the reverse direction, suggesting an inherent instability of ESD [410].

atures, then the stable TSD system is reversed: offspring above a certain threshold temperature develop as male, and those below as female—this 'males high, females low' system is observed in all known fish species with TSD [412].

Explanations for why GSD dominates, despite this advantage to ESD, have focused on sex ratio fluctuations under ESD caused by environmental perturbations [44, 47, 49, 125, 468]; these fluctuations are avoided under GSD. But this selective disadvantage of ESD can be mitigated by responsive maternal nesting behavior [46, 47, 55, 370, 376, 436] and long lifespans [45, 468]. A more robust explanation for the observed instability of ESD is lacking. Here, we propose an explanation based on factors that are expected to operate in all ESD populations, whether or not they can mitigate the problems associated with fluctuating sex ratios in variable environments.

7.3 Results and discussion

Our model is set in a population initially with TSD. We assume underlying fitness effects that lead to a 'females high, males low' system, as described above (Fig. 7.2.2), although our model also applies, with appropriate modifications, to fitness effects that result in the other forms of TSD. Each embryo has a specific 'threshold' temperature θ; if incubated above this temperature, it develops as female, and if below, as male. An embryo's threshold temperature is determined by multiple genes [46, 55, 358, 360]. Allelic variation at these 'threshold loci' results in shifted thresholds: some individuals will develop as female at a slightly lower temperature or a slightly higher temperature than the population average [46, 251, 252]. We shall refer to alleles that decrease their bearers' thresholds as 'female biasing', and those that increase their bearers' thresholds as 'male biasing'. This genetic

variation in thresholds makes our model of a form described as being between GSD and TSD in recent mechanistic models of sex determination [200, 432, 467], though we do not model the mechanistic basis of the genotype-to-phenotype mapping, as these models do [200, 426, 432, 467]; our model is also consistent with more classical models of TSD [55]. In deriving the analytical results below, we assume that almost every individual in the population initially exhibits a threshold close to the evolutionarily stable threshold, θ^* (Fig. 7.2.2b). We later relax this assumption in numerical simulations of our model, to verify that our analytical results are robust to the existence of appreciable initial threshold variation in the population. Environmental temperature varies across the population's range, so that some patches produce mostly males or mostly females (Figs.7.2.2a, 7.3.1a). Under the assumed fitness effects, the population sex ratio associated with the stable average threshold θ^* is expected to be slightly male biased (the proportion of males $m > 1/2$) [44, 81].

We now assume that, at a distinct locus, a new allele arises that does not affect the threshold but confers a fitness benefit s_f when expressed in females, and a fitness cost s_m when expressed in males. We assume this allele to be dominant to the wild-type allele, and $s_m > s_f$, so that the allele is, averaged across the sexes, costly to bear. Such 'sexually antagonistic' alleles are common throughout the genomes of sexual organisms [208, 438, 441], and have been invoked elsewhere in the evolution of sex determining mechanisms to explain why GSD species typically have only one major sex determining gene [439] and to explain transitions within and between heterogametic GSD systems [535, 536]. For brevity, we shall refer to the allele as a 'female-beneficial' allele. If the female-beneficial allele arises on the same chromosome as a threshold locus with a rare dominant female-biasing allele—i.e., one that codes for a lower-than-average threshold $\theta' < \theta^*$, producing a proportion

$m' < m$ of males (Figs. 7.2.2, 7.3.1b)—then the initial TSD system is unstable with respect to invasion of the female-beneficial, female-biasing haplotype if the following condition holds (all mathematical details in [382, Methods and Section S1-3]):

$$\frac{s_f}{2}\left(1-m'\right)\overline{W'_{\female}} - \frac{s_m}{2}m'\overline{W'_{\male}} - s_T > \frac{r}{1-r}. \tag{7.1}$$

Here, r is the rate of recombination of the two loci—the right hand side of Eq. (7.1) is an increasing function of r, ranging from 0 (when $r = 0$) to 1 (when $r = 1/2$). s_T is the marginal fitness cost of bearing the female-biasing threshold allele, ignoring the presence of the female-biasing allele. This cost stems from the fact that the mutant threshold allele systematically causes its bearers to develop as female in some environments where male development would be optimal (Fig. 7.2.2). The general form of s_T is given in Fig. 7.2.2, and derived in [382, Methods]. It depends on various factors, including the size of the difference between the two thresholds θ^* and θ', the nature of the underlying Charnov-Bull fitness functions, and the temperature distribution. Some numerical examples of s_T are given in [382, Figure S3]. $\overline{W'_{\female}}$ and $\overline{W'_{\male}}$ are the average fitnesses of, respectively, female and male bearers of the female-biasing threshold allele who do not bear the female-beneficial sexually antagonistic allele. Therefore, $s_f\left(1-m'\right)\overline{W'_{\female}}/2 - s_m m'\overline{W'_{\male}}/2$ is the marginal benefit of having the mutant female-beneficial allele, conditional on also having the female-biasing threshold allele.

Condition (7.1) is easier to satisfy when the fitness cost to males of the sexually antagonistic allele is not much larger than its fitness benefit to females ($s_m \approx s_f$), and when the female-biasing and female-beneficial alleles are tightly linked (r is small) so that their haplotype is seldom disrupted by recombination. Some numerical examples of values of r for which the haplotype can invade, under reasonable

specifications of the temperature distribution and fitness functions, are given in Fig. 7.3.2. These examples show that the haplotype can invade even when the two loci recombine at an appreciable rate (above 4% in some cases).

We note two caveats to the invasion analysis above. First, we have assumed that almost every individual in the population initially exhibits a threshold close to the evolutionarily stable threshold, θ^*. This assumption was made for the purpose of deriving the simple analytical form of condition (7.1), but ESD populations in fact exhibit considerable threshold variation [46, 251, 252]. To investigate whether condition (7.1) accurately predicts the invasion of the female-biasing, female-beneficial haplotype arising in a population with substantial threshold variation, we turn to simulations of our model. Specifically, we include three or four 'regular' threshold loci along a single chromosome, each segregating for two alleles, one male-biasing and one female-biasing. These regular threshold alleles influence their bearer's threshold in an additive fashion (the model is described in detail in [382, Section S7]). Imposing a normal distribution of temperature across patches and Charnov-Bull fitness effects as described above, we allow the population to evolve for 1000 generations, by which time a stable distribution of genotypes is attained, with an expected male-biased sex ratio (Fig. 7.3.3, Table S1), but with substantial threshold variation (Table S1). We introduce into this population a rare female-biasing, female-beneficial haplotype, and observe if it goes on to attain appreciable frequency (i.e., if it invades). The results are presented in Figs. S5-12, and demonstrate that condition (7.1) is a good predictor of the conditions for invasion when there is initial threshold variation in the population.

Second, we have assumed that both the female-biasing and female-beneficial (and

male-costly) alleles are initially present at low frequency in the population. This could occur if one of the alleles is initially present at a low-frequency mutation-selection balance when the other is introduced into the population by mutation, or if both are initially at mutation-selection balance. It could also occur if the alleles recurrently appear by mutation—though each will usually appear in isolation of the other, and therefore will often go extinct by drift or selection, at some point in evolutionary time the two mutations are expected to co-occur in the same population. This second possibility would imply much less frequent invasion of the haplotype than the first. It is also possible that one of the mutations is initially at a medium-frequency mutation selection balance, instead of the low initial frequency we have assumed in our analysis—this would be expected simply to improve the prospects for invasion of the female-biasing, female-beneficial haplotype.

Our model, and the invasion condition (7.1), bear similarities to W.R. Rice's classic model of, and condition for, the instability of polygenic sex determination with respect to genes of major sex-determining effect [439]. There are key conceptual and biological differences between the models, however. We have directly modelled the Charnov-Bull fitness effects that are thought to be the underlying evolutionary reason for ESD; Rice's model does not, and therefore better applies to other polygenic systems. In addition, Rice's model invokes the spontaneous appearance in the population of a mutation of major sex determining effect (e.g., the *SRY* gene in mammals), while our model invokes already-existing polygenic variation in thresholds, known to be present in populations with TSD [46, 55]. A major sex determining genetic complex is expected eventually to evolve in our model (see below), but it does so gradually, instead of appearing spontaneously as a single, large-effect mutation. We shall demonstrate that this gradual evolution of a sex chromosome

has novel empirical implications, distinct from the implications of Rice's model.

The initial invasion of the female-biasing, female-beneficial haplotype causes the population sex ratio to become more female-biased, which selects for male-biasing threshold alleles in the genome (Figs. 7.3.1c, 7.3.3). Importantly, this selection for male-biasing alleles does not apply to regions tightly linked and in phase with the female-biasing, female-beneficial haplotype, because of the strong selective disadvantage of the haplotype in males. The increase in frequency of male-biasing alleles evens the population sex ratio, relaxing the Fisherian sex ratio selection acting against the female-biasing, female-beneficial haplotype, which can therefore increase further in frequency (Figs. 7.3.1c, 7.3.3). The simulation results that we described previously verify this, showing that the haplotype goes on to attain appreciable frequency after initial invasion (5-25% [382, Figure S5-12]). This is despite our model of multiple threshold loci being highly restrictive, involving, for computational reasons, only a single chromosome with four or fewer threshold loci in addition to the focal locus.

As the haplotype increases in frequency, selection simultaneously acts to reduce recombination between its two loci, because of the average deleterious effect of the female-beneficial allele when uncoupled from the female-biasing allele. If recombination is shut down between the loci (for example, via an inversion), the haplotype becomes, in effect, a single female-biasing, female-beneficial allele [49, 72, 77, 155, 440]. Then, by the same logic as that described above, further female-biasing or female-beneficial alleles that arise near the haplotype will couple with it, creating a larger and larger haplotype that is successively more female-biasing and female-beneficial. This further selects for male-biasing alleles elsewhere in the genome. The end result of this process is a haplotype whose bearers develop as females and whose non-

bearers develop as males under all experienced environmental conditions—that is, a major sex determining factor1 on a neo-W chromosome (Fig. 7.3.1d). We have investigated this process using the simulation model described above. Technical details are in [382, Methods and Section S8]. An example of the gradual evolution of a W chromosome in our simulations is displayed Fig. 7.3.3. There, it can also be seen that the population sex ratio gradually shifts from the male-biased sex ratio expected under ESD with the Charnov-Bull fitness functions we have assumed to the even sex ratio expected under heterogamety. Moreover, mutations that weaken either the female-biasing or female-beneficial tendencies of the haplotype on its way to defining a W chromosome fail to invade [382, Fig. S13], suggesting that the process is irreversible.

The process described above involves the coupling of female-biasing threshold alleles and female-beneficial sexually antagonistic alleles, which leads to a neo-W chromosome and female heterogamety. The symmetric alternative, also possible, is the successive coupling of male-biasing and male-beneficial alleles, leading to a neo-Y chromosome and male heterogamety. A condition similar to Eq. (7.1) can be derived for the invasion of male-biasing, male-beneficial haplotypes [382, Section S4]. These haplotypes can invade if they do not reduce female fitness too much relative to their benefit to male fitness, and if their two loci do not recombine too often. Examples of recombination rates for which male-biasing, male-beneficial haplotype can invade are given in Fig. 7.3.2, and, like for the invasion of female-biasing, female-beneficial haplotypes studied above, can be appreciable.

Despite these similarities, genetic or demographic differences between the sexes might render the invasion of a male-biasing, male-beneficial haplotype more or less likely than a female-biasing, female-beneficial haplotype. For example, a lower

rate of recombination in males relative to females, as observed in many species [524], would allow male-biasing and male-beneficial alleles to couple more tightly—their average rate of recombination being lower because they are more often found in males—promoting the invasion of male-biasing, male-beneficial haplotypes over female-biasing, female-beneficial haplotypes (this is formalized mathematically in [382, Section S5] and displayed in [382, Fig. S4]). This would bias evolution towards male heterogamety, an argument that has previously been given by Trivers for genes of major sex-determining effect [524]. The argument presented here is made especially relevant by the finding of extremely reduced male recombination in a species with TSD, the saltwater crocodile [368].

We have thus far invoked threshold alleles, expressed in zygotes, as a source of heritable sex ratio bias. An alternative and common source of heritable variation in offspring sex ratios is maternal nesting behavior [46, 47, 55, 358, 359, 370, 376, 436]. Applied to our model, the coupling of female-beneficial sexually antagonistic alleles with alleles that cause mothers to nest, for example, in warmer patches (and therefore to produce predominantly female offspring) will eventuate in a neo-W chromosome and female heterogamety. Importantly, male heterogamety is a much less likely result in this 'maternal behavior' scenario, because it would require the repeated expression of male-beneficial (and female-costly) alleles in mothers (this argument is formalized mathematically in [382, Section S6], for the case where Charnov-Bull fitness effects are absent; a similar logic has been given by Tanaka and Iwasa [506] for the different potentials for spread of a Japanese superstition under matrilineal and patrilineal transmission). Sex ratio biases from maternal nesting behavior can arise in many ways, including nest-site choice, nest construction, nesting timing, and the duration of incubation [46, 370, 376], so this route to heterogamety might not

be infrequent relative to that involving threshold alleles acting in embryos. If so, transitions from ESD to female heterogamety should be more common than from ESD to male heterogamety, a pattern that has been observed within reptiles (including birds) [410]. The observed preponderance of male over female heterogamety [49, 232] would then seem to have to be explained by biased transitions between these two systems [232, 534, 536, 547].

Searching for threshold genes in TSD species is an area of active research [343, 465], but is extremely difficult, as males and females have identical genomes, and large-scale gene expression assays at multiple points in development are required. Our model predicts that, in a species that has recently evolved GSD from ancestral TSD (examples in Table 7.3.1), the sex chromosomes will contain ancestral threshold genes (possibly including genes that have translocated from other chromosomes), and moreover, are likely to be enriched for them, relative to other chromosomes. If so, examining the sex chromosomes of species with newly evolved GSD, or their homologs in closely related TSD species (Table 7.3.1), will more readily uncover candidate loci for threshold genes—these can then be studied more closely by measuring expression during development. The jacky dragon, *Amphibolurus muricatus*, is already a model organism for the study of TSD [562, 563], and so, together with the closely related *A. norrisi* (GSD), represents an especially promising species in which to apply this method of search for TSD genes.

Recent evidence suggests that some species previously thought to exhibit exclusively genetic sex determination in fact also exhibit an environmental component at extreme temperatures [28, 239, 431, 433, 530]. Our model for transitions from TSD to GSD can explain this 'environmental override' phenomenon in two ways. First, it could be a late intermediate stage in the gradual transition to true GSD, when

Table 7.3.1: Species in which to search for threshold genes. Closely-related squamate species in clades with ancestral temperature sex determination (TSD), one with the ancestral TSD, and one with recently evolved genetic sex determination (GSD) [427]. Our model predicts that the new sex chromosomes in the GSD species, or their homologs in the TSD species, will be a fruitful place to search for TSD genes.

Genus with ancestral ESD	ESD species	GSD species
Amphibolurus (Agamidae)	*A. muricatus*	*A. norrisi*
Ctenophorus (Agamidae)	*C. pictus*	*C. fordi*
Phelsuma (Gekkonidae)	*P. ornata*	*P. guimbeaui*
Furcifer (Chamaelionidae)	*F. pardalis*	*F. lateralis*

thresholds in the population are shifted towards the extremes of the environmental temperature distribution (Fig 3c,d), so that TSD still operates at these extreme temperatures. Second, our model predicts that thresholds will diverge until, but not further than the point where some genotypes develop as females at all commonly experienced temperatures, while the rest develop as males at all commonly experienced temperatures. The selection we have modelled acts only weakly outside of the range of commonly experienced temperatures. TSD would therefore be expected still to operate at uncommon temperatures, until a gene of major sex determining effect evolves.

For clarity, we summarize the predictions of our model: (1) Transitions from ESD to female heterogamety should be more common in clades with intensive maternal nesting behaviour. This prediction could be tested in a comparative phylogenetic framework. (2) In GSD systems that have recently evolved from ESD, the sex chromosomes should be enriched for genes that were involved in the ancestral ESD system, e.g., genes affecting thresholds if the ancestral system was TSD. Such genes could be identified by sequencing the sex chromosomes of the GSD species or their homolog in a closely related ESD species; candidates identified in this fashion could then be experimentally verified using gene expression assays in the related ESD

species. We have listed some promising candidate species for such testing in Table 7.3.1. (3) 'Mixed' ESD-GSD systems, where at most temperatures sex is determined by the presence or absence of a particular chromosome, but with sex reversal at extreme temperatures, are a natural expectation under our model. Moreover, the pattern of sex reversal is expected to respect the ancestral ESD system. For example, since all known TSD fish species exhibit a 'males high, females low' system, we expect any transitions from TSD to GSD in fishes to be from this particular TSD system. If sex reversal occurs in a derived GSD species, then our model predicts that it should take the form of reversal to male development at very high temperatures, or reversal to female development at very low temperatures. Indeed, all clear cases of sex reversal in GSD fishes involve male development at very high temperatures [412, 425]. We should note that this final prediction, concerning the precise patterns of environmental override in derived GSD species, is unlikely to be unique to our model.

Our arguments can also explain transitions from hermaphroditism (simultaneous or sequential) to dioecy/gonochorism, as a result of the coupling of alleles that increase or prolong female function with alleles that improve female function and worsen male function (or, of course, coupled alleles with the opposite effect). The timing of the transition between sexes in simultaneous hermaphrodites, and the allocation of reproductive expenditure on female and male function in simultaneous hermaphrodites, are both theoretically analogous to the threshold temperature in species with temperature sex determination [79, 80, 180]. Both sequential and simultaneous hermaphroditism are rare among animals, the latter especially so when considering only non-selfing organisms [15, 180, 269]. This rarity of hermaphroditism is in spite of its plausible advantages [82, 180, 269, 269], and, we propose, may be

the result of sexual antagonism coupled with genetic variation for allocation of reproductive expenditure to each sex.

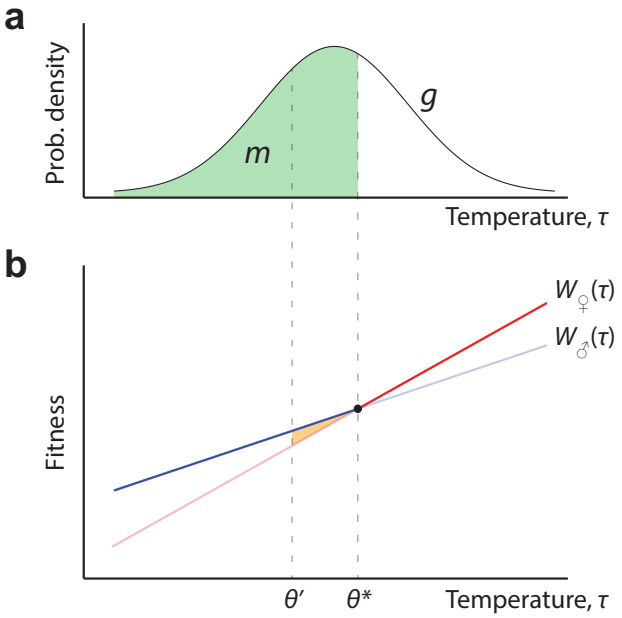

Figure 7.2.2: The advantage of environmental sex determination: exploiting sex-specific benefits of different environments. An example of Charnov-Bull fitness functions [80] that lead, in the absence of other forces, to an evolutionarily stable system of temperature sex determination. a, Temperature τ is distributed across regions in the environment according to the distribution g. b, Offspring of both sexes benefit from developing at higher temperatures, but female offspring benefit more: Female fitness as a function of temperature, $W_{♀}(\tau)$, is steeper than male fitness, $W_{♂}(\tau)$. These fitness functions are derived from underlying male and female viabilities (or fertilities or fecundities); the calculations for this derivation are given in [382, Methods and Section S2]. With these fitness functions, there is a threshold temperature θ^* such that the following system of temperature sex determination is evolutionarily stable: offspring develop as female when incubated at temperatures above θ^*, and as male when incubated below θ^*. The stable threshold θ^* satisfies $W_{♀}(\theta^*) = W_{♂}(\theta^*)$, and in this case is associated with a male-biased sex ratio (proportion of males $m > 1/2$) [52, 79]. When almost all members of the population have thresholds close to θ^*, a rare mutant with a deviant threshold $\theta' < \theta^*$ suffers, all else equal, a fitness cost $s_T = \frac{1}{2}\int_{\theta'}^{\theta^*} \left[W_{♂}(\tau) - W_{♀}(\tau)\right] g(\tau) d\tau > 0$ (see [382, Methods] for details of this calculation). Graphically, this fitness cost is half the area of the orange shaded triangle in b, weighted according to g.

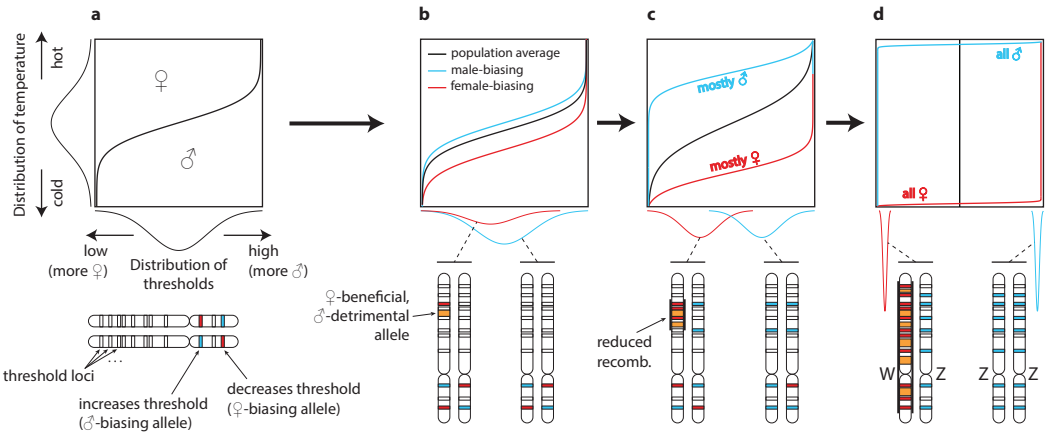

Figure 7.3.1: Genetic sex determination evolves from temperature sex determination via sexually antagonistic genes. An illustration of our general model. a, The population initially exhibits temperature sex determination, with embryos becoming female at high temperatures and male at low. There is variation in threshold temperatures (x axis), owing to male-biasing and female-biasing threshold alleles segregating in the population, but the average embryo has an approximately even chance of developing as male or female given the prevailing distribution of environmental temperatures (y axis). b, A female-beneficial sexually antagonistic allele arises near a female-biasing threshold allele. If they are sufficiently tightly linked [Condition (7.1)], this female-biasing, female-beneficial haplotype increases in frequency, shifting the population sex ratio towards a slight female bias. c, As the female-biasing, female-beneficial haplotype increases in frequency, male-biasing alleles are selected for elsewhere in the genome, to compensate for the population's female bias. Simultaneously, there is selection for reduced recombination between the female-biasing and female-beneficial alleles in the haplotype. The effect of these two selection pressures is to allow the haplotype to increase further in frequency. Those embryos that bear it have low threshold temperatures, and therefore develop as female under most temperatures; non-bearers have high threshold temperatures, and therefore develop as male under most temperatures. d, The female tendency of the haplotype attracts further linked female-biasing and female-beneficial alleles, which in turn selects for reduced recombination within the growing haplotype, as well as more male-biasing alleles elsewhere in the genome. Eventually, embryos that bear the haplotype develop as female at all experienced temperatures, while non-bearers develop as male at all experienced temperatures. Sex in the population is then genetically determined, with the haplotype on a neo-W chromosome.

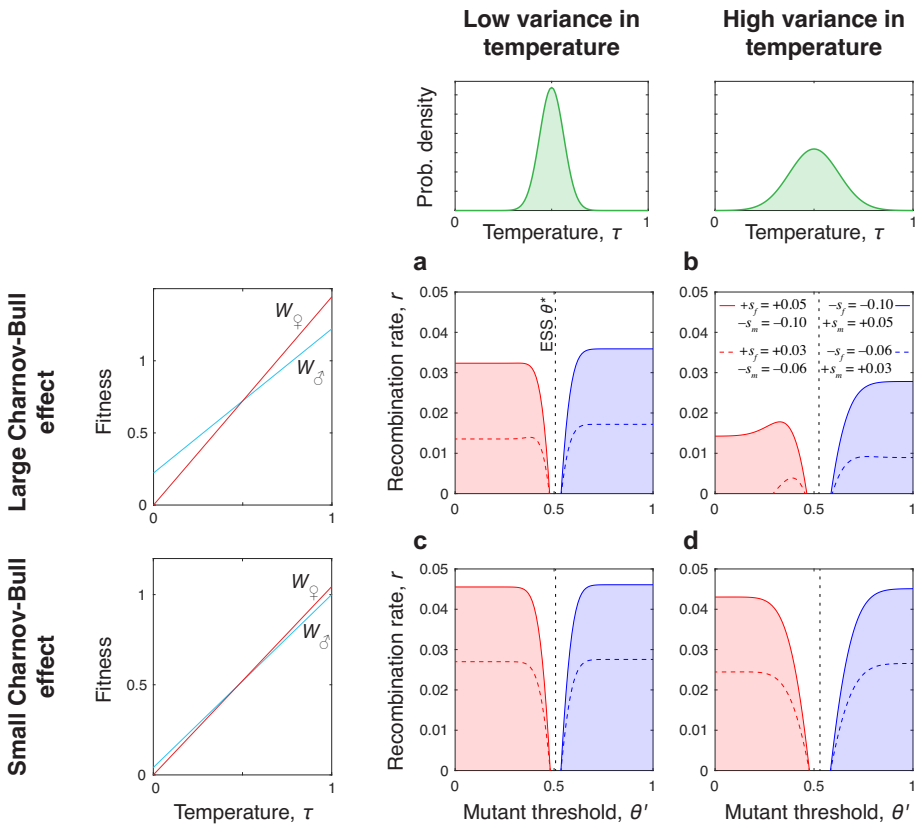

Figure 7.3.2: For sensible empirical specifications of the temperature distribution (normal) and of male and female fitness functions (linear), the figure shows the maximum recombination rates below which female-biasing, female-beneficial (red shading) and male-biasing, male-beneficial (blue shading) haplotypes can invade a population with temperature sex determination. Recombination rates are the same in both sexes. In general, both female-beneficial, female-biasing haplotypes and male-biasing, male-beneficial haplotypes can invade even with appreciable recombination of their constituent alleles. Their invasion is more likely when Charnov-Bull fitness effects are minor (c, d) and the temperature distribution exhibits lower variance (a, c). Invasion is least likely under conditions of high temperature variance and large Charnov-Bull effects (b), but even then, is possible for reasonable recombination rates (up to about 2.5% for the parameters considered here). Details: Temperature is distributed normally with mean $1/2$ and standard deviation $1/16$ ('low variance') or $1/8$ ('high variance'). Individuals homozygous for the wild-type allele a that develop at temperature have viability $V_{♂}(\tau) = k + \tau$ if male and $V_{♀}(\tau) = \lambda\tau$ if female, with $= 1 + 2$k. For 'large Charnov-Bull effect', $k = 2/9$; for 'small Charnov-Bull effect', $k = 2/90$.

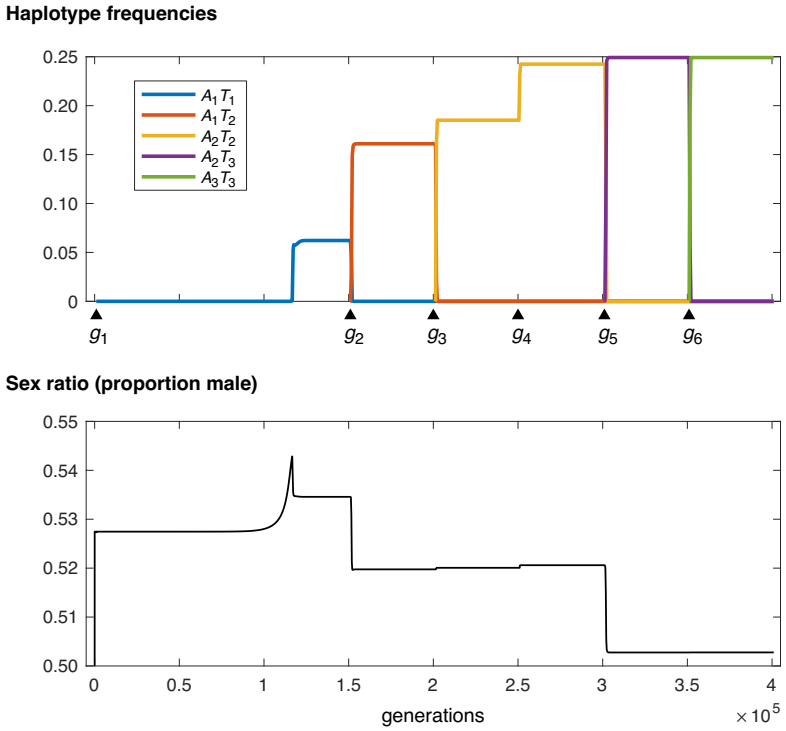

Figure 7.3.3: Gradual evolution of GSD from TSD. After the initial invasion of a female-biasing, female-beneficial haplotype A_1T_1 (in generation g_1), mutations that successively strengthen the female-biasing tendency (T_2 and T_3) and female-beneficial tendency (A_2 and A_3) of the haplotype, as well as the shutting down of recombination between its constituent loci in generation g_4, lead it to attain higher and higher frequency. Eventually, the haplotype is at 25% frequency, and causes almost all its bearers to develop as female. At this point, the haplotype essentially defines a W chromosome, and sex is determined genetically according to a system of female heterogamety. In the gradual transition from TSD to GSD, the sex ratio of the population moves from the male-biased sex ratio that is stable under TSD with the Charnov-Bull fitness effects we have assumed to an almost even sex ratio, as expected under GSD. Simulation details: Model as described in [382, Section S8]. Initial recombination rate between the focal viability and threshold loci: 1%. Temperature distribution and Charnov-Bull effects as in Fig. 7.3.2a. An individual's baseline threshold is determined additively by the number of male-biasing alleles at four regular threshold loci (those in addition to the focal threshold locus): threshold 0.20 if $0/8$ male-biasing alleles, threshold 0.50 if $4/8$ male-biasing alleles, threshold 0.80 if $8/8$ male-biasing alleles. Threshold reductions caused by (dominant) alleles T_1, T_2, and T_3 are 0.1, 0.2, and 0.3 respectively. Fitness effects of sexually antagonistic alleles: A_1: $s_f = +0.04$, $-s_m = -0.08$; A_2: $s_f = +0.06$, $-s_m = -0.12$; A_3: $s_f = +0.08$, $-s_m = -0.16$.

8

A rigorous measure of genome-wide genetic shuffling that takes into account crossover positions and Mendel's second law

8.1 Abstract

Comparative studies in evolutionary genetics rely critically on evaluation of the total amount of genetic shuffling that occurs during gamete production. Such studies have

been hampered by the absence of a direct measure of this quantity. Existing measures consider crossing over by simply counting the average number of crossovers per meiosis. This is qualitatively inadequate because the positions of crossovers along a chromosome are also critical: a crossover towards the middle of a chromosome causes more shuffling than a crossover towards the tip. Moreover, traditional measures fail to consider shuffling from independent assortment of homologous chromosomes (Mendel's second law). Here, we present a rigorous measure of genome-wide shuffling that does not suffer from these limitations. We define the parameter $\bar{r}$ as the probability that the alleles at two randomly chosen loci are shuffled during gamete production. This measure can be decomposed into separate contributions from crossover number and position and from independent assortment. Intrinsic implications of this metric include the fact that $\bar{r}$ is larger when crossovers are more evenly spaced, which suggests a novel selective advantage of crossover interference. Utilization of $\bar{r}$ is enabled by powerful emergent methods for determining crossover positions, either cytologically or by DNA sequencing. Application of our analysis to such data from human male and female reveals that: (i) $\bar{r}$ in humans is close to its maximum possible value of 1/2, (ii) this high level of shuffling is due almost entirely to independent assortment, whose contribution is $\sim$30 times greater than that of crossovers.

8.2 Introduction

The shuffling of maternally and paternally inherited genes during gamete production is an important process in sexual populations [23]. It leads to genetic diversity among gametes and offspring [23], and thus aids adaptation to novel or changing environments [578]. In addition, it improves the long-term efficiency of

adaptation by allowing natural selection to act separately on distinct mutations [150, 154, 230, 357, 380, 381]. Genetic shuffling has further been implicated in protecting populations from rapidly evolving parasites [213, 214] and from the harmful invasion of selfish genetic complexes [37, 59, 206, 207]. The total amount of shuffling that occurs in gamete production is therefore a quantity of considerable importance, and has been the subject of much empirical interest.

Correspondingly, comparative studies of genome-wide shuffling have been carried out across species ([23, 40, 58, 126, 127, 448, 472, 526]; reviewed in [116, 490, 497]), with implications ranging from distinguishing the evolutionary advantages of sex [23, 58, 116, 497, 574] to testing the genomic effects of domestication [58, 448]. A large literature has also studied male/female differences in shuffling [37, 60, 524], prompting several evolutionary theories to explain these differences [37, 60, 206, 312, 313, 524], which could concomitantly be informative of the adaptive value of shuffling [524]. There can also exist differences in shuffling across individuals of the same sex (e.g., in flies [98, 243, 244, 277, 278], mice [128, 288, 335], humans [41, 85, 292, 294, 335, 415], and *Arabidopsis* [456]; reviewed in [445]), and across gametes produced by the same individual [85, 201, 222, 315, 335, 344, 560]. Finally, comparisons have been made of the levels of shuffling within different chromosomes [34, 42, 291], with implications for which chromosomes are most susceptible to harboring selfish genetic complexes [206] or to be used as new sex chromosomes [382, 524].

Quantitative comparisons of such types require a proper measure of genome-wide shuffling. Shuffling is caused both by crossing over and by independent assortment of homologous chromosomes,[1] which comprise 'intra-chromosomal' and 'inter-chromosomal' shuffling, respectively.[2] In previous studies, the most widely used

[1] Gene conversion also causes shuffling, but makes a negligible contribution, as discussed below.
[2] Shuffling caused either by crossing over or independent assortment of homologs is referred to as

measures of shuffling have considered only the contribution of crossing over, and, more specifically, total crossover frequency or map length. Crossover frequency is simply the number of crossovers that occur during meiotic prophase, as measured either cytologically or from sequence data (further discussion below). Map length is average crossover frequency multiplied by 50 centiMorgans (cM), 1 cM being the map distance between two linked loci that are shuffled in 1% of gametes [220]. Another measure that is sometimes used is the number of crossovers in excess of the haploid chromosome number [58]. Since each bivalent usually requires at least one crossover for its chromosomes to segregate properly [117], the 'excess crossover frequency' is the number of crossovers that contribute to shuffling beyond this supposed structurally-required minimum. None of the above measures takes into account shuffling caused by independent assortment of homologs. A fourth measure of aggregate shuffling, which does take into account independent assortment, is Darlington's 'recombination index' (RI) [23, 118, 119], defined as the sum of the haploid chromosome number and the average crossover count. The rationale for this measure derives from the fact that, given no chromatid interference in meiosis [220, 595], two linked loci separated by one or more crossovers shuffle their alleles with probability 1/2 in the formation of a gamete, as if the loci were on separate chromosomes. The RI is therefore the average number of 'freely recombining' segments per meiosis.

Importantly, none of these existing measures takes into account the specific positions of crossovers on the chromosomes. Intuitively, though, crossover position is a critical parameter. For example, a crossover at the far tip of a pair of homologous

'recombination' in the population genetics literature, but 'recombination' has a different meaning—the breakage and rejoining of DNA molecules—in molecular biology. To avoid confusion, we use the unambiguous term 'genetic shuffling' (or just 'shuffling') throughout.

chromosomes does little work in shuffling the genetic material of those chromosomes, while a crossover in the middle causes much shuffling (Fig. 8.2.1). Additionally, two crossovers close together may cancel each other's effect (except for the few loci that lie between them) and thus result in less allelic shuffling than two crossovers spaced further apart.

Therefore, existing measures do not actually define the total genome-wide amount of shuffling, instead serving only as proxies for this critical parameter. This is not a trivial concern. There is significant heterogeneity in the chromosomal positioning of crossovers at all levels of comparison—between species [266, 319, 526], populations within species [233, 321, 322, 565, 572], the sexes [37, 62, 158, 257, 524, 590], individuals [86, 282, 305, 415, 503], and different chromosomes [34, 168, 257, 502], all of which will impact the level of shuffling that these crossovers will cause. Moreover, there can be major differences in chromosome number and size across species [23, 482, 571], which will seriously influence the total amount of shuffling due to independent assortment.

The fact that the positions of crossovers matter for the total amount of shuffling has been recognized for many years (e.g., [23, 62, 157, 195, 568, 571]). The need for a measure of total shuffling that accounts for crossover positions has also previously been recognized. Indeed, Burt, Bell, and Harvey [60] give an explicit formula, identical to Eq. (8.3) below, for 'the proportion of the genome which recombines' (in the population genetics sense—see footnote 2). Colombo [97] also gives an explicit characterization of what we call $\bar{r}$, phrased as a generalization of the RI. Finally, Haag et al. [203], after noting that terminal crossovers cause little shuffling and that map length is therefore an imperfect measure of genome-wide shuffling, suggest a better measure to be 'the average likelihood that a [crossover] occurs between two

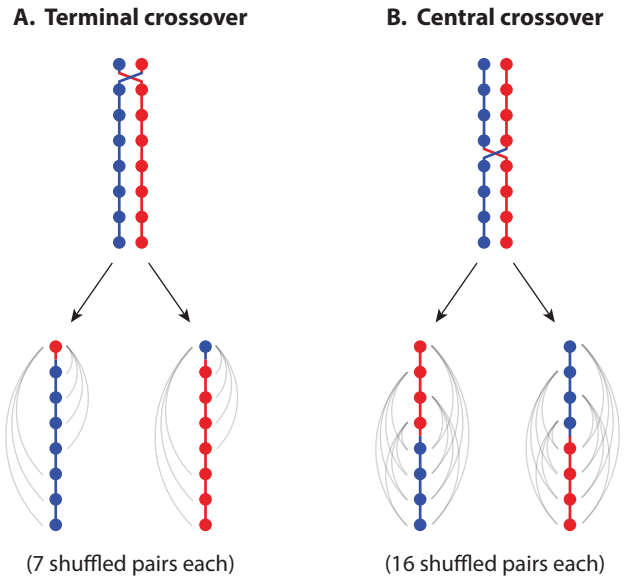

Figure 8.2.1: The position of a crossover affects the amount of genetic shuffling that it causes. The figure shows the number of shuffled locus pairs that result from crossing over between two chromatids in a one-step meiosis. The chromosome is arbitrarily divided into eight loci. (A) A crossover at the tip of the chromosome, between the seventh and eighth loci, causes 7 of the 28 locus pairs to be shuffled in each resulting gamete. (B) A crossover in the middle of the chromosome, between the fourth and fifth loci, causes 16 of the 28 locus pairs to be shuffled in each resulting gamete. The central crossover thus causes more shuffling than the terminal crossover.

randomly chosen genes'. However, no mathematical expression that incorporates crossover position in the measurement of genome-wide shuffling has been developed and implemented.

Here, we present a simple, intuitive measure of the genome-wide level of shuffling. We define $\bar{r}$ as the probability that a randomly chosen pair of loci shuffle their alleles in meiosis, taking into account crossover number and position and the contribution of independent assortment. We have chosen the name '$\bar{r}$' to echo classic population genetics terminology, where the parameter 'r' for a given pair of loci is the probability that they shuffle their alleles in a gamete. Our parameter $\bar{r}$ is simply this quantity averaged across all locus pairs.

$\bar{r}$ is the most direct metric of the primary effect of genetic shuffling, the diversification of gametes and thus the transmission of new genetic combinations to offspring [23]. $\bar{r}$ should therefore be used when such diversification is the quantity of interest, for example in judging the ability of a population to respond a sudden change (or continual fluctuations) in its environment [578]. Genetic shuffling also has indirect effects, such as the gradual reduction of allelic correlations (linkage disequilibrium) within populations over time [150, 230], and the prevention of invasion of selfish genetic complexes [207]. Here, crossover positions and independent assortment again matter, and so standard metrics that simply count crossovers remain inadequate. Therefore, $\bar{r}$ is likely a better measure in these cases too, although we suggest, in the Discussion section below, modifications of $\bar{r}$ that more directly measure these quantities of interest.

In the present work, we define the quantity $\bar{r}$, develop it mathematically and statistically, and document its intrinsic implications, e.g., for crossover interference. We also show how it can be decomposed into separate components deriving

from crossovers and from independent assortment of homologs. We then discuss the approaches now available to allow chromosome-specific and/or genome-wide measurement of crossover positions. With these developments in hand, we present a first application of $\bar{r}$ to quantitative evaluation of shuffling in human males and females.

8.3 Derivation of $\bar{r}$

$\bar{r}$ is the probability that the alleles at two randomly chosen loci are shuffled in the production of a gamete. It can be calculated with knowledge of crossover positions on each chromosome, in conjunction with knowledge of the fraction of the total genomic length (in bp) accounted for by each chromosome (chromosome lengths influence shuffling caused by both independent assortment and crossovers). In what follows, we always assume that there are sufficiently many loci that the difference between sampling them with or without replacement is negligible.

8.3.1 Formulas for $\bar{r}$

In the ideal situation, crossover positions are defined for individual gametes, and the parental origins of the chromosome segments delimited by these crossovers are known. In this case, the proportion p of the gamete's genome that is paternal can be determined, and the probability that the alleles of a randomly chosen pair of loci were shuffled during formation of the gamete (equivalently, the proportion of locus pairs at which the alleles are shuffled), either by crossing over or by independent assortment, is simply the product of the probabilities that one locus is of paternal origin (probability p) and the other of maternal origin (probability $1 - p$), in each

of the two possible combinations:

$$\bar{r} = 2p(1-p). \tag{8.1}$$

Such data can emerge directly from sequencing of single gametes (Fig. 8.3.1B) or of a diploid offspring in which the haploid contribution from a single gamete can be identified (Fig. 8.3.1C).

In some analyses, while crossover positions for a gamete are known, the specific parental identities of the chromosome segments that these crossovers delimit are not known, because the gamete-producer has been sequenced but its parents have not. In this case, we can nonetheless calculate an expected value of $\bar{r}$ for the gamete. The parental origin of segments will alternate across crossovers on each chromosome in the gamete, and so we can still define, for any given chromosome k, the proportions that originate from the two different parents (p_k and $1-p_k$). However, it is not possible to know, from one chromosome to the next, which sets of segments are from the same or different parents. We address this ambiguity by assuming that the probability that the alleles at two loci on separate chromosomes have been shuffled is 1/2, consistent with Mendel's Second Law. If there are n chromosomes in the haploid set, and chromosome k accounts for a fraction L_k of the genome's length, and we determine that a proportion p_k of chromosome k is of one parental origin and $1-p_k$ is of the other, then

$$\mathbb{E}[\bar{r}] = \sum_{k=1}^{n} 2p_k(1-p_k)L_k^2 + \frac{1}{2}\left(1 - \sum_{k=1}^{n} L_k^2\right). \tag{8.2}$$

The first term in Eq. (8.2) is the probability, summed over all chromosomes k, that two randomly chosen loci lie on chromosome k multiplied by the probability that, if

so, they are of different parental origin. The second term is the probability that the two randomly chosen loci lie on different chromosomes, $1-\sum_{k=1}^{n} L_k^2$ (i.e., one minus the probability that a random pair of loci lie on the same chromosome), multiplied by 1/2. This second term is probabilistic, and so Eq. (8.2) is an expectation of $\bar{r}$ rather than the value actually realized in the gamete.[3]

Finally, cytological analysis of meiotic pachytene chromosomes allows to define crossover positions along bivalent chromosomes at that stage of meiotic prophase I. An expected value for $\bar{r}$ can be calculated in this case following the formulas given by Burt, Bell, and Harvey [60] and Colombo [97] (Fig. 8.3.1A). If the haploid number of chromosomes is n and there are a total of I crossovers, then these crossovers divide the bivalents into $n+I$ segments (this is the RI described above). Label the segments in some (arbitrary) order, and suppose that segment i's fraction of total genome length is l_i, with $l_1 + \ldots + l_{n+I} = 1$. For any randomly-selected locus pair to shuffle its alleles in the production of a gamete, the two loci need to be situated on different segments, the probability of which is $1-\sum_{i=1}^{n+I} l_i^2$. If the two loci are indeed situated on different segments, they shuffle their alleles with probability 1/2 (this assumes no chromatid interference, so that two linked loci separated by one or more crossovers at meiosis I shuffle their alleles in a resulting gamete with probability 1/2 [119, 220]). Therefore, given the configuration of crossovers at meiosis I, the probability that the

[3] Given a gamete sequence and knowledge of the paternal and maternal origins of all chromosome segments, the realized value of $\bar{r}$—being the proportion of locus pairs at which alleles have been shuffled—is precisely known. I.e., here it is a 'parameter'. If the maternal and paternal origins are not known, then $\bar{r}$ becomes a random variable, its realized value being different for different assortments of the possible parental origins of the various segments. We therefore calculate its expectation with respect to the distribution of these possible assortments. Similarly, when we observe crossovers along bivalent chromosomes at meiosis I, $\bar{r}$ in a resulting gamete is again a random variable, so we calculate its expected value, but this time with respect to the distribution of possible patterns of chromatid involvement in the resolution of crossovers at meiosis I, and segregation patterns of chromatids thereafter.

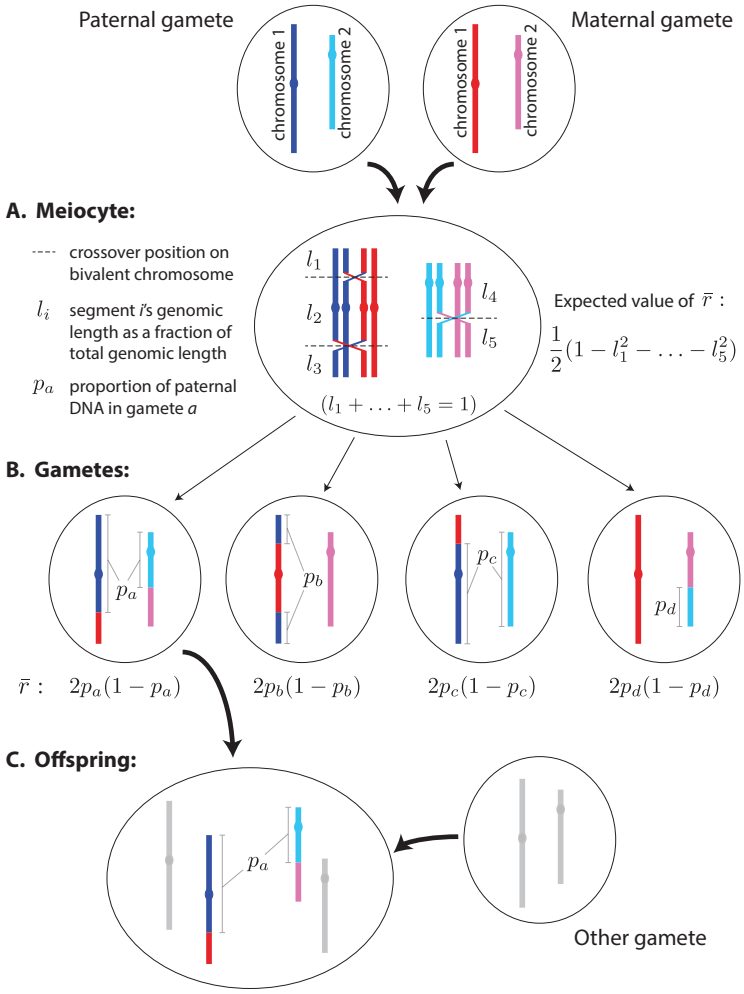

Figure 8.3.1: (A) Calculating the expected value of $\bar{r}$, $\mathbb{E}[\bar{r}]$, at meiosis I using Eq. (8.3). (B,C) Calculating $\bar{r}$ in resulting gametes or offspring using Eq. (8.1).

alleles at a randomly chosen pair of loci are shuffled in a resulting gamete is 1/2 multiplied by the probability that the two loci are on separate segments, or

$$\mathbb{E}[\bar{r}] = \frac{1}{2}\left(1 - \sum_{i=1}^{n+I} l_i^2\right). \tag{8.3}$$

$\mathbb{E}[\bar{r}]$, as defined by Eq. (8.3), is proportional to the Gini-Simpson index [486], a commonly used measure of diversity, especially in ecology [259].

8.3.2 Inter- and intra-chromosomal components of $\bar{r}$

It is often argued that the predominant source of shuffling in sexual species is independent assortment of separate chromosomes, or, correspondingly, that the most effective way for a species to increase genome-wide shuffling in the long term is to increase the number of chromosomes rather than crossover frequency ([23, 109]; though see [57] and *Discussion*). Our formulation of $\bar{r}$ allows us to partition total shuffling into a component deriving from crossovers (intra-chromosomal shuffling) and a component deriving from independent assortment of separate chromosomes (inter-chromosomal shuffling), thereby allowing us to evaluate previous assertions about the relative contributions of each in a rigorous, quantitative way.

The inter-chromosomal component of $\bar{r}$ is the probability that two randomly chosen loci are on separate chromosomes and shuffle their alleles, while the intra-chromosomal component is the probability that two loci are on the same chromosome and shuffle their alleles. We first present this decomposition for $\bar{r}$ in a gamete or haploid complement of an offspring. If chromosome k contains a proportion p_k of

paternal content, then the appropriate decomposition is

$$\bar{r} = \underbrace{\sum_{k=1}^{n} 2p_k(1-p_k)L_k^2}_{\text{Intra-chrom. component}} + \underbrace{\sum_{i\neq j} 2p_i(1-p_j)L_iL_j}_{\text{Inter-chrom. component}}. \tag{8.4}$$

If we know crossover realizations in a haploid complement but not the specific parental origin of the segments they delimit, then we can still calculate a proportion p_k of chromosome k to be of one parental origin and $1-p_k$ of the other (though not knowing which is which), so we retain the first term in Eq. (8.4) but lose information about the second term. The appropriate partition is then

$$\mathbb{E}[\bar{r}] = \underbrace{\sum_{k=1}^{n} 2p_k(1-p_k)L_k^2}_{\text{Intra-chrom. component}} + \underbrace{\frac{1}{2}\left(1-\sum_{k=1}^{n} L_k^2\right)}_{\text{Inter-chrom. component}}, \tag{8.5}$$

which is the same as Eq. (8.2).

We now present the decomposition for $\mathbb{E}[\bar{r}]$ at meiosis I. Suppose that the haploid number of chromosomes is n, and that bivalent k exhibits I_k crossovers, dividing it into segments $i = 1, \ldots, I_k + 1$, whose fractions of the total genomic length are $l_{k,i}$. Chromosome k's fraction of the total genomic length is $L_k = l_{k,1} + l_{k,2} + \ldots + l_{k,I_k+1}$, with $L_1 + L_2 + \ldots + L_n = 1$. Then Eq. (8.3) is partitioned as follows:

$$\mathbb{E}[\bar{r}] = \underbrace{\frac{1}{2}\sum_{k=1}^{n}\left(L_k^2 - \sum_{i=1}^{I_k+1} l_{k,i}^2\right)}_{\text{Intra-chrom. component}} + \underbrace{\frac{1}{2}\left(1-\sum_{k=1}^{n} L_k^2\right)}_{\text{Inter-chrom. component}}. \tag{8.6}$$

8.3.3 Averaging $\bar{r}$

The above measures can be aggregated to obtain the average value of $\bar{r}$ across many gametes (or meiocytes). We denote the average value of a variable x by $\langle x \rangle$. To average $\bar{r}$ given sequence data from many gametes, and supposing that, for each gamete, we can distinguish which sequences are paternal and which are maternal, we can take the average value of Eq. (8.4), noting that the L_k are constants:

$$\langle \bar{r} \rangle = \underbrace{\sum_{k=1}^{n} \langle 2p_k(1-p_k) \rangle \, L_k^2}_{\text{Intra-chrom. component}} + \underbrace{\sum_{i \neq j} \langle 2p_i(1-p_j) \rangle \, L_i L_j}_{\text{Inter-chrom. component}}. \tag{8.7}$$

If segregation is Mendelian, then in a large sample of gametes, $\langle 2p_i(1-p_j) \rangle \approx 1/2$, and so the inter-chromosomal component in Eq. (8.7) will be close to $\frac{1}{2}\left(1 - \sum_{k=1}^{n} L_k^2\right)$.

If we have sequence data from many gametes and can determine crossover positions but not the parental origin of the sequences these crossovers delimit, then we take the average of Eq. (8.5), noting again that the L_k are constants (which, here, means that the inter-chromosomal component is constant):

$$\langle \mathbb{E}[\bar{r}] \rangle = \underbrace{\sum_{k=1}^{n} \langle 2p_k(1-p_k) \rangle \, L_k^2}_{\text{Intra-chrom. component}} + \underbrace{\frac{1}{2}\left(1 - \sum_{k=1}^{n} L_k^2\right)}_{\text{Inter-chrom. component}}. \tag{8.8}$$

Given data of crossover positions along bivalent chromosomes in many meiocytes, we take the average of Eq. (8.6):

$$\langle \mathbb{E}[\bar{r}] \rangle = \underbrace{\frac{1}{2} \sum_{k=1}^{n} \left(L_k^2 - \left\langle \sum_{i=1}^{I_k+1} l_{k,i}^2 \right\rangle \right)}_{\text{Intra-chrom. component}} + \underbrace{\frac{1}{2}\left(1 - \sum_{k=1}^{n} L_k^2\right)}_{\text{Inter-chrom. component}}. \tag{8.9}$$

Eqs. (8.7)–(8.9) mean that we can estimate the average intra-chromosomal contribution to $\bar{r}$ separately for each chromosome, possibly from different sets of data, and then combine these averages into a final measure of $\bar{r}$. This is useful, because often in sequencing or cytological studies of large numbers of gametes or meiosis I nuclei, it is possible (or desired) to obtain accurate measurements for only a subset of the chromosomes in each cell, so that the sets of cells from which measurements are taken for two chromosomes will in general not overlap. This is the case, for example, in the very rich cytological data from human pachytene nuclei in [201]. In such cases, Eqs. (8.7)–(8.9) state that the average intra-chromosomal contribution of one chromosome can be estimated from the set of cells from which measurements of that chromosome were possible, while the contribution of another chromosome can be estimated from the set of cells from which measurements of that chromosome were possible (possibly from different sets of data); these two separate estimates can then be combined in Eqs. (8.7)–(8.9).

Unrelated to the averaging of $\bar{r}$ across multiple measurements of individual gametes or meiocytes, an average value for $\bar{r}$ can also be calculated directly given pairwise average rates of shuffling for all loci. As discussed below, these can be estimated from linkage maps generated from pooled sequence data. Suppose that we have measured, for each locus pair (i, j), their rate of shuffling r_{ij}. $\langle \bar{r} \rangle$ is then simply the average value of r_{ij} across all locus pairs (i, j). If Λ is the total number of loci, then

$$\langle \bar{r} \rangle = \sum_{i<j} r_{ij} \Big/ \binom{\Lambda}{2} = \underbrace{\sum_{\substack{i<j \\ \text{linked}}} r_{ij} \Big/ \binom{\Lambda}{2}}_{\text{Intra-chrom.}} + \underbrace{\sum_{\substack{i<j \\ \text{unlinked}}} r_{ij} \Big/ \binom{\Lambda}{2}}_{\text{Inter-chrom.}}, \tag{8.10}$$

where $\binom{\Lambda}{2} = \Lambda(\Lambda-1)/2$. When $r_{ij} = 1/2$ for all unlinked locus pairs (i, j), the inter-chromosomal component simplifies to $(1-\sum_{k=1}^{n} L_k^2)/2$, where L_k is chromosome k's proportion of total genomic length.

8.4 Properties and intrinsic implications of $\bar{r}$

8.4.1 Properties

We note three properties of $\bar{r}$. First, its minimum value is 0, and its maximum value is 1/2, the latter relying on our assumption of many loci. The maximum value of $\bar{r}$ in a gamete can occur by chance equal segregation of maternal and paternal DNA to the gamete. The maximum value of $\mathbb{E}[\bar{r}]$ at meiosis I requires, unrealistically, that every pair of loci are either on separate chromosomes or experience at least one crossover between them in every meiosis. The minimum value of $\bar{r}$ in a gamete could result from chance segregation of only crossover-less chromatids of one parental origin to the gamete. The minimum value of $\mathbb{E}[\bar{r}]$ at meiosis I requires crossing over to be absent (as in *Drosophila* males and *Lepidoptera* females [571]), and either a karyotype of one chromosome or a meiotic process that causes multiple chromosomes to segregate as a single linkage group (as in some species in the evening primrose genus, *Oenothera* [91]).

Second, $\bar{r}$ satisfies the intuitive property that a crossover at the tip of a chromosome causes less shuffling than a crossover in the middle (some example calculations of $\bar{r}$ are given in Fig. 8.4.1). This is easily seen in Eq. (8.3). Consider a bivalent chromosome on which a single crossover will be placed. This will divide the chromosome into two segments of length l_1 and l_2, where $l_1 + l_2 = L$ is the chromosome's fraction of total genomic length. The contribution of this crossover to $\mathbb{E}[\bar{r}]$ is seen from Eq. (8.3) to be $1/2-(l_1^2+l_2^2)/2$, which can be rewritten $l_1 l_2 + 1/2 - (l_1+l_2)^2/2$,

which simplifies to $l_1 l_2$ under the constraint $l_1 + l_2 = L$. $l_1 l_2$ is maximized when $l_1 = l_2 = L/2$, i.e., when the crossover is placed in the middle of the bivalent. The quantity is minimized when either $l_1 = 0$ or $l_2 = 0$, i.e., when the crossover is placed at one of the far ends of the bivalent. In general, as the crossover is moved further from the middle of the bivalent, $\mathbb{E}[\bar{r}]$ steadily decreases. This is true regardless of the positions of the crossovers on other chromosomes. Importantly, this relationship also holds if, instead of considering where to place a single crossover on a whole bivalent, we consider where to place a new crossover on a segment already delimited by two crossovers (or by a crossover and a chromosome end). In general, if we are to place any fixed number of crossovers along a single chromosome, $\mathbb{E}[\bar{r}]$ is increased if they are evenly spaced [548, Appendix].

Third, $\bar{r}$ will tend to increase sub-linearly with both the number of crossovers and the number of chromosomes (Fig. 8.4.1D,E,F). For example, increasing the number of crossovers by some factor will increase the intra-chromosomal component of $\bar{r}$ by a lesser factor (and $\bar{r}$ as a whole by a yet lesser factor, because its inter-chromosomal component is unaffected). Similarly, doubling the number of chromosomes in the haploid set will cause a less-than-twofold increase in the inter-chromosomal component of $\bar{r}$. That is, there are 'diminishing returns' to genome-wide shuffling from having increasingly more crossovers and more chromosomes. These effects are described in mathematical detail in [548, Appendix].

8.4.2 Intrinsic implications

We have noted above that, given some number of crossovers along a chromosome at meiosis I, $\mathbb{E}[\bar{r}]$ is maximized if they are evenly spaced. This observation carries the interesting implication that positive crossover interference—a classical phenomenon

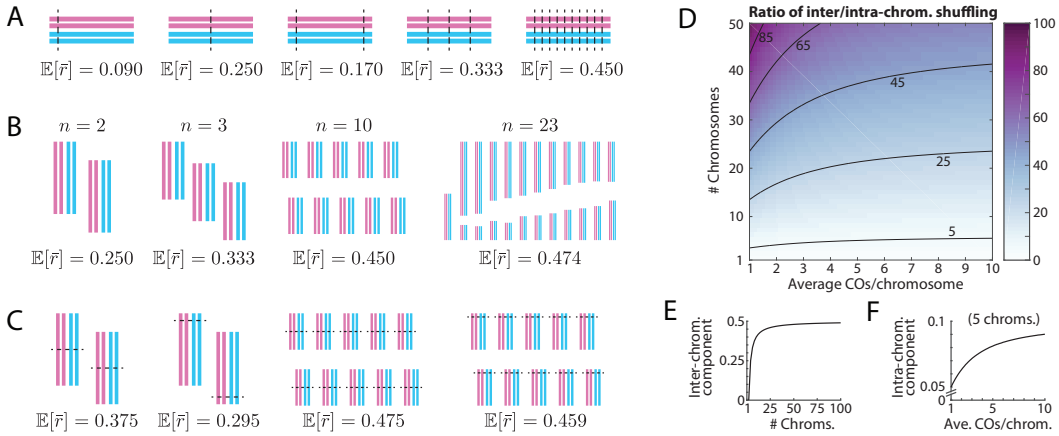

Figure 8.4.1: (A-C) Example values of the expected value of $\bar{r}$, $\mathbb{E}[\bar{r}]$, at meiosis I. In each case, $\mathbb{E}[\bar{r}]$ is calculated according to Eq. (8.3). (A) Various crossover numbers and positions in a diploid organism with only one chromosome. Notice that $\mathbb{E}[\bar{r}]$ increases sub-linearly with crossover number, even when crossovers are evenly spaced so as to maximize $\mathbb{E}[\bar{r}]$. (B) Various chromosome numbers for a diploid organism without crossing over. Notice that $\mathbb{E}[\bar{r}]$ increases sub-linearly with chromosome number, even when chromosomes are evenly sized so as to maximize $\mathbb{E}[\bar{r}]$. Notice too that, when the number of chromosomes is not small, $\mathbb{E}[\bar{r}]$ is close to its maximum value of $1/2$. The rightmost panel represents a crossover-less meiosis in a human female, in which case $\mathbb{E}[\bar{r}]$ is 0.474, close to its maximum value of $1/2$. (C) Various configurations of crossovers in a diploid organism with multiple chromosomes. (D) The ratio of contributions to $\mathbb{E}[\bar{r}]$ from independent assortment of homologs (inter-chromosomal shuffling) and crossing over (intra-chromosomal shuffling). Isoclines indicate CO and chromosome number combinations across which this ratio is constant. For example, the '45' isocline indicates where independent assortment contributes 45 times more shuffling than crossovers do. Chromosomes are assumed to be of equal size, and crossovers are assumed always to be evenly spaced along chromosomes. For each combination of $n \geq 2$ chromosomes in the haploid set and $I \geq 1$ crossovers per chromosome on average, we simulate 10^5 nuclei. For each of the n bivalent chromosomes in a nucleus, we draw a value from a Poisson distribution with parameter $I - 1$ and add it to 1 mandatory crossover to get the total number of crossovers for that chromosome. We then calculate the average total intra-chromosomal contribution to $\mathbb{E}[\bar{r}]$ across the nuclei, and compare it to the inter-chromosomal contribution (which is constant across nuclei). When the number of chromosomes is not small, the inter-chromosomal component dominates. (E) The inter-chromosomal component increases at a decreasing rate as chromosome number increases. (F) Similarly, holding constant the number of chromosomes (here, 5), the intra-chromosomal component increases at a decreasing rate as average crossover number increases.

[379, 501] where the presence of a crossover at some point along a bivalent chromosome inhibits the formation of nearby crossovers—will tend to increase $\bar{r}$. It thus suggests a possible selective advantage for this phenomenon (see Discussion).

Also, the general 'diminishing returns' to $\bar{r}$ of having more crossovers (above) carries particular implications for differences in total autosomal shuffling in the two sexes of a species. When the number of crossovers and/or their localization does not differ grossly between the sexes, then the amount of shuffling will be similar in both sexes (e.g., for male and female humans, as discussed below).

8.5 Experimental determination of crossover positions

Measurement of the quantity $\bar{r}$ requires that crossover positions along chromosomes can be accurately determined. While this was previously not possible, cytological advances have made it possible to efficiently and accurately visualize the positions of crossovers on pachytene bivalent chromosomes [8, 168, 335, 373, 502], while rapid technological advances in DNA sequencing have allowed crossover positions to be determined at a fine genomic scale using sequence/marker analysis of pedigrees [41, 294, 446, 484], individual gametes [332, 557] and meiotic triads/tetrads [96, 241, 338, 415]. These technological advances allow simple estimation of $\bar{r}$.

8.5.1 Cytological analysis

The physical positions of crossovers along the axes of pachytene chromosomes can be determined reliably in spread pachytene nuclei (or in 3D reconstructions from serial sectioning), either with electron microscopy by direct visualization of 'late recombination nodules' (which mark all crossovers [9, 481, 553, 596]), or with light microscopy using immunofluorescent staining techniques to detect 'type I' (inter-

fering) crossovers (reviewed in [221]; see Fig. 8.6.1), which are the vast majority in most organisms [245]. The latter method is now most commonly used.

Visualization of the chromosome axes can be achieved by staining either the axes or the SC central region (e.g., SYCP1-3). Crossover positions along the axes can be visualized by staining molecules specific to crossover recombination complexes (e.g., MLH1). If desired, the positions of centromeres along the axes can be visualized by staining for centromeric proteins such as CENP-A, and individual chromosomes can be identified by fluorescence in situ hybridization (FISH) or locus-specific fluorescent tags (e.g., FROS arrays), or, in favorable cases (e.g., *Arabidopsis* [166]), by relative chromosome length. Spread pachytene nuclei immuno-stained for crossover positions are now common in the literature, and have been generated for many species (e.g., 28 bovid species in [450] alone).

Only physical distances (in μm) along chromosomes can be directly inferred from cytological data, and so the measurement of $\bar{r}$ from such data requires a way to convert physical distances into genomic distances (in bp). The use of pachytene-stage chromosomes in the measurement of $\bar{r}$ (Fig. 8.6.1) is particularly advantageous in this regard because, at this stage of meiosis, genomic distance is proportional to physical distance along the chromosome axes (below and [548, Appendix]).

The physical structure of these chromosomes is highly regular: The chromatin of each chromatid is arranged in a linear array of loops, the bases of which lie at regular intervals along a common axis (reviewed in [285, 372, 596]). Almost all of the DNA is accommodated in the loops, with very little DNA in the axis between loop bases [285, 323, 372, 596]. Therefore, the genomic lengths of the loops directly define the genomic distance per unit of physical distance along a pachytene bivalent axis (the local 'packing ratio') [285, 286, 394, 450, 596]. Moreover, the local packing

ratio along and across different chromosomes is approximately constant within each nucleus, at least at the relatively crude scale of inter-crossover distances required for analysis of $\bar{r}$, as indicated by two criteria. First, physical loop lengths can be measured directly, and, in a variety of species, appear to vary minimally along and across chromosomes within nuclei (e.g., [276, 331, 372, 394, 429]; reviewed in [596]). Second, the relative genomic lengths of chromosomes closely match their relative physical axis lengths at pachytene (see [548, Fig. S2] for examples from diverse species), from which we infer that the average packing ratio of different chromosomes within a nucleus is approximately constant. Given these considerations, the chromosome segments' fractions of total genomic length (bp), as required for calculation of $\mathbb{E}[\bar{r}]$, correspond to, and thus can be defined by, their fractions of total physical axis length (μm). Therefore, their fractions of total axis length (easily measured from cytological spreads) can be substituted into the formulas derived above for $\mathbb{E}[\bar{r}]$ and its components.[4]

8.5.2 Sequence analysis

The genomic positions of crossovers in an individual's meioses can be inferred by sequencing the individual products of those meioses—either directly by sequencing individual gametes or polar bodies, or by inferring gametic genomes by sequencing individual diploid offspring—provided the individual's diploid genome has been haplophased. Haplophasing can be achieved either by sequencing an extended pedigree involving the individual [41, 86, 215], by sequencing multiple offspring, gametes, and/or polar bodies of the individual [89, 104, 241, 291, 332, 415], or by isolat-

[4] In some species (e.g., tomato [593]), it has been reported that loops are longer in heterochromatin than in euchromatin. While the data in [548, Fig. S2] suggest that this is not generally the case, in such species appropriate adjustments would be needed to convert physical lengths to genomic lengths.

ing individual chromosomes from a somatic cell and sequencing them separately [146, 557]. $\bar{r}$ can be calculated directly from gametic genome sequencing.

$\bar{r}$ can also be calculated from linkage maps derived from pooled sequencing data (as obtained, for example, from population pedigrees [41] or pooled sperm [254]). A linkage map gives the map distance (in cM) between pairs of linked markers. Using this, we can generate an evenly spaced grid of loci for each chromosome (to ensure even sampling of loci in the calculation of $\bar{r}$), and impute map distances between these pseudomarkers by linear interpolation from distances between true markers in the linkage map (details in [548, Appendix]). Thus, we generate a map distance d_{ij} between every pair of linked loci (i, j), which we can convert to a rate of shuffling r_{ij} using a map function [220], e.g., Kosambi's [297]: $r_{ij} = r(d_{ij}) = \frac{1}{2}\tanh(2d_{ij})$. This gives a rate of shuffling for every linked locus pair, from which we can calculate the average intra-chromosomal component of $\langle\bar{r}\rangle$ using Eq. (8.10). Assuming that unlinked locus pairs shuffle their alleles with probability 1/2, we can calculate the average value of shuffling across all locus pairs, $\langle\bar{r}\rangle$, using Eq. (8.10).

8.6 Measuring $\bar{r}$ in humans

8.6.1 Analysis of cytological data

Fig. 8.6.1 shows the calculation of $\mathbb{E}[\bar{r}]$ from the immunostained pachytene chromosomes of a single human spermatocyte [221] and oocyte [85]. For both spermatocyte and oocyte, $\mathbb{E}[\bar{r}]$ is close to its maximum value of 1/2. This high level of shuffling is due almost entirely to independent assortment: in both cases, the inter-chromosomal component of $\mathbb{E}[\bar{r}]$ is much larger than the intra-chromosomal component (from crossovers), by a factor of about 35 in the male and about 27 in

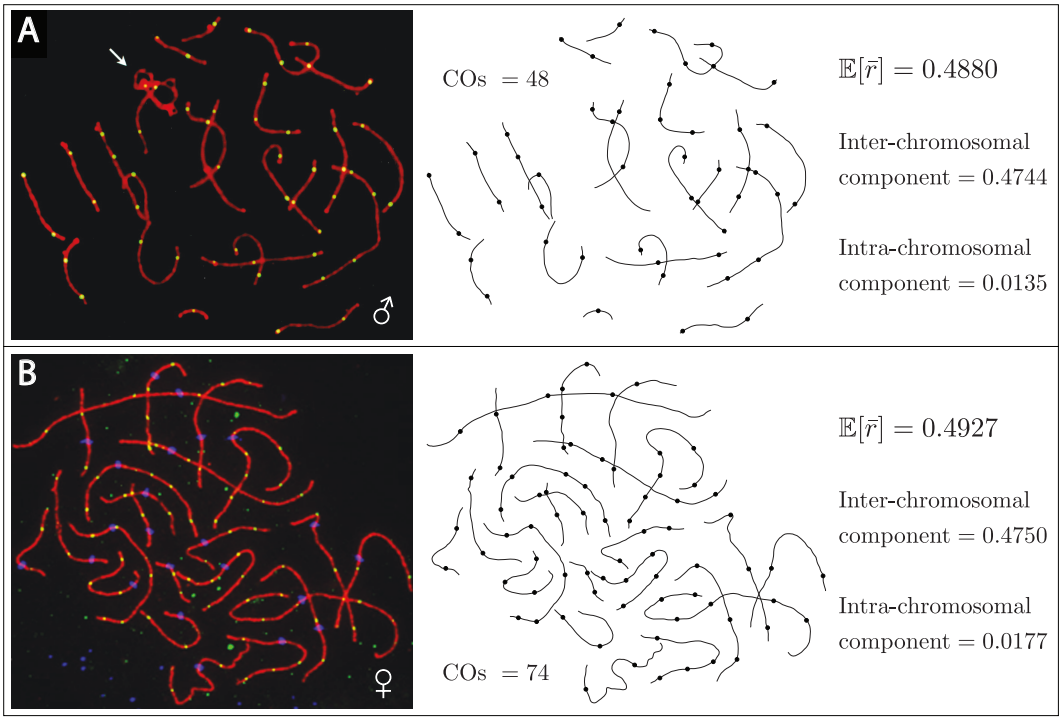

Figure 8.6.1: Calculation of $\mathbb{E}[\bar{r}]$ from crossover patterns at meiosis I in humans. The left panels are micrographs of immunostained spreads of a pachytene spermatocyte (A) and a pachytene oocyte (B). The red lines show localization of synaptonemal complex protein SYCP3, and demarcate the structural axes of the chromosomes. The green dots along the axes show foci of the protein MLH1, and demarcate the positions of crossover associations along the axes. The white arrow in (A) points to the paired X and Y chromosomes. In (B), the blue dots along the chromosome axes mark the centromeres. The paired X chromosomes in (B) have not been identified, and are included in the calculation of $\mathbb{E}[\bar{r}]$. The central panels show the traced axes and crossover positions from the spreads. From these, the lengths of the segments separated by the crossovers can be measured, and converted to fractions of the total physical axis length (these measurements can be found in [548, File S1]). The segments' fractions of total physical length can be taken to be approximately equal to their fractions of total genomic length, for reasons described in the text. With these fractions of genomic length, $\mathbb{E}[\bar{r}]$ may be calculated for each spread according to Eq. (8.3), and its inter- and intra-chromosomal components determined according to Eq. (8.6). The results of these calculations are given in the right panels. Notice that we do not require individual chromosomes to be identified to calculate $\mathbb{E}[\bar{r}]$ or its intra- and inter-chromosomal components.

the female.

Owing to the male-heterogametic (XX/XY) system of sex determination in humans, the spermatocyte in Fig. 8.6.1A contains easily identified, partially paired X and Y chromosomes, while the oocyte in Fig. 8.6.1B contains a bivalent of paired X chromosomes which in this case has not been distinguished from the other bivalents (e.g., by FISH). Therefore, the X chromosome is included in the calculation for the oocyte, and so the inter-chromosomal components of $\mathbb{E}[\bar{r}]$ for the spermatocyte and oocyte are not expected to be equal. Though we have estimated them directly from the single cytological spreads in Fig. 8.6.1, they can be calculated exactly from known genomic lengths of the chromosomes. Substituting the chromosome lengths reported in assembly GRCh38.p11 of the human reference genome (available online at www.ncbi.nlm.nih.gov/grc/human/data?asm=GRCh38.p11; lengths listed in [548, File S1]) into the first term in Eq. (8.6), we find that the value for the spermatocyte should be 0.4730, close to the value of 0.4744 calculated in Fig. 8.6.1A, while the value for the oocyte should be 0.4744, close to the value of 0.4750 calculated in Fig. 8.6.1B. This close match between the exact values and those deduced from physical chromosome axis lengths illustrates the reliability of physical length as a proxy for genomic length in the calculation of $\mathbb{E}[\bar{r}]$.

Interestingly, although the female spread exhibits about 50% more crossovers than the male spread (74 vs. 48), the intra-chromosomal component of $\mathbb{E}[\bar{r}]$ for the female spread is only about 30% larger than that of the male spread. This is expected from the general arguments given earlier concerning the 'diminishing returns' of more crossovers (Fig. 8.4.1D,F).

We have carried out measurement of $\mathbb{E}[\bar{r}]$ using data from 824 spermatocytes collected from 10 male humans (data from [324], kindly provided by F. Sun). Us-

ing Eq. (8.9), we calculate each chromosome's average contribution to the intra-chromosomal component of $\mathbb{E}[\bar{r}]$ (these are listed in SI Table S1). Summing these values, we find that the average intra-chromosomal component of $\mathbb{E}[\bar{r}]$ is 0.0143, which is similar to the value calculated for the single spermatocyte in Fig. 8.6.1A. Restricting attention to the 715 cells in which data were collected for every chromosome allows us to calculate the average and standard deviation of the intra-chromosomal component of $\mathbb{E}[\bar{r}]$ for each of the 10 individuals. The standard deviation of the intra-chromosomal component of $\mathbb{E}[\bar{r}]$ across the spermatocytes of each individual is of order 0.0015 (SI Table S2), or about 10% of the average value. There is some variation among the individuals for the average value of the intra-chromosomal component of $\mathbb{E}[\bar{r}]$: the minimum value is 0.0130, while the maximum is 0.0153. Interestingly, these minimum and maximum average values do not come from the individuals with, respectively, the smallest and largest average crossover frequencies (SI Table S2). In fact, the individual with the largest average value of the intra-chromosomal component of $\mathbb{E}[\bar{r}]$ has only the fourth (out of ten) largest average number of crossovers per spermatocyte. This further highlights the importance of crossover position for the amount of genetic shuffling, and hints that individuals might differ systematically in their crossover positioning in ways that quantitatively affect the amount of shuffling in their gametes.

8.6.2 Analysis of gamete sequence data

Hou et al. [241] sequenced the products of multiple meioses (first polar bodies, second polar bodies, and ova) of several females, and haplophased these females directly from the sequences of the meiotic products, allowing the crossover points in those products to be determined. Fig. 8.6.2 shows the crossover points along

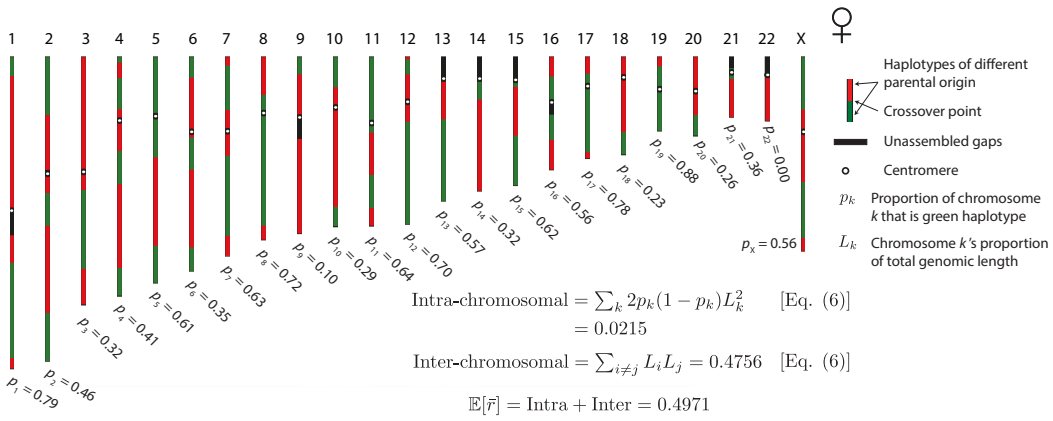

Figure 8.6.2: Calculation of $\bar{r}$ from the sequence of an individual egg obtained from a haplophased human female. Points of crossing over along chromosomes can be estimated directly from the gamete sequence. With no sequencing of an extended pedigree, we cannot tell which of the haplotypes separated by crossover points are maternal and which are paternal. Therefore, we cannot directly calculate p, the proportion of the egg's DNA that is paternal. We can, however, for each chromosome k find the proportion p_k that is of one parental origin (without knowing which), and then use Eq. (8.5) to calculate $\bar{r}$ and its components.

the chromosomes of an egg cell from one of the individuals. Because relatives of the individual were not sequenced, the paternal and maternal sequences cannot be discerned. Therefore, calculation of $\mathbb{E}[\bar{r}]$ proceeds according to Eq. (8.2), with its inter- and intra-chromosomal components determined according to Eq. (8.5). Carrying out this calculation for all chromosomes, including the X, reveals a value of $\mathbb{E}[\bar{r}] = 0.4971$, with an inter-chromosomal component of 0.4756 (calculated using chromosome lengths as they appear in Fig. 8.6.2) and an intra-chromosomal component of 0.0215 (all details in [548, File S2]). The inter-chromosomal contribution is about 22 times larger than the intra-chromosomal contribution. If we instead restrict attention to the autosomes, we find $\mathbb{E}[\bar{r}] = 0.4965$, with an inter-chromosomal component of 0.4735, and an intra-chromosomal component of 0.0230.

Fan et al. [146] haplophased a male using microfluidic techniques, and Wang et al. [557] sequenced 91 individual sperm cells from this male, using the haplophasing

from [146] to determine the points of crossing over in each sperm's sequence (given in Table S2 of [557]). From these, and because maternal and paternal sequences are not known, we use Eq. (8.8) to calculate the average value, across all 91 gametes, of $\mathbb{E}[\bar{r}]$ and its components. Carrying out this calculation yields an average value of $\mathbb{E}[\bar{r}]$ of 0.4856, with an average inter-chromosomal component of 0.4729, and an average intra-chromosomal component of 0.0127 (MATLAB code for these and the following calculations is provided in [548, File S3]). The average inter-chromosomal contribution is therefore about 37 times larger than the average intra-chromosomal contribution. In calculating the inter-chromosomal component of $\mathbb{E}[\bar{r}]$, because some shuffled SNP positions for this individual exceeded the chromosome lengths of the human reference genome, we used the position of the last SNP on each chromosome (as reported in [146] in their Supplemental Data Set 2) as our proxy of that chromosome's genomic length. Because there is no information about the parental origin of the sequences in each sperm, the inter-chromosomal component for each sperm is an average, deduced from the fixed genomic lengths of the individual's chromosomes [using Eq. (8.5)]. There is therefore no variance across gametes in this component. The standard deviation of the intra-chromosomal component of $\bar{r}$ across gametes is 0.0026, resulting in a coefficient of variation of about 0.2. The minimum value of the intra-chromosomal component across all 91 sperm is 0.0058; the maximum value is 0.0178. The average intra-chromosomal component of this individual is low relative to the average value of the intra-chromosomal component calculated from spermatocytes in the previous subsection (0.0143). This is expected, as he is homozygous for a variant of the *RNF212* gene that, in homozygous form, is associated with a reduction of ∼5-7.5% in crossover numbers in males [89, 293]. Indeed, the 91 sperm show, on average, 22.8 crossovers each (minimum 12; maximum 32), as compared to

the previously cited averages of 25.9 for Icelandic males [291] and 26.2 for Hutterite males [104].

8.6.3 Analysis of linkage map data

Kong et al. [294] sequenced 8,850 mother-offspring and 6,407 father-offspring pairs of Icelandics to generate high-density linkage maps for both sexes (data publicly available at http://www.decode.com/addendum). For each sex, we apply the method described above for generating a linkage map of evenly spaced 'pseudomarker' loci, and we estimate rates of shuffling for all linked locus pairs from the map distances between them using the Kosambi map function. We then estimate the intra-chromosomal component of $\langle \bar{r} \rangle$ using Eq. (8.10) (the inter-chromosomal component is calculated form known chromosome lengths). This yields a male value of 0.0138, similar to the value of 0.0143 calculated above from 824 spermatocytes (the chromosome-specific contributions are similar too; SI Table S4). This concordance indicates the validity of the linkage-data approach to estimating $\bar{r}$. The female value, including the X chromosome, is 0.0183, similar to the value of 0.0177 calculated from the single oocyte spread in Fig. 8.6.1, but smaller than the value of 0.0215 calculated from the single egg in Fig. 8.6.2. Excluding the X chromosome, the female value is 0.0193.

8.7 Discussion

The most common current measures of genome-wide genetic shuffling—crossover frequency and map length—do not take into account the positions of crossovers. This is a significant limitation, because terminal crossovers cause less shuffling than central crossovers. Traditional measures of aggregate shuffling also do not take into

account independent assortment of homologs in meiosis. Here, we have proposed a measure of genome-wide shuffling that naturally takes both of these features into account. This measure, $\bar{r}$, is the probability that a randomly chosen pair of loci shuffle their alleles in meiosis.

8.7.1 $\bar{r}$ should be the measure of choice for evaluation and comparison of genetic shuffling

$\bar{r}$ is the most direct measure of the aggregate amount of shuffling that occurs in the production of gametes. Application of this measure should therefore significantly improve the possibility of understanding the nature, basis, and significance of genetic shuffling and its variation across different situations (e.g., across species). We hope that this will become common practice where possible. In support of this possibility, we have demonstrated that $\bar{r}$ can readily be measured from standard sequence and cytological data.

8.7.2 Distinguishing the contributions of crossing over and Mendel's Second Law

We have shown that $\bar{r}$ can be decomposed into a component from crossovers and a component from independent assortment of homologs. The relative importance of crossing over and independent assortment as sources of shuffling has long been discussed [23, 57, 58, 109]. Theories of the adaptive value of shuffling fall roughly into two categories: those positing a short-term advantage (offspring diversification; e.g., the Tangled Bank [23, 181] and sib-competition [346, 578] theories) and those positing a long-term advantage (e.g., the 'Fisher-Muller' theory that gradually reducing allelic correlations over time allows natural selection to operate more efficiently on

genes at different loci [150, 154, 230, 380, 381]).

Burt [57] has argued that crossovers are more effective than independent assortment in gradually reducing allelic associations (because independent assortment shuffles genomes at fixed points, whereas crossovers can occur at many points along a chromosome). Under this view, the crossover component of $\bar{r}$ would be more important than the independent assortment component for long-term theories of the adaptive value of shuffling. On the other hand, the short-term theories rely on aggregate shuffling *per se*. We have shown, using humans as an example, that independent assortment will typically be the greatest contributor to aggregate shuffling. Therefore, the independent assortment component of $\bar{r}$ may be more important than the crossover component for short-term theories of the adaptive purpose of shuffling. Our decomposition of $\bar{r}$ into these separate components allows these distinctions to be tested quantitatively.

8.7.3 Crossover interference increases genetic shuffling

A property of the intra-chromosomal component of $\bar{r}$ is that it increases as crossovers become more evenly spread out. Thus, intriguingly, interference among crossovers will tend to increase the amount of shuffling that they cause (similar points have been made by Goldstein, Bergman, and Feldman [190], and Gorlov and Gorlova [194]). In [548, Appendix], we quantify this effect for human males using the spermatocyte data from [324], described above. Following the method employed in [338, 557] for sampling crossovers without interference, for each chromosome we calculate an interference-less average contribution to intra-chromosomal $\mathbb{E}[\bar{r}]$ by resampling, in each spermatocyte, the positions of the crossovers independently from the empirical distribution pooled across all spermatocytes. We find that the observed average

value of the intra-chromosomal contribution to $\mathbb{E}[\bar{r}]$ is about 15% higher than this interference-less value.

Crossover interference, first described more than a century ago [501], is a deeply conserved feature of the meiotic program [231, 558]. Despite this, its adaptive function, if any, remains unclear [245, 314, 452]. One category of hypotheses invokes mechanical advantages of spread-out crossovers, either to bivalent stability in prophase [541] or to homolog segregation at meiosis I [298]. However, such ideas are challenged by the fact that meiotic segregation proceeds without trouble in organisms that lack crossover interference (e.g., fission yeast and *Aspergillus* [135]) or that have had interference experimentally reduced or eliminated [152, 478]. The present study raises the possibility of a qualitatively different idea, that crossover interference provides an evolutionary advantage via its effects on genetic transmission. By explicitly taking into account the positions of crossovers in quantifying how much shuffling they cause, we show that crossover interference serves to increase the shuffling caused by a given number of crossovers. This finding therefore suggests a new possibility for the adaptive function of crossover interference.

8.7.4 Additional measures of genetic shuffling

$\bar{r}$ is a suitable measure of the total amount of shuffling, linearly aggregating the rates of shuffling between different locus pairs. In this way, it quantifies the first-order effect of shuffling, the genetic diversification of gametes/offspring [23]. However, certain population genetic properties exhibit non-linear dependence on the rates of shuffling between loci. For example, theoretical studies have determined that certain allelic associations across loci can jointly increase in frequency only if their constituent loci shuffle their alleles at a rate below some critical threshold value. This

has been shown for co-adapted gene complexes exhibiting positive fitness epistasis [110, 389, 567], 'poison-antidote' gamete-killing haplotypes involved in meiotic drive [75, 207, 218, 325], and associations between sex-determining genes and genes with sexually antagonistic fitness effects [382, 439, 535, 536]. Similarly, Hill-Robertson interference is effective only among loci that are tightly linked, shuffling their alleles at a rate below a small threshold (which depends on the effective population size and other parameters) [364]. In quantifying these various properties at an aggregate level, a more suitable measure would be the proportion of locus pairs that shuffle their alleles at a rate below the critical threshold. Such measures would be informative, for example, of which chromosomes are most likely to be co-opted as new sex chromosomes, or of how susceptible a species is to the invasion of 'poison-antidote' meiotic drive complexes (or, within species, which chromosomes are most likely to harbor such complexes), or of the average fitness reduction caused by Hill-Robertson interference. Calculating these threshold-based aggregate measures would require estimates of the average rates of shuffling for specific locus pairs. High-density linkage maps would therefore be especially promising for such measurements.

8.7.5 Taking gene density into account

The calculation of $\bar{r}$, as we have defined it, treats all regions of equal genomic length as of the same importance. However, the quantity we seek to measure is really the amount of shuffling of functional genetic elements—it is largely irrelevant if two functionless pseudogenes shuffle, for example. Therefore, correcting the calculation of $\bar{r}$ to take gene density into account is an important extension, a point already noted by Burt, Bell, and Harvey [60]. This is especially so if the distribution of genes is non-random along or across chromosomes. Accounting for the gene densities of

different genomic regions would be easiest with sequence data, especially in species with well-annotated genomes. For species without well-annotated genomes, proxies of the gene density of genomic regions, such as euchromatin content or GC-richness, could be used. Accounting for gene density with cytological data would be more complicated, since it requires knowledge of the identity and orientation of the various chromosomes. At a crude resolution, this can be achieved with chromosome-specific FISH probes (and, if required, centromere localization). Finer-scale identification of different genomic regions in cytological spreads could be achieved using high-resolution FISH [21, 22, 559]. In any case, the usual problems would arise in deciding which parts of the genome are 'functional' (see [131, 132] for reviews of recent debates on this topic).

8.7.6 Taking heterozygosity into account

Genetic shuffling of alleles at two loci in meiosis is practically relevant only if both loci are heterozygous. A simple modification of $\bar{r}$ that measures the extent of such 'effective' shuffling in meiosis is the proportion of locus pairs that shuffle their alleles and are both heterozygous. Again, we are mostly interested in the shuffling of functional elements, in which case estimation of this measure requires knowledge of the landscape of 'functional' heterozygosity across the genome (e.g., non-synonymous heterozygosity in protein-coding genes, as available for humans [311]) together with knowledge of linkage disequilibrium between nearby loci (e.g., for humans [517]).

8.7.7 Taking gene conversion into account

Another source of shuffling, in addition to crossing over and independent assortment, is gene conversion (GC) [95, 495]: the unidirectional copying of a DNA sequence

tract from one chromatid (the donor) to a homologous chromatid (the acceptor), either in mitosis or meiosis. In [548, Appendix], we show how to take both mitotic and meiotic GC into account in measuring $\bar{r}$. In meiosis, chromosome pairing involves many points of interaction between homologous chromatids ($\sim$ 200 across all chromosomes in mouse spermatocytes [592]), each induced by a double-strand break on one of the chromatids. In most organisms, only a minority of these interactions result in crossovers [94, 245, 287], the majority instead resulting in non-crossovers. Both outcomes are associated with short tracts of GC, (e.g., $\sim$ 100bp for non-crossover GCs and $\sim$ 500bp for crossover GCs in mice [96, 592]). These tracts, though numerous, are too short to seriously affect the total amount of shuffling [for example, the contribution from meiotic GCs in mammals will be of order 10,000 times smaller than the contribution from crossovers [548, Appendix]; in yeast, this figure is smaller—about 200 [548, Appendix]—owing to their longer GC tracts and smaller genomes], though they may have important local effects [10, 495]. Mitotic GC tracts result from homologous chromosome repair, are typically much longer than meiotic GC tracts (often of order 10kb; e.g., [242, 307]), and, if they occur in germline cell divisions leading to meiocytes, can lead to shuffling of maternal and paternal DNA in gametes (which should especially affect males, who have more germline cell divisions). Too little is presently known about the global frequency of these events for us to give a reasonable quantitative estimate of how much shuffling they cause.

9

Per-nucleus crossover covariation and implications for evolution

9.1 Abstract

Crossing-over is a nearly-universal feature of sexual reproduction. Here, analysis of crossover numbers on a per-chromosome and per-nucleus basis reveals a fundamental, evolutionarily-conserved feature of meiosis: within individual nuclei, crossover frequencies co-vary across different chromosomes. This effect results from per-

nucleus covariation of chromosome axis lengths. Crossovers can promote evolutionary adaptation. However, the benefit of creating favorable new allelic combinations must outweigh the cost of disrupting existing favorable combinations. Covariation concomitantly increases the frequencies of gametes with especially high, or especially low, numbers of crossovers, and thus might concomitantly enhance the benefits of crossing-over while reducing its costs. A four-locus population genetic model suggests that such an effect can pertain in situations where the environment fluctuates: hyper-crossover gametes are advantageous when the environment changes while hypo-crossover gametes are advantageous in periods of environmental stasis. These findings reveal a new feature of the basic meiotic program and suggest a possible adaptive advantage.

9.2 Introduction

Meiosis is the specialized cellular program that yields gametes for sexual reproduction. DNA recombination is a central feature of this program. Cross-over (CO) recombination shuffles the alleles along chromosomes, leading to genetic diversity of gametes and thus progeny [23, 548]. The nearly-universal occurrence of CO recombination in sexually-reproducing organisms is assumed to imply a fundamental adaptive role [347]. However, the ability of COs to create favorable new allelic combinations must be balanced against their seemingly opposing ability to break apart existing combinations that have been selected for. These opposing potentials are sometimes referred to as the "good" and "bad" effects of crossing-over [413, 497].

In some organisms, this dilemma is addressed by alternation between sexual and asexual reproductive lifestyles, usually with the sexual phase involving dispersal to new environments and/or being triggered by information that the environment

is changing [23, 578]. Other organisms utilize programmed variations of sexual reproduction in which recombination frequency is specifically elevated in conditions of stress, where new genetic combinations may be beneficial [23].

In the general case, including obligately sexual organisms, theoretical modeling suggests that the advantage of crossing-over comes into play in at least two ways [479]. First, in the long-term evolution of populations, COs can accelerate adaptation by bringing together favorable alleles that would otherwise compete with one another and by separating favorable alleles from linked unfavorable alleles that otherwise would impede the spread of the favorable alleles [150, 230, 357]. Second, in conditions where the environment fluctuates in time or space, COs can generate previously rare (or absent) genetic combinations that allow immediate adaptation [70, 214, 347, 459, 578].

Previous studies of crossing-over, beginning with classical genetic analyses, primarily analyzed recombination patterns on a per-chromosome basis. Such studies revealed not only the occurrence of crossing-over but also the phenomenon of crossover interference, a one-dimensional spatial patterning process that results, ultimately, in even spacing of crossovers along each chromosome [258]. Here we analyze CO patterns from a different perspective: with respect to the numbers of COs along individual chromosomes in single meiotic nuclei. Such information is provided by both cytological and DNA sequencing approaches.

Analysis of such data reveals a new basic feature of the meiotic recombination program: the numbers of CO-fated recombination interactions (and thus COs) tend to co-vary across different chromosomes, at higher or lower levels, within individual meiotic nuclei. Further, in accord with diverse evidences that axis length determines recombination/CO levels [560], the proximate basis for this effect is analogous per-

nucleus covariation of different chromosome axis lengths. Since chromosome axis length is known to be determined by chromatin loop length (e.g., [560]; below), global loop length modulation could underlie global modulation of CO frequencies.

Per-nucleus CO covariation results in an over-dispersed distribution of total CO levels per nucleus. The practical consequence of this effect is to elevate the frequencies of nuclei, and thereafter gametes, that contain either very many or very few COs, coordinately on all chromosomes. This outcome triggered the idea that CO covariation might increase the ability of COs to promote evolutionary adaptation. Both hyper- and hypo-CO gametes would be available, at all times, to provide either more or less genetic shuffling according to the dictates of the circumstances. Using a four-locus population genetic model, we provide support for this adaptive advantage of CO covariation across a range of situations in which the environment fluctuates: hyper-CO gametes are advantageous when the environment changes while hypo-CO gametes are advantageous in periods of environmental stasis. These findings suggest that CO covariation, an intrinsic feature of the basic meiotic chromosomal program and apparently common to most sexual organisms, has the potential to increase the power of crossing-over to enhance evolutionary adaptation.

9.3 Results

9.3.1 Per-nucleus analysis of COs.

Two methodologies can define the numbers and positions of crossover events along each chromosome (bivalent) in individual meiotic nuclei: (i) cytological analysis and (ii) DNA sequencing. (i) At the pachytene stage of meiotic prophase, the axes of homologous chromosomes are linked at 100nm along their lengths by a "pairing structure", the synaptonemal complex (SC). In spread chromosomal preparations

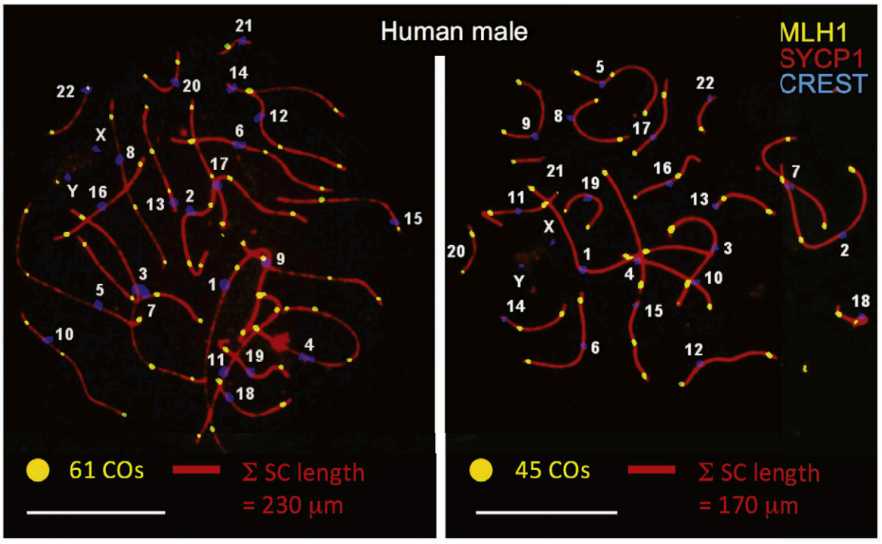

Figure 9.3.1: Per-nucleus analysis of COs. (A) Human male pachytene nuclei immunostained for chromosome axis (SYCP3; red), CO recombination complexes (MLH1; yellow) and centromeres (CREST, blue) for 22 autosomes. Left and right panels illustrate nuclei with longer axes and more COs (left) or shorter axes and fewer COs (right). See also [561, Figure S1A-D].

subjected to immunofluorescent staining, the positions of all crossover (CO) events, along each individual SC, are specifically marked by foci of particular proteins, e.g., MLH1 or Hei10-T3, as defined for many different organisms (e.g., Figure 9.3.1; [561, Figure S1CD]). Cytological analyses can analogously define the numbers of foci that mark the sites of early recombination intermediates (e.g., RPA or Hei10-T2; [561, Figure S1AB]) as well as underlying SC lengths in the same nuclei at both the CO and early intermediate stages. (ii) DNA sequence analysis has been applied only to a few organisms thus far. Data suitable for per-nucleus analysis is available from human female, where numbers and positions of COs along all chromosomes in individual nuclei are known for the egg and the two polar bodies of individual oocytes [241, 415] and from individual human male sperm [332, 557] which can be related to per-nucleus data (below).

CO-correlated cytologically-defined foci accurately report final CO numbers. Where tested, their average number corresponds well to the average number of COs detected either by DNA sequence analysis or as the number of chiasmata, the cytological manifestations of COs seen at diplotene. For example, analyses of human male report average numbers of 49.1 MLH1 foci [201, 560], 49.6 chiasmata [304], 50.7 COs (sperm sequencing [332]); and 50 COs (pedigree studies such as HapMap, deCODE etc.; further discussions in [9, 122, 341]). This agreement reflects the fact that the period when CO foci are present is long-lived and the number of foci remains stable throughout different substages (e.g., [122, 341]). Correspondingly, our analyses of DNA sequence data and CO focus data yield the same results (below).

9.3.2 The distribution of total COs per nucleus is over-dispersed relative to the hypothesis of independence across chromosomes.

Previous analyses by several methods show that the total number of CO events per nucleus varies significantly from one nucleus to another (e.g., [241, 332, 336, 450, 503, 560]) (Figure 9.3.1 left vs right; [561, Table S1]; below). Such variability could simply reflect intrinsic variability in the numbers of COs on different chromosomes as determined independently on those different chromosomes (hereafter "intrinsic variation"). To investigate this possibility, we asked whether the experimental distribution of COs per nucleus corresponded to that predicted if all variation resulted from independent variability on different chromosomes. To do so, we pooled all of the bivalents analyzed in experimental data, separately for each chromosome, and then created artificial nuclei "in silico", each containing one bivalent of each chromosome drawn at random from the corresponding pool [561, Methods]. Analysis of human male data shows that the per-nucleus CO numbers observed experimentally

vary much more widely than predicted from the artificial nuclei assembled in silico by the "hypothesis of independence", with Coefficients of Variation (CVs) of 0.1 and 0.05 respectively (Figure 9.3.2A; Figure 9.3.2B top panel, blue versus red; [561, Figure S1E]). As a result, the observed percentages of nuclei that contain either more or fewer COs are both substantially greater than those predicted by the hypothesis of independence for in silico nuclei (Figure 9.3.2B top, blue versus red; bottom, blue and orange). For human male, hyper- and hypo-CO nuclei each comprise 16% of the total. We define the sum of these percentages, 32% in human male, as the "Variability Index" (VI) (Figure 9.3.2C, data and corresponding best-fit normal distributions "dist"; [561, Figure S1F]). The VI provides a useful quantitative indicator of the magnitude of this effect. These various effects are observed for nuclei from several different individuals, indicating that they are a common general feature of human male meiosis [561, Figure S1EF].

The same over-dispersion seen in human male is observed in several other organisms as defined by CO focus data for two other mammals (tiger and elephant shrew), the higher plant tomato, and the filamentous fungus Sordaria, and by DNA sequence data for "meiotic tetrads" in human female (Figure 9.3.2DF; [561, Figure S2A]). All data sets exhibit: (i) a significantly higher CV for total COs per nucleus in experimental data as compared to those predicted for the hypothesis of independence from in silico nuclei; (ii) VIs ranging from 20% to 50%; and (iii) roughly equal numbers of hyper- and hypo-CO nuclei. These effects thus appear to be an evolutionarily conserved feature of the basic meiotic program.

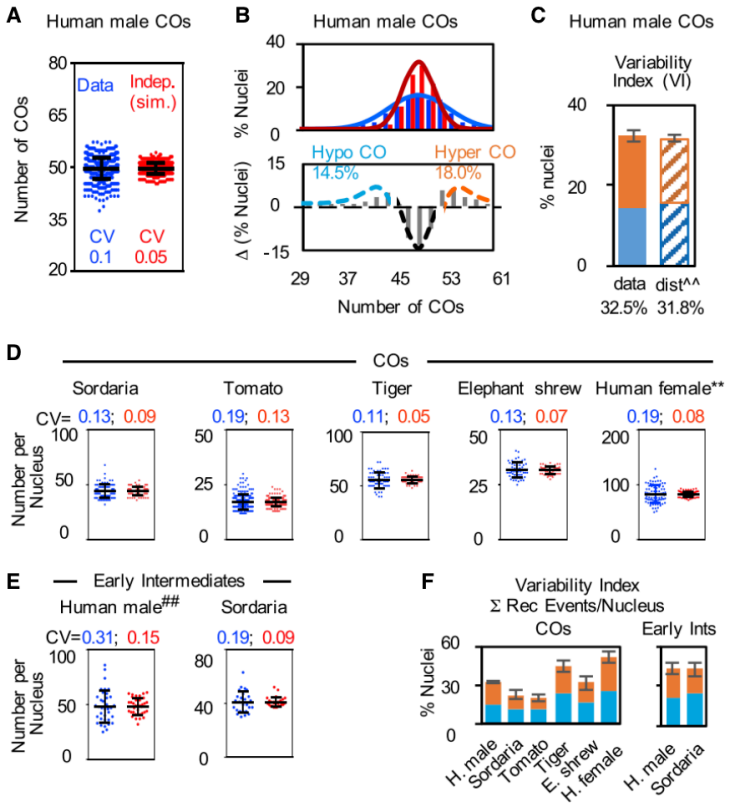

Figure 9.3.2: Over-dispersed distribution of total COs per nucleus, and resultant hyper- and hypo-CO nuclei. (A, B top). Experimental distribution of total CO number per nucleus in human male pachytene nuclei (blue; n=755) is compared with the distribution predicted if COs were determined independently on different chromosomes (the hypothesis of independence for in silico nuclei; text; red). Solid lines are best-fit normal distributions (B top; details in [561, Figure S2A]). The difference between these two distributions defines the frequencies of hypo- and hyper-CO nuclei (B bottom; blue, orange). (C) The sum of the frequencies of hypo-CO (blue) and hyper-CO (orange) nuclei is defined as the variability index (VI), determined from the data (left) and the corresponding normal distributions (right; [561, Figure S2A]). (D, F left) Comparisons as in (A) for COs in the five indicated organisms. **Female data come from DNA sequencing. (E, F right) Comparisons as in (A, C, D) for early intermediates in the two indicated organisms. ##Data are available only for chromosomes 13, 14, 15, 21 and 22. Data sources and details of statistical analysis are given in [561, Methods]. For human male, Sordaria, tomato, tiger, elephant shrew, and human female at CO stages, and human male and Sordaria at early intermediate stages, n = 755, 94, 111, 59, 63, 69, 36 and 26, respectively. Error bars indicate SD (A, D, E) or SE (C, F). See also [561, Figure S1-3].

9.3.3 Per-nucleus covariation of COs.

Overdispersion in the distribution of COs per nucleus directly implies that the numbers of COs on different chromosomes tend to covary, at higher or lower levels, within individual nuclei. This tendency for covariation can be observed experimentally. If chromosomes of an experimental sample are divided into two comparable groups, e.g., odd-numbered and even-numbered autosomes [561, Methods], the numbers of events on bivalents in the two groups are seen to be correlated within individual nuclei (Figure 9.3.3A). Per-nucleus correlation is also seen between: (i) the numbers of events on two different individual chromosomes (Figure 9.3.3B) and (ii) the number of events on one bivalent with the number on all other bivalents in the same nucleus [561, Figure S2B]. Accordingly, groups of nuclei exhibiting high, intermediate or low total numbers of COs exhibit the same hierarchy of CO levels for every chromosome (Figure 9.3.3C). Further, for human male, the CV for COs per nucleus and the degree of covariation between odd- and even-numbered chromosomes exhibit exactly the predicted relationship (Figure 9.3.3E; [561, Methods]).

9.3.4 Covariation contributes half or more of the total variance in the number of COs per nucleus.

The total variance of CO number per nucleus ("A") can be decomposed mathematically into two sources (Equation 7.2 in Table 9.3.1A): the sum of the "intrinsic variance" of CO numbers on each chromosome ("B"), and the sum of the covariances of CO numbers across all pairs of distinct chromosomes ("C"). Values of A, B, and C can be calculated directly from the experimental data. The proportional contribution of CO covariance to the total variance in CO number is given by the

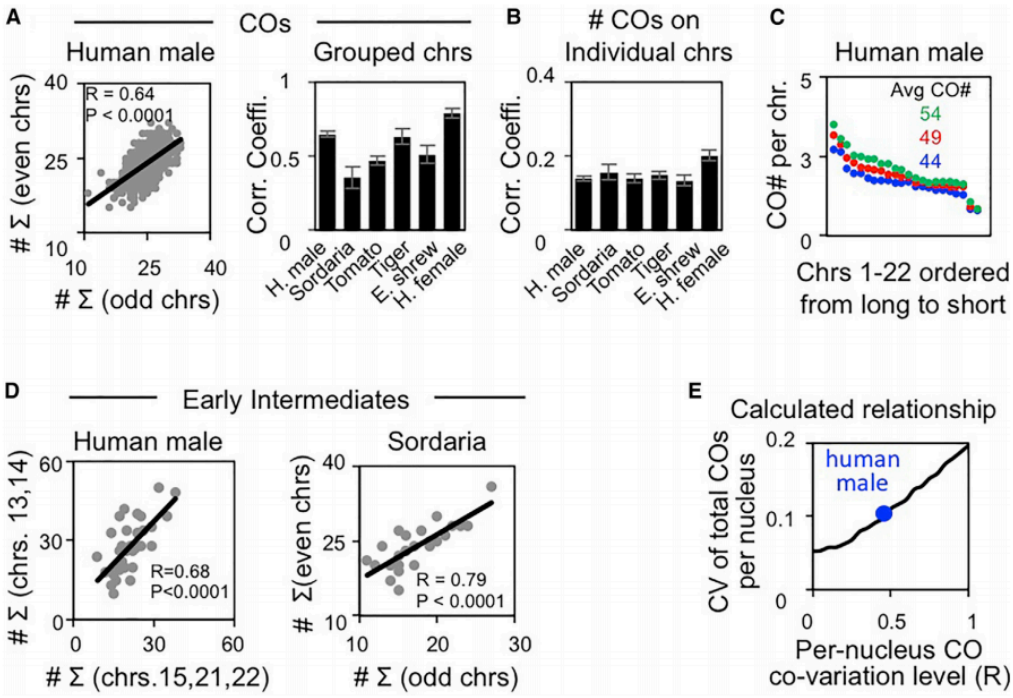

Figure 9.3.3: (A,B) For the six organisms analyzed for COs in Figure 9.3.2, the numbers of CO foci in single individual nuclei are correlated for two matched groups of chromosomes (e.g., odd vs even chromosomes in panel A left) and on pairs of individual chromosomes (B) for all possible combinations. (C) Human male nuclei with high, medium and low total CO numbers exhibit the same hierarchy for all 22 autosomes. (D) For the two organisms analyzed for early intermediates in Figure 9.3.2, the numbers of CO foci in single individual nuclei are correlated for two matched groups of chromosomes. (E) Simulations [561, Methods] confirm that stronger per-nucleus co-variation of COs gives increased variation in the total number of COs per nucleus (defined by CV). Sample sizes as in Figure 9.3.2. Error bars = SE (A-right and B). Data sources and details of statistical analysis are given in [561, Methods]. See also [561, Figure S1-2].

ratio C/A. All of the per-nucleus CO data sets described above exhibit positive values for total covariance (column (C) in Table 9.3.1B-I). Moreover, the contribution of covariation comprises 48%-83% of the total observed variance (C/A = 0.48-0.83; Table 9.3.1B-I) and thus is a major determining factor in all cases. [Note: the observed covariance cannot be due to the fact that every pair of homologs almost always acquires at least one CO (as required to ensure their regular segregation; Introduction) because, mathematically, neither variance nor covariance change when one CO is removed from every bivalent.]

Interestingly, the variation in COs per nucleus is particularly large in human female (e.g., Figure 9.3.2D, Table 9.3.1B-I). This difference results from the fact that human female meiosis is afflicted by a unique feature, CO maturation inefficiency (CMI), which acts at a late stage in the recombination process to effectively "subtract" COs stochastically from the original array set up by CO designation and interference [560]. Nonetheless, covariance is still the predominant factor in determining total variance (C/A = 83%; Table 9.3.1B-I).

These findings are confirmed and extended by analysis of DNA sequence data from post-prophase products of human male and female meiosis (Table 9.3.1B-V; [561, Methods]). CO patterns in individual sperm exhibit CO covariation, at exactly the level predicted for gametes from MLH1 focus analysis under the assumption of no chromatid interference. This correspondence has three implications. (i) Prophase focus data accurately report final CO numbers. (ii) Chromatid interference is either absent or extremely weak in human male, as has been found in other organisms [338, 595] and in human female [241]. (iii) Covariation set up at prophase, as seen in MLH1 focus patterns, is maintained essentially unaltered through gamete formation, without any detectable influence of covariation-induced biases in the loss

Table 9.3.1: Analysis of variance.

A. $\underbrace{\mathrm{Var}\left(\sum_{k=1}^{n} \mathrm{CO}_k\right)}_{(A)} = \underbrace{\sum_{k=1}^{n} \mathrm{Var}\left(\mathrm{CO}_k\right)}_{(B)} + \underbrace{\sum_{i \neq j} \mathrm{Covar}\left(\mathrm{CO}_i, \mathrm{CO}_j\right)}_{(C)}$ (Equation 9.2)[a]

B. Decomposition of Variance

	Organism	(A) = Obs. Total Var.	(B) = Var. if Indep.	(C) = Covar.	$(C)/(A)$	CV
I.	COs per nucleus					
	H. male	25.3	6.2	19.1	0.75	0.10
	Sordaria	8.9	4.6	4.3	0.48	0.13
	Tomato	11.3	4.9	6.4	0.57	0.19
	Tiger	47.0	13.0	34.0	0.72	0.11
	E. shrew	13.3	5.3	8.0	0.60	0.13
	H. female[b]	257.0	44.4	212.6	0.83	0.19
II.	Early intermediates per nucleus					
	H. male[c]	218.4	76.3	142.1	0.65	0.31
	Sordaria	62.9	16.1	46.8	0.74	0.19
III.	CO stage – axis length per nucleus[d]					
	H. male	19,827.1	2,541.3	17,286.4	0.87	0.16
	Sordaria	56.9	11.8	45.2	0.79	0.14
	Tomato	325.6	36.9	288.7	0.89	0.07
	Tiger	164,804.3	13,817.4	150,987.1	0.92	0.14
	E. shrew	121,045.2	29,112.1	91,933.3	0.76	0.13
IV.	Early intermediate stage – axis length per nucleus					
	H. male[c]	196.2	64.7	131.3	0.67	0.17
	Sordaria	114.5	26.2	88.4	0.77	0.14
V.	COs per gamete					
	H. sperms[b]	19.4	14.3	5.1	0.26	0.18
	H. sperms pred.	18.7	13.9	4.8	0.26	0.18
	H. eggs[b]	79.0	28.3	50.7	0.64	0.21
	H. eggs pred.	85.4	32.2	53.2	0.62	0.22

[a] n is the number of chromosomes in the haploid set. CO_k is the number of crossovers on chromosome k, but an analogous equation holds for any quantity, e.g., the axis length of chromosome k.

[b] From DNA sequence data (all other data from recombination foci).

[c] For human male, RPA foci and axis/SC length data are available only for chromosomes 13, 14, 15, 21, and 22.

[d] Female axis lengths at the CO stage are not available because data come from DNA sequence analysis (text).

of hypo- or hyper-CO gametes. These conclusions are bolstered by the fact that, for human female, covariation observed in gametes (eggs) is the same as that predicted for gametes from full prophase "tetrads", each reconstituted from an egg plus the associated first and second polar bodies (Table 9.3.1B-V). We also note that these findings for human gametes explain the "gamete effect" of Kong et al. [291, 295], who observe, in sequenced human pedigrees, that the number of crossovers transmitted to a given offspring is correlated across chromosomes.

9.3.5 Early recombination intermediates exhibit per-nucleus covariation.

During meiosis, CO sites are designated (with accompanying CO interference) at early/mid prophase from among a much larger array of early recombination interactions, each set up by a corresponding initiating double-strand break [245]. All of the patterns described above for COs are also observed for these early intermediates, as defined by analysis of RPA foci in human male and Hei10 T2 foci in Sordaria, including: (1) an overdispersed distribution of total foci per nucleus, with high VI's and roughly equal numbers of hyper- and hypo-focus nuclei (Figure 9.3.2EF; [561, Figure S1AB]); (2) per-nucleus correlations in the numbers of foci observed in two equivalent chromosome groups (Figure 9.3.3D); and (3) positive levels of total covariance and large contributions of covariance to total variance (Table IB-II).

9.3.6 Prophase chromosome axis lengths exhibit per-nucleus covariation.

Every experimental feature diagnostic of per-nucleus covariation of COs, and of early recombination events, is also observed analogously for bivalent axis (SC) lengths at

the corresponding stages. (1) Total axis lengths per nucleus are overdispersed, with high VI's and roughly equal numbers of hyper- and hypo-axis length nuclei (Figure 9.3.4; [561, Figure S1GH]). (2) Per-nucleus covariation is seen for axis lengths between different groups of chromosomes or of individual chromosomes (Figure 9.3.5ABD; [561, Figure S2D-F]), or an individual chromosome and a chromosome group [561, Figure 2C]. Accordingly, groups of nuclei exhibiting high, intermediate or low total axis lengths exhibit the same hierarchy of axis lengths for every chromosome (Figure 9.3.5C). (3) Axis lengths at both stages exhibit positive values of total covariance and large contributions of total covariance to total variance (Table 9.3.1B-III, IV).

9.3.7 Per-nucleus covariation of prophase chromosome axis lengths dictates per-nucleus CO covariation.

The axis length of an individual chromosome determines the number of initiated recombination events (DSBs), total early recombination interactions and, then, interference-mediated COs. Correlations between axis length and event number are documented in several organisms (e.g., human male and female meiosis; Figure 9.3.1; [560]). Moreover: (i) Axis lengths are the same regardless of whether recombination has been initiated, not initiated, or initiated at a reduced level [94, 500, 516, 593, 594]. (ii) Mutations in axis components coordinately alter not only axis length but also CO levels [176, 367, 394, 437, 594]; and (iii) human male and female meiosis exhibit, respectively, shorter/longer axes, and fewer/more COs, but have identical recombination processes including the density of early recombination interactions per axis length and the parameters governing CO designation

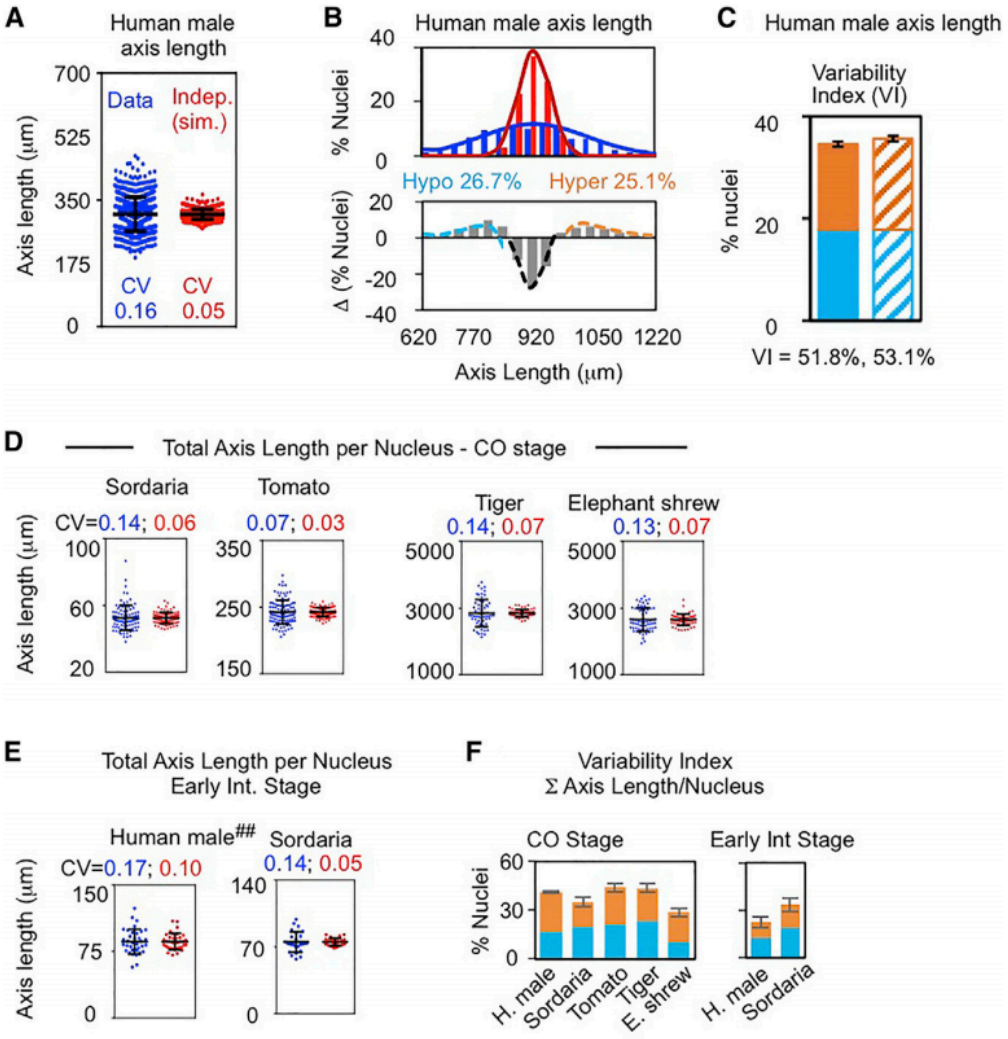

Figure 9.3.4: Over-dispersed distribution of total axis lengths per nucleus. Panels (A-F) are exactly analogous to panels (A-F) of Figure 9.3.2 except that they pertain to axis lengths at the CO and early intermediate stages rather than the corresponding recombination events. ##Data are available only for chromosomes 13, 14, 15, 21 and 22. Sample sizes as in Figure 9.3.2. See also [561, Figure S1-2].

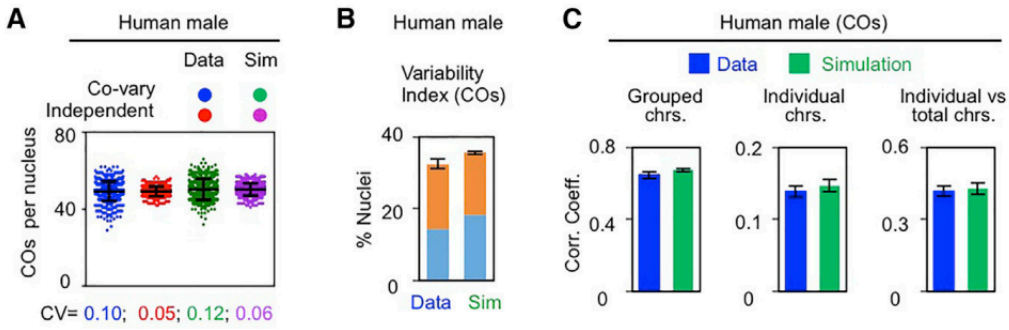

Figure 9.3.5: Panels (A-D) are exactly analogous to panels (A-D) of Figure 9.3.3 except that they pertain to axis lengths at the CO and early intermediate stages rather than the corresponding recombination events. Sample sizes as in Figure 9.3.2. Data sources and details of statistical analysis are given in [561, Methods]. See also [561, Figure S1-2].

and interference [560].

If chromosome axis length determines the average number of COs per bivalent, it follows directly that per-nucleus covariation of axis lengths should determine per-nucleus covariation of COs. In accord with this causality, per-nucleus correlation coefficients for grouped chromosomes, and the proportion of total variance resulting from covariation (C/A, above), are both substantially higher for axis lengths than for COs (R >0.9 versus 0.4-0.8; and 76%-92% versus 48%-83%, respectively (Figures 9.3.5A and 9.3.3A; and Table 9.3.1B-I, III, respectively)).

Additionally, simulation of recombination patterns shows that per-nucleus covariation of axis lengths can quantitatively explain CO covariation. In previous work, we used this approach to determine, for human male meiosis, the values of all parameters that define the basic features of CO recombination (e.g., the array of total early interactions and the nature of CO site specification by CO designation and interference) [560]. We have now included in the simulation algorithm two additional parameters that specify (i) intrinsic variation in axis lengths; and (ii) covariation among axis lengths of different bivalents in the same nucleus [561, Methods]. When

the values of these two parameters are set at the levels defined experimentally [561, Methods and Figure S2C-E, S3A], simulation of human male CO patterns yields a nearly perfect match to experimental data with respect to: (i) the CV for the total number of COs per nucleus (Figure 9.3.6A, green vs blue), the CV for total COs per nucleus predicted for in silico nuclei by the hypothesis of independence (Figure 9.3.6A, purple vs red), and the accompanying percentages of hyper- and hypo-CO nuclei and the VI (Figure 9.3.6B); (ii) the per-nucleus correlation coefficients for COs in odd versus even chromosome groups, for pairs of individual chromosomes, and for individual chromosomes versus a chromosome group (Figure 9.3.6C green vs blue); (iii) total variance, intrinsic variance, and co-variance and, thus the contribution of covariance to total variance, of COs per nucleus; and (iv) previously-analyzed features [561, Figure S3B].

Finally, in most organisms, axis lengths are set up early in prophase where they determine not only CO frequencies but the frequencies of total initiating double-strand breaks and of early intermediates, among which a selected subset are CO sites [560, 593, 594]. In accord with this progression, covariation is also observed for early intermediates and their corresponding axis lengths, by all criteria (Figures 9.3.2-9.3.5; Table 9.3.1B-III, IV). By implication: (i) covariation will apply also to gene conversion (GC) events, which arise from all types of early intermediates but primarily from those that yield "non-crossover" products [95], and (ii) individual nuclei (and gametes) will tend to exhibit especially high or especially low levels coordinately for both GCs and COs.

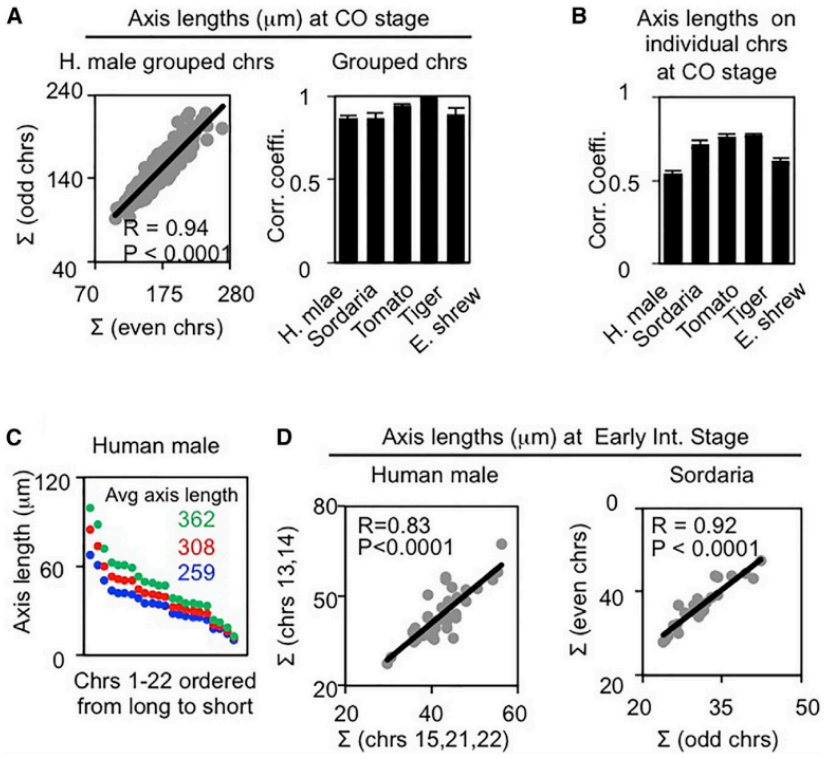

Figure 9.3.6: Simulation analysis shows that intrinsic variation and covariation of axis lengths can quantitatively explain per-nucleus covariation of COs in human male. Recombination event patterns were predicted by an enhanced simulation analysis that parameterizes both intrinsic variation and covariation of chromosome axis lengths (text; [561, Methods]). For human male COs, simulation using the experimentally-defined values for both of these parameters perfectly predicts all experimentally-observed features including the CV of total COs per nucleus (Panel A, green versus blue) and the three per-nucleus correlations in CO numbers on grouped and/or individual chromosomes as described in Figure 9.3.3AB and [561, Figure S2B]. Moreover, simulation using the experimentally-defined axis variation but zero axis-length co-variation perfectly predicts the outcome of the "hypothesis of independence" (text) (Panel A, purple vs red). Correspondingly, predicted levels of hyper-CO (orange) and hypo-CO (blue) nuclei and the corresponding VI exactly match those defined from experimental data (B). Data sources and details of statistical analysis are given in [561, Methods]. See also [561, Figure S1-3].

9.3.8 Per-nucleus CO covariation aids evolutionary adaptation in a sporadically fluctuating environment.

Per-nucleus CO covariation has the effect of increasing the proportions of gametes with extremely low and with extremely high CO numbers (above). During sexual reproduction, gametes with few COs tend to lead to offspring that are phenotypically similar to their parents, while gametes with many COs lead to offspring with substantial phenotypic variation. CO covariation, by elevating hypo-CO and hyper-CO gametes, concomitantly increases the proportions of both of these classes of offspring. At the same time, by reducing the proportion of mid-CO gametes, it reduces the number of offspring whose phenotypes are intermediately different from their parents' (Figure 9.3.7A). The effect of CO covariation on CO levels in gametes is thus expected to have significant consequences for the fitness of the resulting offspring according to the environment(s) in which they find themselves.

Covariation is predicted to confer an advantage in a fluctuating environment. One circumstance in which CO covariation could potentially confer an advantage is where a species experiences occasional fluctuations in its environment, across time or space. Such environmental fluctuations, either biotic or abiotic, are faced by the majority of species [578]. If the environment does not change between a parental generation and an offspring generation, then selection will tend to favor offspring that are similar to their parents, whose phenotypes (and perhaps those of their parents, etc.) were tried and tested in the same environment (Figure 9.3.7B). In this situation, the fittest offspring are likely to be enriched for those produced from hypo-CO gametes (Figure 9.3.7A); this will favor parents whose gametes exhibited CO covariation. If, instead, the environment changes between the parental and

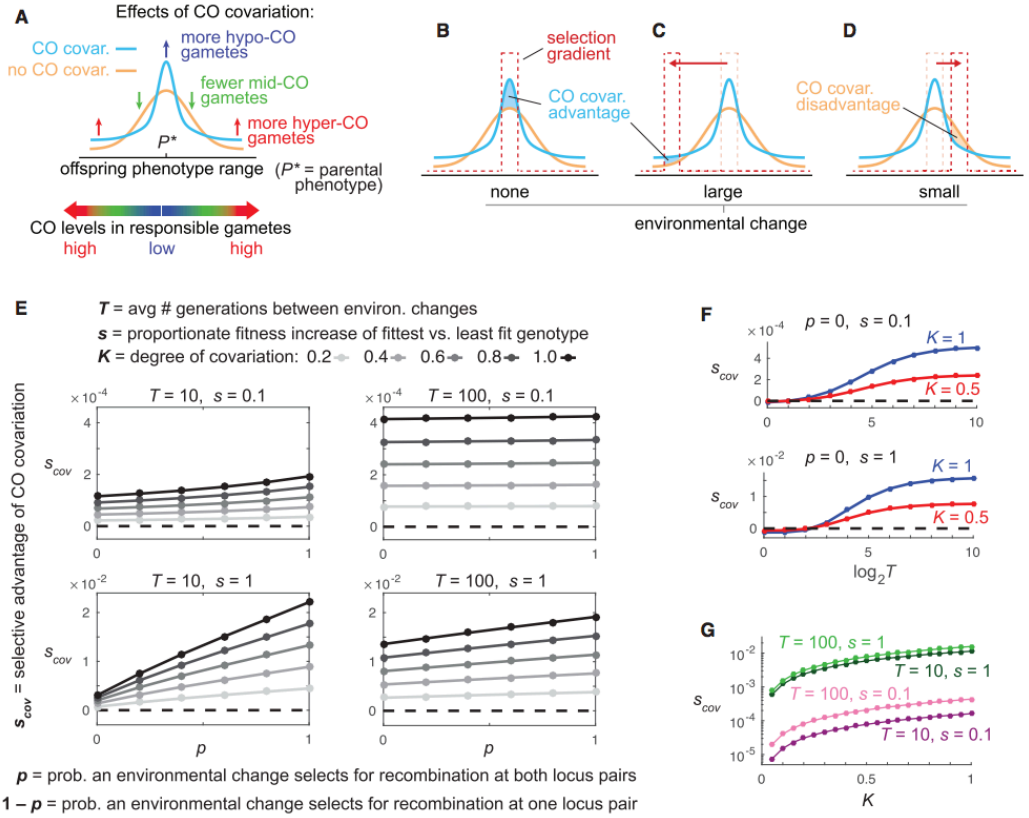

Figure 9.3.7: Mathematical modelling demonstrates the evolutionary advantage of crossover covariation. (A) CO covariation causes an overproduction of hypo-CO and hyper-CO gametes, which, respectively, increase the frequencies of offspring with trait values very close to, and very far from, the parental value. (B) When the environment does not change, offspring with trait values near the parental value are favored, and thus covariation is favored. (C) When the environment changes substantially, offspring with trait values far from the parental value become favored, and thus covariation is again favored. (D) Only when the environment changes a little is covariation disfavored. (E) The selective advantage of covariation is revealed formally in a four locus population genetic model with a fluctuating environment. CO covariation enjoys a selective advantage in all scenarios. The selective advantage of covariation increases with p, the probability that each environmental change favors hyper-CO gametes with COs between both locus pairs. However, covariation is favored even when $p = 0$, so that environmental changes always favor gametes with a CO between only one locus pair, and thus always disfavor covariation. Here, the benefit of covariation derives from its overproduction of hypo-CO gametes in the periods of stasis between environmental changes. (F,G) Consistent with this logic, when $p = 0$, the advantage of covariation grows as the average period of stasis, T, grows. (H) The advantage to covariation increases monotonically with the degree of covariation. See also [561, Figure S4-6].

offspring generations, then selection will shift to favoring a phenotype different from that favored in the parental generation, and thus can favor new genetic combinations produced by crossing-over. If the environmental shift is large, the fittest offspring will tend to be enriched for those with many new genetic combinations (Figure 9.3.7C). This again will favor parents who exhibited CO covariation, due to their elevated levels of hyper-CO gametes (Figure 9.3.7A). This selection for hyper-CO gametes will be stronger, the more severe the environmental change. Only in the case where the environmental changes, but the change is mild, can mid-CO gametes be favored (Figure 9.3.7D), and, thus, CO covariation disfavored (Figure 9.3.7A).

Population genetic modeling defines the advantage of covariation in a fluctuating environment. To investigate the above logic more formally, we have constructed a minimal population genetic model of selection in a fluctuating environment (full details in [561, Methods]). For convenience, the model organism is a unisexual haploid, and sexual reproduction occurs by the fusion of two individuals, followed by meiosis. To allow for CO covariation across chromosomes, four loci are considered—one pair of loci on each of two different chromosomes—with alleles A/a and B/b; and C/c and D/d respectively. In a given generation, there is a favored combination of alleles on each chromosome: e.g., AB and ab on chromosome 1, and CD and cd on chromosome 2. (This symmetry—e.g., if aB is favored then so is Ab—ensures that polymorphism is maintained at all loci, and thus allows us to focus directly on the effect of recombination without having to worry about drastic swings in the frequencies of particular alleles, e.g., [70, 459].) The favored combination of alleles remains constant in periods of environmental stasis and changes to a different combination when/after the environment changes.

Our general strategy was to simulate separately, and then compare, the evolu-

tionary dynamics of a population that exhibits no CO covariation between the two locus pairs and of a population that does exhibit CO covariation (full recursion equations provided in [561, Methods]). In each simulation, we calculated the average growth rate (geometric mean fitness) of the population across 10^7 generations. For a given comparison, if the population employing CO covariation has a higher average growth rate than the population employing no CO covariation, we expect that CO covariation would usually outcompete no covariation in a population mixed for the two strategies [264].

Simulations were carried out over a range of values of five specified parameters: (1) A baseline rate of recombination between each locus pair, r. This rate is chosen arbitrarily, recognizing that the recombination rate between each locus pair could have evolved for reasons other than, or in addition to, environmental fluctuations (e.g., alleviation of Hill-Robertson interference). (2) The level of covariation of COs at the two locus pairs, K, which ranges from 0 (no covariation) to 1 (maximal covariation). (3) The average period of environmental fluctuations, T generations. Specifically, in each generation, there is a probability $1/T$ that the environment changes. (4) The probability p that, when the environment does change, the newly-favored allele combination changes on both chromosomes (e.g., from AB/ab and CD/cd to Ab/aB and Cd/cD). $1-p$ is then the probability that the newly-favored allele combination changes on only one of the two chromosomes (each equally likely). (5) The strength of selection, s, defined as the relative selective advantage of the fittest genotype over the least fit genotype.

We focused primarily on a selection scenario where only those offspring that are best genetically equipped for their environment are likely to survive and reproduce. This scenario applies to the majority of extant species, and likely also to those an-

cestral species in which the basic features of sex and recombination evolved [578]. In this case, across a wide range of parameter specifications, the population employing CO covariation virtually always enjoys a higher average growth rate than the population without CO covariation. Moreover, the advantage of covariation increases as the degree of covariation increases (Figure 9.3.7E greyscale; Figure 9.3.7FG, red versus blue; Figure 9.3.7H, [561, Figure S4C]). These findings provide a proof of principle that CO covariation can be evolutionarily advantageous in populations faced with fluctuating environments. We obtain similar results when selection is more even across genotypes (multiplicative across locus pairs) [561, Figure S5]. However, in the opposite case to that we have focused on, where selection acts so that all but the very least fit reproduce, the results are more equivocal, with CO covariation sometimes being advantageous, and sometimes not [561, Figure S6].

Additional findings support our specific prediction that the advantage of covariation derives from its elevation of both hyper- and hypo-CO gametes, due to their different advantages in changed or static conditions, respectively. Consistent with this: (i) The advantage of CO covariation tends to be larger when environmental shifts more often alter the favored genetic combinations at both locus pairs; i.e., when p is larger (Figure 9.3.7E; [561, Figure S4A]). Intuitively, this can be understood as the case where environmental changes are often large (Figure 9.3.7C), with the positive effects of covariation in creating new combinations coordinately on two (or more) chromosomes resulting from elevation of hyper-CO gametes (Figure 9.3.7A). (ii) However: the advantage of CO covariation is also apparent at low values of p (Figure 9.3.7E). In the extreme case of $p = 0$, a change in the environment always favors recombination at only one locus pair. Intuitively, this corresponds to the case where environmental shifts are always small (Figure 9.3.7D). In this case,

environmental changes always disfavor CO covariation because small environmental shifts select for mid-CO gametes (in our model, 1 CO; Figure 9.3.7AD). Therefore, we infer that covariation's advantage in the case of small p must derive from a benefit conferred in the periods of stasis between environmental changes, and, specifically, from overproduction of hypo-CO gametes in these periods (Figure 9.3.7AB). This interpretation is directly supported by an additional finding: when $p = 0$, the advantage of CO covariation is typically greater if the average period of stasis between environmental changes, T, is longer (Figure 9.3.7FG; [561, Figure S4B]).

To more comprehensively study the effects of the various parameters on the evolutionary success of CO covariation, we focused on a simple specification of the model where, when the environment changes, a new set of favored alleles is selected, with all of the alternative combinations being equally likely. Under this specification, we find again that CO covariation typically improves the average population growth rate relative to no CO covariation. The size of this advantage is: (i) monotonic in the degree of CO covariation (Figure 9.3.7H; [561, Figure S4C]); (ii) tends to increase with the average period between environmental changes, T, unless selection is very strong [561, Figure S4D]; and (iii) increases with the strength of selection [561, Figure S4E].

9.4 Discussion

Here we identify a fundamental new feature of meiotic recombination: per-nucleus CO covariation. This feature is evolutionarily conserved, as seen by documentation in three mammals, a higher plant, and a fungus. The existence of per-nucleus CO covariation raises two general questions. What is the mechanism? And what is its significance? We have begun to provide answers to both questions.

9.4.1 Mechanism.

We show that the proximate basis for per-nucleus covariation of COs is analogous per-nucleus covariation of chromosome axis lengths. This conclusion is concordant with, and a direct extension of, diverse evidences that chromosome axis length determines CO number, as documented above. What could determine CO axis length? It has been shown that the density of chromatin loops along prophase chromosome axes is evolutionarily conserved [285]. This feature, in turn, directly implies that axis length and chromatin loop length are inversely related. Correspondingly, longer/shorter axes in correlation with shorter/longer loops have been documented in a number of situations: in the two sexes of a given organism (including human) [201, 515], domainally in heterochromatin vs euchromatin in tomato (e.g., [496]), in the PAR region of mammalian X and Y chromosomes [267]. Further, in mouse, deletion of a single meiotic axis component, $smc1\beta$, is sufficient to confer shorter chromosome axes and correspondingly larger chromatin loops [394, 437]. These observations imply that global modulation of loop length is a general mechanism for determining chromosome axis length and, therefore, the number of COs per chromosome (discussion in [560]). Thus, in the present case, per-nucleus covariation of CO numbers could be a natural consequence of global determination of chromatin loop size.

9.4.2 Significance for Evolution.

The distribution of total COs per nucleus, as observed experimentally, is significantly broader than that predicted if CO numbers were specified independently on different chromosomes, and this difference is driven by covariation of CO number across chromosomes within nuclei. As a direct consequence, CO covariation significantly

increases the frequencies of nuclei (and thus gametes) that have especially high or especially low levels of COs, coordinately on all chromosomes. We reasoned that this feature might increase the ability of COs to promote evolutionary adaptation: on the one hand, hyper-CO gametes would be available when new genetic combinations are needed for adaptation; on the other hand, hypo-CO gametes would be available when it is more advantageous to retain ancestral, well-evolved combinations. The question then arises: in which specific situation(s) would the increased availability of these two types of gametes confer a selective advantage?

We further reasoned that covariation could be advantageous in a fluctuating environment. More hyper-CO gametes would be available for times of environmental change, when new genetic combinations become favored, and more hypo-CO would be available for periods of stasis, when the environment is not changing and creation of new combinations by crossing-over would tend to be deleterious. Population genetic modeling provides support for the validity of these predictions. In scenarios where environmental changes are separated by periods of stasis, covariation significantly increases mean fitness, in proportion to the degree of covariation, and over a wide range of parameter specifications. Moreover, details of the observed effects provide specific evidence that covariation is favorable via its elevations of both hyper-CO and hypo-CO gametes (above).

This analysis provides an initial proof of principle that CO covariation can be advantageous in fluctuating environments, as probably faced by all species [578]. If so, CO covariation expands the power of meiotic recombination to promote evolutionary adaptation.

COs have diverse roles in adaptation, whose relative contributions to the evolutionary maintenance of recombiation are much debated (e.g., [17, 18, 23, 150, 347,

413, 578]). Importantly, by the logic above, CO covariation will aid in the response to environmental fluctuations even if other factors are the predominant reasons for the maintenance of COs. We note, however, that the model we employed is, by necessity, highly simplified, ignoring a number of biological complexities that could plausibly affect the degree to which CO covariation is advantageous, e.g., analysis of only four loci, inclusion of only two chromosomes, and a limited number of environmental fluctuation regimes [561, Methods]. In addition, a more direct demonstration of the advantage of CO covariation in our model would involve competing alleles at a fifth, unlinked "modifier" locus, the alleles at which have no direct effect on fitness but influence the level of CO covariation among the other four loci. Future studies can address these complexities.

We also note that Hadany and Beker [204] argue that it is favorable for low-fitness individuals to recombine their genomes substantially, but not for high-fitness individuals to do so. Such "fitness associated recombination" is directly apparent when high recombination is induced by, or associated with, environmental change (Introduction), but is also mirrored in the situation described here, where environmental change reduces the fitness of currently-common genotypes while environmental stasis maintains the fitness dominance of common genotypes.

Additional advantages of CO covariation can also be considered. First, we note that chromosomes lacking even a single CO are prone to mis-segregation [596]. CO covariation does not confer an overall increase in the frequency of chromosomes lacking a CO, which is a function of the basic mechanism by which meiotic CO patterns are determined [570, 593, 594]. However, it does tend to bundle zero-CO chromosomes into a smaller fraction of nuclei (e.g., [560]) and will thereby decrease the overall probability that a nucleus will exhibit aberrant segregation(s) at Meiosis

I. This effect, while small, represents an effective additional benefit of covariation.

Second, while we have focused here on scenarios involving short-term effects of recombination in a fluctuating environment, it is not impossible that CO covariation might also be beneficial for in longer-term evolution, even in stable environments. Laboratory evolution experiments show that, under constant environmental conditions, population fitness increases over time, seemingly without bound, as new beneficial mutations (and combinations of mutations) continually arise and are incorporated (e.g., [581]). In this case, it is the "allelic environment" of the organism that is constantly changing over time. Correspondingly, it is possible that, in some regimes, in the presence of co-variation, hyper-CO gametes will increase the rates at which independently-arising favorable mutations become linked and favorable mutations become separated from linked deleterious ones (Introduction) whereas hypo-CO gametes will keep new mutations together once they have become linked.

Third, when DNA is introgressed, via hybridization, from the genome of one species into another's, introgressed genes that are incompatible with the recipient genome are purged by purifying selection. This process also removes introgressed DNA surrounding the incompatible genes, with larger blocks removed in regions of low recombination. Higher recombination thus causes finer "trimming", allowing greater retention of introgressed DNA that is neutral or beneficial [38, 133, 342, 466]. Introgression and purging, like CO covariation, are genome-wide events; and the time-scale of purging is short—e.g., < 100 generations [217, 466]. After a pulse of introgression, hypo-CO gametes are expected to be favorable if there are many incompatible genes and few beneficial genes in the introgressed DNA, since hypo-CO gametes allow rapid purging of many large blocks of introgressed DNA. Under this scenario, CO covariation would speed the purging of incompatibilities by providing

an excess of hypo-CO gametes. If, on the other hand, introgressed DNA harbors many beneficial new genes, then hyper-CO gametes will be favorable in rapidly unlinking these beneficial genes from linked incompatible genes, so that a greater number of beneficial genes can be retained in the recipient species' genome.

We also note that CO covariation is of general significance for population genetic modeling. Classical population genetic models that probe the evolutionary advantages of recombination mostly involve only two loci, although multi-locus models have been developed to understand genomic evolution and the evolution of recombination (e.g., [17, 76, 214, 312, 414]). Since CO covariation appears to be conserved across eukaryotes, future multi-locus population genetic models must take this phenomenon into account if they are to be empirically realistic.

References

[1] I. Alger and J. W. Weibull. Homo moralis–preference evolution under incomplete information and assortative matching. *Econometrica*, 81(6):2269–2302, 2013.

[2] B. Allen and M. A. Nowak. Games on graphs. *EMS Surveys in Mathematical Sciences*, 1(1):113–151, 2014.

[3] B. Allen and M. A. Nowak. Games among relatives revisited. *Journal of Theoretical Biology*, 378:103–116, 2015.

[4] B. Allen and C. E. Tarnita. Measures of success in a class of evolutionary models with fixed population size and structure. *Journal of Mathematical Biology*, 68(1-2):109–143, 2014.

[5] B. Allen, M. A. Nowak, and U. Dieckmann. Adaptive dynamics with interaction structure. *American Naturalist*, 181(6):E139–E163, 2013.

[6] D. Almond and L. Edlund. Trivers–Willard at birth and one year: evidence from US natality data 1983–2001. *Proceedings of the Royal Society of London B: Biological Sciences*, 274(1624):2491–2496, 2007.

[7] P. M. Altrock, C. S. Gokhale, and A. Traulsen. Stochastic slowdown in evolutionary processes. *Physical Review E*, 82(1):011925, 2010.

[8] L. K. Anderson, A. Reeves, L. M. Webb, and T. Ashley. Distribution of crossing over on mouse synaptonemal complexes using immunofluorescent localization of MLH1 protein. *Genetics*, 151:1569–1579, 1999.

[9] L. K. Anderson, L. D. Lohmiller, X. Tang, D. B. Hammond, L. Javernick, L. Shearer, S. Basu-Roy, O. C. Martin, and M. Falque. Combined fluorescent and electron microscopic imaging unveils the specific properties of two classes of meiotic crossovers. *Proceedings of the National Academy of Sciences USA USA*, 111:13415–13420, 2014.

[10] P. Andolfatto and M. Nordborg. The effect of gene conversion on intralocus associations. *Genetics*, 148:1397–1399, 1998.

[11] M. Archetti and I. Scheuring. Review: Game theory of public goods in one-shot social dilemmas without assortment. *Journal of Theoretical Biology*, 299: 9–20, 2012.

[12] P. S. Ashton, T. J. Givnish, and S. Appanah. Staggered flowering in the Dipterocarpaceae: new insights into floral induction and the evolution of mast fruiting in the aseasonal tropics. *American Naturalist*, 132(1):44–66, 1988.

[13] R. Axelrod. *The Evolution of Cooperation*. Basic Books, 1984.

[14] D. Bachtrog, M. Kirkpatrick, J. E. Mank, S. F. McDaniel, J. C. Pires, W. Rice, and N. Valenzuela. Are all sex chromosomes created equal? *Trends in Genetics*, 27(9):350–357, 2011.

[15] D. Bachtrog, J. E. Mank, C. L. Peichel, M. Kirkpatrick, S. P. Otto, T.-L. Ashman, M. W. Hahn, J. Kitano, I. Mayrose, R. Ming, et al. Sex determination: why so many ways of doing it? *PLoS Biology*, 12(7):e1001899, 2014.

[16] Z. Baker, M. Schumer, Y. Haba, L. Bashkirova, C. Holland, G. G. Rosenthal, and M. Przeworski. Repeated losses of prdm9-directed recombination despite the conservation of prdm9 across vertebrates. *eLife*, 6:e24133, 2017.

[17] N. Barton. A general model for the evolution of recombination. *Genetics Research*, 65(2):123–144, 1995.

[18] N. H. Barton and B. Charlesworth. Why sex and recombination? *Science*, 281(5385):1986–1990, 1998.

[19] F. Baudat, J. Buard, C. Grey, A. Fledel-Alon, C. Ober, M. Przeworski, G. Coop, and B. De Massy. PRDM9 is a major determinant of meiotic recombination hotspots in humans and mice. *Science*, 327(5967):836–840, 2010.

[20] T. Becking, I. Giraud, M. Raimond, B. Moumen, C. Chandler, R. Cordaux, and G. Clément. Diversity and evolution of sex determination systems in terrestrial isopods. *Scientific Reports*, 7:1084, 2017.

[21] B. J. Beliveau, E. F. Joyce, N. Apostolopoulos, F. Yilmaz, C. Y. Fonseka, R. B. McCole, Y. Chang, J. B. Li, T. N. Senaratne, B. R. Williams, et al. Versatile design and synthesis platform for visualizing genomes with Oligopaint FISH probes. *Proceedings of the National Academy of Sciences USA USA*, 109: 21301–21306, 2012.

[22] B. J. Beliveau, A. N. Boettiger, M. S. Avendaño, R. Jungmann, R. B. McCole, E. F. Joyce, C. Kim-Kiselak, F. Bantignies, C. Y. Fonseka, J. Erceg, et al. Single-molecule super-resolution imaging of chromosomes and in situ haplotype visualization using Oligopaint FISH probes. *Nat Comm*, 6, 2015.

[23] G. Bell. *The Masterpiece of Nature: The Evolution and Genetics of Sexuality*. University of California Press, 1982.

[24] T. Bereczkei and R. I. M. Dunbar. Female-biased reproductive strategies in a Hungarian Gypsy population. *Proceedings of the Royal Society of London B: Biological Sciences*, 264(1378):17–22, 1997.

[25] C. T. Bergstrom and P. Godfrey-Smith. On the evolution of behavioral heterogeneity in individuals and populations. *Biology and Philosophy*, 13(2): 205–231, 1998.

[26] C. T. Bergstrom and M. Lachmann. The Red King effect: when the slowest runner wins the coevolutionary race. *Proceedings of the National Academy of Sciences USA*, 100(2):593–598, 2003.

[27] T. C. Bergstrom. The algebra of assortative encounters and the evolution of cooperation. *International Game Theory Review*, 5(03):211–228, 2003.

[28] L. W. Beukeboom and N. Perrin. *The evolution of sex determination*. Oxford University Press, 2014.

[29] A. J. Bewick, D. W. Anderson, and B. J. Evans. Evolution of the closely related, sex-related genes DM-W and DMRT1 in African Clawed Frogs (*Xenopus*). *Evolution*, 65(3):698–712, 2011.

[30] P. Bijma and D. Aanen. Assortment, Hamilton's rule and multilevel selection. *Proceedings of the Royal Society of London B: Biological Sciences*, 277(1682): 673–675, 2010.

[31] K. Binmore and L. Samuelson. Muddling through: Noisy equilibrium selection. *Journal of Economic Theory*, 74(2):235–265, 1997.

[32] A. J. Black, A. Traulsen, and T. Galla. Mixing times in evolutionary game dynamics. *Physical Review Letters*, 109(2):028101, 2012.

[33] L. E. Blume. The statistical mechanics of strategic interaction. *Games and Economic Behavior*, 5(3):387–424, 1993.

[34] M. Bojko. Human meiosis IX. Crossing over and chiasma formation in oocytes. *Carlsberg Research Communications*, 50:43–72, 1985.

[35] A. Boulton, R. S. Myers, and R. J. Redfield. The hotspot conversion paradox and the evolution of meiotic recombination. *Proceedings of the National Academy of Sciences USA*, 94(15):8058–8063, 1997.

[36] D. Brandis. Biological notes on Indian bamboos. *Indian Forester*, 25:1–25, 1899.

[37] Y. Brandvain and G. Coop. Scrambling eggs: meiotic drive and the evolution of female recombination rates. *Genetics*, 190:709–723, 2012.

[38] Y. Brandvain, A. M. Kenney, L. Flagel, G. Coop, and A. L. Sweigart. Speciation and introgression between *Mimulus nasutus* and *Mimulus guttatus*. *PLoS Genetics*, 10(6):e1004410, 2014.

[39] C. B. Bridges. Triploid intersexes in *Drosophila melanogaster*. *Science*, 54: 252–254, 1921.

[40] C. Brion, S. Legrand, J. Peter, C. Caradec, D. Pflieger, J. Hou, A. Friedrich, B. Llorente, and J. Schacherer. Variation of the meiotic recombination landscape and properties over a broad evolutionary distance in yeasts. *PLoS Genetics*, 13:e1006917, 2017.

[41] K. W. Broman, J. C. Murray, V. C. Sheffield, R. L. White, and J. L. Weber. Comprehensive human genetic maps: individual and sex-specific variation in recombination. *Am J Human Genet*, 63:861–869, 1998.

[42] L. D. Brooks and R. W. Marks. The organization of genetic variation for recombination in *Drosophila melanogaster*. *Genetics*, 114:525–547, 1986.

[43] G. R. Brown. Sex-biased investment in nonhuman primates: can Trivers & Willard's theory be tested? *Animal Behaviour*, 61(4):683–694, 2001.

[44] J. Bull. Sex ratio evolution when fitness varies. *Heredity*, 46(1):9, 1981.

[45] J. Bull and M. G. Bulmer. Longevity enhances selection of environmental sex determination. *Heredity*, 63(3):315, 1989.

[46] J. Bull, R. C. Vogt, and M. Bulmer. Heritability of sex ratio in turtles with environmental sex determination. *Evolution*, 36(2):333–341, 1982.

[47] J. J. Bull. Sex determination in reptiles. *Quarterly Review of Biology*, 55(1): 3–21, 1980.

[48] J. J. Bull. Evolution of environmental sex determination from genotypic sex determination. *Heredity*, 47(2):173–184, 1981.

[49] J. J. Bull. *The evolution of sex determining mechanisms*. Benjamin Cummings, 1983.

[50] J. J. Bull. Sex determining mechanisms: an evolutionary perspective. In S. C. Stearns, editor, *The Evolution of Sex and its Consequences*, pages 93–115. Springer, 1987.

[51] J. J. Bull. Virulence. *Evolution*, 48(5):1423–1437, 1994.

[52] J. J. Bull and M. G. Bulmer. The evolution of XY females in mammals. *Heredity*, 47(3):347–365, 1981.

[53] J. J. Bull and E. L. Charnov. Changes in the heterogametic mechanism of sex determination. *Heredity*, 39(1):1–14, 1977.

[54] J. J. Bull and E. L. Charnov. On irreversible evolution. *Evolution*, 39(5): 1149–1155, 1985.

[55] M. Bulmer and J. Bull. Models of polygenic sex determination and sex ratio control. *Evolution*, 36(1):13–26, 1982.

[56] M. G. Bulmer. Periodical insects. *American Naturalist*, 111(982):1099–1117, 1977.

[57] A. Burt. Perspective: sex, recombination, and the efficacy of selection–was Weismann right? *Evolution*, 54:337–351, 2000.

[58] A. Burt and G. Bell. Mammalian chiasma frequencies as a test of two theories of recombination. *Nature*, 326(6115):803–805, 1987.

[59] A. Burt and R. L. Trivers. *Genes in conflict*. Belknap Press, 2006.

[60] A. Burt, G. Bell, and P. H. Harvey. Sex differences in recombination. *Journal of Evolutionary Biologyl*, 4:259–277, 1991.

[61] E. J. Caldera and C. R. Currie. The population structure of antibiotic-producing bacterial symbionts of *Apterostigma dentigerum* ants: impacts of coevolution and multipartite symbiosis. *Am Nat*, 180(5):604–617, 2012.

[62] H. G. Callan and P. E. Perry. Recombination in male and female meiocytes contrasted. *Philosophical Transactions of the Royal Society of London B: Biological Sciences*, 277:227–233, 1977.

[63] E. Z. Cameron and F. Dalerum. A Trivers-Willard effect in contemporary humans: male-biased sex ratios among billionaires. *PLoS One*, 4(1):e4195–e4195, 2009.

[64] E. Z. Cameron and W. L. Linklater. Individual mares bias investment in sons and daughters in relation to their condition. *Animal Behaviour*, 60(3): 359–367, 2000.

[65] E. Z. Cameron and W. L. Linklater. Sex bias in studies of sex bias: the value of daughters to mothers in poor condition. *Animal Behaviour*, 63(2):F5–F8, 2002.

[66] E. Z. Cameron and W. L. Linklater. Extreme sex ratio variation in relation to change in condition around conception. *Biology Letters*, 3(4):395–397, 2007.

[67] J. Carranza. What did Trivers and Willard really predict? *Animal Behaviour*, 63(2):F1–F3, 2002.

[68] L. Carroll. *Through the Looking-Glass*. Macmillan, 1871.

[69] C. Y. Chang and E. Witschi. Genic control and hormonal reversal of sex differentiation in *Xenopus*. *Proceedings of the Society for Experimental Biology and Medicine*, 93(1):140–144, 1956.

[70] B. Charlesworth. Recombination modification in a fluctuating environment. *Genetics*, 83(1):181–195, 1976.

[71] B. Charlesworth. Model for evolution of Y chromosomes and dosage compensation. *Proceedings of the National Academy of Sciences USA*, 75(11): 5618–5622, 1978.

[72] B. Charlesworth. The evolution of sex chromosomes. *Science*, 251(4997): 1030–1033, 1991.

[73] B. Charlesworth. Effective population size and patterns of molecular evolution and variation. *Nature Reviews Genetics*, 10(3):195–205, 2009.

[74] B. Charlesworth and D. Charlesworth. The degeneration of Y chromosomes. *Philosophical Transactions of the Royal Society of London B: Biological Sciences*, 355(1403):1563, 2000.

[75] B. Charlesworth and D. L. Hartl. Population dynamics of the segregation distorter polymorphism of *Drosophila melanogaster*. *Genetics*, 89:171–192, 1978.

[76] B. Charlesworth, M. Morgan, and D. Charlesworth. The effect of deleterious mutations on neutral molecular variation. *Genetics*, 134(4):1289–1303, 1993.

[77] D. Charlesworth and B. Charlesworth. Sex differences in fitness and selection for centric fusions between sex-chromosomes and autosomes. *Genetics Research*, 35(2):205–214, 1980.

[78] D. Charlesworth, B. Charlesworth, and G. Marais. Steps in the evolution of heteromorphic sex chromosomes. *Heredity*, 95(2):118–128, 2005.

[79] E. L. Charnov. *The Theory of Sex Allocation*. Princeton University Press, 1982.

[80] E. L. Charnov and J. Bull. When is sex environmentally determined? *Nature*, 266(5605):828, 1977.

[81] E. L. Charnov and J. Bull. Non-fisherian sex ratios with sex change and environmental sex determination. *Nature*, 338(6211):148, 1989.

[82] E. L. Charnov, J. J. Bull, and J. M. Smith. Why be an hermaphrodite? *Nature*, 263(5573):125, 1976.

[83] E. L. Charnov, R. L. Los-den Hartogh, W. T. Jones, and J. van den Assem. Sex ratio evolution in a variable environment. *Nature*, 289(5793):27, 1981.

[84] M.-Y. Chen. Giant timber bamboo in Alabama. *Journal of Forestry*, 71(12): 777, 1973.

[85] E. Y. Cheng, P. A. Hunt, T. A. Naluai-Cecchini, C. L. Fligner, V. Y. Fujimoto, T. L. Pasternack, J. M. Schwartz, J. E. Steinauer, T. J. Woodruff, S. M. Cherry, et al. Meiotic recombination in human oocytes. *PLoS Genetics*, 5: e1000661, 2009.

[86] V. G. Cheung, J. T. Burdick, D. Hirschmann, and M. Morley. Polymorphic variation in human meiotic recombination. *Am J Human Genet*, 80:526–530, 2007.

[87] I.-K. Cho and D. M. Kreps. Signaling games and stable equilibria. *The Quarterly Journal of Economics*, 102(2):179–221, 1987.

[88] T. Chotibut and D. R. Nelson. Population genetics with fluctuating population sizes. *Journal of Statistical Physics*, 167(3-4):777–791, 2017.

[89] R. Chowdhury, P. R. J. Bois, E. Feingold, S. L. Sherman, and V. G. Cheung. Genetic analysis of variation in human meiotic recombination. *PLoS Genetics*, 5:e1000648, 2009.

[90] E. Clancey and J. A. Byers. The definition and measurement of individual condition in evolutionary studies. *Ethology*, 120(9):845–854, 2014.

[91] R. E. Cleland. *Oenothera: Cytogenetics and Evolution*. Academic Press, 1972.

[92] T. H. Clutton-Brock, S. D. Albon, and F. E. Guinness. Maternal dominance, breeding success and birth sex ratios in red deer. *Nature*, 308(5957):358–360, 1984.

[93] T. H. Clutton-Brock, S. D. Albon, and F. E. Guinness. Great expectations: dominance, breeding success and offspring sex ratios in red deer. *Animal Behaviour*, 34(2):460–471, 1986.

[94] F. Cole, L. Kauppi, J. Lange, I. Roig, R. Wang, S. Keeney, and M. Jasin. Homeostatic control of recombination is implemented progressively in mouse meiosis. *Nat Cell Biol*, 14(4), 2012.

[95] F. Cole, S. Keeney, and M. Jasin. Preaching about the converted: how meiotic gene conversion influences genomic diversity. *Ann NY Acad Sci*, 1267:95–102, 2012.

[96] F. Cole, F. Baudat, C. Grey, S. Keeney, B. de Massy, and M. Jasin. Mouse tetrad analysis provides insights into recombination mechanisms and hotspot evolutionary dynamics. *Nat Genet*, 46:1072–1080, 2014.

[97] P. C. Colombo. A new index for estimating genetic recombination from chiasma distribution data. *Heredity*, 69:412–415, 1992.

[98] J. M. Comeron, R. Ratnappan, and S. Bailin. The many landscapes of recombination in *Drosophila melanogaster*. *PLoS Genetics*, 8:e1002905, 2012.

[99] G. W. A. Constable, A. J. McKane, and T. Rogers. Stochastic dynamics on slow manifolds. *J. Phys. A: Math. Theor.*, 46:295002, 2013.

[100] G. W. A. Constable, T. Rogers, A. J. McKane, and C. E. Tarnita. Demographic noise can reverse the direction of deterministic selection. *Proceedings of the National Academy of Sciences USA*, 113(32):E4745–E4754, 2016.

[101] J. M. Cook and J.-Y. Rasplus. Mutualists with attitude: coevolving fig wasps and figs. *Trends Ecol Evol*, 18(5):241–248, 2003.

[102] D. Cooney and C. Veller. Assortment and the evolution of cooperation in a Moran process with exponential fitness. *arXiv:1509.05757*, 2015.

[103] D. Cooney, B. Allen, and C. Veller. Assortment and the evolution of cooperation in a Moran process with exponential fitness. *Journal of Theoretical Biology*, 409:38–46, 2016.

[104] G. Coop, X. Wen, C. Ober, J. K. Pritchard, and M. Przeworski. High-resolution mapping of crossovers reveals extensive variation in fine-scale recombination patterns among humans. *Science*, 319:1395–1398, 2008.

[105] V. P. Crawford and J. Sobel. Strategic information transmission. *Econometrica*, 50(6):1431–1451, 1982.

[106] M. J. Crawley and C. R. Long. Alternate bearing, predator satiation and seedling recruitment in *Quercus robur* L. *Journal of Ecology*, 83:683–696, 1995.

[107] R. Cressman. *Evolutionary dynamics and extensive form games*. MIT Press, 2003.

[108] L. Cronk. Low Socioeconomic Status and Female-Biased Parental Investment: The Mukogodo Example. *American Anthropologist*, 91(2):414–429, 1989.

[109] J. F. Crow. The importance of recombination. In R. E. Michod and B. R. Levin, editors, *The evolution of sex: an examination of current ideas*. Sinauer, 1988.

[110] J. F. Crow and M. Kimura. Evolution in sexual and asexual populations. *Am Nat*, 99:439–450, 1965.

[111] J. F. Crow and M. Kimura. *An Introduction to Population Genetics Theory*. Harper & Row, 1970.

[112] R. Cui, M. Schumer, K. Kruesi, R. Walter, P. Andolfatto, and G. G. Rosenthal. Phylogenomics reveals extensive reticulate evolution in *Xiphophorus* fishes. *Evolution*, 67(8):2166–2179, 2013.

[113] L. M. Curran and M. Leighton. Vertebrate responses to spatiotemporal variation in seed production of mast-fruiting Dipterocarpaceae. *Ecological Monographs*, 70(1):101–128, 2000.

[114] L. M. Curran and C. O. Webb. Experimental tests of the spatiotemporal scale of seed predation in mast-fruiting Dipterocarpaceae. *Ecological Monographs*, 70(1):129–148, 2000.

[115] J. A. Damore and J. Gore. A slowly evolving host moves first in symbiotic interactions. *Evolution*, 65(8):2391, 2011.

[116] A. L. Dapper and B. A. Payseur. Connecting theory and data to understand recombination rate evolution. *Philosophical Transactions of the Royal Society of London B: Biological Sciences*, 372:20160469, 2017.

[117] C. D. Darlington. *Recent Advances in Cytology*. Churchill, 1932.

[118] C. D. Darlington. The biology of crossing-over. *Nature*, 140:759–761, 1937.

[119] C. D. Darlington. *The Evolution of Genetic Systems*. Cambridge University Press, 1939.

[120] B. Davies, E. Hatton, N. Altemose, J. G. Hussin, F. Pratto, G. Zhang, A. G. Hinch, D. Moralli, D. Biggs, R. Diaz, et al. Re-engineering the zinc fingers of PRDM9 reverses hybrid sterility in mice. *Nature*, 530(7589):171–176, 2016.

[121] R. Dawkins and J. R. Krebs. Arms races between and within species. *Proceedings of the Royal Society of London B: Biological Sciences*, 205(1161):489–511, 1979.

[122] A. De Muyt, L. Zhang, T. Piolot, N. Kleckner, E. Espagne, and D. Zickler. E3 ligase hei10: a multifaceted structure-based signaling molecule with roles within and beyond meiosis. *Genes & development*, 28(10):1111–1123, 2014.

[123] M. Doebeli and N. Knowlton. The evolution of interspecific mutualisms. *Proceedings of the National Academy of Sciences USA*, 95(15):8676–8680, 1998.

[124] L. Dollo. Les lois de l'evolution. *Bull. Soc. Belge. Géol. Pal. Hydr*, 7:164–167, 1893.

[125] T. J. V. Dooren and O. Leimar. The evolution of environmental and genetic sex determination in fluctuating environments. *Evolution*, 57(12):2667–2677, 2003.

[126] B. L. Dumont and B. A. Payseur. Evolution of the genomic rate of recombination in mammals. *Evolution*, 62:276–294, 2008.

[127] B. L. Dumont and B. A. Payseur. Evolution of the genomic recombination rate in murid rodents. *Genetics*, 187:643–657, 2011.

[128] B. L. Dumont, K. W. Broman, and B. A. Payseur. Variation in genomic recombination rates among heterogeneous stock mice. *Genetics*, 182:1345–1349, 2009.

[129] C. Düsing. Die Faktoren welche die Sexualität entscheiden. *Jenaische Zeitschrift für Naturwissenschaft*, 16(2):428–464, 1883.

[130] M. L. East, O. P. Höner, B. Wachter, K. Wilhelm, T. Burke, and H. Hofer. Maternal effects on offspring social status in spotted hyenas. *Behavioral Ecology*, 20(3):478–483, 2009.

[131] S. R. Eddy. The C-value paradox, junk DNA and ENCODE. *Current Biology*, 22:R898–R899, 2012.

[132] S. R. Eddy. The ENCODE project: missteps overshadowing a success. *Current Biology*, 23:R259–R261, 2013.

[133] N. B. Edelman, P. Frandsen, M. Miyagi, B. J. Clavijo, J. Davey, R. Dikow, G. G. Accinelli, S. M. Van Belleghem, N. J. Patterson, D. E. Neafsey, et al. Genomic architecture and introgression shape a butterfly radiation. *bioRxiv*, 2018. https://doi.org/10.1101/527655.

[134] A. W. F. Edwards. An analysis of geissler's data on the human sex ratio. *Annals of Human Genetics*, 23(1):6–15, 1958.

[135] R. Egel. The synaptonemal complex and the distribution of meiotic recombination events. *Trends in Genetics*, 11:206–208, 1995.

[136] H. Ellegren, L. Gustafsson, and B. C. Sheldon. Sex ratio adjustment in relation to paternal attractiveness in a wild bird population. *Proceedings of the National Academy of Sciences USA*, 93(21):11723–11728, 1996.

[137] G. Ellison. Learning, local interaction, and coordination. *Econometrica*, 61 (5):1047–71, 1993.

[138] G. Ellison and D. Fudenberg. Word-of-mouth communication and social learning. *The Quarterly Journal of Economics*, 110(1):93–125, 1995.

[139] I. Eshel and L. L. Cavalli-Sforza. Assortment of encounters and evolution of cooperativeness. *Proceedings of the National Academy of Sciences USA*, 79 (4):1331–1335, 1982.

[140] S. N. Ethier and T. Nagylaki. Diffusion approximations of Markov chains with two time scales and applications to population genetics. *Advances in Applied Probability*, 12:14–49, 1980.

[141] W. J. Ewens. Numerical results and diffusion approximations in a genetic process. *Biometrika*, 50(3 and 4):241–249, 1963.

[142] W. J. Ewens. The pseudo-transient distribution and its uses in genetics. *Journal of Applied Probability*, 1(1):141–156, 1964.

[143] W. J. Ewens. *Mathematical Population Genetics 1. Theoretical Introduction*. Springer-Verlag, 2004.

[144] T. Ezaz, R. Stiglec, F. Veyrunes, and J. A. M. Graves. Relationships between vertebrate ZW and XY sex chromosome systems. *Current Biology*, 16(17): R736–R743, 2006.

[145] T. Ezaz, S. Sarre, D. O'Meally, J. Marshall Graves, and A. Georges. Sex chromosome evolution in lizards: independent origins and rapid transitions. *Cytogenetic and Genome Research*, 127(2-4):249–260, 2009.

[146] H. C. Fan, J. Wang, A. Potanina, and S. R. Quake. Whole-genome molecular haplotyping of single cells. *Nat Biotech*, 29:51–57, 2011.

[147] T. W. Fawcett, B. Kuijper, I. Pen, and F. J. Weissing. Should attractive males have more sons? *Behavioral Ecology*, 18(1):71–80, 2007.

[148] B. Feldmeyer, M. Kozielska, B. Kuijper, F. J. Weissing, L. W. Beukeboom, and I. Pen. Climatic variation and the geographical distribution of sex-determining mechanisms in the housefly. *Evolutionary Ecology Research*, 10(6):797–809, 2008.

[149] J. Felsenstein. Inbreeding and variance effective numbers in populations with overlapping generations. *Genetics*, 68:581–597, 1971.

[150] J. Felsenstein. The evolutionary advantage of recombination. *Genetics*, 78: 737–756, 1974.

[151] M. W. Fenner. *Seed ecology*. Chapman and Hall, 1985.

[152] J. B. Fernandes, M. Seguéla-Arnaud, C. Larchevêque, A. H. Lloyd, and R. Mercier. Unleashing meiotic crossovers in hybrid plants. *Proceedings of the National Academy of Sciences USA*, 115:2431–2436, 2018.

[153] A. E. Fisher, J. K. Triplett, C.-S. Ho, A. D. Schiller, K. A. Oltrogge, E. S. Schroder, S. A. Kelchner, and L. G. Clark. Paraphyly in the bamboo subtribe Chusqueinae (Poaceae: Bambusoideae) and a revised infrageneric classification for *Chusquea*. *Systematic Botany*, 34(4):673–683, 2009.

[154] R. A. Fisher. *The Genetical Theory of Natural Selection*. Clarendon Press, 1930.

[155] R. A. Fisher. The evolution of dominance. *Biological reviews*, 6(4):345–368, 1931.

[156] M. A. Fishman. Asymmetric evolutionary games with non-linear pure strategy payoffs. *Games and Economic Behavior*, 63(1):77–90, 2008.

[157] H. L. Fletcher. Sex and recombination. *Nature*, 331:492, 1988.

[158] H. L. Fletcher and G. M. Hewitt. A comparison of chiasma frequency and distribution between sexes in three species of grasshoppers. *Chromosoma*, 77: 129–144, 1980.

[159] J. A. Fletcher and M. Doebeli. A simple and general explanation for the evolution of altruism. *Proceedings of the Royal Society of London B: Biological Sciences*, 276(1654):13–19, 2009.

[160] D. Foster and P. Young. Stochastic evolutionary game dynamics. *Theoretical Population Biology*, 38(2):219–232, 1990.

[161] M. Franco, P. Rubini, and M. Vecchi. Sex-determinants and their distribution in various populations of *Musca domestica* L. of Western Europe. *Genetical Research*, 40(03):279–293, 1982.

[162] S. A. Frank. Individual and population sex allocation patterns. *Theoretical Population Biology*, 31(1):47–74, 1987.

[163] S. A. Frank. *Foundations of Social Evolution*. Princeton University Press, 1998.

[164] S. A. Frank. Natural selection. VII. History and interpretation of kin selection theory. *Journal of Evolutionary Biology*, 26(6):1151–1184, 2013.

[165] D. C. Franklin. Synchrony and asynchrony: observations and hypotheses for the flowering wave in a long-lived semelparous bamboo. *Journal of Biogeography*, 31(5):773–786, 2004.

[166] P. Fransz, S. Armstrong, C. Alonso-blanco, T. C. Fischer, R. A. Torres-ruiz, and G. Jones. Cytogenetics for the model system *Arabidopsis thaliana*. *The Plant Journal*, 13(6):867–876, 1998.

[167] M. E. Frederickson, A. Ravenscraft, G. A. Miller, L. M. Arcila Hernández, G. Booth, and N. E. Pierce. The direct and ecological costs of an ant-plant symbiosis. *Am Nat*, 179(6):768–778, 2012.

[168] L. Froenicke, L. K. Anderson, J. Wienberg, and T. Ashley. Male mouse recombination maps for each autosome identified by chromosome painting. *Am J Human Genet*, 71:1353–1368, 2002.

[169] F. Fu, M. A. Nowak, N. A. Christakis, and J. H. Fowler. The evolution of homophily. *Scientific Reports*, 2, 2012.

[170] D. Fudenberg and L. A. Imhof. Imitation processes with small mutations. *Journal of Economic Theory*, 131(1):251–262, 2006.

[171] D. Fudenberg and L. A. Imhof. Monotone imitation dynamics in large populations. *Journal of Economic Theory*, 140(1):229–245, 2008.

[172] D. Fudenberg and D. K. Levine. *The Theory of Learning in Games*. MIT Press, 1998.

[173] D. Fudenberg and J. Tirole. *Game Theory*. MIT Press, 1991.

[174] D. Fudenberg, M. A. Nowak, C. Taylor, and L. A. Imhof. Evolutionary game dynamics in finite populations with strong selection and weak mutation. *Theoretical Population Biology*, 70(3):352–363, 2006.

[175] M. Fujita, E. Roth, Y.-J. Lo, C. Hurst, J. Vollner, and A. Kendell. In poor families, mothers' milk is richer for daughters than sons: a test of Trivers-Willard hypothesis in agropastoral settlements in Northern Kenya. *American Journal of Physical Anthropology*, 149(1):52–59, 2012.

[176] J. C. Fung, B. Rockmill, M. Odell, and G. S. Roeder. Imposition of crossover interference through the nonrandom distribution of synapsis initiation complexes. *Cell*, 116(6):795–802, 2004.

[177] B. L. Furman and B. J. Evans. Sequential turnovers of sex chromosomes in African clawed frogs (*Xenopus*) suggest some genomic regions are good at sex determination. *G3: Genes | Genomes | Genetics*, 6(11):3625–3633, 2016.

[178] C. W. Gardiner. *Handbook of Stochastic Methods*. Springer, Berlin, 2009.

[179] S. J. C. Gaulin and C. J. Robbins. Trivers-Willard effect in contemporary North American society. *American Journal of Physical Anthropology*, 85(1): 61–69, 1991.

[180] M. T. Ghiselin. The evolution of hermaphroditism among animals. *Quarterly Review of Biology*, 44(2):189–208, 1969.

[181] M. T. Ghiselin. *The Economy of Nature and the Evolution of Sex*. University of California Press, 1974.

[182] J. H. Gillespie. Natural selection for within-generation variance in offspring number. *Genetics*, 76(3):601–606, 1974.

[183] J. H. Gillespie. Natural selection for variances in offspring numbers: a new evolutionary principle. *American Naturalist*, 111(981):1010–1014, 1977.

[184] H. C. J. Godfray. Models for clutch size and sex ratio with sibling interaction. *Theoretical Population Biology*, 30(2):215–231, 1986.

[185] C. S. Gokhale and A. Traulsen. Evolutionary games in the multiverse. *Proceedings of the National Academy of Sciences USA*, 107(12):5500–5504, 2010.

[186] C. S. Gokhale and A. Traulsen. Strategy abundance in evolutionary many-player games with multiple strategies. *Journal of Theoretical Biology*, 283(1): 180–191, 2011.

[187] C. S. Gokhale and A. Traulsen. Mutualism and evolutionary multiplayer games: revisiting the Red King. *Proceedings of the Royal Society B*, 279 (1747):4611–4616, 2012.

[188] C. S. Gokhale and A. Traulsen. Evolutionary multiplayer games. *Dynamic Games and Applications*, 4(4):468–488, 2014.

[189] C. S. Gokhale, A. Papkou, A. Traulsen, and H. Schulenburg. Lotka–Volterra dynamics kills the Red Queen: population size fluctuations and associated stochasticity dramatically change host-parasite coevolution. *BMC Evol Biol*, 13(254), 2013.

[190] D. B. Goldstein, A. Bergman, and M. W. Feldman. The evolution of interference: reduction of recombination among three loci. *Theoretical Population Biology*, 44:246–259, 1993.

[191] E. Goles, O. Schulz, and M. Markus. Prime number selection of cycles in a predator-prey model. *Complexity*, 6(4):33–38, 2001.

[192] M. E. Gonzalez and C. Donoso. Producción de semillas y hojarasca en *Chusquea quila* (poaceae: Bambusoideae), posterior a su floración sincrónica en la zona centro-sur de chile. *Revista Chilena de Historia Natural*, 72(2): 169–180, 1999.

[193] J. Gore, H. Youk, and A. Van Oudenaarden. Snowdrift game dynamics and facultative cheating in yeast. *Nature*, 459(7244):253–256, 2009.

[194] I. P. Gorlov and O. Y. Gorlova. Cost–benefit analysis of recombination and its application for understanding of chiasma interference. *Journal of Theoretical Biology*, 213:1–8, 2001.

[195] I. P. Gorlov, A. I. Zhelezova, and O. Y. Gorlova. Sex differences in chiasma distribution along two marked mouse chromosomes: differences in chiasma distribution as a reason for sex differences in recombination frequency. *Genet Res*, 64:161–166, 1994.

[196] S. J. Gould. *Ever since Darwin: Reflections in natural history.* WW Norton & Company, 1992.

[197] A. Grafen. The hawk-dove game played between relatives. *Animal Behaviour*, 27(3):905–907, 1979.

[198] A. Grafen. Biological signals as handicaps. *Journal of Theoretical Biology*, 144(4):517–546, 1990.

[199] J. M. Greeff. Offspring allocation in externally ovipositing fig wasps with varying clutch size and sex ratio. *Behavioral Ecology*, 8(5):500–505, 1997.

[200] C. Grossen, S. Neuenschwander, and N. Perrin. Temperature-dependent turnovers in sex-determination mechanisms: a quantitative model. *Evolution*, 65(1):64–78, 2011.

[201] J. R. Gruhn, C. Rubio, K. W. Broman, P. A. Hunt, and T. Hassold. Cytological studies of human meiosis: sex-specific differences in recombination originate at, or prior to, establishment of double-strand breaks. *PLOS one*, 8: e85075, 2013.

[202] C. Guerreiro. Flowering cycles of woody bamboos native to southern South America. *Journal of plant research*, 127(2):307–313, 2014.

[203] C. R. Haag, L. Theodosiou, R. Zahab, and T. Lenormand. Low recombination rates in sexual species and sex-asex transitions. *Philosophical Transactions of the Royal Society of London B: Biological Sciences*, 372:20160461, 2017.

[204] L. Hadany and T. Beker. On the evolutionary advantage of fitness-associated recombination. *Genetics*, 165(4):2167–2179, 2003.

[205] D. Haig. Brood reduction and optimal parental investment when offspring differ in quality. *American Naturalist*, 136(4):550–556, 1990.

[206] D. Haig. Games in tetrads: segregation, recombination, and meiotic drive. *Am Nat*, 176:404–413, 2010.

[207] D. Haig and A. Grafen. Genetic scrambling as a defence against meiotic drive. *Journal of Theoretical Biology*, 153(4):531–558, 1991.

[208] D. Haig, F. Úbeda, and M. M. Patten. Specialists and generalists: the sexual ecology of the genome. *Cold Spring Harbor perspectives in biology*, 6(9): a017525, 2014.

[209] W. D. Hamilton. The genetical evolution of social behaviour. I. *Journal of Theoretical Biology*, 7(1):1–16, 1964.

[210] W. D. Hamilton. The moulding of senescence by natural selection. *Journal of Theoretical Biology*, 12:12–45, 1966.

[211] W. D. Hamilton. Extraordinary sex ratios. *Science*, 156(3774):477–488, 1967.

[212] W. D. Hamilton. Selection of selfish and altruistic behaviour in some extreme models. In J. F. Eisenberg and W. S. Dillon, editors, *Man and Beast: Comparative Social Behavior*, pages 57–91. Smithsonian Press, Washington, D.C., 1971.

[213] W. D. Hamilton. Sex versus non-sex versus parasite. *Oikos*, 35:282–290, 1980.

[214] W. D. Hamilton, R. Axelrod, and R. Tanese. Sexual reproduction as an adaptation to resist parasites (a review). *Proceedings of the National Academy of Sciences USA USA*, 87:3566–3573, 1990.

[215] A. H. Handyside, G. L. Harton, B. Mariani, A. R. Thornhill, N. Affara, M.-A. Shaw, and D. K. Griffin. Karyomapping: a universal method for genome wide analysis of genetic disease based on mapping crossovers between parental haplotypes. *J Med Genet*, 47:651–658, 2010.

[216] T. F. Hansen. On the definition and measurement of fitness in finite populations. *Journal of Theoretical Biology*, 419:36–43, 2017.

[217] K. Harris and R. Nielsen. The genetic cost of Neanderthal introgression. *Genetics*, 203(2):881–891, 2016.

[218] D. L. Hartl. Modifier theory and meiotic drive. *Theor Popul Biol*, 7:168–174, 1975.

[219] D. L. Hartl and A. G. Clark. *Principles of population genetics*. Sinauer, 4th edition, 2007.

[220] D. L. Hartl and M. Ruvolo. *Genetics: Analysis of Genes and Genomes*. Jones & Bartlett Learning, 8th edition, 2012.

[221] T. Hassold, S. Sherman, and P. Hunt. Counting cross-overs: characterizing meiotic recombination in mammals. *Human Mol Genet*, 9:2409–2419, 2000.

[222] T. Hassold, L. Judis, E. R. Chan, S. Schwartz, A. Seftel, and A. Lynn. Cytological studies of meiotic recombination in human males. *Cytogen Genome Res*, 107:249–255, 2004.

[223] C. Hauert, F. Michor, M. A. Nowak, and M. Doebeli. Synergy and discounting of cooperation in social dilemmas. *Journal of Theoretical Biology*, 239(2):195–202, 2006.

[224] C. Hauert, A. Traulsen, H. De Silva, M. A. Nowak, and K. Sigmund. Public goods with punishment and abstaining in finite and infinite populations. *Biol Theor*, 3(2):114–122, 2008.

[225] G. Hausfater, J. Altmann, and S. Altmann. Long-term consistency of dominance relations among female baboons (*Papio cynocephalus*). *Science*, 217 (4561):752–755, 1982.

[226] S. Henikoff, K. Ahmad, and H. S. Malik. The centromere paradox: stable inheritance with rapidly evolving DNA. *Science*, 293(5532):1098–1102, 2001.

[227] E. A. Herre, N. Knowlton, U. G. Mueller, and S. A. Rehner. The evolution of mutualisms: exploring the paths between conflict and cooperation. *Trends Ecol Evol*, 14(2):49–53, 1999.

[228] A. J. M. Hewison and J.-M. Gaillard. Successful sons or advantaged daughters? The Trivers–Willard model and sex-biased maternal investment in ungulates. *Trends in Ecology & Evolution*, 14(6):229–234, 1999.

[229] C. Hilbe, M. A. Nowak, and K. Sigmund. Evolution of extortion in Iterated Prisoner's Dilemma games. *Proceedings of the National Academy of Sciences USA*, 110(17):6913–6918, 2013.

[230] W. G. Hill and A. Robertson. The effect of linkage on limits to artificial selection. *Genet Res*, 8:269–294, 1966.

[231] K. J. Hillers. Crossover interference. *Current Biology*, 14:R1036–R1037, 2004.

[232] D. M. Hillis and D. M. Green. Evolutionary changes of heterogametic sex in the phylogenetic history of amphibians. *Journal of Evolutionary Biology*, 3 (1-2):49–64, 1990.

[233] A. G. Hinch, A. Tandon, N. Patterson, Y. Song, N. Rohland, C. D. Palmer, G. K. Chen, K. Wang, S. G. Buxbaum, E. L. Akylbekova, et al. The landscape of recombination in African Americans. *Nature*, 476:170–175, 2011.

[234] K. Hinde. First-time macaque mothers bias milk composition in favor of sons. *Current Biology*, 17(22):R958–R959, 2007.

[235] K. Hinde. Richer milk for sons but more milk for daughters: Sex-biased investment during lactation varies with maternal life history in rhesus macaques. *American Journal of Human Biology*, 21(4):512–519, 2009.

[236] J. Hofbauer. Evolutionary dynamics for bimatrix games: a Hamiltonian system? *Journal of Mathematical Biology*, 34(5-6):675–688, 1996.

[237] J. Hofbauer and K. Sigmund. *The Theory of Evolution and Dynamical Systems: Mathematical Aspects of Selection*. Cambridge University Press, 1988.

[238] J. Hofbauer and K. Sigmund. *Evolutionary Games and Population Dynamics*. Cambridge University Press, 1998.

[239] C. E. Holleley, D. O'Meally, S. D. Sarre, J. A. M. Graves, T. Ezaz, K. Matsubara, B. Azad, X. Zhang, and A. Georges. Sex reversal triggers the rapid transition from genetic to temperature-dependent sex. *Nature*, 523(7558):79–82, 2015.

[240] E. F. Y. Hom, P. Aiyar, D. Schaeme, M. Mittag, and S. Sasso. A chemical perspective on microalgal–microbial interactions. *Trends Plant Sci*, 20(11): 689–693, 2015.

[241] Y. Hou, W. Fan, L. Yan, R. Li, Y. Lian, J. Huang, J. Li, L. Xu, F. Tang, X. S. Xie, et al. Genome analyses of single human oocytes. *Cell*, 155:1492–1506, 2013.

[242] Y. F. Hum and S. Jinks-Robertson. Mitotic gene conversion tracts associated with repair of a defined double-strand break in *Saccharomyces cerevisiae*. *Genetics*, 207:115–128, 2017.

[243] C. Hunter and N. Singh. Do males matter? Testing the effects of male genetic background on female meiotic crossover rates in *Drosophila melanogaster*. *Evolution*, 68:2718–2726, 2014.

[244] C. Hunter, W. Huang, T. Mackay, and N. Singh. The genetic architecture of natural variation in recombination rate in *Drosophila melanogaster*. *PLoS Genetics*, 12:e1005951, 2016.

[245] N. Hunter. Meiotic recombination: the essence of heredity. *Cold Spring Harbor perspectives in biology*, 7:a016618, 2015.

[246] L. D. Hurst and H. Ellegren. Sex biases in the mutation rate. *Trends in Genetics*, 14(11):446–452, 1998.

[247] L. A. Imhof and M. A. Nowak. Evolutionary game dynamics in a Wright-Fisher process. *Journal of Mathematical Biology*, 52(5):667–681, 2006.

[248] V. A. Jansen and M. Van Baalen. Altruism through beard chromodynamics. *Nature*, 440(7084):663–666, 2006.

[249] D. H. Janzen. Tropical blackwater rivers, animals, and mast fruiting by the Dipterocarpaceae. *Biotropica*, 6:69–103, 1974.

[250] D. H. Janzen. Why bamboos wait so long to flower. *Annual Review of Ecology and Systematics*, 7(1):347–391, 1976.

[251] F. J. Janzen. Heritable variation for sex ratio under environmental sex determination in the common snapping turtle (*Chelydra serpentina*). *Genetics*, 131 (1):155–161, 1992.

[252] F. J. Janzen and G. L. Paukstis. Environmental sex determination in reptiles: ecology, evolution, and experimental design. *Quarterly Review of Biology*, 66 (2):149–179, 1991.

[253] F. J. Janzen and P. C. Phillips. Exploring the evolution of environmental sex determination, especially in reptiles. *Journal of Evolutionary Biology*, 19(6): 1775–1784, 2006.

[254] A. J. Jeffreys, J. K. Holloway, L. Kauppi, C. A. May, R. Neumann, M. T. Slingsby, and A. J. Webb. Meiotic recombination hot spots and human DNA diversity. *Philosophical Transactions of the Royal Society of London B: Biological Sciences*, 359:141–152, 2004.

[255] A. J. Jeffreys, V. E. Cotton, R. Neumann, and K.-W. G. Lam. Recombination regulator PRDM9 influences the instability of its own coding sequence in humans. *Proceedings of the National Academy of Sciences USA*, 110:600–605, 2013.

[256] M. K. Jensen and A. Rigos. Evolutionary games and matching rules. *International Journal of Game Theory*, 47(3):707–735, 2018.

[257] S. E. Johnston, J. Huisman, P. A. Ellis, and J. M. Pemberton. A high-density linkage map reveals sexually-dimorphic recombination landscapes in red deer (*Cervus elaphus*). *G3*, 7:2859–2870, 2017.

[258] G. H. Jones and F. C. H. Franklin. Meiotic crossing-over: obligation and interference. *Cell*, 126(2):246–248, 2006.

[259] L. Jost. Entropy and diversity. *Oikos*, 113:363–375, 2006.

[260] V. B. Kaiser and D. Bachtrog. Evolution of sex chromosomes in insects. *Annual Review of Genetics*, 44:91–112, 2010.

[261] K. D. Kallman. Genetics and geography of sex determination in the poeciliid fish, *Xiphophorus maculatus*. *Zoologica*, 50(1):151–190, 1965.

[262] K. D. Kallman. Evidence for the existence of transformer genes for sex in the teleost *Xiphophorus maculatus*. *Genetics*, 60(4):811, 1968.

[263] M. Kandori, G. J. Mailath, and R. Rob. Learning, mutation, and long run equilibria in games. *Econometrica*, 61(1):29–56, 1993.

[264] S. Karlin and J. McGregor. Towards a theory of the evolution of modifier genes. *Theoretical population biology*, 5(1):59–103, 1974.

[265] S. Karlin and H. M. Taylor. *A First Course in Stochastic Processes*. Academic Press, 1975.

[266] L. Kauppi, A. J. Jeffreys, and S. Keeney. Where the crossovers are: recombination distributions in mammals. *Nat Rev Genet*, 5:413–424, 2004.

[267] L. Kauppi, M. Barchi, F. Baudat, P. J. Romanienko, S. Keeney, and M. Jasin. Distinct properties of the XY pseudoautosomal region crucial for male meiosis. *Science*, 331(6019):916–920, 2011.

[268] S. Kawamura. On the periodical flowering of the bamboo. *Jpn J Bot*, 3: 335–349, 1927.

[269] E. Kazancıoğlu and S. H. Alonzo. A comparative analysis of sex change in Labridae supports the size advantage hypothesis. *Evolution*, 64(8):2254–2264, 2010.

[270] J. E. Keeley and W. J. Bond. Mast flowering and semelparity in bamboos: the bamboo fire cycle hypothesis. *American Naturalist*, 154(3):383–391, 1999.

[271] S. A. Kelchner and B. P. Group. Higher level phylogenetic relationships within the bamboos (Poaceae: Bambusoideae) based on five plastid markers. *Molecular Phylogenetics and Evolution*, 67(2):404–413, 2013.

[272] M. C. Keller, R. M. Nesse, and S. Hofferth. The Trivers-Willard hypothesis of parental investment: no effect in the contemporary United States. *Evolution and Human Behavior*, 22(5):343–360, 2001.

[273] D. Kelly. The evolutionary ecology of mast seeding. *Trends in Ecology & Evolution*, 9(12):465–470, 1994.

[274] D. Kelly and V. L. Sork. Mast seeding in perennial plants: why, how, where? *Annual review of ecology and systematics*, 33(1):427–447, 2002.

[275] B. Kerr, P. Godfrey-Smith, and M. W. Feldman. What is altruism? *Trends in Ecology & Evolution*, 19(3):135–140, 2004.

[276] H.-G. Keyl. Lampbrush chromosomes in spermatocytes of *Chironomus*. *Chromosoma*, 51:75–91, 1975.

[277] M. G. Kidwell. Genetic change of recombination value in *Drosophila melanogaster*. I. Artificial selection for high and low recombination and some properties of recombination-modifying genes. *Genetics*, 70:419–432, 1972.

[278] M. G. Kidwell. Genetic change of recombination value in *Drosophila melanogaster*. II. Simulated natural selection. *Genetics*, 70:433–443, 1972.

[279] M. Kimura. On the probability of fixation of mutant genes in a population. *Genetics*, 47(6):713–719, 1962.

[280] M. Kimura. *The neutral theory of molecular evolution*. Cambridge University Press, 1983.

[281] M. Kimura and T. Ohta. The average number of generations until fixation of a mutant gene in a finite population. *Genetics*, 61(3):763, 1969.

[282] M. King and D. Hayman. Seasonal variation of chiasma frequency in *Phyllodactylus marmoratus* (Gray)(Gekkonidae – Reptilia). *Chromosoma*, 69:131–154, 1978.

[283] S. B. Kingan, D. Garrigan, and D. L. Hartl. Recurrent selection on the Winters sex-ratio genes in *Drosophila simulans*. *Genetics*, 184(1):253–265, 2010.

[284] T. Kitzberger, E. J. Chaneton, and F. Caccia. Indirect effects of prey swamping: differential seed predation during a bamboo masting event. *Ecology*, 88 (10):2541–2554, 2007.

[285] N. Kleckner. Chiasma formation: chromatin/axis interplay and the role (s) of the synaptonemal complex. *Chromosoma*, 115:175–194, 2006.

[286] N. Kleckner, A. Storlazzi, and D. Zickler. Coordinate variation in meiotic pachytene SC length and total crossover/chiasma frequency under conditions of constant DNA length. *Trends in Genetics*, 19:623–628, 2003.

[287] N. Kleckner, L. Zhang, B. Weiner, and D. Zickler. Meiotic chromosome dynamics. In K. Rippe, editor, *Genome Organization and Functioon in the Cell Nucleus*, pages 487–523. Wiley VCH, 2012.

[288] K. E. Koehler, J. P. Cherry, A. Lynn, P. A. Hunt, and T. J. Hassold. Genetic control of mammalian meiotic recombination. I. Variation in exchange frequencies among males from inbred mouse strains. *Genetics*, 162:297–306, 2002.

[289] W. D. Koenig, R. L. Mumme, W. J. Carmen, and M. T. Stanback. Acorn production by oaks in central coastal california: variation within and among years. *Ecology*, 75(1):99–109, 1994.

[290] O. Kogan, M. Khasin, B. Meerson, D. Schneider, and C. R. Myers. Two-strain competition in quasi-neutral stochastic disease dynamics. *Phys. Rev. E*, 90: 042149, 2014.

[291] A. Kong, D. F. Gudbjartsson, J. Sainz, G. M. Jonsdottir, S. A. Gudjonsson, B. Richardsson, S. Sigurdardottir, J. Barnard, B. Hallbeck, G. Masson, et al. A high-resolution recombination map of the human genome. *Nat Genet*, 31: 241–247, 2002.

[292] A. Kong, J. Barnard, D. F. Gudbjartsson, G. Thorleifsson, G. Jonsdottir, S. Sigurdardottir, B. Richardsson, J. Jonsdottir, T. Thorgeirsson, M. L. Frigge, et al. Recombination rate and reproductive success in humans. *Nat Genet*, 36:1203–1206, 2004.

[293] A. Kong, G. Thorleifsson, H. Stefansson, G. Masson, A. Helgason, D. F. Gudbjartsson, G. M. Jonsdottir, S. A. Gudjonsson, S. Sverrisson, T. Thorlacius, et al. Sequence variants in the *RNF212* gene associate with genome-wide recombination rate. *Science*, 319:1398–1401, 2008.

[294] A. Kong, G. Thorleifsson, D. F. Gudbjartsson, G. Masson, A. Sigurdsson, A. Jonasdottir, G. B. Walters, A. Jonasdottir, A. Gylfason, K. T. Kristinsson, et al. Fine-scale recombination rate differences between sexes, populations and individuals. *Nature*, 467:1099–1103, 2010.

[295] A. Kong, G. Thorleifsson, M. L. Frigge, G. Masson, D. F. Gudbjartsson, R. Villemoes, E. Magnusdottir, S. B. Olafsdottir, U. Thorsteinsdottir, and K. Stefansson. Common and low-frequency variants associated with genome-wide recombination rate. *Nature Genetics*, 46(1):11, 2014.

[296] P. Koopman, J. Gubbay, N. Vivian, P. Goodfellow, and R. Lovell-Badge. Male development of chromosomally female mice transgenic for *Sry*. *Nature*, 351 (6322):117, 1991.

[297] D. D. Kosambi. The estimation of map distance from recombination values. *Annals of Eugenics*, 12:172–175, 1944.

[298] R. Koszul, M. Meselson, K. Van Doninck, J. Vandenhaute, and D. Zickler. The centenary of Janssens's chiasmatype theory. *Genetics*, 191(2):309–317, 2012.

[299] P. R. Krugman. Increasing returns, monopolistic competition, and international trade. *J Int Econ*, 9(4):469–479, 1979.

[300] B. Kuijper, I. Pen, and F. J. Weissing. A guide to sexual selection theory. *Annual Review of Ecology, Evolution, and Systematics*, 43:287–311, 2012.

[301] F. E. Kydland and E. C. Prescott. Rules Rather than Discretion: The Inconsistency of Optimal Plans. *The Journal of Political Economy*, 85(3):473–492, 1977.

[302] R. Lanfear, H. Kokko, and A. Eyre-Walker. Population size and the rate of evolution. *Trends in Ecology & Evolution*, 29(1):33–41, 2014.

[303] V. Laporte and B. Charlesworth. Effective population size and population subdivision in demographically structured populations. *Genetics*, 162(1):501–519, 2002.

[304] D. Laurie and M. Hulten. Further studies on bivalent chiasma frequency in human males with normal karyotypes. *Annals of Human Genetics*, 49(3): 189–201, 1985.

[305] D. Laurie and G. Jones. Inter-individual variation in chiasma distribution in *Chorthippus brunneus* (Orthoptera: Acrididae). *Heredity*, 47:409–416, 1981.

[306] B. Y. Lee, G. Hulata, and T. D. Kocher. Two unlinked loci controlling the sex of blue tilapia (*Oreochromis aureus*). *Heredity*, 92(6):543–549, 2004.

[307] P. S. Lee, P. W. Greenwell, M. Dominska, M. Gawel, M. Hamilton, and T. D. Petes. A fine-structure map of spontaneous mitotic crossovers in the yeast *Saccharomyces cerevisiae*. *PLoS Genetics*, 5:e1000410, 2009.

[308] L. Lehmann and F. Rousset. How life history and demography promote or inhibit the evolution of helping behaviours. *Philosophical Transactions of the Royal Society of London B: Biological Sciences*, 365(1553):2599–2617, 2010.

[309] E. G. Leigh. The evolution of mutualism. *Journal of Evolutionary Biologyl*, 23(12):2507–2528, 2010.

[310] O. Leimar. Life-history analysis of the Trivers and Willard sex-ratio problem. *Behavioral Ecology*, 7(3):316–325, 1996.

[311] M. Lek, K. J. Karczewski, E. V. Minikel, K. E. Samocha, E. Banks, T. Fennell, A. H. O'Donnell-Luria, J. S. Ware, A. J. Hill, B. B. Cummings, et al. Analysis of protein-coding genetic variation in 60,706 humans. *Nature*, 536:285–291, 2016.

[312] T. Lenormand. The evolution of sex dimorphism in recombination. *Genetics*, 163(2):811–822, 2003.

[313] T. Lenormand and J. Dutheil. Recombination difference between sexes: a role for haploid selection. *PLoS Biology*, 3:e63, 2005.

[314] T. Lenormand, J. Engelstädter, S. E. Johnston, E. Wijnker, and C. R. Haag. Evolutionary mysteries in meiosis. *Philosophical Transactions of the Royal Society of London B: Biological Sciences*, 371(1706):20160001, 2016.

[315] M. L. Lenzi, J. Smith, T. Snowden, M. Kim, R. Fishel, B. K. Poulos, and P. E. Cohen. Extreme heterogeneity in the molecular events leading to the establishment of chiasmata during meiosis I in human oocytes. *Am J Human Genet*, 76:112–127, 2005.

[316] Y. Lesecque, S. Glémin, N. Lartillot, D. Mouchiroud, and L. Duret. The Red Queen model of recombination hotspots evolution in the light of archaic and modern human genomes. *PLoS Genetics*, 10(11):e1004790, 2014.

[317] S. Lessard. Long-term stability from fixation probabilities in finite populations: New perspectives for ESS theory. *Theoretical Population Biology*, 68 (1):19–27, 2005.

[318] C. M. Lessells. A theoretical framework for sex-biased parental care. *Animal Behaviour*, 56(2):395–407, 1998.

[319] A. Levan. Cytological studies in *Allium*, VI. The chromosome morphology of some diploid species of *Allium*. *Hereditas*, 20:289–330, 1935.

[320] D. A. Levin, Y. Peres, and E. L. Wilmer. *Markov chains and mixing times*. American Mathematical Society, 2009.

[321] R. P. Levine and E. E. Levine. The genotypic control of crossing over in *Drosophila pseudoobscura*. *Genetics*, 39:677–691, 1954.

[322] R. P. Levine and E. E. Levine. Variable crossing over arising in different strains of *Drosophila pseudoobscura*. *Genetics*, 40:399–405, 1955.

[323] S. Li, M. Meistrich, W. Brock, T. Hsu, and M. Kuo. Isolation and preliminary characterization of the synaptonemal complex from rat pachytene spermatocytes. *Exp Cell Res*, 144:63–72, 1983.

[324] J. Lian, Y. Yin, M. Oliver-Bonet, T. Liehr, E. Ko, P. Turek, F. Sun, and R. H. Martin. Variation in crossover interference levels on individual chromosomes from human males. *Human Molecular Genetics*, 17(17):2583–2594, 2008.

[325] U. Liberman. Modifier theory of meiotic drive: is Mendelian segregation stable? *Theoretical Population Biology*, 10(2):127–132, 1976.

[326] Y. T. Lin, H. Kim, and C. R. Doering. Features of fast living: On the weak selection for longevity in degenerate birth-death processes. *J. Stat. Phys.*, 148: 646–662, 2012.

[327] S. Lion and M. van Baalen. Self-structuring in spatial evolutionary ecology. *Ecology Letters*, 11(3):277–295, 2008.

[328] M. Lipson, P.-R. Loh, S. Sankararaman, N. Patterson, B. Berger, and D. Reich. Calibrating the human mutation rate via ancestral recombination density in diploid genomes. *PLoS Genetics*, 11(11), 2015.

[329] M. Lloyd and H. S. Dybas. The periodical cicada problem. I. Population ecology. *Evolution*, 20(2):133–149, 1966.

[330] M. Lloyd and H. S. Dybas. The periodical cicada problem. II. Evolution. *Evolution*, 20(4):466–505, 1966.

[331] B. C. Lu. Spreading the synaptonemal complex of *Neurospora crassa*. *Chromosoma*, 102:464–472, 1993.

[332] S. Lu, C. Zong, W. Fan, M. Yang, J. Li, A. R. Chapman, P. Zhu, X. Hu, L. Xu, L. Yan, et al. Probing meiotic recombination and aneuploidy of single sperm cells by whole-genome sequencing. *Science*, 338:1627–1630, 2012.

[333] M. Lynch. *The Origins of Genome Architecture*. Sinauer Associates, 2007.

[334] M. Lynch. Evolution of the mutation rate. *Trends in Genetics*, 26(8):345–352, 2010.

[335] A. Lynn, K. E. Koehler, L. Judis, E. R. Chan, J. P. Cherry, S. Schwartz, A. Seftel, P. A. Hunt, and T. J. Hassold. Covariation of synaptonemal complex length and mammalian meiotic exchange rates. *Science*, 296:2222–2225, 2002.

[336] A. Lynn, T. Ashley, and T. Hassold. Variation in human meiotic recombination. *Annual Review of Genomics and Human Genetics*, 5:317–349, 2004.

[337] H. S. Malik and S. Henikoff. Conflict begets complexity: the evolution of centromeres. *Curr Opinion Genet Dev*, 12(6):711–718, 2002.

[338] E. Mancera, R. Bourgon, A. Brozzi, W. Huber, and L. M. Steinmetz. High-resolution mapping of meiotic crossovers and noncrossovers in yeast. *Nature*, 454:479–485, 2008.

[339] J. E. Mank and J. C. Avise. Evolutionary diversity and turn-over of sex determination in teleost fishes. *Sexual Development*, 3(2-3):60–67, 2009.

[340] J. E. Mank, D. E. L. Promislow, and J. C. Avise. Evolution of alternative sex-determining mechanisms in teleost fishes. *Biological Journal of the Linnean Society*, 87(1):83–93, 2006.

[341] E. Marcon and P. Moens. MLH1p and MLH3p localize to precociously induced chiasmata of okadaic-acid-treated mouse spermatocytes. *Genetics*, 165(4): 2283–2287, 2003.

[342] S. H. Martin, J. W. Davey, C. Salazar, and C. D. Jiggins. Recombination rate variation shapes barriers to introgression across butterfly genomes. *PLoS Biology*, 17(2):e2006288, 2019.

[343] Y. Matsumoto and D. Crews. Molecular mechanisms of temperature-dependent sex determination in the context of ecological developmental biology. *Molecular and Cellular Endocrinology*, 354(1-2):103–110, 2012.

[344] I. Maudlin. Developmental variation of chiasma frequency in *Chorthippus brunneus*. *Heredity*, 29:259–262, 1972.

[345] R. M. May. Periodical cicadas. *Nature*, 277(5695):347–349, 1979.

[346] J. Maynard Smith. A short-term advantage for sex and recombination through sib-competition. *Journal of Theoretical Biology*, 63:245–258, 1976.

[347] J. Maynard Smith. *The evolution of sex*. Cambridge University Press, 1978.

[348] J. Maynard Smith. A new theory of sexual investment. *Behavioral Ecology and Sociobiology*, 7(3):247–251, 1980.

[349] J. Maynard Smith. *Evolution and the Theory of Games*. Cambridge University Press, 1982.

[350] J. Maynard Smith and G. A. Parker. The logic of asymmetric contests. *Animal behaviour*, 24(1):159–175, 1976.

[351] A. McAvoy. Comment on "Imitation processes with small mutations" [J. Econ. Theory 131 (2006) 251–262]. *Journal of Economic Theory*, 159: 66–69, 2015.

[352] A. McAvoy. Stochastic selection processes. *arXiv:1511.05390*, 2015.

[353] A. McAvoy and C. Hauert. Asymmetric evolutionary games. *PLoS Computational Biology*, 11(8):e1004349, 2015.

[354] A. McAvoy and C. Hauert. Structure coefficients and strategy selection in multiplayer games. *Journal of Mathematical Biology*, 72(1-2):203–238, 2016.

[355] D. M. McCandlish and A. Stoltzfus. Modeling evolution using the probability of fixation: History and implications. *Quarterly Review of Biology*, 89(3): 225–252, 2014.

[356] D. M. McCandlish, C. L. Epstein, and J. B. Plotkin. The inevitability of unconditionally deleterious substitutions during adaptation. *Evolution*, 68(5): 1351–1364, 2014.

[357] M. J. McDonald, D. P. Rice, and M. M. Desai. Sex speeds adaptation by altering the dynamics of molecular evolution. *Nature*, 531:233–236, 2016.

[358] S. McGaugh and F. Janzen. Effective heritability of targets of sex-ratio selection under environmental sex determination. *Journal of Evolutionary Biology*, 24(4):784–794, 2011.

[359] S. E. McGaugh, L. E. Schwanz, R. M. Bowden, J. E. Gonzalez, and F. J. Janzen. Inheritance of nesting behaviour across natural environmental variation in a turtle with temperature-dependent sex determination. *Proceedings of the Royal Society of London B: Biological Sciences*, 277(1685):1219–1226, 2009.

[360] S. E. McGaugh, R. M. Bowden, C.-H. Kuo, and F. J. Janzen. Field-measured heritability of the threshold for sex determination in a turtle with temperature-dependent sex determination. *Evolutionary Ecology Research*, 13:75, 2011.

[361] A. McKane, T. Biancalani, and T. Rogers. Stochastic pattern formation and spontaneous polarisation: The linear noise approximation and beyond. *Bulletin of Mathematical Biology*, 76:895, 2014.

[362] R. N. McLaughlin and H. S. Malik. Genetic conflicts: the usual suspects and beyond. *Journal of Experimental Biology*, 220(1):6–17, 2017.

[363] M. McPherson, L. Smith-Lovin, and J. M. Cook. Birds of a feather: Homophily in social networks. *Annual Review of Sociology*, pages 415–444, 2001.

[364] G. A. T. McVean and B. Charlesworth. The effects of Hill-Robertson interference between weakly selected mutations on patterns of molecular evolution and variation. *Genetics*, 155:929–944, 2000.

[365] L. Mealey and W. Mackey. Variation in offspring sex ratio in women of differing social status. *Ethology and Sociobiology*, 11(2):83–95, 1990.

[366] R. P. Meisel, T. Davey, J. H. Son, A. C. Gerry, T. Shono, and J. G. Scott. Is multifactorial sex determination in the house fly, *Musca domestica* (L.), stable over time? *Journal of Heredity*, 107(7):615–625, 2016.

[367] D. G. Mets and B. J. Meyer. Condensins regulate meiotic DNA break distribution, thus crossover frequency, by controlling chromosome structure. *Cell*, 139(1):73–86, 2009.

[368] L. G. Miles, S. R. Isberg, T. C. Glenn, S. L. Lance, P. Dalzell, P. C. Thomson, and C. Moran. A genetic linkage map for the saltwater crocodile (*Crocodylus porosus*). *Bmc Genomics*, 10(1):339, 2009.

[369] P. Milgrom and J. Roberts. Predation, reputation, and entry deterrence. *Journal of Economic Theory*, 27(2):280–312, 1982.

[370] T. S. Mitchell, J. A. Maciel, and F. J. Janzen. Does sex-ratio selection influence nest-site choice in a reptile with temperature-dependent sex determination? *Proceedings of the Royal Society of London B: Biological Sciences*, 280(1772): 20132460, 2013.

[371] I. Miura, H. Ohtani, M. Nakamura, Y. Ichikawa, and K. Saitoh. The origin and differentiation of the heteromorphic sex chromosomes Z, W, X, and Y in the frog *Rana rugosa*, inferred from the sequences of a sex-linked gene, ADP/ATP translocase. *Molecular biology and evolution*, 15(12):1612–1619, 1998.

[372] P. B. Møens and R. E. Pearlman. Chromatin organization at meiosis. *BioEssays*, 9:151–153, 1988.

[373] P. B. Møens, N. K. Kolas, M. Tarsounas, E. Marcon, P. E. Cohen, and B. Spyropoulos. The time course and chromosomal localization of recombination-related proteins at meiosis in the mouse are compatible with models that can resolve the early DNA-DNA interactions without reciprocal recombination. *J Cell Sci*, 115:1611–1622, 2002.

[374] N. A. Moran and J. J. Wernegreen. Lifestyle evolution in symbiotic bacteria: insights from genomics. *Trends Ecol Evol*, 15(8):321–326, 2000.

[375] P. A. P. Moran. Random processes in genetics. *Proceedings of the Cambridge Philosophical Society*, 54(01):60–71, 1958.

[376] C. L. Morjan. How rapidly can maternal behavior affecting primary sex ratio evolve in a reptile with environmental sex determination? *American Naturalist*, 162(2):205–219, 2003.

[377] D. Morris. *Chusquea abietifolia. Gardener's Chronicle*, 20:524, 1886.

[378] R. Moss, P. Rothery, and I. B. Trenholm. The inheritance of social dominance rank in red grouse (*Lagopus lagopus scoticus*). *Aggressive Behavior*, 11(3): 253–259, 1985.

[379] H. J. Muller. The mechanism of crossing-over. *Am Nat*, 50:193–221, 1916.

[380] H. J. Muller. Some genetic aspects of sex. *Am Nat*, 66:118–138, 1932.

[381] H. J. Muller. The relation of recombination to mutational advance. *Mut Res*, 1:2–9, 1964.

[382] P. Muralidhar and C. Veller. Sexual antagonism and the instability of environmental sex determination. *Nature Ecology & Evolution*, 2:343–351, 2018.

[383] S. Myers, R. Bowden, A. Tumian, R. E. Bontrop, C. Freeman, T. S. MacFie, G. McVean, and P. Donnelly. Drive against hotspot motifs in primates implicates the *PRDM9* gene in meiotic recombination. *Science*, 327(5967):876–879, 2010.

[384] R. S. Nadgauda, V. A. Parasharami, and A. F. Mascarenhas. Precocious flowering and seeding behaviour in tissue-cultured bamboos. *Nature*, 344(6264): 335–336, 1990.

[385] C. J. Nagelkerke. Simultaneous optimization of egg distribution and sex allocation in a patch-structured population. *American Naturalist*, 144(2):262–284, 1994.

[386] J. F. Nash Jr. The bargaining problem. *Econometrica*, 18(2):155–162, 1950.

[387] C. G. Nathanson, C. E. Tarnita, and M. A. Nowak. Calculating evolutionary dynamics in structured populations. *PLoS Computational Biology*, 5(12): e1000615, 2009. ISSN 1553-7358.

[388] S. Nee. Antagonistic co-evolution and the evolution of genotypic randomization. *Journal of Theoretical Biology*, 140(4):499–518, 1989.

[389] R. A. Neher and B. I. Shraiman. Competition between recombination and epistasis can cause a transition from allele to genotype selection. *Proceedings of the National Academy of Sciences USA USA*, 106:6866–6871, 2009.

[390] M. G. Newberry, D. M. McCandlish, and J. B. Plotkin. Assortative mating can impede or facilitate fixation of underdominant alleles. *Theoretical Population Biology*, 112:14–21, 2016.

[391] S. G. Nilsson and U. Wastljung. Seed predation and cross-pollination in mast-seeding beech (*Fagus sylvatica*) patches. *Ecology*, 68(2):260–265, 1987.

[392] M. Nishioka, I. Miura, and K. Saitoh. Sex chromosomes of *Rana rugosa* with special reference to local differences in sex-determining mechanism. *Scientific report of the Laboratory for Amphibian Biology, Hiroshima University*, 12: 55–81, 1993.

[393] D. A. Norton and D. Kelly. Mast seeding over 33 years by *Dacrydium cupressinum* Lamb.(rimu)(Podocarpaceae) in New Zealand: the importance of economies of scale. *Functional ecology*, 2:399–408, 1988.

[394] I. Novak, H. Wang, E. Revenkova, R. Jessberger, H. Scherthan, and C. Höög. Cohesin Smc1β determines meiotic chromatin axis loop organization. *J Cell Biol*, 180:83–90, 2008.

[395] M. A. Nowak. What is a quasispecies? *Trends in Ecology & Evolution*, 7(4): 118–121, 1992.

[396] M. A. Nowak. *Evolutionary dynamics*. Harvard University Press, 2006.

[397] M. A. Nowak. Five rules for the evolution of cooperation. *Science*, 314(5805): 1560–1563, 2006.

[398] M. A. Nowak. Evolving cooperation. *Journal of Theoretical Biology*, 299:1–8, 2012.

[399] M. A. Nowak and R. M. May. Evolutionary games and spatial chaos. *Nature*, 359(6398):826–829, 1992.

[400] M. A. Nowak and R. M. May. Superinfection and the evolution of parasite virulence. *Proceedings of the Royal Society of London B: Biological Sciences*, 255(1342):81–89, 1994.

[401] M. A. Nowak, A. Sasaki, C. Taylor, and D. Fudenberg. Emergence of cooperation and evolutionary stability in finite populations. *Nature*, 428(6983): 646–650, 2004.

[402] M. Numata. Conservational implications of bamboo flowering and death in japan. *Biological Conservation*, 2(3):227–9, 1970.

[403] M. Ogata, H. Ohtani, T. Igarashi, Y. Hasegawa, Y. Ichikawa, and I. Miura. Change of the heterogametic sex from male to female in the frog. *Genetics*, 164(2):613–620, 2003.

[404] T. Ohta. Slightly deleterious mutant substitutions in evolution. *Nature*, 246 (5428):96–98, 1973.

[405] T. Ohta. The nearly neutral theory of molecular evolution. *Annual Review of Ecology, Evolution, and Systematics*, 23:263–286, 1992.

[406] H. Ohtsuki. Stochastic evolutionary dynamics of bimatrix games. *Journal of Theoretical Biology*, 264(1):136–142, 2010.

[407] H. Ohtsuki. Evolutionary dynamics of n-player games played by relatives. *Philosophical Transactions of the Royal Society of London B: Biological Sciences*, 369(1642):20130359, 2014.

[408] H. Ohtsuki, C. Hauert, E. Lieberman, and M. A. Nowak. A simple rule for the evolution of cooperation on graphs and social networks. *Nature*, 441:502–505, 2006.

[409] S. Okasha and J. Martens. Hamilton's rule, inclusive fitness maximization, and the goal of individual behaviour in symmetric two-player games. *Journal of Evolutionary Biology*, 29(3):473–482, 2016.

[410] C. L. Organ and D. E. Janes. Evolution of sex chromosomes in Sauropsida. *Integrative and Comparative Biology*, 48(4):512–519, 2008.

[411] S. H. Orzack, J. J. Sohn, K. D. Kallman, S. A. Levin, and R. Johnston. Maintenance of the three sex chromosome polymorphism in the platyfish, *Xiphophorus maculatus*. *Evolution*, 34(4):663–672, 1980.

[412] N. Ospina-Alvarez and F. Piferrer. Temperature-dependent sex determination in fish revisited: prevalence, a single sex ratio response pattern, and possible effects of climate change. *PloS one*, 3(7):e2837, 2008.

[413] S. P. Otto. The evolutionary enigma of sex. *American Naturalist*, 174(S1): S1–S14, 2009.

[414] S. P. Otto and S. L. Nuismer. Species interactions and the evolution of sex. *Science*, 304(5673):1018–1020, 2004.

[415] C. S. Ottolini, L. J. Newnham, A. Capalbo, S. A. Natesan, H. A. Joshi, D. Cimadomo, D. K. Griffin, K. Sage, M. C. Summers, A. R. Thornhill, et al. Genome-wide maps of recombination and chromosome segregation in human oocytes and embryos show selection for maternal recombination rates. *Nat Genet*, 47:727–735, 2015.

[416] C. Pal, M. D. Maciá, A. Oliver, I. Schachar, and A. Buckling. Coevolution with viruses drives the evolution of bacterial mutation rates. *Nature*, 450 (7172):1079–1081, 2007.

[417] A. Papkou, C. S. Gokhale, A. Traulsen, and H. Schulenburg. Host–parasite coevolution: why changing population size matters. *Zoology*, 119(4):330–338, 2016.

[418] G. A. Parker and J. Maynard Smith. Optimality theory in evolutionary biology. *Nature*, 348(6296):27–33, 1990.

[419] T. L. Parsons and T. Rogers. Dimension reduction via timescale separation in stochastic dynamical systems. *arXiv:1510.07031*, 2015.

[420] T. L. Parsons, C. Quince, and J. B. Plotkin. Some consequences of demographic stochasticity in population genetics. *Genetics*, 185(4):1345–1354, 2010.

[421] E. D. Parvanov, P. M. Petkov, and K. Paigen. *Prdm9* controls activation of mammalian recombination hotspots. *Science*, 327(5967):835–835, 2010.

[422] I. Pen and F. J. Weissing. Sexual selection and the sex ratio: an ESS analysis. *Selection*, 1(1-3):111–122, 2001.

[423] J. Peña, L. Lehmann, and G. Nöldeke. Gains from switching and evolutionary stability in multi-player matrix games. *Journal of Theoretical Biology*, 346: 23–33, 2014.

[424] J. Peña, B. Wu, and A. Traulsen. Ordering structured populations in multiplayer cooperation games. *Journal of the Royal Society Interface*, 13:20150881, 2016.

[425] N. Perrin. Sex reversal: a fountain of youth for sex chromosomes? *Evolution*, 63(12):3043–3049, 2009.

[426] N. Pezaro, J. S. Doody, and M. B. Thompson. The ecology and evolution of temperature-dependent reaction norms for sex determination in reptiles: a mechanistic conceptual model. *Biological Reviews*, 92(3):1348–1364, 2017.

[427] M. Pokorna and L. Kratochvíl. Phylogeny of sex-determining mechanisms in squamate reptiles: are sex chromosomes an evolutionary trap? *Zoological Journal of the Linnean Society*, 156(1):168–183, 2009.

[428] C. P. Ponting. What are the genomic drivers of the rapid evolution of PRDM9? *Trends in Genetics*, 27(5):165–171, 2011.

[429] P. J. Pukkila and B. C. Lu. Silver staining of meiotic chromosomes in the fungus, *Coprinus cinereus*. *Chromosoma*, 91:108–112, 1985.

[430] R. J. Quinlan, M. B. Quinlan, and M. V. Flinn. Parental investment and age at weaning in a Caribbean village. *Evolution and Human Behavior*, 24(1): 1–16, 2003.

[431] A. E. Quinn, A. Georges, S. D. Sarre, F. Guarino, T. Ezaz, and J. A. M. Graves. Temperature sex reversal implies sex gene dosage in a reptile. *Science*, 316(5823):411–411, 2007.

[432] A. E. Quinn, S. D. Sarre, T. Ezaz, J. A. Marshall Graves, and A. Georges. Evolutionary transitions between mechanisms of sex determination in vertebrates. *Biology Letters*, 7(3):443–448, 2011.

[433] R. S. Radder, A. E. Quinn, A. Georges, S. D. Sarre, and R. Shine. Genetic evidence for co-occurrence of chromosomal and thermal sex-determining systems in a lizard. *Biology Letters*, 4(2):176–178, 2007.

[434] D. G. Rand, C. E. Tarnita, H. Ohtsuki, and M. A. Nowak. Evolution of fairness in the one-shot anonymous Ultimatum Game. *Proceedings of the National Academy of Sciences USA*, 110(7):2581–2586, 2013.

[435] A. Rapoport and A. M. Chammah. *Prisoner's dilemma: A study in conflict and cooperation*. University of Michigan Press, 1965.

[436] J. M. Refsnider, C. Milne-Zelman, D. A. Warner, and F. J. Janzen. Population sex ratios under differing local climates in a reptile with environmental sex determination. *Evolutionary ecology*, 28(5):977–989, 2014.

[437] E. Revenkova, M. Eijpe, C. Heyting, C. A. Hodges, P. A. Hunt, B. Liebe, H. Scherthan, and R. Jessberger. Cohesin SMC1β is required for meiotic chromosome dynamics, sister chromatid cohesion and DNA recombination. *Nature Cell Biology*, 6(6):555, 2004.

[438] W. Rice and A. Chippindale. Intersexual ontogenetic conflict. *Journal of Evolutionary Biology*, 14(5):685–693, 2001.

[439] W. R. Rice. On the instability of polygenic sex determination: the effect of sex-specific selection. *Evolution*, 40(3):633–639, 1986.

[440] W. R. Rice. The accumulation of sexually antagonistic genes as a selective agent promoting the evolution of reduced recombination between primitive sex chromosomes. *Evolution*, 41(4):911–914, 1987.

[441] W. R. Rice. Sexually antagonistic genes: experimental evidence. *Science*, 256 (5062):1436–1439, 1992.

[442] W. R. Rice. Male fitness increases when females are eliminated from gene pool: implications for the Y chromosome. *Proceedings of the National Academy of Sciences USA*, 95(11):6217–6221, 1998.

[443] A. Rigos and H. H. Nax. Assortativity evolving from social dilemmas. *Journal of Theoretical Biology*, 395:194–203, 2016.

[444] H. Risken. *The Fokker-Planck Equation*. Springer, Berlin, 1989.

[445] K. R. Ritz, M. A. F. Noor, and N. D. Singh. Variation in recombination rate: adaptive or not? *Trends in Genetics*, 33:364–374, 2017.

[446] J. Roach, G. Glusman, A. Smit, C. Huff, R. Hubley, P. Shannon, L. Rowen, K. Pant, N. Goodman, M. Bamshad, et al. Analysis of genetic inheritance in a family quartet by whole-genome sequencing. *Science*, 328(5978):636–639, 2010.

[447] Á. S. Roco, A. W. Olmstead, S. J. Degitz, T. Amano, L. B. Zimmerman, and M. Bullejos. Coexistence of Y, W, and Z sex chromosomes in *Xenopus tropicalis*. *Proceedings of the National Academy of Sciences USA*, 112(34): E4752–E4761, 2015.

[448] J. Ross-Ibarra. The evolution of recombination under domestication: a test of two hypotheses. *Am Nat*, 163:105–112, 2004.

[449] B. E. Rubin and C. S. Moreau. Comparative genomics reveals convergent rates of evolution in ant–plant mutualisms. *Nature Communications*, 7:12679, 2016.

[450] A. Ruiz-Herrera, M. Vozdova, J. Fernández, H. Sebestova, L. Capilla, J. Frohlich, C. Vara, A. Hernández-Marsal, J. Sipek, T. J. Robinson, et al. Recombination correlates with synaptonemal complex length and chromatin loop size in bovids–insights into mammalian meiotic chromosomal organization. *Chromosoma*, 126:615–631, 2017.

[451] S. Saha and H. F. Howe. The bamboo fire cycle hypothesis: a comment. *American Naturalist*, 158(6):659–663, 2001.

[452] T. T. Saito and M. P. Colaiácovo. Regulation of crossover frequency and distribution during meiotic recombination. *Cold Spring Harb Symp Quant Biol*, 2017.

[453] S. C. Salop. Strategic entry deterrence. *American Economic Review*, 69(2): 335–38, 1979.

[454] L. Samuelson. *Evolutionary Games and Equilibrium Selection*. MIT Press, 1998.

[455] L. Samuelson and J. Zhang. Evolutionary stability in asymmetric games. *Journal of Economic Theory*, 57(2):363–391, 1992.

[456] E. Sanchez-Moran, S. Armstrong, J. Santos, F. Franklin, and G. Jones. Variation in chiasma frequency among eight accessions of *Arabidopsis thaliana*. *Genetics*, 162:1415–1422, 2002.

[457] W. H. Sandholm. *Population Games and Evolutionary Dynamics*. MIT press, 2010.

[458] W. H. Sandholm. Stochastic imitative game dynamics with committed agents. *Journal of Economic Theory*, 147(5):2056–2071, 2012.

[459] A. Sasaki and Y. Iwasa. Optimal recombination rate in fluctuating environments. *Genetics*, 115(2):377–388, 1987.

[460] M. Schartl. Sex chromosome evolution in non-mammalian vertebrates. *Current opinion in genetics & development*, 14(6):634–641, 2004.

[461] T. C. Schelling. *The Strategy of Conflict*. Harvard University Press, 1960.

[462] H. Schenk, A. Traulsen, and C. S. Gokhale. Chaotic provinces in the kingdom of the Red Queen. *Journal of Theoretical Biology*, 431:1–10, 2017.

[463] A. F. W. Schimper. *Plant-geography upon a physiological basis*. Clarendon Press, 1902.

[464] S. Schindler, J.-M. Gaillard, A. Grüning, P. Neuhaus, L. W. Traill, S. Tuljapurkar, and T. Coulson. Sex-specific demography and generalization of the Trivers-Willard theory. *Nature*, 526, 2015.

[465] A. L. Schroeder, K. J. Metzger, A. Miller, and T. Rhen. A novel candidate gene for temperature-dependent sex determination in the common snapping turtle. *Genetics*, 203(1):557–571, 2016.

[466] M. Schumer, C. Xu, D. L. Powell, A. Durvasula, L. Skov, C. Holland, J. C. Blazier, S. Sankararaman, P. Andolfatto, G. G. Rosenthal, et al. Natural selection interacts with recombination to shape the evolution of hybrid genomes. *Science*, 360(6389):656–660, 2018.

[467] L. Schwanz, T. Ezaz, B. Gruber, and A. Georges. Novel evolutionary pathways of sex-determining mechanisms. *Journal of Evolutionary Biology*, 26(12):2544–2557, 2013.

[468] L. E. Schwanz and S. R. Proulx. Mutual information reveals variation in temperature-dependent sex determination in response to environmental fluctuation, lifespan and selection. *Proceedings of the Royal Society of London B: Biological Sciences*, 275(1650):2441–2448, 2008.

[469] J. J. Schwartz, D. J. Roach, J. H. Thomas, and J. Shendure. Primate evolution of the recombination regulator PRDM9. *Nature Communications*, 5, 2014.

[470] F. M. Scudo. Sex population genetics. *La Ricerca Scientifica, Anno 34, Serie 2, II-B*, 5(2):93–143, 1964.

[471] F. M. Scudo. Criteria for the analysis of multifactorial sex determination. *Monitore Zoologico Italiano*, 1:1–21, 1967.

[472] J. Segura, L. Ferretti, S. Ramos-Onsins, L. Capilla, M. Farré, F. Reis, M. Oliver-Bonet, H. Fernández-Bellón, F. Garcia, M. Garcia-Caldés, et al. Evolution of recombination in eutherian mammals: insights into mechanisms that affect recombination rates and crossover interference. *Proceedings of the Royal Society of London B: Biological Sciences*, 280(1771):20131945, 2013.

[473] W. Seifriz. Observations on the causes of gregarious flowering in plants. *American Journal of Botany*, 10(2):93–112, 1923.

[474] W. Seifriz. Gregarious flowering of *Chusquea*. *Nature*, 165(4199):635–636, 1950.

[475] T. Sekiguchi and H. Ohtsuki. Fixation probabilities of strategies for bimatrix games in finite populations. *Dynamic Games and Applications*, pages 1–19, 2015.

[476] R. Selten. A note on evolutionarily stable strategies in asymmetric animal conflicts. *Journal of Theoretical Biology*, 84(1):93–101, 1980.

[477] J. R. Ser, R. B. Roberts, and T. D. Kocher. Multiple interacting loci control sex determination in Lake Malawi cichlid fish. *Evolution*, 64(2):486–501, 2010.

[478] H. Serra, C. Lambing, C. H. Griffin, S. D. Topp, D. C. Nageswaran, C. J. Underwood, P. A. Ziolkowski, M. Séguéla-Arnaud, J. B. Fernandes, R. Mercier, et al. Massive crossover elevation via combination of *HEI10* and *recq4a recq4b* during *Arabidopsis* meiosis. *Proceedings of the National Academy of Sciences USA*, 115:2437–2442, 2018.

[479] N. P. Sharp and S. P. Otto. Evolution of sex: Using experimental genomics to select among competing theories. *BioEssays*, 38(8):751–757, 2016.

[480] B. C. Sheldon and S. A. West. Maternal dominance, maternal condition, and offspring sex ratio in ungulate mammals. *American Naturalist*, 163(1):40–54, 2004.

[481] J. D. Sherman and S. M. Stack. Two-dimensional spreads of synaptonemal complexes from solanaceous plants. VI. High-resolution recombination nodule map for tomato (*Lycopersicon esculentum*). *Genetics*, 141:683–708, 1995.

[482] P. W. Sherman. Insect chromosome numbers and eusociality. *Am Nat*, 113: 925–935, 1979.

[483] T. N. Sherratt. The evolution of Müllerian mimicry. *Naturwissenschaften*, 95 (8):681–695, 2008.

[484] S. Shifman, J. T. Bell, R. R. Copley, M. S. Taylor, R. W. Williams, R. Mott, and J. Flint. A high-resolution single nucleotide polymorphism genetic map of the mouse genome. *PLoS Biology*, 4:e395, 2006.

[485] R. Shine. Why is sex determined by nest temperature in many reptiles? *Trends in Ecology & Evolution*, 14(5):186–189, 1999.

[486] E. H. Simpson. Measurement of diversity. *Nature*, 163:688–688, 1949.

[487] B. Skyrms. *Social Dynamics*. Oxford University Press, 2014.

[488] C. C. Smith, J. L. Hamrick, and C. L. Kramer. The advantage of mast years for wind pollination. *American Naturalist*, 136(2):154–166, 1990.

[489] N. G. C. Smith, M. T. Webster, and H. Ellegren. Deterministic mutation rate variation in the human genome. *Genome research*, 12(9):1350–1356, 2002.

[490] C. S. Smukowski and M. A. F. Noor. Recombination rate variation in closely related species. *Heredity*, 107:496–508, 2011.

[491] P. D. Sniegowski, P. J. Gerrish, R. E. Lenski, et al. Evolution of high mutation rates in experimental populations of *E. coli*. *Nature*, 387(6634):703–705, 1997.

[492] P. D. Sniegowski, P. J. Gerrish, T. Johnson, A. Shaver, et al. The evolution of mutation rates: separating causes from consequences. *BioEssays*, 22(12): 1057–1066, 2000.

[493] Y. Song, C. S. Gokhale, A. Papkou, H. Schulenburg, and A. Traulsen. Host-parasite coevolution in populations of constant and variable size. *BMC Evol Biol*, 15(212), 2015.

[494] A. M. Spence. Job market signaling. *The Quarterly Journal of Economics*, 87 (3):355–374, 1973.

[495] C. C. Spencer, P. Deloukas, S. Hunt, J. Mullikin, S. Myers, B. Silverman, P. Donnelly, D. Bentley, and G. McVean. The influence of recombination on human genetic diversity. *PLoS Genetics*, 2:e148, 2006.

[496] S. Stack, S. Royer, L. Shearer, S. Chang, J. Giovannoni, D. Westfall, R. White, and L. Anderson. Role of fluorescence in situ hybridization in sequencing the tomato genome. *Cytogenetic and Genome Research*, 124(3-4):339–350, 2009.

[497] J. Stapley, P. G. Feulner, S. E. Johnston, A. W. Santure, and C. M. Smadja. Recombination: the good, the bad and the variable. *Philosophical Transactions of the Royal Society of London B: Biological Sciences*, 372(1736), 2017.

[498] S. C. Stearns, M. Ackermann, M. Doebeli, and M. Kaiser. Experimental evolution of aging, growth, and reproduction in fruitflies. *Proceedings of the National Academy of Sciences USA*, 97(7):3309–3313, 2000.

[499] W. Stephan, B. Charlesworth, and G. McVean. The effect of background selection at a single locus on weakly selected, partially linked variants. *Genet. Res., Camb.*, 73:133–146, 1999.

[500] A. Storlazzi, S. Tessé, S. Gargano, F. James, N. Kleckner, and D. Zickler. Meiotic double-strand breaks at the interface of chromosome movement, chromosome remodeling, and reductional division. *Genes & development*, 17(21): 2675–2687, 2003.

[501] A. H. Sturtevant. The linear arrangement of six sex-linked factors in *Drosophila*, as shown by their mode of association. *J Exp Zoo A*, 14:43–59, 1913.

[502] F. Sun, M. Oliver-Bonet, T. Liehr, H. Starke, E. Ko, A. Rademaker, J. Navarro, J. Benet, and R. H. Martin. Human male recombination maps for individual chromosomes. *Am J Human Genet*, 74:521–531, 2004.

[503] F. Sun, M. Oliver-Bonet, T. Liehr, H. Starke, P. Turek, E. Ko, A. Rademaker, and R. H. Martin. Variation in MLH1 distribution in recombination maps for individual chromosomes from human males. *Human Mol Genet*, 15:2376–2391, 2006.

[504] F. Taddei, M. Radman, J. Maynard Smith, B. Toupance, P. H. Gouyon, and B. Godelle. Role of mutator alleles in adaptive evolution. *Nature*, 387:700–702, 1997.

[505] Y. Takehana, M. Matsuda, T. Myosho, M. L. Suster, K. Kawakami, T. Shin, Y. Kohara, Y. Kuroki, A. Toyoda, A. Fujiyama, et al. Co-option of *Sox3* as the male-determining factor on the Y chromosome in the fish *Oryzias dancena*. *Nature communications*, 5, 2014.

[506] C. M. Tanaka and Y. Iwasa. Cultural evolution of a belief controlling human mate choice: Dynamic modeling of the hinoeuma superstition in Japan. *Journal of Theoretical Biology*, 309:20–28, 2012.

[507] Y. Tao, L. Araripe, S. B. Kingan, Y. Ke, H. Xiao, and D. L. Hartl. A sex-ratio meiotic drive system in *Drosophila simulans*. II: an X-linked distorter. *PLoS Biology*, 5(11):e293, 2007.

[508] Y. Tao, J. P. Masly, L. Araripe, Y. Ke, and D. L. Hartl. A sex-ratio meiotic drive system in *Drosophila simulans*. I: an autosomal suppressor. *PLoS Biology*, 5(11):e292, 2007.

[509] C. E. Tarnita, T. Antal, H. Ohtsuki, and M. A. Nowak. Evolutionary dynamics in set structured populations. *Proceedings of the National Academy of Sciences USA*, 106(21):8601–8604, 2009.

[510] C. E. Tarnita, H. Ohtsuki, T. Antal, F. Fu, and M. A. Nowak. Strategy selection in structured populations. *Journal of Theoretical Biology*, 259(3): 570 – 581, 2009.

[511] C. Taylor, D. Fudenberg, A. Sasaki, and M. A. Nowak. Evolutionary game dynamics in finite populations. *Bulletin of Mathematical Biology*, 66(6):1621–1644, 2004.

[512] P. D. Taylor. Inclusive fitness in a homogeneous environment. *Proceedings of the Royal Society of London B: Biological Sciences*, 249(1326):299–302, 1992.

[513] P. D. Taylor and A. Sauer. The selective advantage of sex-ratio homeostasis. *American Naturalist*, 116(2):305–310, 1980.

[514] P. D. Taylor, T. Day, and G. Wild. Evolution of cooperation in a finite homogeneous graph. *Nature*, 447(7143):469–472, 2007.

[515] C. Tease and M. A. Hultén. Inter-sex variation in synaptonemal complex lengths largely determine the different recombination rates in male and female germ cells. *Cytogen. Genome Res.*, 107:208–215, 2004.

[516] S. Tessé, A. Storlazzi, N. Kleckner, S. Gargano, and D. Zickler. Localization and roles of Ski8p protein in Sordaria meiosis and delineation of three mechanistically distinct steps of meiotic homolog juxtaposition. *Proceedings of the National Academy of Sciences USA*, 100(22):12865–12870, 2003.

[517] The 1000 Genomes Project Consortium. A global reference for human genetic variation. *Nature*, 526:68–74, 2015.

[518] A. Traulsen and C. Hauert. Stochastic evolutionary game dynamics. In H. G. Schuster, editor, *Review of Nonlinear Dynamics and Complexity*, volume 2, pages 25–61. Wiley-VCH, 2009.

[519] A. Traulsen, J. M. Pacheco, and L. A. Imhof. Stochasticity and evolutionary stability. *Physical Review E*, 74(2):021905, 2006.

[520] A. Traulsen, N. Shoresh, and M. A. Nowak. Analytical results for individual and group selection of any intensity. *Bulletin of Mathematical Biology*, 70(5): 1410–1424, 2008.

[521] W. Traut and U. Willhoeft. A jumping sex determining factor in the fly *Megaselia scalaris*. *Chromosoma*, 99(6):407–412, 1990.

[522] Tree of Sex Consortium. Tree of Sex: A database of sexual systems. *Scientific Data*, 1, 2014.

[523] J. K. Triplett and L. G. Clark. Phylogeny of the temperate bamboos (Poaceae: Bambusoideae: Bambuseae) with an emphasis on *Arundinaria* and allies. *Systematic Botany*, 35(1):102–120, 2010.

[524] R. L. Trivers. Sex differences in rates of recombination and sexual selection. In R. E. Michod and B. R. Levin, editors, *The evolution of sex: an examination of current ideas*. Sinauer, 1988.

[525] R. L. Trivers and D. E. Willard. Natural selection of parental ability to vary the sex ratio of offspring. *Science*, 179(4068):90–92, 1973.

[526] J. R. True, J. M. Mercer, and C. C. Laurie. Differences in crossover frequency and distribution among three sibling species of *Drosophila*. *Genetics*, 142: 507–523, 1996.

[527] J. R. G. Turner. The evolutionary dynamics of Batesian and Muellerian mimicry: similarities and differences. *Ecological Entomology*, 12(1):81–95, 1987.

[528] F. Úbeda and J. F. Wilkins. The Red Queen theory of recombination hotspots. *Journal of Evolutionary Biologyl*, 24(3):541–553, 2011.

[529] Y. Uno, C. Nishida, Y. Oshima, S. Yokoyama, I. Miura, Y. Matsuda, and M. Nakamura. Comparative chromosome mapping of sex-linked genes and identification of sex chromosomal rearrangements in the Japanese wrinkled frog (*Rana rugosa*, Ranidae) with ZW and XY sex chromosome systems. *Chromosome Research*, 16(4):637–647, 2008.

[530] N. Valenzuela, D. C. Adams, and F. J. Janzen. Pattern does not equal process: exactly when is sex environmentally determined? *American Naturalist*, 161 (4):676–683, 2003.

[531] J. Van Cleve. Social evolution and genetic interactions in the short and long term. *Theoretical Population Biology*, 103:2–26, 2015.

[532] J. Van Cleve and E. Akçay. Pathways to social evolution: reciprocity, relatedness, and synergy. *Evolution*, 68(8):2245–2258, 2014.

[533] J. Van Cleve and L. Lehmann. Stochastic stability and the evolution of coordination in spatially structured populations. *Theoretical Population Biology*, 89:75–87, 2013.

[534] G. S. van Doorn. Evolutionary transitions between sex-determining mechanisms: a review of theory. *Sexual Development*, 8(1-3):7–19, 2014.

[535] G. S. van Doorn and M. Kirkpatrick. Turnover of sex chromosomes induced by sexual conflict. *Nature*, 449:909–912, 2007.

[536] G. S. van Doorn and M. Kirkpatrick. Transitions between male and female heterogamety caused by sex-antagonistic selection. *Genetics*, 186(2):629–645, 2010.

[537] L. Van Valen. A new evolutionary law. *Evol Theor*, 1:1–30, 1973.

[538] M. Van Veelen. Group selection, kin selection, altruism and cooperation: when inclusive fitness is right and when it can be wrong. *Journal of Theoretical Biology*, 259(3):589–600, 2009.

[539] M. Van Veelen. The replicator dynamics with n players and population structure. *Journal of Theoretical Biology*, 276(1):78–85, 2011.

[540] M. van Veelen, J. García, D. G. Rand, and M. A. Nowak. Direct reciprocity in structured populations. *Proceedings of the National Academy of Sciences USA*, 109(25):9929–9934, 2012.

[541] J. van Veen and R. Hawley. Meiosis: when even two is a crowd. *Current Biology*, 13:R831–R833, 2003.

[542] V. V. Vasconcelos, F. P. Santos, F. C. Santos, and J. M. Pacheco. Stochastic dynamics through hierarchically embedded markov chains. *Physical Review Letters*, 118(5):058301, 2017.

[543] C. Veller and L. K. Hayward. Finite-population evolution with rare mutations in asymmetric games. *Journal of Economic Theory*, 162:93–113, 2016.

[544] C. Veller, M. A. Nowak, and C. C. Davis. Extended flowering intervals of bamboos evolved by discrete multiplication. *Ecology letters*, 18(7):653–659, 2015.

[545] C. Veller, D. Haig, and M. A. Nowak. The Trivers–Willard hypothesis: sex ratio or investment? *Proceedings of the Royal Society of London B: Biological Sciences*, 283(1830):20160126, 2016.

[546] C. Veller, L. K. Hayward, C. Hilbe, and M. A. Nowak. The Red Queen and King in finite populations. *Proceedings of the National Academy of Sciences USA*, 114(27):E5396–E5405, 2017.

[547] C. Veller, P. Muralidhar, G. W. Constable, and M. A. Nowak. Drift-induced selection between male and female heterogamety. *Genetics*, 207(2):711–727, 2017.

[548] C. Veller, N. Kleckner, and M. A. Nowak. A rigorous measure of genome-wide genetic shuffling that takes into account crossover positions and Mendel's second law. *Proceedings of the National Academy of Sciences USA*, 116(5): 1659–1668, 2019.

[549] M. Vérin, F. Menu, and E. Rajon. The biased evolution of generation time. *arXiv:1502.05508*, 2016.

[550] J. Verner. Selection for sex ratio. *American Naturalist*, 99(908):419–421, 1965.

[551] B. Vicoso and D. Bachtrog. Numerous transitions of sex chromosomes in Diptera. *PLoS Biology*, 13(4):e1002078, 2015.

[552] M. E. Visser. Keeping up with a warming world; assessing the rate of adaptation to climate change. *Proceedings of the Royal Society of London B: Biological Sciences*, 275(1635):649–659, 2008.

[553] D. von Wettstein, S. W. Rasmussen, and P. B. Holm. The synaptonemal complex in genetic segregation. *Annual Review of Genetics*, 18(1):331–411, 1984.

[554] S. Vuilleumier, R. Lande, J. Van Alphen, and O. Seehausen. Invasion and fixation of sex-reversal genes. *Journal of Evolutionary Biology*, 20(3):913–920, 2007.

[555] L. M. Wahl. Evolving the division of labour: generalists, specialists and task allocation. *Journal of Theoretical Biology*, 219(3):371–388, 2002.

[556] K. Wander and S. M. Mattison. The evolutionary ecology of early weaning in Kilimanjaro, Tanzania. *Proceedings of the Royal Society of London B: Biological Sciences*, 280(1768):20131359, 2013.

[557] J. Wang, H. C. Fan, B. Behr, and S. R. Quake. Genome-wide single-cell analysis of recombination activity and de novo mutation rates in human sperm. *Cell*, 150:402–412, 2012.

[558] S. Wang, D. Zickler, N. Kleckner, and L. Zhang. Meiotic crossover patterns: obligatory crossover, interference and homeostasis in a single process. *Cell Cycle*, 14:305–314, 2015.

[559] S. Wang, J.-H. Su, B. J. Beliveau, B. Bintu, J. R. Moffitt, C.-t. Wu, and X. Zhuang. Spatial organization of chromatin domains and compartments in single chromosomes. *Science*, 353:598–602, 2016.

[560] S. Wang, T. Hassold, P. Hunt, M. A. White, D. Zickler, N. Kleckner, and Z. Zhang. Inefficient crossover maturation underlies elevated aneuploidy in human female meiosis. *Cell*, 168:977–989, 2017.

[561] S. Wang, C. Veller, F. Sun, A. Ruiz-Herrera, Y. Shang, H. Liu, D. Zickler, Z. Chen, N. Kleckner, and L. Zhang. Per-nucleus crossover covariation and implications for evolution. *Cell*, 177:326–338, 2019.

[562] D. Warner and R. Shine. The adaptive significance of temperature-dependent sex determination in a reptile. *Nature*, 451(7178):566, 2008.

[563] D. A. Warner and R. Shine. The adaptive significance of temperature-dependent sex determination: experimental tests with a short-lived lizard. *Evolution*, 59(10):2209–2221, 2005.

[564] D. Waxman and S. Gavrilets. 20 questions on adaptive dynamics. *Journal of Evolutionary Biology*, 18:1139–1154, 2005.

[565] D. Wegmann, D. E. Kessner, K. R. Veeramah, R. A. Mathias, D. L. Nicolae, L. R. Yanek, Y. V. Sun, D. G. Torgerson, N. Rafaels, T. Mosley, et al. Recombination rates in admixed individuals identified by ancestry-based inference. *Nat Genet*, 43:847–853, 2011.

[566] J. W. Weibull. *Evolutionary Game Theory*. MIT press, 1997.

[567] D. M. Weinreich and L. Chao. Rapid evolutionary escape by large populations from local fitness peaks is likely in nature. *Evolution*, 59:1175–1182, 2005.

[568] D. B. Weissman. Geographical variability in the pericentric inversion system of the grasshopper *Trimerotropis pseudofasciata*. *Chromosoma*, 55:325–347, 1976.

[569] S. A. West, K. E. Flanagan, and H. C. J. Godfray. Sex allocation and clutch size in parasitoid wasps that produce single-sex broods. *Animal Behaviour*, 57(2):265–275, 1999.

[570] M. A. White, S. Wang, L. Zhang, and N. Kleckner. Quantitative modeling and automated analysis of meiotic recombination. *Methods Mol Biol*, 1471: 305–323, 2017.

[571] M. J. D. White. *Animal Cytology and Evolution*. Cambridge University Press, 3rd edition, 1973.

[572] C. Whitehouse, L. Edgar, G. Jones, and J. Parker. The population cytogenetics of *Crepis capillaris* I. Chiasma variation. *Heredity*, 47:95–103, 1981.

[573] M. C. Whitlock. Fixation probability and time in subdivided populations. *Genetics*, 164(2):767–779, 2003.

[574] L. Wilfert, J. Gadau, and P. Schmid-Hempel. Variation in genomic recombination rates among animal taxa and the case of social insects. *Heredity*, 98: 189–197, 2007.

[575] A. S. Wilkins. Moving up the hierarchy: a hypothesis on the evolution of a genetic sex determination pathway. *BioEssays*, 17(1):71–77, 1995.

[576] E. J. B. Williams and L. D. Hurst. The proteins of linked genes evolve at similar rates. *Nature*, 407(6806):900–903, 2000.

[577] G. C. Williams. Pleiotropy, natural selection, and the evolution of senescence. *Evolution*, 11(4):398–411, 1957.

[578] G. C. Williams. *Sex and Evolution*. Princeton University Press, 1975.

[579] G. C. Williams. The question of adaptive sex ratio in outcrossed vertebrates. *Proceedings of the Royal Society of London B: Biological Sciences*, 205(1161): 567–580, 1979.

[580] K. S. Williams and C. Simon. The ecology, behavior, and evolution of periodical cicadas. *Annual review of entomology*, 40(1):269–295, 1995.

[581] M. J. Wiser, N. Ribeck, and R. E. Lenski. Long-term dynamics of adaptation in asexual populations. *Science*, 342(6164):1364–1367, 2013.

[582] K. H. Wolfe, P. M. Sharp, and W.-H. Li. Mutation rates differ among regions of the mammalian genome. *Nature*, 337(6204):283–285, 1989.

[583] J. O. Wolff. Population fluctuations of mast-eating rodents are correlated with production of acorns. *Journal of Mammalogy*, 77(3):850–856, 1996.

[584] S. Wright. Evolution in Mendelian populations. *Genetics*, 16(2):97–159, 1931.

[585] B. Wu, P. M. Altrock, L. Wang, and A. Traulsen. Universality of weak selection. *Physical Review E*, 82(4):046106, Oct 2010.

[586] B. Wu, C. S. Gokhale, L. Wang, and A. Traulsen. How small are small mutation rates? *Journal of Mathematical Biology*, 64(5):803–827, 2012.

[587] B. Wu, A. Traulsen, and C. S. Gokhale. Dynamic properties of evolutionary multi-player games in finite populations. *Games*, 4(2):182–199, 2013.

[588] G. A. K. Wyatt, E. T. Kiers, A. Gardner, and S. A. West. Restricting mutualistic partners to enforce trade reliance. *Nature Communications*, 7, 2016.

[589] J. Yoshimura. The evolutionary origins of periodical cicadas during ice ages. *American Naturalist*, 149(1):112–124, 1997.

[590] A. Young. *The Evolutionary Feedback between Genetic Conflict and Genome Architecture*. PhD thesis, Harvard University, 2014.

[591] H. P. Young. The evolution of conventions. *Econometrica*, 61(1):57–84, 1993.

[592] M. J. Zelazowski, M. Sandoval, L. Paniker, H. M. Hamilton, J. Han, M. A. Gribbell, R. Kang, and F. Cole. Age-dependent alterations in meiotic recombination cause chromosome segregation errors in spermatocytes. *Cell*, 171: 601–614, 2017.

[593] L. Zhang, Z. Liang, J. Hutchinson, and N. Kleckner. Crossover patterning by the beam-film model: analysis and implications. *PLoS Genetics*, 10:e1004042, 2014.

[594] L. Zhang, S. Wang, S. Yin, S. Hong, K. P. Kim, and N. Kleckner. Topoisomerase ii mediates meiotic crossover interference. *Nature*, 511(7511):551, 2014.

[595] H. Zhao, M. S. McPeek, and T. P. Speed. Statistical analysis of chromatid interference. *Genetics*, 139(2):1057–1065, 1995.

[596] D. Zickler and N. Kleckner. Meiotic chromosomes: integrating structure and function. *Annual Review of Genetics*, 33:603–754, 1999.